FAO Irrigation and Drainage Paper

No. 56

Crop Evapotranspiration

(guidelines for computing crop water requirements)

by
Richard G. ALLEN
Utah State University
Logan, Utah, U.S.A.

Luis S. PEREIRA
Instituto Superior de Agronomia
Lisbon, Portugal

Dirk RAES
Katholieke Universiteit Leuven
Leuven, Belgium

Martin SMITH
FAO, Water Resources, Development and Management Service
Rome, Italy

Preface

This publication presents an updated procedure for calculating reference and crop evapotranspiration from meteorological data and crop coefficients. The procedure, first presented in the FAO Irrigation and Drainage Paper No. 24 'Crop Water Requirements', is termed the 'K_c ET_o' approach, whereby the effect of the climate on crop water requirements is given by the reference evapotranspiration ET_o and the effect of the crop by the crop coefficient K_c. Other procedures developed in FAO Irrigation and Drainage Paper No. 24 such as the estimation of dependable and effective rainfall, the calculation of irrigation requirements and the design of irrigation schedules are not presented in this publication but will be the subject of later papers in the series.

Since the publication of FAO Irrigation and Drainage Paper No. 24 in 1977, advances in research and more accurate assessment of crop water use have revealed the need to update the FAO methodologies for calculating ET_o. The FAO Penman method was found to frequently overestimate ET_o while the other FAO recommended equations, namely the radiation, the Blaney-Criddle, and the pan evaporation methods, showed variable adherence to the grass reference crop evapotranspiration.

In May 1990, FAO organized a consultation of experts and researchers in collaboration with the International Commission for Irrigation and Drainage and with the World Meteorological Organization, to review the FAO methodologies on crop water requirements and to advise on the revision and update of procedures.

The panel of experts recommended the adoption of the Penman-Monteith combination method as a new standard for reference evapotranspiration and advised on procedures for calculating the various parameters. The FAO Penman-Monteith method was developed by defining the reference crop as a hypothetical crop with an assumed height of 0.12 m, with a surface resistance of 70 s m^{-1} and an albedo of 0.23, closely resembling the evaporation from an extensive surface of green grass of uniform height, actively growing and adequately watered. The method overcomes the shortcomings of the previous FAO Penman method and provides values that are more consistent with actual crop water use data worldwide. Furthermore, recommendations have been developed using the FAO Penman-Monteith method with limited climatic data, thereby largely eliminating the need for any other reference evapotranspiration methods and creating a consistent and transparent basis for a globally valid standard for crop water requirement calculations.

The FAO Penman-Monteith method uses standard climatic data that can be easily measured or derived from commonly measured data. All calculation procedures have been standardized according to the available weather data and the time scale of computation. The calculation methods, as well as the procedures for estimating missing climatic data, are presented in this publication.

In the 'K_c-ET_o' approach, differences in the crop canopy and aerodynamic resistance relative to the reference crop are accounted for within the crop coefficient. The K_c coefficient serves as an aggregation of the physical and physiological differences between crops. Two calculation methods

to derive crop evapotranspiration from ET_o are presented. The first approach integrates the relationships between evapotranspiration of the crop and the reference surface into a single K_c coefficient. In the second approach, K_c is split into two factors that separately describe the evaporation (K_e) and transpiration (K_{cb}) components. The selection of the K_c approach depends on the purpose of the calculation and the time step on which the calculations are to be executed.

The final chapters present procedures that can be used to make adjustments to crop coefficients to account for deviations from standard conditions, such as water and salinity stress, low plant density, environmental factors and management practices.

Examples demonstrate the various calculation procedures throughout the publication. Most of the computations, namely all those required for the reference evapotranspiration and the single crop coefficient approach, can be performed using a pocket calculator, calculation sheets and the numerous tables given in the publication. The user may also build computer algorithms, either using a spreadsheet or any programming language.

These guidelines are intended to provide guidance to project managers, consultants, irrigation engineers, hydrologists, agronomists, meteorologists and students for the calculation of reference and crop evapotranspiration. They can be used for computing crop water requirements for both irrigated and rainfed agriculture, and for computing water consumption by agricultural and natural vegetation.

Acknowledgements

These guidelines constitute the efforts of eight years of deliberations and consultations by the authors, who together formed the working group to pursue the recommendations of the FAO expert consultation that was held in May 1990 in Rome. The consultation was organized to review the then current FAO guidelines to determine Crop Water Requirements, published in 1977 as FAO Irrigation and Drainage paper No. 24 (FAO-24) and authored by J. Doorenbos and W. Pruitt. The conceptual framework for the revised methodologies introduced in this publication came forth out of the advice of the group of eminent experts congregated in the 1990 meetings and who have importantly contributed to the development of the further studies conducted in the framework of the publication. Members of the 1990 FAO expert consultation included Dr P. Fleming of Australia, Dr A. Perrier of France, Drs L. Cavazza and L. Tombesi from Italy, Drs R. Feddes and J. Doorenbos of the Netherlands, Dr L.S. Pereira of Portugal, Drs J.L. Monteith and H. Gunston from the United Kingdom, Drs R. Allen, M. Jensen and W.O. Pruitt of USA, Dr D. Rijks from the World Meteorological Organization and various staff of FAO .

Many other experts and persons from different organizations and institutes have provided, in varying degrees and at different stages, important advice and contributions. Special acknowledgements for this are due in particular to Prof. W.O. Pruitt (retired) of the University of California, Davis and J. Doorenbos of FAO (retired) who set the standard and template for this work in the predecessor FAO-24, and to Prof. J.L. Monteith whose unique work set the scientific basis for the ET_0 review. Prof. Pruitt, despite his emeritus status, has consistently contributed in making essential data available and in advising on critical concepts. Dr James L. Wright of the USDA, Kimberly, Idaho, further contributed in providing data from the precision lysimeter for several crops. Further important contributions or reviews at critical stages of the publication were received from Drs M. Jensen, G. Hargreaves and C. Stockle of USA, Dr B. Itier of France, and various members of technical working groups of the International Commission on Irrigation and Drainage (ICID) and the American Societies of Civil and Agricultural Engneers.

The authors thank their respective institutions, Utah State University, Instituto Superior de Agronomia of Lisbon, Katholieke Universiteit Leuven and FAO for the generous support of faculty time and staff services during the development of this publication.

The authors wish to express their gratitude to Mr H. Wolter, Director of the Land and Water Development Division for his encouragement in the preparation of the guidelines and to FAO colleagues and others who have reviewed the document and made valuable comments.

Special thanks are due to Ms Chrissi Redfern for her patience and valuable assistance in the preparation and formatting of the text. Mr Julian Plummer further contributed in editing the final document.

Contents

Page

List of figures

List of tables

List of boxes

List of examples

List of equations

List of principal symbols and acronyms

a_{psy}	coefficient of psychrometer [°C^{-1}]
a_s	fraction of extraterrestrial radiation reaching the earth on an overcast day [-]
a_s+b_s	fraction of extraterrestrial radiation reaching the earth on a clear day [-]
c_p	specific heat [MJ kg^{-1} °C^{-1}]
c_s	soil heat capacity [MJ m^{-3} °C^{-1}]
CR	capillary rise [mm day^{-1}]
D_e	cumulative depth of evaporation (depletion) from the soil surface layer [mm]
D_r	cumulative depth of evapotranspiration (depletion) from the root zone [mm]
d	zero plane displacement height [m]
d_r	inverse relative distance Earth-Sun [-]
DP	deep percolation [mm]
DP_e	deep percolation from the evaporation layer [mm]
E	evaporation [mm day^{-1}]
E_{pan}	pan evaporation [mm day^{-1}]
e°(T)	saturation vapour pressure at air temperature T [kPa]
e_s	saturation vapour pressure for a given time period [kPa]
e_a	actual vapour pressure [kPa]
e_s- e_a	saturation vapour pressure deficit
EC_e	electrical conductivity of the saturation extract of the soil [dS m^{-1}]
$EC_{e,\ threshold}$	electrical conductivity of the saturation extract of the soil above which yield begins to decrease [dS m^{-1}]
ET	evapotranspiration [mm day^{-1}]
ET_o	reference crop evapotranspiration [mm day^{-1}]
ET_c	crop evapotranspiration under standard conditions [mm day^{-1}]
$ET_{c\ adj}$	crop evapotranspiration under non-standard conditions [mm day^{-1}]
exp[x]	2.7183 (base of natural logarithm) raised to the power x
F_r	resistance correction factor [-]

f_c	fraction of soil surface covered by vegetation (as observed from overhead) [-]
$f_{c\ eff}$	effective fraction of soil surface covered by vegetation [-]
$1-f_c$	exposed soil fraction [-]
f_w	fraction of soil surface wetted by rain or irrigation [-]
f_{ew}	fraction of soil that is both exposed and wetted (from which most evaporation occurs) [-]
G	soil heat flux [MJ m^{-2} day^{-1}]
G_{day}	soil heat flux for day and ten-day periods [MJ m^{-2} day^{-1}]
G_{hr}	soil heat flux for hourly or shorter periods [MJ m^{-2} $hour^{-1}$]
G_{month}	soil heat flux for monthly periods [MJ m^{-2} day^{-1}]
G_{sc}	solar constant [0.0820 MJ m^{-2} min^{-1}]
H	sensible heat [MJ m^{-2} day^{-1}]
HWR	height to width ratio
h	crop height [m]
I	irrigation depth [mm]
I_w	irrigation depth for that part of the surface wetted [mm]
J	number of day in the year [-]
K_c	crop coefficient [-]
$K_{c\ ini}$	crop coefficient during the initial growth stage [-]
$K_{c\ mid}$	crop coefficient during the mid-season growth stage [-]
$K_{c\ end}$	crop coefficient at end of the late season growth stage [-]
$K_{c\ max}$	maximum value of crop coefficient (following rain or irrigation) [-]
$K_{c\ min}$	minimum value of crop coefficient (dry soil with no ground cover) [-]
K_{cb}	basal crop coefficient [-]
$K_{cb\ full}$	basal crop coefficient during mid-season (at peak plant size or height) for vegetation with full ground cover of LAI > 3 [-]
$K_{cb\ ini}$	basal crop coefficient during the initial growth stage [-]
$K_{cb\ mid}$	basal crop coefficient during the mid-season growth stage [-]
$K_{cb\ end}$	basal crop coefficient at end of the late season growth stage [-]
K_e	soil evaporation coefficient [-]
K_p	pan coefficient [-]
K_r	soil evaporation reduction coefficient [-]

K_s	water stress coefficient [-]
K_y	yield response factor [-]
k	von Karman's constant [0.41] [-]
k_{Rs}	adjustment coefficient for the Hargreaves' radiation formula [$°C^{-0.5}$]
L_{ini}	length of initial growth stage [day]
L_{dev}	length of crop development growth stage [day]
L_{mid}	length of mid-season growth stage [day]
L_{late}	length of late season growth stage [day]
L_z	longitude of centre of local time zone [degrees west of Greenwich]
L_m	longitude [degrees west of Greenwich]
LAI	leaf area index [m^2 (leaf area) m^{-2} (soil surface)]
LAI_{active}	active (sunlit) leaf area index [-]
N	maximum possible sunshine duration in a day, daylight hours [hour]
n	actual duration of sunshine in a day [hour]
n/N	relative sunshine duration [-]
P	rainfall [mm], atmospheric pressure [kPa]
p	evapotranspiration depletion factor [-]
R	specific gas constant [0.287 kJ kg^{-1} K^{-1}]
R_a	extraterrestrial radiation [MJ m^{-2} day^{-1}]
R_l	longwave radiation [MJ m^{-2} day^{-1}]
R_n	net radiation [MJ m^{-2} day^{-1}]
R_{nl}	net longwave radiation [MJ m^{-2} day^{-1}]
R_{ns}	net solar or shortwave radiation [MJ m^{-2} day^{-1}]
R_s	solar or shortwave radiation [MJ m^{-2} day^{-1}]
R_{so}	clear-sky solar or clear-sky shortwave radiation [MJ m^{-2} day^{-1}]
r_a	aerodynamic resistance [s m^{-1}]
r_l	bulk stomatal resistance of well-illuminated leaf [s m^{-1}]
r_s	(bulk) surface or canopy resistance [s m^{-1}]
R_s/R_{so}	relative solar or relative shortwave radiation [-]
RAW	readily available soil water of the root zone [mm]

REW	readily evaporable water (i.e., maximum depth of water that can be evaporated from the soil surface layer without restriction during stage 1) [mm]
RH	relative humidity [%]
RH_{hr}	average hourly relative humidity
RH_{max}	daily maximum relative humidity [%]
RH_{mean}	daily mean relative humidity [%]
RH_{min}	daily minimum relative humidity [%]
RO	surface runoff [mm]
S_c	seasonal correction factor for solar time [hour]
SF	subsurface flow [mm]
T	air temperature [°C]
T_K	air temperature [K]
T_{Kv}	virtual air temperature [K]
T_{dew}	dewpoint temperature [°C]
T_{dry}	temperature of dry bulb [°C]
T_{max}	daily maximum air temperature [°C]
$T_{max,K}$	daily maximum air temperature [K]
T_{mean}	daily mean air temperature [°C]
T_{min}	daily minimum air temperature [°C]
$T_{min,K}$	daily minimum air temperature [K]
T_{wet}	temperature of wet bulb [°C]
TAW	total available soil water of the root zone [mm]
TEW	total evaporable water (i.e., maximum depth of water that can be evaporated from the soil surface layer)[mm]
t	time [hour]
u_2	wind speed at 2 m above ground surface [m s^{-1}]
u_z	wind speed at z m above ground surface [m s^{-1}]
W	soil water content [mm]
Y_a	actual yield of the crop [kg ha^{-1}]
Y_m	maximum (expected) yield of the crop in absence of environment or water stresses [kg ha^{-1}]
Z_e	depth of surface soil layer subjected to drying by evaporation [m]

Z_r	rooting depth [m]
z	elevation, height above sea level [m]
z_h	height of humidity measurements [m]
z_m	height of wind measurements [m]
z_{om}	roughness length governing momentum transfer [m]
z_{oh}	roughness length governing heat and vapour transfer [m]
α	albedo [-]
γ	psychrometric constant [kPa °C^{-1}]
γ_{psy}	psychrometric constant of instrument [kPa °C^{-1}]
Δ	slope of saturation vapour pressure curve [kPa °C^{-1}]
ΔSW	variation in soil water content [mm]
Δt	length of time interval [day]
Δz	effective soil depth [m]
δ	solar declination [rad]
ε	ratio molecular weight of water vapour/dry air (= 0.622)
η	mean angle of the sun above the horizon
θ	soil water content [m^3(water) m^{-3}(soil)]
θ_{FC}	soil water content at field capacity [m^3(water) m^{-3}(soil)]
θ_t	threshold soil water content below which transpiration is reduced due to water stress [m^3(water) m^{-3}(soil)]
θ_{WP}	soil water content at wilting point [m^3(water) m^{-3}(soil)]
λ	latent heat of vaporization [MJ kg^{-1}]
λET	latent heat flux [MJ m^{-2} day^{-1}]
ρ_a	mean air density [kg m^{-3}]
ρ_w	density of water [kg m^{-3}]
σ	Stefan-Boltzmann constant [4.903 10^{-9} MJ K^{-4} m^{-2} day^{-1}]
φ	latitude [rad]
ω	solar time angle at midpoint of hourly or shorter period [rad]
ω_1	solar time angle at beginning of hourly or shorter period [rad]
ω_2	solar time angle at end of hourly or shorter period [rad]
ω_s	sunset hour angle [rad]

Chapter 1

Introduction to evapotranspiration

This chapter explains the concepts of and the differences between reference crop evapotranspiration (ET_o) and crop evapotranspiration under standard conditions (ET_c) and various management and environmental conditions ($ET_{c\ adj}$). It also examines the factors that affect evapotranspiration, the units in which it is normally expressed and the way in which it can be determined.

EVAPOTRANSPIRATION PROCESS

The combination of two separate processes whereby water is lost on the one hand from the soil surface by evaporation and on the other hand from the crop by transpiration is referred to as evapotranspiration (ET).

Evaporation

Evaporation is the process whereby liquid water is converted to water vapour (vaporization) and removed from the evaporating surface (vapour removal). Water evaporates from a variety of surfaces, such as lakes, rivers, pavements, soils and wet vegetation.

Energy is required to change the state of the molecules of water from liquid to vapour. Direct solar radiation and, to a lesser extent, the ambient temperature of the air provide this energy. The driving force to remove water vapour from the evaporating surface is the difference between the water vapour pressure at the evaporating surface and that of the surrounding atmosphere. As evaporation proceeds, the surrounding air becomes gradually saturated and the process will slow down and might stop if the wet air is not transferred to the atmosphere. The replacement of the saturated air with drier air depends greatly on wind speed. Hence, solar radiation, air temperature, air humidity and wind speed are climatological parameters to consider when assessing the evaporation process.

Where the evaporating surface is the soil surface, the degree of shading of the crop canopy and the amount of water available at the evaporating surface are other factors that affect the evaporation process. Frequent rains, irrigation and water transported upwards in a soil from a shallow water table wet the soil surface. Where the soil is able to supply water fast enough to satisfy the evaporation demand, the evaporation from the soil is determined only by the meteorological conditions. However, where the interval between rains and irrigation becomes large and the ability of the soil to conduct moisture to near the surface is small, the water content in the topsoil drops and the soil surface dries out. Under these circumstances the limited availability of water exerts a controlling influence on soil evaporation. In the absence of any supply of water to the soil surface, evaporation decreases rapidly and may cease almost completely within a few days.

FIGURE 1
Schematic representation of a stoma

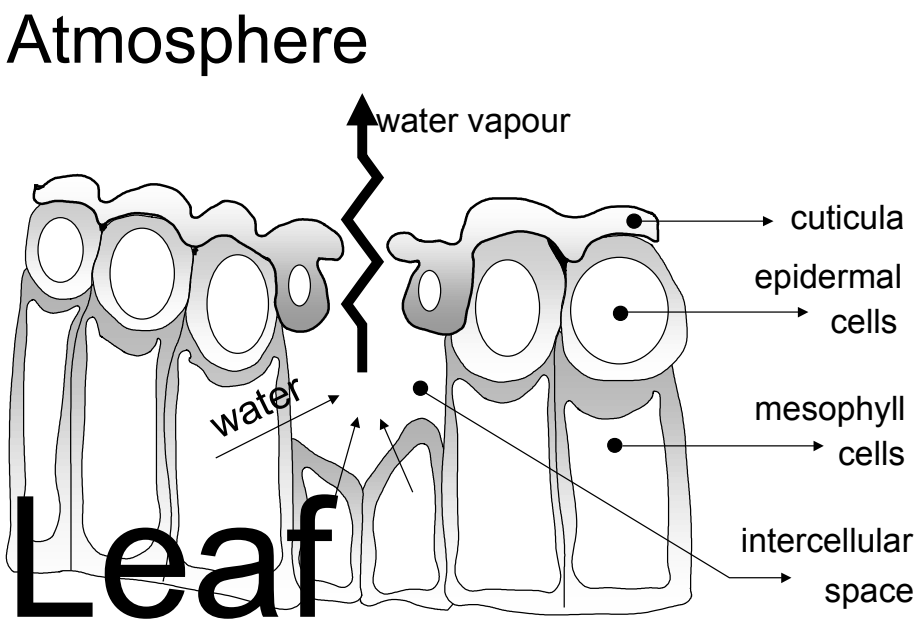

FIGURE 2
The partitioning of evapotranspiration into evaporation and transpiration over the growing period for an annual field crop

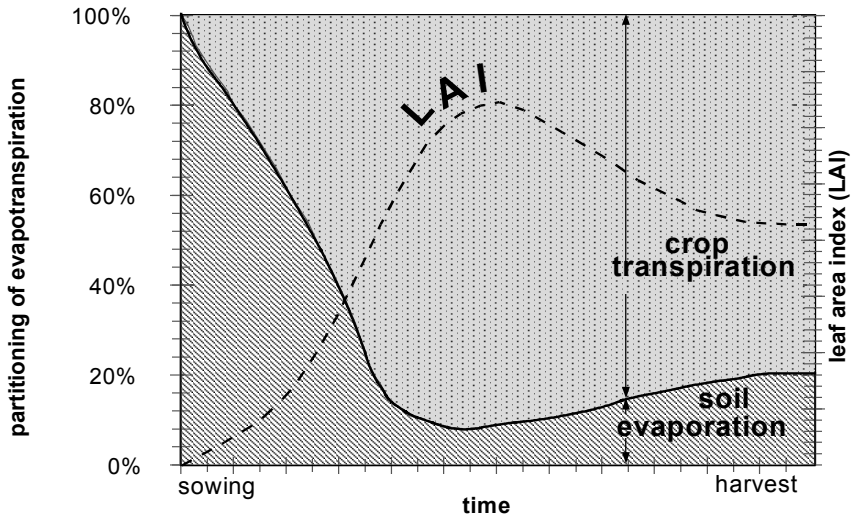

Transpiration

Transpiration consists of the vaporization of liquid water contained in plant tissues and the vapour removal to the atmosphere. Crops predominately lose their water through stomata. These are small openings on the plant leaf through which gases and water vapour pass (Figure 1). The water, together with some nutrients, is taken up by the roots and transported through the plant. The vaporization occurs within the leaf, namely in the intercellular spaces, and the vapour exchange with the atmosphere is controlled by the stomatal aperture. Nearly all water taken up is lost by transpiration and only a tiny fraction is used within the plant.

Transpiration, like direct evaporation, depends on the energy supply, vapour pressure gradient and wind. Hence, radiation, air temperature, air humidity and wind terms should be considered when assessing transpiration. The soil water content and the ability of the soil to conduct water to the roots also determine the transpiration rate, as do waterlogging and soil water salinity. The transpiration rate is also influenced by crop characteristics, environmental aspects and cultivation practices. Different kinds of plants may have different transpiration rates. Not only the type of crop, but also the crop development, environment and management should be considered when assessing transpiration.

Evapotranspiration (ET)

Evaporation and transpiration occur simultaneously and there is no easy way of distinguishing between the two processes. Apart from the water availability in the topsoil, the evaporation from a cropped soil is mainly determined by the fraction of the solar radiation reaching the soil surface. This fraction decreases over the growing period as the crop develops and the crop canopy shades more and more of the ground area. When the crop is small, water is predominately lost by soil evaporation, but once the crop is well developed and completely covers the soil, transpiration becomes the main process. In Figure 2 the partitioning of evapotranspiration into evaporation and transpiration is plotted in correspondence to leaf area per unit surface of soil below it. At sowing nearly 100% of ET comes from evaporation, while at full crop cover more than 90% of ET comes from transpiration.

UNITS

The evapotranspiration rate is normally expressed in millimetres (mm) per unit time. The rate expresses the amount of water lost from a cropped surface in units of water depth. The time unit can be an hour, day, decade, month or even an entire growing period or year.

As one hectare has a surface of 10 000 m^2 and 1 mm is equal to 0.001 m, a loss of 1 mm of water corresponds to a loss of 10 m^3 of water per hectare. In other words, 1 mm day^{-1} is equivalent to 10 m^3 ha^{-1} day^{-1}.

Water depths can also be expressed in terms of energy received per unit area. The energy refers to the energy or heat required to vaporize free water. This energy, known as the latent heat of vaporization (λ), is a function of the water temperature. For example, at 20°C, λ is about 2.45 MJ kg^{-1}. In other words, 2.45 MJ are needed to vaporize 1 kg or 0.001 m^3 of water. Hence, an energy input of 2.45 MJ per m^2 is able to vaporize 0.001 m or 1 mm of water, and therefore 1 mm of water is equivalent to 2.45 MJ m^{-2}. The evapotranspiration rate expressed in units of MJ m^{-2} day^{-1} is represented by λET, the latent heat flux.

Table 1 summarizes the units used to express the evapotranspiration rate and the conversion factors.

TABLE 1
Conversion factors for evapotranspiration

	depth	volume per unit area		energy per unit area *
	mm day^{-1}	**m^3 ha^{-1} day^{-1}**	**l s^{-1} ha^{-1}**	**MJ m^{-2} day^{-1}**
1 mm day^{-1}	1	10	0.116	2.45
1 m^3 ha^{-1} day^{-1}	0.1	1	0.012	0.245
1 l s^{-1} ha^{-1}	8.640	86.40	1	21.17
1 MJ m^{-2} day^{-1}	0.408	4.082	0.047	1

* For water with a density of 1 000 kg m^{-3} and at 20°C.

EXAMPLE 1
Converting evaporation from one unit to another

On a summer day, net solar energy received at a lake reaches 15 MJ per square metre per day. If 80% of the energy is used to vaporize water, how large could the depth of evaporation be?

From Table 1:	1 MJ m^{-2} day^{-1} =	0.408	mm day^{-1}
Therefore:	0.8 x 15 MJ m^{-2} day^{-1} = 0.8 x 15 x 0.408 mm d^{-1} =	4.9	mm day^{-1}

The evaporation rate could be 4.9 mm/day

FIGURE 3
Factors affecting evapotranspiration with reference to related ET concepts

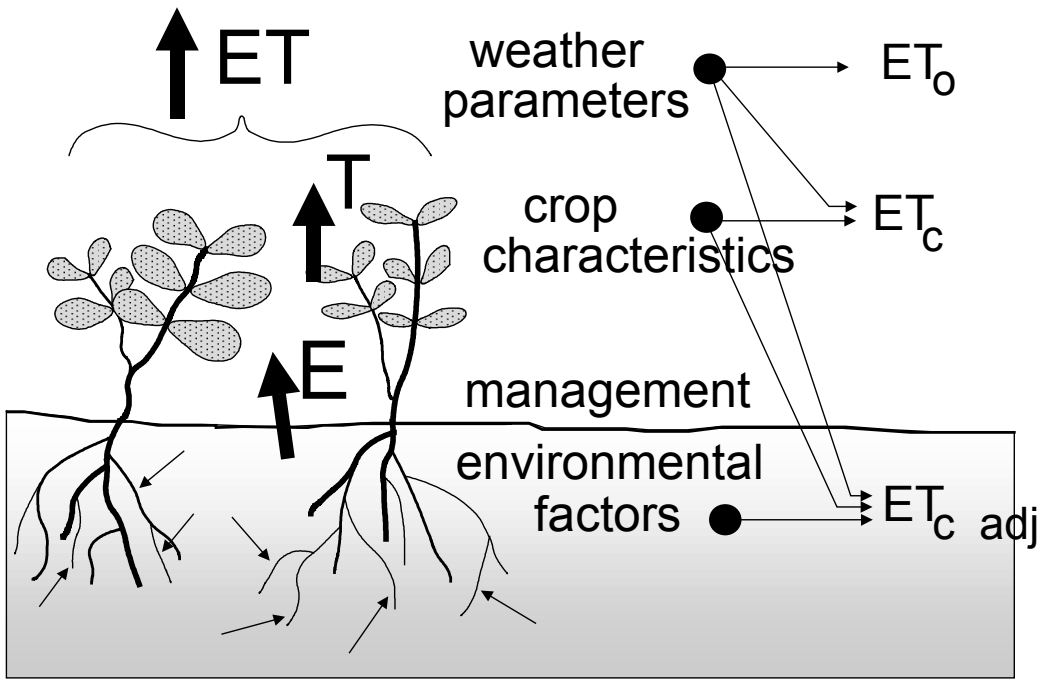

FACTORS AFFECTING EVAPOTRANSPIRATION

Weather parameters, crop characteristics, management and environmental aspects are factors affecting evaporation and transpiration. The related ET concepts presented in Figure 3 are discussed in the section on evapotranspiration concepts.

Weather parameters

The principal weather parameters affecting evapotranspiration are radiation, air temperature, humidity and wind speed. Several procedures have been developed to assess the evaporation rate from these parameters. The evaporation power of the atmosphere is expressed by the reference crop evapotranspiration (ET_o). The reference crop evapotranspiration represents the evapotranspiration from a standardized vegetated surface. The ET_o is described in detail later in this Chapter and in Chapters 2 and 4.

Crop factors

The crop type, variety and development stage should be considered when assessing the evapotranspiration from crops grown in large, well-managed fields. Differences in resistance to transpiration, crop height, crop roughness, reflection, ground cover and crop rooting characteristics result in different ET levels in different types of crops under identical environmental conditions. Crop evapotranspiration under standard conditions (ET_c) refers to the evaporating demand from crops that are grown in large fields under optimum soil water, excellent management and environmental conditions, and achieve full production under the given climatic conditions.

Management and environmental conditions

Factors such as soil salinity, poor land fertility, limited application of fertilizers, the presence of hard or impenetrable soil horizons, the absence of control of diseases and pests and poor soil management may limit the crop development and reduce the evapotranspiration. Other factors to be considered when assessing ET are ground cover, plant density and the soil water content. The effect of soil water content on ET is conditioned primarily by the magnitude of the water deficit and the type of soil. On the other hand, too much water will result in waterlogging which might damage the root and limit root water uptake by inhibiting respiration.

When assessing the ET rate, additional consideration should be given to the range of management practices that act on the climatic and crop factors affecting the ET process. Cultivation practices and the type of irrigation method can alter the microclimate, affect the crop characteristics or affect the wetting of the soil and crop surface. A windbreak reduces wind velocities and decreases the ET rate of the field directly beyond the barrier. The effect can be significant especially in windy, warm and dry conditions although evapotranspiration from the trees themselves may offset any reduction in the field. Soil evaporation in a young orchard, where trees are widely spaced, can be reduced by using a well-designed drip or trickle irrigation system. The drippers apply water directly to the soil near trees, thereby leaving the major part of the soil surface dry, and limiting the evaporation losses. The use of mulches, especially when the crop is small, is another way of substantially reducing soil evaporation. Anti-transpirants, such as stomata-closing, film-forming or reflecting material, reduce the water losses from the crop and hence the transpiration rate.

FIGURE 4
Reference (ET_o), crop evapotranspiration under standard (ET_c) and non-standard conditions ($ET_{c\ adj}$)

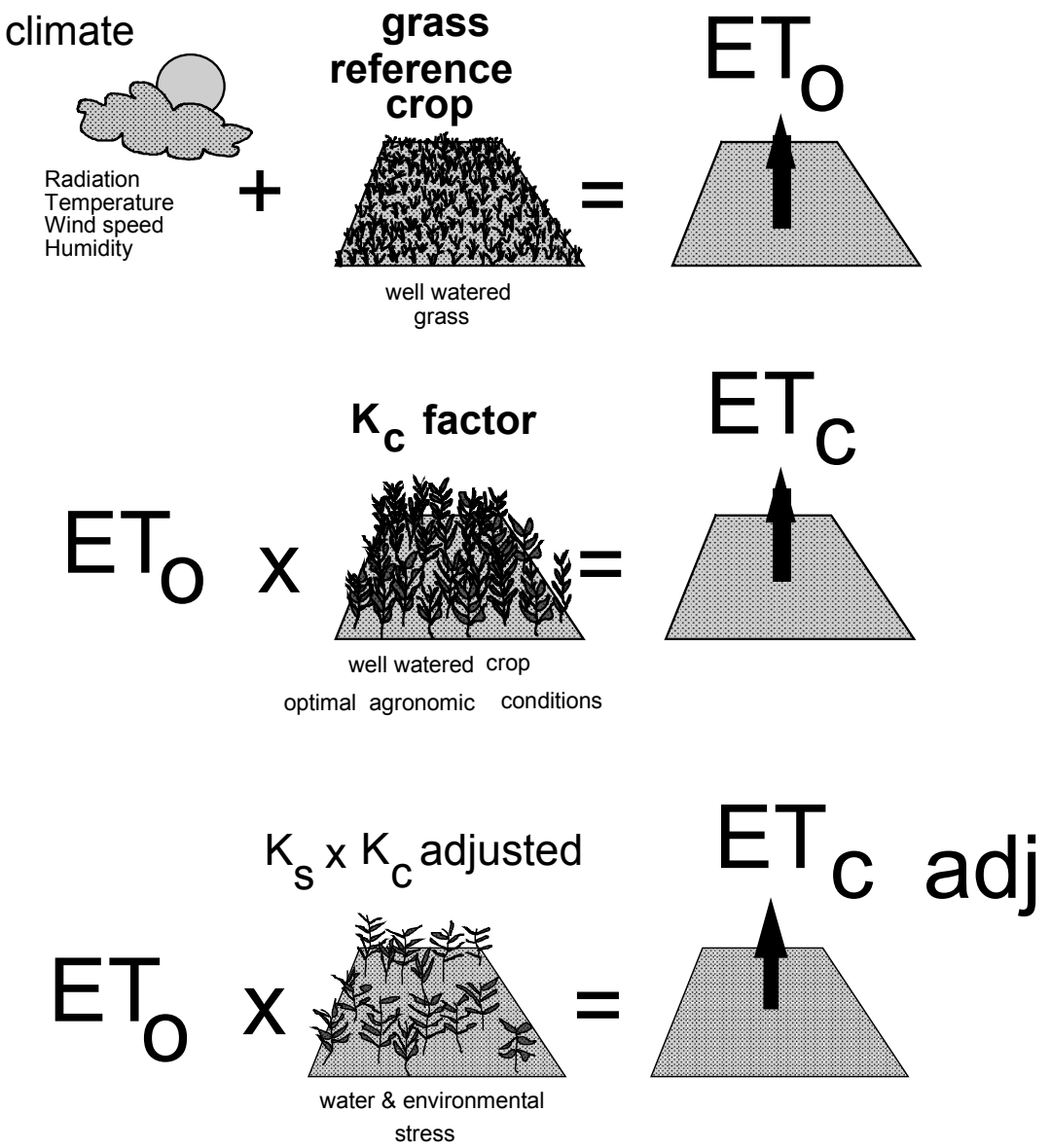

Where field conditions differ from the standard conditions, correction factors are required to adjust ET_c. The adjustment reflects the effect on crop evapotranspiration of the environmental and management conditions in the field.

EVAPOTRANSPIRATION CONCEPTS

Distinctions are made (Figure 4) between reference crop evapotranspiration (ET_o), crop evapotranspiration under standard conditions (ET_c) and crop evapotranspiration under non-standard conditions ($ET_{c\ adj}$). ET_o is a climatic parameter expressing the evaporation power of the atmosphere. ET_c refers to the evapotranspiration from excellently managed, large, well-watered fields that achieve full production under the given climatic conditions. Due to sub-optimal crop management and environmental constraints that affect crop growth and limit evapotranspiration, ET_c under non-standard conditions generally requires a correction.

Reference crop evapotranspiration (ET_o)

The evapotranspiration rate from a reference surface, not short of water, is called the reference crop evapotranspiration or reference evapotranspiration and is denoted as ET_o. The reference surface is a hypothetical grass reference crop with specific characteristics. The use of other denominations such as potential ET is strongly discouraged due to ambiguities in their definitions.

The concept of the reference evapotranspiration was introduced to study the evaporative demand of the atmosphere independently of crop type, crop development and management practices. As water is abundantly available at the reference evapotranspiring surface, soil factors do not affect ET. Relating ET to a specific surface provides a reference to which ET from other surfaces can be related. It obviates the need to define a separate ET level for each crop and stage of growth. ET_o values measured or calculated at different locations or in different seasons are comparable as they refer to the ET from the same reference surface.

The only factors affecting ET_o are climatic parameters. Consequently, ET_o is a climatic parameter and can be computed from weather data. ET_o expresses the evaporating power of the atmosphere at a specific location and time of the year and does not consider the crop characteristics and soil factors. The FAO Penman-Monteith method is recommended as the sole method for determining ET_o. The method has been selected because it closely approximates grass ET_o at the location evaluated, is physically based, and explicitly incorporates both physiological and aerodynamic parameters. Moreover, procedures have been developed for estimating missing climatic parameters.

Typical ranges for ET_o values for different agroclimatic regions are given in Table 2. These values are intended to familiarize inexperienced users with typical ranges, and are not intended for direct application. The calculation of the reference crop evapotranspiration is discussed in Part A of this handbook (Box 1).

Crop evapotranspiration under standard conditions (ET_c)

The crop evapotranspiration under standard conditions, denoted as ET_c, is the evapotranspiration from disease-free, well-fertilized crops, grown in large fields, under optimum soil water conditions, and achieving full production under the given climatic conditions.

TABLE 2
Average ET_o for different agroclimatic regions in mm/day

Regions	Mean daily temperature (°C)		
	Cool ~ 10°C	**Moderate 20°C**	**Warm > 30°C**
Tropics and subtropics			
- humid and sub-humid	2 - 3	3 - 5	5 - 7
- arid and semi-arid	2 - 4	4 - 6	6 - 8
Temperate region			
- humid and sub-humid	1 - 2	2 - 4	4 - 7
- arid and semi-arid	1 - 3	4 - 7	6 - 9

BOX 1
Chapters concerning the calculation of the reference crop evapotranspiration (ET_o)

PART A -----
Chapter 2 - FAO Penman-Monteith equation:
This chapter introduces the user to the need to standardize one method to compute ET_o from meteorological data. The FAO Penman-Monteith method is recommended as the method for determining reference ET_o. The method and the corresponding definition of the reference surface are described.

Chapter 3 - Meteorological data:
The FAO Penman-Monteith method requires radiation, air temperature, air humidity and wind speed data. Calculation procedures to derive climatic parameters from the meteorological data are presented. Procedures to estimate missing meteorological variables required for calculating ET_o are outlined. This allows for estimation of ET_o with the FAO Penman-Monteith method under all circumstances, even in the case of missing climatic data.

Chapter 4 - Determination of ET_o:
The calculation of ET_o by means of the FAO Penman-Monteith equation, with different time steps, from the principal weather parameters and with missing data is described. The determination of ET_o from pan evaporation is also presented.

BOX 2
Chapters concerning the calculation of crop evapotranspiration under standard conditions (ET_c)

PART B -----
Chapter 5 - Introduction to crop evapotranspiration:
This chapter introduces the user to the 'K_c ET_o' approach for calculating crop evapotranspiration. The effects of characteristics that distinguish field crops from the reference grass crop are integrated into the crop coefficient K_c. Depending on the purpose of the calculation, the required accuracy, the available climatic data and the time step with which the calculations have to be executed, a distinction is made between two calculation methods.

Chapter 6 - ET_c - Single crop coefficient (K_c):
This chapter presents the first calculation method for crop evapotranspiration whereby the difference in evapotranspiration between the cropped and reference grass surface is combined into a single crop coefficient (K_c).

Chapter 7 - ET_c - Dual crop coefficient ($K_c = K_{cb} + K_e$):
This chapter presents the other calculation method for crop evapotranspiration. K_c is split into two separate coefficients, one for crop transpiration (i.e., the basal crop coefficient K_{cb}) and one for soil evaporation (K_e).

The amount of water required to compensate the evapotranspiration loss from the cropped field is defined as crop water requirement. Although the values for crop evapotranspiration and crop water requirement are identical, crop water requirement refers to the amount of water that needs to be supplied, while crop evapotranspiration refers to the amount of water that is lost through evapotranspiration. The irrigation water requirement basically represents the difference between the crop water requirement and effective precipitation. The irrigation water requirement also includes additional water for leaching of salts and to compensate for non-uniformity of water application. Calculation of the irrigation water requirement is not covered in this publication, but will be the topic of a future Irrigation and Drainage Paper.

Crop evapotranspiration can be calculated from climatic data and by integrating directly the crop resistance, albedo and air resistance factors in the Penman-Monteith approach. As there is still a considerable lack of information for different crops, the Penman-Monteith method is used for the estimation of the standard reference crop to determine its evapotranspiration rate, i.e., ET_o. Experimentally determined ratios of ET_c/ET_o, called crop coefficients (K_c), are used to relate ET_c to ET_o or $ET_c = K_c\ ET_o$.

Differences in leaf anatomy, stomatal characteristics, aerodynamic properties and even albedo cause the crop evapotranspiration to differ from the reference crop evapotranspiration under the same climatic conditions. Due to variations in the crop characteristics throughout its growing season, K_c for a given crop changes from sowing till harvest. The calculation of crop evapotranspiration under standard conditions (ET_c) is discussed in Part B of this handbook (Box 2).

Crop evapotranspiration under non-standard conditions ($ET_{c\ adj}$)

The crop evapotranspiration under non-standard conditions ($ET_{c\ adj}$) is the evapotranspiration from crops grown under management and environmental conditions that differ from the standard conditions. When cultivating crops in fields, the real crop evapotranspiration may deviate from ET_c due to non-optimal conditions such as the presence of pests and diseases, soil salinity, low soil fertility, water shortage or waterlogging. This may result in scanty plant growth, low plant density and may reduce the evapotranspiration rate below ET_c.

The crop evapotranspiration under non-standard conditions is calculated by using a water stress coefficient K_s and/or by adjusting K_c for all kinds of other stresses and environmental constraints on crop evapotranspiration. The adjustment to ET_c for water stress, management and environmental constraints is discussed in Part C of this handbook (Box 3).

DETERMINING EVAPOTRANSPIRATION

ET measurement

Evapotranspiration is not easy to measure. Specific devices and accurate measurements of various physical parameters or the soil water balance in lysimeters are required to determine evapotranspiration. The methods are often expensive, demanding in terms of accuracy of measurement and can only be fully exploited by well-trained research personnel. Although the methods are inappropriate for routine measurements, they remain important for the evaluation of ET estimates obtained by more indirect methods.

BOX 3
Chapters concerning the calculation of crop evapotranspiration under non-standard conditions ($ET_{c\ adj}$)

PART C -----
Chapter 8 - ET_c under soil water stress conditions:
This chapter discusses the reduction in transpiration induced by soil moisture stress or soil water salinity. The resulting evapotranspiration will deviate from the crop evapotranspiration under standard conditions. The evapotranspiration is computed by using a water stress coefficient, K_s, describing the effect of water stress on crop transpiration.

Chapter 9 - ET_c for natural, non-typical and non-pristine vegetation:
Procedures that can be used to make adjustments to the K_c to account for less than perfect growing conditions or stand characteristics are discussed. The procedures can also be used to determine K_c for agricultural crops not listed in the tables of Part B.

Chapter 10 - ET_c under various management practices:
This chapter discusses various types of management practices that may cause the values for K_c and ET_c to deviate from the standard conditions described in Part B. Adjustment procedures for K_c to account for surface mulches, intercropping, small areas of vegetation and management induced stress are presented.

Chapter 11 - ET_c during non-growing periods:
This chapter describes procedures for predicting ET_c during non-growing periods under various types of surface conditions.

FIGURE 5
Schematic presentation of the diurnal variation of the components of the energy balance above a well-watered transpiring surface on a cloudless day

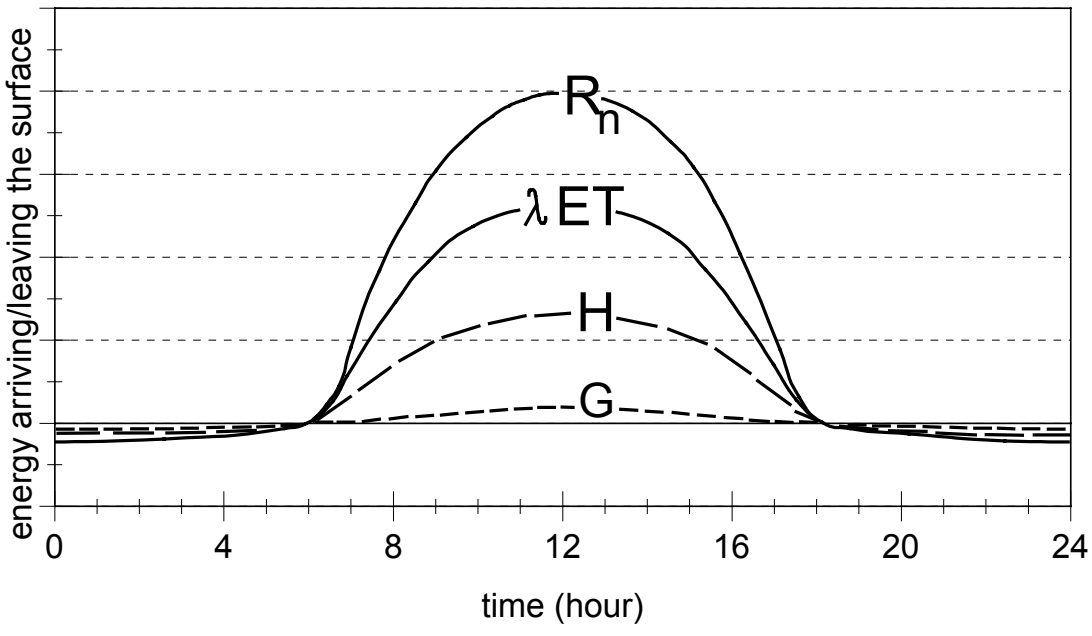

Energy balance and microclimatological methods

Evaporation of water requires relatively large amounts of energy, either in the form of sensible heat or radiant energy. Therefore the evapotranspiration process is governed by energy exchange at the vegetation surface and is limited by the amount of energy available. Because of this limitation, it is possible to predict the evapotranspiration rate by applying the principle of energy conservation. The energy arriving at the surface must equal the energy leaving the surface for the same time period.

All fluxes of energy should be considered when deriving an energy balance equation. The equation for an evaporating surface can be written as:

$$R_n - G - \lambda ET - H = 0 \qquad (1)$$

where R_n is the net radiation, H the sensible heat, G the soil heat flux and λET the latent heat flux. The various terms can be either positive or negative. Positive R_n supplies energy to the surface and positive G, λET and H remove energy from the surface (Figure 5).

In Equation 1 only vertical fluxes are considered and the net rate at which energy is being transferred horizontally, by advection, is ignored. Therefore the equation is to be applied to large, extensive surfaces of homogeneous vegetation only. The equation is restricted to the four components: R_n, λET, H and G. Other energy terms, such as heat stored or released in the plant, or the energy used in metabolic activities, are not considered These terms account for only a small fraction of the daily net radiation and can be considered negligible when compared with the other four components.

The latent heat flux (λET) representing the evapotranspiration fraction can be derived from the energy balance equation if all other components are known. Net radiation (R_n) and soil heat fluxes (G) can be measured or estimated from climatic parameters. Measurements of the sensible heat (H) are however complex and cannot be easily obtained. H requires accurate measurement of temperature gradients above the surface.

Another method of estimating evapotranspiration is the mass transfer method. This approach considers the vertical movement of small parcels of air (eddies) above a large homogeneous surface. The eddies transport material (water vapour) and energy (heat, momentum) from and towards the evaporating surface. By assuming steady state conditions and that the eddy transfer coefficients for water vapour are proportional to those for heat and momentum, the evapotranspiration rate can be computed from the vertical gradients of air temperature and water vapour via the Bowen ratio. Other direct measurement methods use gradients of wind speed and water vapour. These methods and other methods such as eddy covariance, require accurate measurement of vapour pressure, and air temperature or wind speed at different levels above the surface. Therefore, their application is restricted to primarily research situations.

Soil water balance

Evapotranspiration can also be determined by measuring the various components of the soil water balance. The method consists of assessing the incoming and outgoing water flux into the crop root zone over some time period (Figure 6). Irrigation (I) and rainfall (P) add water to the root zone. Part of I and P might be lost by surface runoff (RO) and by deep percolation

(DP) that will eventually recharge the water table. Water might also be transported upward by capillary rise (CR) from a shallow water table towards the root zone or even transferred horizontally by subsurface flow in (SF_{in}) or out of (SF_{out}) the root zone. In many situations, however, except under condititions with large slopes, SF_{in} and SF_{out} are minor and can be ignored. Soil evaporation and crop transpiration deplete water from the root zone. If all fluxes other than evapotranspiration (ET) can be assessed, the evapotranspiration can be deduced from the change in soil water content (ΔSW) over the time period:

$$ET = I + P - RO - DP + CR \pm \Delta SF \pm \Delta SW \qquad (2)$$

Some fluxes such as subsurface flow, deep percolation and capillary rise from a water table are difficult to assess and short time periods cannot be considered. The soil water balance method can usually only give ET estimates over long time periods of the order of week-long or ten-day periods.

FIGURE 6
Soil water balance of the root zone

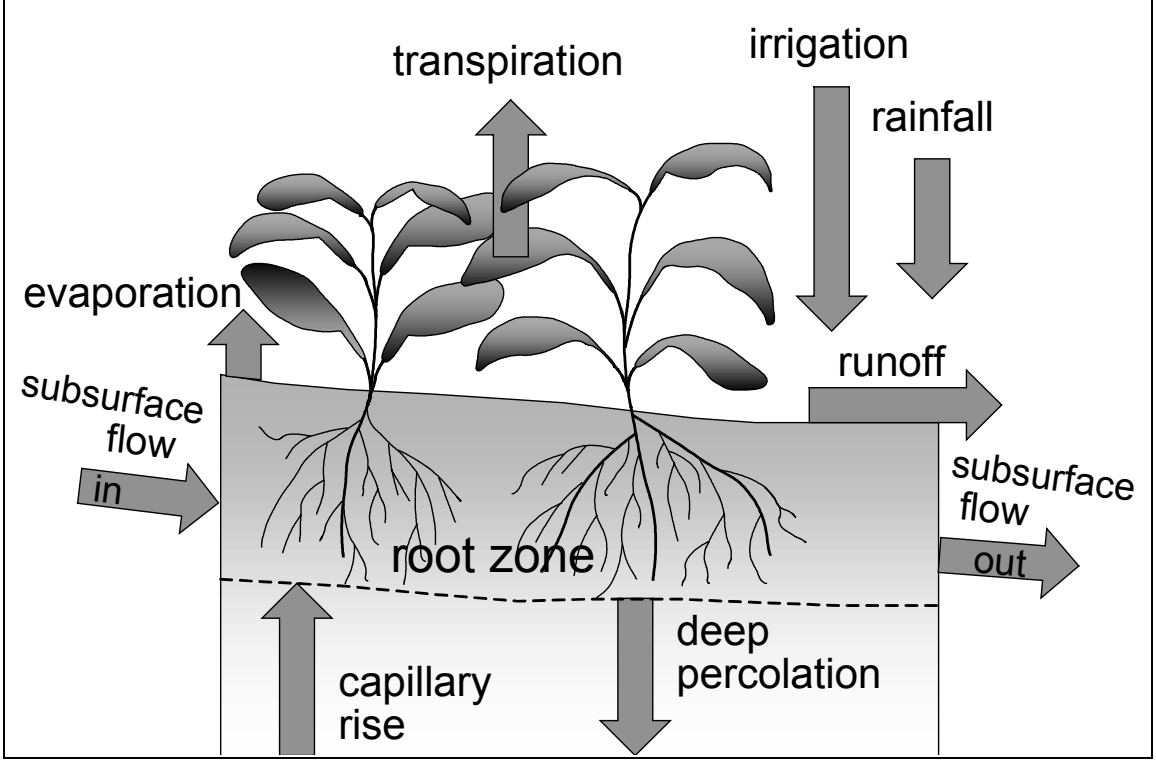

Lysimeters

By isolating the crop root zone from its environment and controlling the processes that are difficult to measure, the different terms in the soil water balance equation can be determined with greater accuracy. This is done in lysimeters where the crop grows in isolated tanks filled with either disturbed or undisturbed soil. In precision weighing lysimeters, where the water loss is directly measured by the change of mass, evapotranspiration can be obtained with an accuracy of a few hundredths of a millimetre, and small time periods such as an hour can be

considered. In non-weighing lysimeters the evapotranspiration for a given time period is determined by deducting the drainage water, collected at the bottom of the lysimeters, from the total water input.

A requirement of lysimeters is that the vegetation both inside and immediately outside of the lysimeter be perfectly matched (same height and leaf area index). This requirement has historically not been closely adhered to in a majority of lysimeter studies and has resulted in severely erroneous and unrepresentative ET_c and K_c data.

As lysimeters are difficult and expensive to construct and as their operation and maintenance require special care, their use is limited to specific research purposes.

ET computed from meteorological data

Owing to the difficulty of obtaining accurate field measurements, ET is commonly computed from weather data. A large number of empirical or semi-empirical equations have been developed for assessing crop or reference crop evapotranspiration from meteorological data. Some of the methods are only valid under specific climatic and agronomic conditions and cannot be applied under conditions different from those under which they were originally developed.

Numerous researchers have analysed the performance of the various calculation methods for different locations. As a result of an Expert Consultation held in May 1990, the FAO Penman-Monteith method is now recommended as the standard method for the definition and computation of the reference evapotranspiration, ET_o. The ET from crop surfaces under standard conditions is determined by crop coefficients (K_c) that relate ET_c to ET_o. The ET from crop surfaces under non-standard conditions is adjusted by a water stress coefficient (K_s) and/or by modifying the crop coefficient.

ET estimated from pan evaporation

Evaporation from an open water surface provides an index of the integrated effect of radiation, air temperature, air humidity and wind on evapotranspiration. However, differences in the water and cropped surface produce significant differences in the water loss from an open water surface and the crop. The pan has proved its practical value and has been used successfully to estimate reference evapotranspiration by observing the evaporation loss from a water surface and applying empirical coefficients to relate pan evaporation to ET_o. The procedure is outlined in Chapter 3.

Part A

Reference evapotranspiration (ET_o)

Part A deals with the evapotranspiration from the reference surface, the so-called reference crop evapotranspiration or reference evapotranspiration, denoted as ET_o. The reference surface is a hypothetical grass reference crop with an assumed crop height of 0.12 m, a fixed surface resistance of 70 s m^{-1} and an albedo of 0.23. The reference surface closely resembles an extensive surface of green, well-watered grass of uniform height, actively growing and completely shading the ground. The fixed surface resistance of 70 s m^{-1} implies a moderately dry soil surface resulting from about a weekly irrigation frequency.

ET_o can be computed from meteorological data. As a result of an Expert Consultation held in May 1990, the FAO Penman-Monteith method is now recommended as the sole standard method for the definition and computation of the reference evapotranspiration. The FAO Penman-Monteith method requires radiation, air temperature, air humidity and wind speed data. Calculation procedures to derive climatic parameters from meteorological data and to estimate missing meteorological variables required for calculating ET_o are presented in this Part (Chapter 3). The calculation procedures in this Publication allow for estimation of ET_o with the FAO Penman-Monteith method under all circumstances, even in the case of missing climatic data.

ET_o can also be estimated from pan evaporation. Pans have proved their practical value and have been used successfully to estimate ET_o by observing the water loss from the pan and using empirical coefficients to relate pan evaporation to ET_o. However, special precautions and management must be applied.

Chapter 2

FAO Penman-Monteith equation

This chapter introduces the user to the need to standardize one method to compute reference evapotranspiration (ET_o) from meteorological data. The FAO Penman-Monteith method is recommended as the sole ET_o method for determining reference evapotranspiration. The method, its derivation, the required meteorological data and the corresponding definition of the reference surface are described in this chapter.

NEED FOR A STANDARD ET_o METHOD

A large number of more or less empirical methods have been developed over the last 50 years by numerous scientists and specialists worldwide to estimate evapotranspiration from different climatic variables. Relationships were often subject to rigorous local calibrations and proved to have limited global validity. Testing the accuracy of the methods under a new set of conditions is laborious, time-consuming and costly, and yet evapotranspiration data are frequently needed at short notice for project planning or irrigation scheduling design. To meet this need, guidelines were developed and published in the FAO Irrigation and Drainage Paper No. 24 'Crop water requirements'. To accommodate users with different data availability, four methods were presented to calculate the reference crop evapotranspiration (ET_o): the Blaney-Criddle, radiation, modified Penman and pan evaporation methods. The modified Penman method was considered to offer the best results with minimum possible error in relation to a living grass reference crop. It was expected that the pan method would give acceptable estimates, depending on the location of the pan. The radiation method was suggested for areas where available climatic data include measured air temperature and sunshine, cloudiness or radiation, but not measured wind speed and air humidity. Finally, the publication proposed the use of the Blaney-Criddle method for areas where available climatic data cover air temperature data only.

These climatic methods to calculate ET_o were all calibrated for ten-day or monthly calculations, not for daily or hourly calculations. The Blaney-Criddle method was recommended for periods of one month or longer. For the pan method it was suggested that calculations should be done for periods of ten days or longer. Users have not always respected these conditions and calculations have often been done on daily time steps.

Advances in research and the more accurate assessment of crop water use have revealed weaknesses in the methodologies. Numerous researchers analysed the performance of the four methods for different locations. Although the results of such analyses could have been influenced by site or measurement conditions or by bias in weather data collection, it became evident that the proposed methods do not behave the same way in different locations around the world. Deviations from computed to observed values were often found to exceed ranges indicated by FAO. The modified Penman was frequently found to overestimate ET_o, even by

up to 20% for low evaporative conditions. The other FAO recommended equations showed variable adherence to the reference crop evapotranspiration standard of grass.

To evaluate the performance of these and other estimation procedures under different climatological conditions, a major study was undertaken under the auspices of the Committee on Irrigation Water Requirements of the American Society of Civil Engineers (ASCE). The ASCE study analysed the performance of 20 different methods, using detailed procedures to assess the validity of the methods compared to a set of carefully screened lysimeter data from 11 locations with variable climatic conditions. The study proved very revealing and showed the widely varying performance of the methods under different climatic conditions. In a parallel study commissioned by the European Community, a consortium of European research institutes evaluated the performance of various evapotranspiration methods using data from different lysimeter studies in Europe.

The studies confirm the overestimation of the modified Penman introduced in FAO Irrigation and Drainage Paper No. 24, and the variable performance of the different methods depending on their adaptation to local conditions. The comparative studies may be summarized as follows:

- The Penman methods may require local calibration of the wind function to achieve satisfactory results.
- The radiation methods show good results in humid climates where the aerodynamic term is relatively small, but performance in arid conditions is erratic and tends to underestimate evapotranspiration.
- Temperature methods remain empirical and require local calibration in order to achieve satisfactory results. A possible exception is the 1985 Hargreaves' method which has shown reasonable ET_o results with a global validity.
- Pan evapotranspiration methods clearly reflect the shortcomings of predicting crop evapotranspiration from open water evaporation. The methods are susceptible to the microclimatic conditions under which the pans are operating and the rigour of station maintenance. Their performance proves erratic.
- The relatively accurate and consistent performance of the Penman-Monteith approach in both arid and humid climates has been indicated in both the ASCE and European studies.

The analysis of the performance of the various calculation methods reveals the need for formulating a standard method for the computation of ET_o. The FAO Penman-Monteith method is recommended as the sole standard method. It is a method with strong likelihood of correctly predicting ET_o in a wide range of locations and climates and has provision for application in data-short situations. The use of older FAO or other reference ET methods is no longer encouraged.

FORMULATION OF THE PENMAN-MONTEITH EQUATION

Penman-Monteith equation

In 1948, Penman combined the energy balance with the mass transfer method and derived an equation to compute the evaporation from an open water surface from standard climatological records of sunshine, temperature, humidity and wind speed. This so-called combination

method was further developed by many researchers and extended to cropped surfaces by introducing resistance factors.

The resistance nomenclature distinguishes between aerodynamic resistance and surface resistance factors (Figure 7). The surface resistance parameters are often combined into one parameter, the 'bulk' surface resistance parameter which operates in series with the aerodynamic resistance. The surface resistance, r_s, describes the resistance of vapour flow through stomata openings, total leaf area and soil surface. The aerodynamic resistance, r_a, describes the resistance from the vegetation upward and involves friction from air flowing over vegetative surfaces. Although the exchange process in a vegetation layer is too complex to be fully described by the two resistance factors, good correlations can be obtained between measured and calculated evapotranspiration rates, especially for a uniform grass reference surface.

FIGURE 7
Simplified representation of the (bulk) surface and aerodynamic resistances for water vapour flow

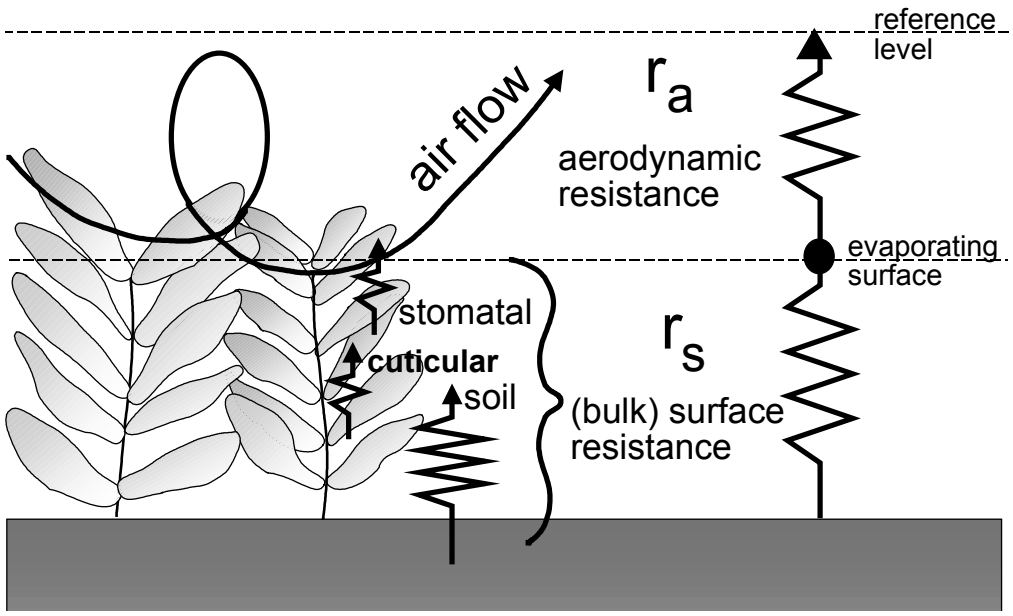

The Penman-Monteith form of the combination equation is:

$$\lambda ET = \frac{\Delta(R_n - G) + \rho_a c_p \dfrac{(e_s - e_a)}{r_a}}{\Delta + \gamma\left(1 + \dfrac{r_s}{r_a}\right)} \qquad (3)$$

where R_n is the net radiation, G is the soil heat flux, $(e_s - e_a)$ represents the vapour pressure deficit of the air, ρ_a is the mean air density at constant pressure, c_p is the specific heat of the air, Δ represents the slope of the saturation vapour pressure temperature relationship, γ is the

psychrometric constant, and r_s and r_a are the (bulk) surface and aerodynamic resistances. The parameters of the equation are defined in Chapter 3.

The Penman-Monteith approach as formulated above includes all parameters that govern energy exchange and corresponding latent heat flux (evapotranspiration) from uniform expanses of vegetation. Most of the parameters are measured or can be readily calculated from weather data. The equation can be utilized for the direct calculation of any crop evapotranspiration as the surface and aerodynamic resistances are crop specific.

Aerodynamic resistance (r_a)

The transfer of heat and water vapour from the evaporating surface into the air above the canopy is determined by the aerodynamic resistance:

$$r_a = \frac{\ln\left[\frac{z_m - d}{z_{om}}\right] \ln\left[\frac{z_h - d}{z_{oh}}\right]}{k^2 u_z} \qquad (4)$$

where
- r_a aerodynamic resistance [s m^{-1}],
- z_m height of wind measurements [m],
- z_h height of humidity measurements [m],
- d zero plane displacement height [m],
- z_{om} roughness length governing momentum transfer [m],
- z_{oh} roughness length governing transfer of heat and vapour [m],
- k von Karman's constant, 0.41 [-],
- u_z wind speed at height z [m s^{-1}].

The equation is restricted for neutral stability conditions, i.e., where temperature, atmospheric pressure, and wind velocity distributions follow nearly adiabatic conditions (no heat exchange). The application of the equation for short time periods (hourly or less) may require the inclusion of corrections for stability. However, when predicting ET_o in the well-watered reference surface, heat exchanged is small, and therefore stability correction is normally not required.

Many studies have explored the nature of the wind regime in plant canopies. Zero displacement heights and roughness lengths have to be considered when the surface is covered by vegetation. The factors depend upon the crop height and architecture. Several empirical equations for the estimate of d, z_{om} and z_{oh} have been developed. The derivation of the aerodynamic resistance for the grass reference surface is presented in Box 4.

(Bulk) surface resistance (r_s)

The 'bulk' surface resistance describes the resistance of vapour flow through the transpiring crop and evaporating soil surface. Where the vegetation does not completely cover the soil, the resistance factor should indeed include the effects of the evaporation from the soil surface. If the crop is not transpiring at a potential rate, the resistance depends also on the water status of the vegetation. An acceptable approximation to a much more complex relation of the surface resistance of dense full cover vegetation is:

BOX 4
The aerodynamic resistance for a grass reference surface

For a wide range of crops the zero plane displacement height, d [m], and the roughness length governing momentum transfer, z_{om} [m], can be estimated from the crop height h [m] by the following equations:

$$d = 2/3\ h$$

$$z_{om} = 0.123\ h$$

The roughness length governing transfer of heat and vapour, z_{oh} [m], can be approximated by:

$$z_{oh} = 0.1\ z_{om}$$

Assuming a constant crop height of 0.12 m and a standardized height for wind speed, temperature and humidity at 2 m ($z_m = z_h = 2$ m), the aerodynamic resistance r_a [s m^{-1}] for the grass reference surface becomes (Eq. 4):

$$r_a = \frac{\ln\left[\frac{2-2/3(0.12)}{0.123(0.12)}\right] \ln\left[\frac{2-2/3(0.12)}{(0.1)0.123(0.12)}\right]}{(0.41)^2 u_2} = \frac{208}{u_2}$$

where u_2 is the wind speed [m s^{-1}] at 2 m.

$$r_s = \frac{r_l}{LAI_{active}} \qquad (5)$$

where r_s (bulk) surface resistance [s m^{-1}],
r_l bulk stomatal resistance of the well-illuminated leaf [s m^{-1}],
LAI_{active} active (sunlit) leaf area index [m^2 (leaf area) m^{-2} (soil surface)].

The Leaf Area Index (LAI), a dimensionless quantity, is the leaf area (upper side only) per unit area of soil below it. It is expressed as m^2 leaf area per m^2 ground area. The active LAI is the index of the leaf area that actively contributes to the surface heat and vapour transfer. It is generally the upper, sunlit portion of a dense canopy. The LAI values for various crops differ widely but values of 3-5 are common for many mature crops. For a given crop, green LAI changes throughout the season and normally reaches its maximum before or at flowering (Figure 8). LAI further depends on the plant density and the crop variety.

The bulk stomatal resistance, r_l, is the average resistance of an individual leaf. This resistance is crop specific and differs among crop varieties and crop management. It usually increases as the crop ages and begins to ripen. There is, however, a lack of consolidated information on changes in r_l over time for the different crops. The information available in the literature on stomatal conductance or resistance is often oriented toward physiological or ecophysiological studies.

The stomatal resistance, r_l, is influenced by climate and by water availability. However, influences vary from one crop to another and different varieties can be affected differently. The resistance increases when the crop is water stressed and the soil water availability limits

FIGURE 8
Typical presentation of the variation in the active (green) Leaf Area Index over the growing season for a maize crop

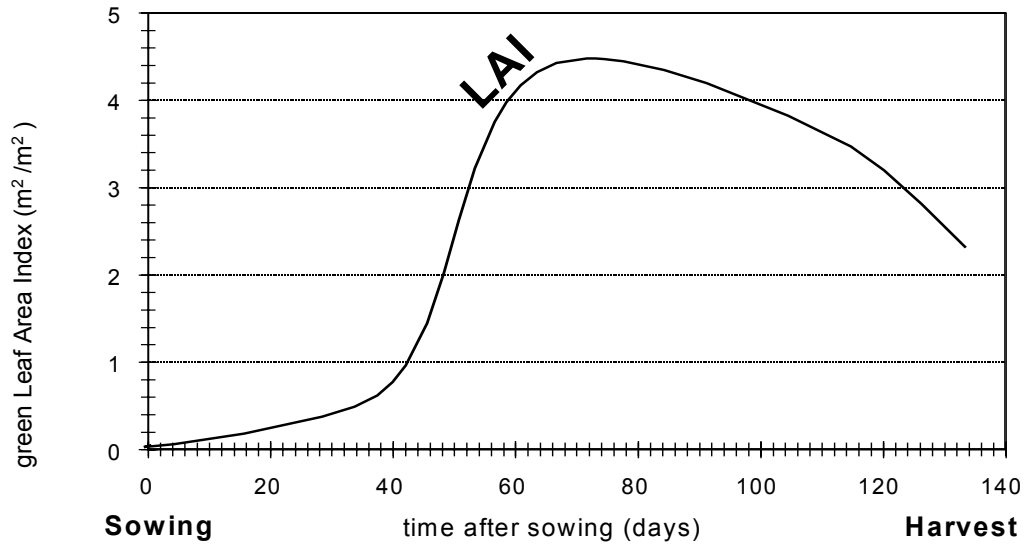

crop evapotranspiration. Some studies indicate that stomatal resistance is influenced to some extent by radiation intensity, temperature, and vapour pressure deficit. The derivation of the surface resistance for the grass reference surface is presented in Box 5.

BOX 5
The (bulk) surface resistance for a grass reference crop

A general equation for LAI_{active} is:

$$\mathbf{LAI_{active} = 0.5\ LAI}$$

which takes into consideration the fact that generally only the upper half of dense clipped grass is actively contributing to the surface heat and vapour transfer. For clipped grass a general equation for LAI is:

$$\mathbf{LAI = 24\ h}$$

where h is the crop height [m].

The stomatal resistance, r_l, of a single leaf has a value of about 100 s m^{-1} under well-watered conditions. By assuming a crop height of 0.12 m, the surface resistance, r_s [s m^{-1}], for the grass reference surface becomes (Eq. 5):

$$r_s = \frac{100}{0.5(24)(0.12)} \approx 70 \text{ s m}^{-1}$$

REFERENCE SURFACE

To obviate the need to define unique evaporation parameters for each crop and stage of growth, the concept of a reference surface was introduced. Evapotranspiration rates of the various crops are related to the evapotranspiration rate from the reference surface (ET_o) by means of crop coefficients.

In the past, an open water surface has been proposed as a reference surface. However, the differences in aerodynamic, vegetation control and radiation characteristics present a strong challenge in relating ET to measurements of free water evaporation. Relating ET_o to a specific crop has the advantage of incorporating the biological and physical processes involved in ET from cropped surfaces.

Grass, together with alfalfa, is a well-studied crop regarding its aerodynamic and surface characteristics and is accepted worldwide as a reference surface. Because the resistance to diffusion of vapour strongly depends on crop height, ground cover, LAI and soil moisture conditions, the characteristics of the reference crop should be well defined and fixed. Changes in crop height result in variations in the roughness and LAI. Consequently, the associated canopy and aerodynamic resistances will vary appreciably with time. Moreover, water stress and the degree of ground cover have an effect on the resistances and also on the albedo.

To avoid problems of local calibration which would require demanding and expensive studies, a hypothetical grass reference has been selected. Difficulties with a living grass reference result from the fact that the grass variety and morphology can significantly affect the evapotranspiration rate, especially during peak water use. Large differences may exist between warm-season and cool-season grass types. Cool-season grasses have a lower degree of stomatal control and hence higher rates of evapotranspiration. It may be difficult to grow cool-season grasses in some arid, tropical climates.

The FAO Expert Consultation on Revision of FAO Methodologies for Crop Water Requirements accepted the following unambiguous definition for the reference surface:

> **"A hypothetical reference crop with an assumed crop height of 0.12 m, a fixed surface resistance of 70 s m^{-1} and an albedo of 0.23."**

The reference surface closely resembles an extensive surface of green grass of uniform height, actively growing, completely shading the ground and with adequate water. The requirements that the grass surface should be extensive and uniform result from the assumption that all fluxes are one-dimensional upwards.

The FAO Penman-Monteith method is selected as the method by which the evapotranspiration of this reference surface (ET_o) can be unambiguously determined, and as the method which provides consistent ET_o values in all regions and climates.

FAO PENMAN-MONTEITH EQUATION

Equation

A consultation of experts and researchers was organized by FAO in May 1990, in collaboration with the International Commission for Irrigation and Drainage and with the World Meteorological Organization, to review the FAO methodologies on crop water requirements and to advise on the revision and update of procedures.

FIGURE 9
Characteristics of the hypothetical reference crop

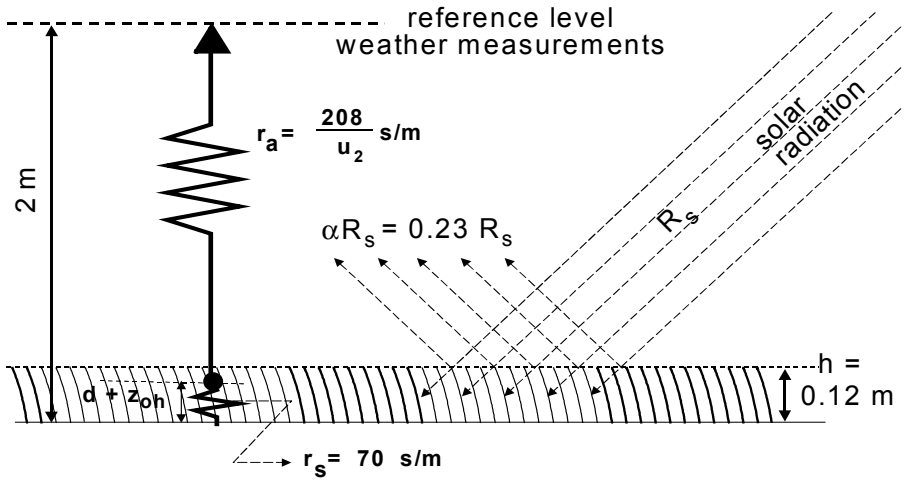

The panel of experts recommended the adoption of the Penman-Monteith combination method as a new standard for reference evapotranspiration and advised on procedures for calculation of the various parameters. By defining the reference crop as a hypothetical crop with an assumed height of 0.12 m having a surface resistance of 70 s m^{-1} and an albedo of 0.23, closely resembling the evaporation of an extension surface of green grass of uniform height, actively growing and adequately watered, the FAO Penman-Monteith method was developed. The method overcomes shortcomings of the previous FAO Penman method and provides values more consistent with actual crop water use data worldwide.

From the original Penman-Monteith equation (Equation 3) and the equations of the aerodynamic (Equation 4) and surface resistance (Equation 5), the FAO Penman-Monteith method to estimate ET_o can be derived (Box 6):

$$ET_o = \frac{0.408\Delta(R_n - G) + \gamma \frac{900}{T+273} u_2 (e_s - e_a)}{\Delta + \gamma(1 + 0.34 u_2)} \qquad (6)$$

where
- ET_o reference evapotranspiration [mm day^{-1}],
- R_n net radiation at the crop surface [MJ m^{-2} day^{-1}],
- G soil heat flux density [MJ m^{-2} day^{-1}],
- T mean daily air temperature at 2 m height [°C],
- u_2 wind speed at 2 m height [m s^{-1}],
- e_s saturation vapour pressure [kPa],
- e_a actual vapour pressure [kPa],
- e_s-e_a saturation vapour pressure deficit [kPa],
- Δ slope vapour pressure curve [kPa $°C^{-1}$],
- γ psychrometric constant [kPa $°C^{-1}$].

The reference evapotranspiration, ET_o, provides a standard to which:

- evapotranspiration at different periods of the year or in other regions can be compared;
- evapotranspiration of other crops can be related.

The equation uses standard climatological records of solar radiation (sunshine), air temperature, humidity and wind speed. To ensure the integrity of computations, the weather measurements should be made at 2 m (or converted to that height) above an extensive surface of green grass, shading the ground and not short of water.

No weather-based evapotranspiration equation can be expected to predict evapotranspiration perfectly under every climatic situation due to simplification in formulation and errors in data measurement. It is probable that precision instruments under excellent environmental and biological management conditions will show the FAO Penman-Monteith equation to deviate at times from true measurements of grass ET_o. However, the Expert Consultation agreed to use the hypothetical reference definition of the FAO Penman-Monteith equation as the definition for grass ET_o when deriving and expressing crop coefficients.

It is important, when comparing the FAO Penman-Monteith equation to ET_o measurements, that the full Penman-Monteith equation (Equation 3) and associated equations for r_a and r_s (Equations 4 and 5) be used to enable accounting for variation in ET due to variation in height of the grass measured. Variations in measurement height can significantly change LAI, d and z_{om} and the corresponding ET_o measurement and predicted value. When evaluating results, it should be noted that local environmental and management factors, such as watering frequency, also affect ET_o observations.

The FAO Penman-Monteith equation is a close, simple representation of the physical and physiological factors governing the evapotranspiration process. By using the FAO Penman-Monteith definition for ET_o, one may calculate crop coefficients at research sites by relating the measured crop evapotranspiration (ET_c) with the calculated ET_o, i.e., $K_c = ET_c/ET_o$. In the crop coefficient approach, differences in the crop canopy and aerodynamic resistance relative to the hypothetical reference crop are accounted for within the crop coefficient. The K_c factor serves as an aggregation of the physical and physiological differences between crops and the reference definition.

Data

Apart from the site location, the FAO Penman-Monteith equation requires air temperature, humidity, radiation and wind speed data for daily, weekly, ten-day or monthly calculations. The computation of all data required for the calculation of the reference evapotranspiration is given in Chapter 3. It is important to verify the units in which the weather data are reported. Factors to convert common units to the standard unit are presented in Annex I.

Location

Altitude above sea level (m) and latitude (degrees north or south) of the location should be specified. These data are needed to adjust some weather parameters for the local average value of atmospheric pressure (a function of the site elevation above mean sea level) and to compute extraterrestrial radiation (R_a) and, in some cases, daylight hours (N). In the calculation procedures for R_a and N, the latitude is expressed in radian (i.e., decimal degrees times $\pi/180$).

BOX 6
Derivation of the FAO Penman-Monteith equation for the hypothetical grass reference crop

With standardized height for wind speed, temperature and humidity measurements at 2 m ($z_m = z_h = 2$ m) and the crop height $h = 0.12$ m, the aerodynamic and surface resistances become (Boxes 4 & 5):
$r_a = 208/u_2$ s m^{-1}, (with u_2 wind speed at 2 m height)
$r_s = 70$ s m^{-1}
$(1 + r_s/r_a) = (1 + 0.34\ u_2)$

R_n and G is energy available per unit area and expressed in MJ m^{-2} day^{-1}. To convert the energy units for radiation to equivalent water depths (mm) the latent heat of vaporization, λ is used as a conversion factor (Chapter 1). The conversion from energy values to equivalent depths of water or vice versa is given by (Eq. 20):

$$\text{Radiation [mm day}^{-1}] \approx \frac{\text{Radiation [MJ m}^{-2}\text{ day}^{-1}]}{2.45} = 0.408\ \text{Radiation [MJ m}^{-2}\text{ day}^{-1}]$$

By substituting c_p with a rearrangement of Eq. 8:

$$c_p = \frac{\gamma\ \varepsilon\ \lambda}{P}$$

and considering the ideal gas law for ρ_a :

$$\rho a = \frac{P}{T_{Kv}\ R}$$

where T_{Kv}, the virtual temperature, may be substituted by:

$$T_{Kv} = 1.01(T+273)$$

results in:

$$\frac{c_p\ \rho_a}{r_a} = \frac{\gamma\ \varepsilon\ \lambda}{1.01(T+273)R(208)}\ u_2 \qquad [\text{MJ m}^{-2}\ {}^{o}\text{C}^{-1}\ \text{s}^{-1}]$$

where c_p specific heat at constant pressure [MJ kg^{-1} °C^{-1}],
ρ_a mean air density at constant pressure [kg m^{-3}],
r_a aerodynamic resistance [s m^{-1}],
γ psychrometric constant [kPa °C^{-1}],
ε ratio molecular weight of water vapour/dry air = 0.622,
λ latent heat of vaporization [MJ kg^{-1}],
u_2 wind speed at 2 m [m s^{-1}],
R specific gas constant = 0.287 kJ kg^{-1} K^{-1},
T air temperature [°C],
P atmospheric pressure [kPa],

$$= 86400\ \frac{\gamma\ (0.622)\ \lambda}{1.01(T+273)(0.287)(208)}\ u_2 \qquad [\text{MJ m}^{-2}\ {}^{o}\text{C}^{-1}\ \text{day}^{-1}]$$

or, when divided by λ ($\lambda = 2.45$),

$$\approx \gamma\ \frac{900}{T+273}\ u_2 \qquad [\text{mm}\ {}^{o}\text{C}^{-1}\ \text{day}^{-1}]$$

A positive value is used for the northern hemisphere and a negative value for the southern hemisphere.

Temperature

The (average) daily maximum and minimum air temperatures in degrees Celsius (°C) are required. Where only (average) mean daily temperatures are available, the calculations can still be executed but some underestimation of ET_o will probably occur due to the non-linearity of the saturation vapour pressure - temperature relationship (Figure 11). Using mean air temperature instead of maximum and minimum air temperatures yields a lower saturation vapour pressure e_s, and hence a lower vapour pressure difference (e_s - e_a), and a lower reference evapotranspiration estimate.

Humidity

The (average) daily actual vapour pressure, e_a, in kilopascals (kPa) is required. The actual vapour pressure, where not available, can be derived from maximum and minimum relative humidity (%), psychrometric data (dry and wet bulb temperatures in °C) or dewpoint temperature (°C) according to the procedures outlined in Chapter 3.

Radiation

The (average) daily net radiation expressed in megajoules per square metre per day (MJ m^{-2} day^{-1}) is required. These data are not commonly available but can be derived from the (average) shortwave radiation measured with a pyranometer or from the (average) daily actual duration of bright sunshine (hours per day) measured with a (Campbell-Stokes) sunshine recorder. The calculation procedures are outlined in Chapter 3.

Wind speed

The (average) daily wind speed in metres per second (m s^{-1}) measured at 2 m above the ground level is required. It is important to verify the height at which wind speed is measured, as wind speeds measured at different heights above the soil surface differ. The calculation procedure to adjust wind speed to the standard height of 2 m is presented in Chapter 3.

Missing climatic data

Situations might occur where data for some weather variables are missing. The use of an alternative ET_o calculation procedure, requiring only limited meteorological parameters, should generally be avoided. It is recommended that one calculate ET_o using the standard FAO Penman-Monteith method after resolving the specific problem of the missing data. Procedures for estimating missing climatic data are outlined in Chapter 3. Differences between ET_o values obtained with the FAO Penman-Monteith equation with, on the one hand, a limited data set and, on the other hand, a full data set, are expected to be smaller than or of similar magnitude to the differences resulting from the use of an alternative ET_o equation.

Even where the data set contains only maximum and minimum air temperature it is still possible to obtain reasonable estimates of ten-day or monthly ET_o with the FAO Penman-Monteith equation. As outlined in Chapter 3, radiation data can be derived from the air temperature difference, or, along with wind speed and humidity data, can be imported from a

nearby weather station. Humidity data can also be estimated from daily minimum air temperature. After evaluating the validity of the use of data from another station, ten-day or monthly estimates of ET_o can be calculated.

The procedures for estimating missing data should be validated at the regional level. This can be done for weather stations with full data sets by comparing ET_o calculated with full and with limited data sets. The ratio should be close to one. Where the ratio deviates significantly from one, the ratio can be used as a correction factor for estimates made with the limited data set. Where the standard error of estimate exceeds 20% of the mean ET_o, a sensitivity analysis should be performed to determine causes (and limits) for the method utilized to import the missing data. A validation should be completed for each month and variable, for the monthly as well as for the daily estimates.

Chapter 3

Meteorological data

The methods for calculating evapotranspiration from meteorological data require various climatological and physical parameters. Some of the data are measured directly in weather stations. Other parameters are related to commonly measured data and can be derived with the help of a direct or empirical relationship. This chapter discusses the source, measurement and computation of all data required for the calculation of the reference evapotranspiration by means of the FAO Penman-Monteith method. Different examples illustrate the various calculation procedures. Appropriate procedures for estimating missing data are also provided.

Meteorological data can be expressed in several units. Conversion factors between various units and standard S.I. units are given in Annex 1. Climatic parameters, calculated by means of the equations presented in this chapter are tabulated and displayed for different meteorological conditions in Annex 2. Only the standardized relationships are presented in this chapter. The background of certain relationships and more information about certain procedures are given in Annex 3. Annexes 4, 5 and 6 list procedures for the statistical analysis, assessment, correction and completion of partial or missing weather data.

METEOROLOGICAL FACTORS DETERMINING ET

The meteorological factors determining evapotranspiration are weather parameters which provide energy for vaporization and remove water vapour from the evaporating surface. The principal weather parameters to consider are presented below.

Solar radiation

The evapotranspiration process is determined by the amount of energy available to vaporize water. Solar radiation is the largest energy source and is able to change large quantities of liquid water into water vapour. The potential amount of radiation that can reach the evaporating surface is determined by its location and time of the year. Due to differences in the position of the sun, the potential radiation differs at various latitudes and in different seasons. The actual solar radiation reaching the evaporating surface depends on the turbidity of the atmosphere and the presence of clouds which reflect and absorb major parts of the radiation. When assessing the effect of solar radiation on evapotranspiration, one should also bear in mind that not all available energy is used to vaporize water. Part of the solar energy is used to heat up the atmosphere and the soil profile.

Air temperature

The solar radiation absorbed by the atmosphere and the heat emitted by the earth increase the air temperature. The sensible heat of the surrounding air transfers energy to the crop and exerts as such a controlling influence on the rate of evapotranspiration. In sunny, warm weather the loss of water by evapotranspiration is greater than in cloudy and cool weather.

FIGURE 10
Illustration of the effect of wind speed on evapotranspiration in hot-dry and humid-warm weather conditions

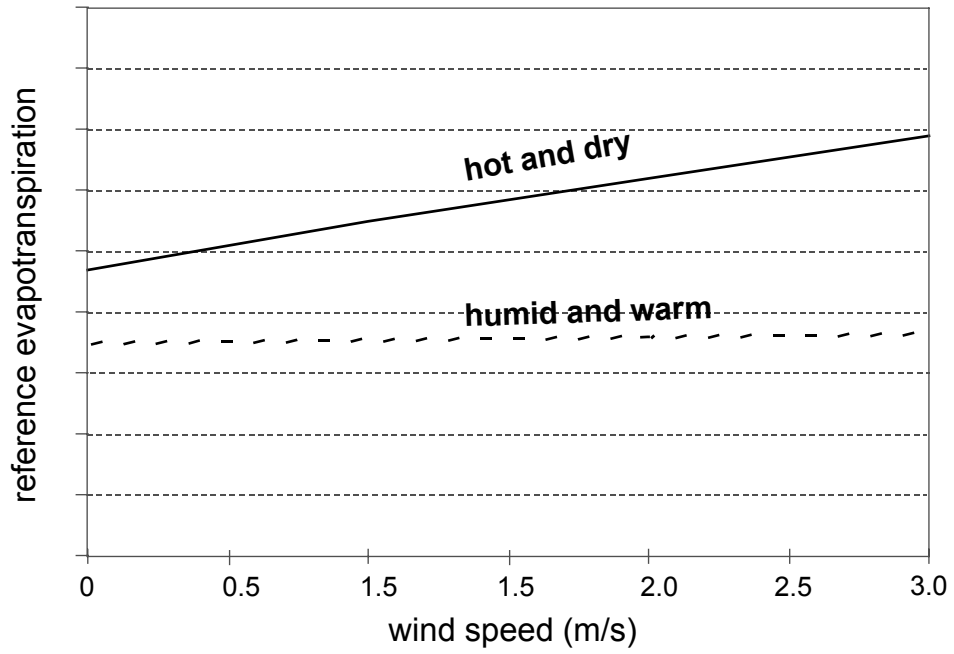

Air humidity

While the energy supply from the sun and surrounding air is the main driving force for the vaporization of water, the difference between the water vapour pressure at the evapotranspiring surface and the surrounding air is the determining factor for the vapour removal. Well-watered fields in hot dry arid regions consume large amounts of water due to the abundance of energy and the desiccating power of the atmosphere. In humid tropical regions, notwithstanding the high energy input, the high humidity of the air will reduce the evapotranspiration demand. In such an environment, the air is already close to saturation, so that less additional water can be stored and hence the evapotranspiration rate is lower than in arid regions.

Wind speed

The process of vapour removal depends to a large extent on wind and air turbulence which transfers large quantities of air over the evaporating surface. When vaporizing water, the air above the evaporating surface becomes gradually saturated with water vapour. If this air is not continuously replaced with drier air, the driving force for water vapour removal and the evapotranspiration rate decreases.

The combined effect of climatic factors affecting evapotranspiration is illustrated in Figure 10 for two different climatic conditions. The evapotranspiration demand is high in hot dry weather due to the dryness of the air and the amount of energy available as direct solar radiation and latent heat. Under these circumstances, much water vapour can be stored in the air

while wind may promote the transport of water allowing more water vapour to be taken up. On the other hand, under humid weather conditions, the high humidity of the air and the presence of clouds cause the evapotranspiration rate to be lower. The effect on evapotranspiration of increasing wind speeds for the two different climatic conditions is illustrated by the slope of the curves in Figure 10. The drier the atmosphere, the larger the effect on ET and the greater the slope of the curve. For humid conditions, the wind can only replace saturated air with slightly less saturated air and remove heat energy. Consequently, the wind speed affects the evapotranspiration rate to a far lesser extent than under arid conditions where small variations in wind speed may result in larger variations in the evapotranspiration rate.

ATMOSPHERIC PARAMETERS

Several relationships are available to express climatic parameters. The effect of the principal weather parameters on evapotranspiration can be assessed with the help of these equations. Some of the relationships require parameters which express a specific characteristic of the atmosphere. Before studying the four principal weather parameters, some atmospheric parameters will be discussed.

Atmospheric pressure (P)

The atmospheric pressure, P, is the pressure exerted by the weight of the earth's atmosphere. Evaporation at high altitudes is promoted due to low atmospheric pressure as expressed in the psychrometric constant. The effect is, however, small and in the calculation procedures, the average value for a location is sufficient. A simplification of the ideal gas law, assuming 20°C for a standard atmosphere, can be employed to calculate P:

$$P = 101.3\left(\frac{293 - 0.0065\,z}{293}\right)^{5.26} \qquad (7)$$

where P atmospheric pressure [kPa],
z elevation above sea level [m],

Values for atmospheric pressure as a function of altitude are given in Annex 2 (Table 2.1).

Latent heat of vaporization (λ)

The latent heat of vaporization, λ, expresses the energy required to change a unit mass of water from liquid to water vapour in a constant pressure and constant temperature process. The value of the latent heat varies as a function of temperature. At a high temperature, less energy will be required than at lower temperatures. As λ varies only slightly over normal temperature ranges a single value of 2.45 MJ kg^{-1} is taken in the simplification of the FAO Penman-Monteith equation. This is the latent heat for an air temperature of about 20°C.

Psychrometric constant (γ)

The psychrometric constant, γ, is given by:

$$\gamma = \frac{c_p \ P}{\varepsilon \ \lambda} = 0.665 \times 10^{-3} \ P \qquad (8)$$

where
- γ psychrometric constant [kPa °C^{-1}],
- P atmospheric pressure [kPa],
- λ latent heat of vaporization, 2.45 [MJ kg^{-1}],
- c_p specific heat at constant pressure, 1.013 10^{-3} [MJ kg^{-1} °C^{-1}],
- ε ratio molecular weight of water vapour/dry air = 0.622.

The specific heat at constant pressure is the amount of energy required to increase the temperature of a unit mass of air by one degree at constant pressure. Its value depends on the composition of the air, i.e., on its humidity. For average atmospheric conditions a value c_p = 1.013 10^{-3} MJ kg^{-1} °C^{-1} can be used. As an average atmospheric pressure is used for each location (Equation 7), the psychrometric constant is kept constant for each location. Values for the psychrometric constant as a function of altitude are given in Annex 2 (Table 2.2).

EXAMPLE 2
Determination of atmospheric parameters.

Determine the atmospheric pressure and the psychrometric constant at an elevation of 1 800 m.

With:	z =	1 800	m
From Eq. 7:	P = 101.3 [(293 - (0.0065) 1800)/293]$^{5.26}$ =	81.8	kPa
From Eq. 8:	γ = 0.665 10^{-3} (81.8) =	0.054	kPa °C^{-1}
The average value of the atmospheric pressure is 81.8 kPa. The psychrometric constant, γ, is 0.054 kPa/°C.			

AIR TEMPERATURE

Agrometeorology is concerned with the air temperature near the level of the crop canopy. In traditional and modern automatic weather stations the air temperature is measured inside shelters (Stevenson screens or ventilated radiation shields) placed in line with World Meteorological Organization (WMO) standards at 2 m above the ground. The shelters are designed to protect the instruments from direct exposure to solar heating. The louvered construction allows free air movement around the instruments. Air temperature is measured with thermometers, thermistors or thermocouples mounted in the shelter. Minimum and maximum thermometers record the minimum and maximum air temperature over a 24-hour period. Thermographs plot the instantaneous temperature over a day or week. Electronic weather stations often sample air temperature each minute and report hourly averages in addition to 24-hour maximum and minimum values.

Due to the non-linearity of humidity data required in the FAO Penman-Monteith equation, the vapour pressure for a certain period should be computed as the mean between the vapour pressure at the daily maximum and minimum air temperatures of that period. The daily maximum air temperature (T_{max}) and daily minimum air temperature (T_{min}) are, respectively, the maximum and minimum air temperature observed during the 24-hour period, beginning at midnight. T_{max} and T_{min} for longer periods such as weeks, 10-day's or months are obtained by dividing the sum of the respective daily values by the number of days in the period. The mean

daily air temperature (T_{mean}) is only employed in the FAO Penman-Monteith equation to calculate the slope of the saturation vapour pressure curves (Δ) and the impact of mean air density (P_a) as the effect of temperature variations on the value of the climatic parameter is small in these cases. For standardization, T_{mean} for 24-hour periods is defined as the mean of the daily maximum (T_{max}) and minimum temperatures (T_{min}) rather than as the average of hourly temperature measurements.

$$T_{mean} = \frac{T_{max} + T_{min}}{2} \qquad (9)$$

The temperature is given in degrees Celsius (°C) or Fahrenheit (°F). The conversion table is given in Annex 1. In some calculation procedures, temperature is required in Kelvin (K), which can be obtained by adding 273.16 to the temperature expressed in degrees Celsius (in practice K = °C + 273.16). The Kelvin and Celsius scale have the same scale interval.

AIR HUMIDITY

Concepts

The water content of the air can be expressed in several ways. In agrometeorology, vapour pressure, dewpoint temperature and relative humidity are common expressions to indicate air humidity.

Vapour pressure

Water vapour is a gas and its pressure contributes to the total atmospheric pressure. The amount of water in the air is related directly to the partial pressure exerted by the water vapour in the air and is therefore a direct measure of the air water content.

In standard S.I. units, pressure is no longer expressed in centimetre of water, millimetre of mercury, bars, atmosphere, etc., but in pascals (Pa). Conversion factors between various units and Pa are given in Annex 1. As a pascal refers to a relatively small force (1 newton) applied on a relatively large surface (1 m^2), multiples of the basic unit are often used. In this handbook, vapour pressure is expressed in kilopascals (kPa = 1 000 Pa).

When air is enclosed above an evaporating water surface, an equilibrium is reached between the water molecules escaping and returning to the water reservoir. At that moment, the air is said to be saturated since it cannot store any extra water molecules. The corresponding pressure is called the saturation vapour pressure ($e^o(T)$). The number of water molecules that can be stored in the air depends on the temperature (T). The higher the air temperature, the higher the storage capacity, the higher its saturation vapour pressure (Figure 11).

As can be seen from Figure 11, the slope of the curve changes exponentially with temperature. At low temperatures, the slope is small and varies only slightly as the temperature rises. At high temperatures, the slope is large and small changes in T result in large changes in slope. The slope of the saturation vapour pressure curve, Δ, is an important parameter in describing vaporization and is required in the equations for calculating ET_o from climatic data.

FIGURE 11
Saturation vapour pressure shown as a function of temperature: e°(T) curve

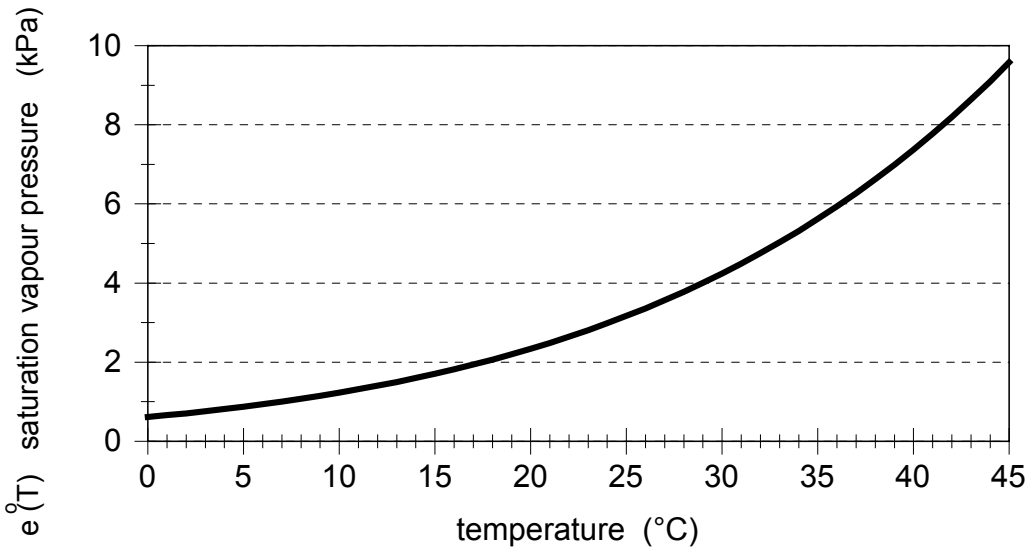

FIGURE 12
Variation of the relative humidity over 24 hours for a constant actual vapour pressure of 2.4 kPa

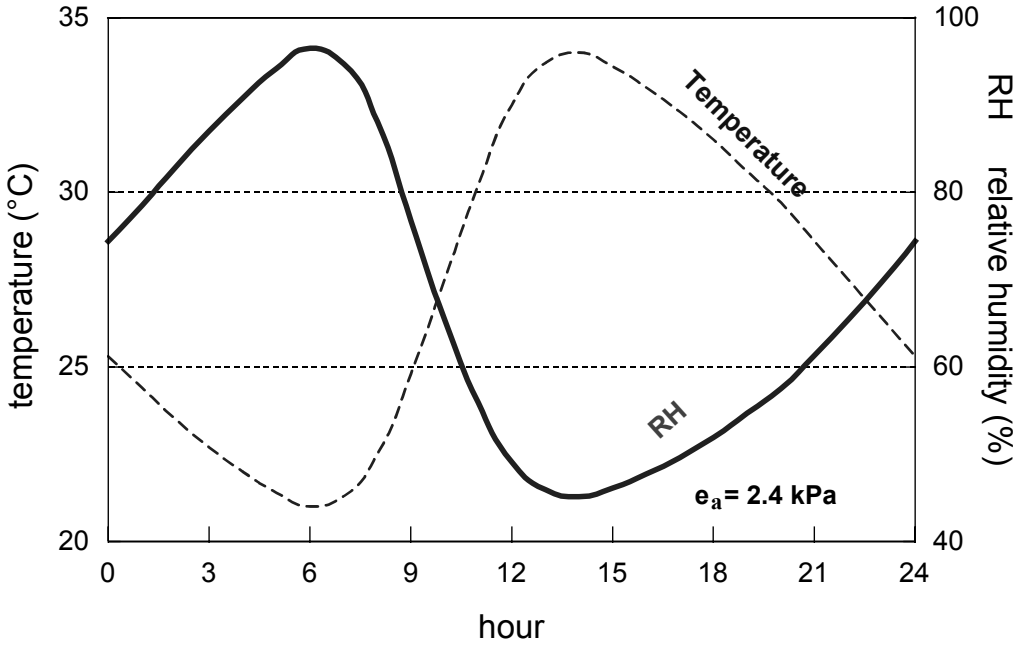

The actual vapour pressure (e_a) is the vapour pressure exerted by the water in the air. When the air is not saturated, the actual vapour pressure will be lower than the saturation vapour pressure. The difference between the saturation and actual vapour pressure is called the vapour pressure deficit or saturation deficit and is an accurate indicator of the actual evaporative capacity of the air.

Dewpoint temperature

The dewpoint temperature is the temperature to which the air needs to be cooled to make the air saturated. The actual vapour pressure of the air is the saturation vapour pressure at the dewpoint temperature. The drier the air, the larger the difference between the air temperature and dewpoint temperature.

Relative humidity

The relative humidity (RH) expresses the degree of saturation of the air as a ratio of the actual (e_a) to the saturation ($e^o(T)$) vapour pressure at the same temperature (T):

$$RH = 100 \frac{e_a}{e^o(T)} \qquad (10)$$

Relative humidity is the ratio between the amount of water the ambient air actually holds and the amount it could hold at the same temperature. It is dimensionless and is commonly given as a percentage. Although the actual vapour pressure might be relatively constant throughout the day, the relative humidity fluctuates between a maximum near sunrise and a minimum around early afternoon (Figure 12). The variation of the relative humidity is the result of the fact that the saturation vapour pressure is determined by the air temperature. As the temperature changes during the day, the relative humidity also changes substantially.

Measurement

It is not possible to directly measure the actual vapour pressure. The vapour pressure is commonly derived from relative humidity or dewpoint temperature.

Relative humidity is measured directly with hygrometers. The measurement is based on the nature of some material such as hair, which changes its length in response to changes in air humidity, or using a capacitance plate, where the electric capacitance changes with RH. Vapour pressure can be measured indirectly with psychrometers which measure the temperature difference between two thermometers, the so-called dry and wet bulb thermometers. The dry bulb thermometer measures the temperature of the air. The bulb of the wet bulb thermometer is covered with a constantly saturated wick. Evaporation of water from the wick, requiring energy, lowers the temperature of the thermometer. The drier the air, the larger the evaporative cooling and the larger the temperature drop. The difference between the dry and wet bulb temperatures is called the wet bulb depression and is a measure of the air humidity.

The dewpoint temperature is measured with dewpoint meters. The underlying principle of some types of apparatus is the cooling of the ambient air until dew formation occurs. The corresponding temperature is the dewpoint temperature.

Relative humidity and dewpoint temperature data are notoriously plagued by measurement errors. Measurement error is common for both older hygrothermograph types of instruments and for the more modern electronic instruments. These instruments are described in Annex 5. Great care should be made to assess the accuracy and integrity of RH and dewpoint data. The user is encouraged to always compare computed dewpoint temperatures to daily minimum air temperatures, as described at the end of this chapter and in Annexes 5 and 6. Frequently, it is better to utilize a dewpoint temperature that is predicted from daily minimum air temperature, rather than to use unreliable relative humidity measurements. The user is encouraged to utilize good judgement in this area.

Calculation procedures

Mean saturation vapour pressure (e_s)

As saturation vapour pressure is related to air temperature, it can be calculated from the air temperature. The relationship is expressed by:

$$e^o(T) = 0.6108 \exp\left[\frac{17.27\ T}{T + 237.3}\right] \qquad (11)$$

where $e°(T)$ saturation vapour pressure at the air temperature T [kPa],
T air temperature [°C],
$\exp[..]$ 2.7183 (base of natural logarithm) raised to the power [..].

Values of saturation vapour pressure as a function of air temperature are given in Annex 2 (Table 2.3). Due to the non-linearity of the above equation, the mean saturation vapour pressure for a day, week, decade or month should be computed as the mean between the saturation vapour pressure at the mean daily maximum and minimum air temperatures for that period:

$$e_s = \frac{e^o(T_{max}) + e^o(T_{min})}{2} \qquad (12)$$

Using mean air temperature instead of daily minimum and maximum temperatures results in lower estimates for the mean saturation vapour pressure. The corresponding vapour pressure deficit (a parameter expressing the evaporating power of the atmosphere) will also be smaller and the result will be some underestimation of the reference crop evapotranspiration. Therefore, the mean saturation vapour pressure should be calculated as the mean between the saturation vapour pressure at both the daily maximum and minimum air temperature.

EXAMPLE 3
Determination of mean saturation vapour pressure

The daily maximum and minimum air temperature are respectively 24.5 and 15°C.
Determine the saturation vapour pressure for that day.

From Eq. 11	$e°(T_{max}) = 0.6108 \exp[17.27(24.5)/(24.5+237.3)]$	3.075	kPa
From Eq. 11	$e°(T_{min}) = 0.6108 \exp[17.27(15)/(15+237.3)]$	1.705	kPa
From Eq. 12	$e_s = (3.075 + 1.705)/2$	2.39	kPa
	Note that for temperature 19.75°C (which is T_{mean}), $e°(T)$ =	2.30	kPa

The mean saturation vapour pressure is 2.39 kPa.

Slope of saturation vapour pressure curve (Δ)

For the calculation of evapotranspiration, the slope of the relationship between saturation vapour pressure and temperature, Δ, is required. The slope of the curve (Figure 11) at a given temperature is given by.

$$\Delta = \frac{4098\left[0.6108\exp\left(\frac{17.27\ T}{T+237.3}\right)\right]}{(T+237.3)^2} \qquad (13)$$

where Δ slope of saturation vapour pressure curve at air temperature T [kPa °C^{-1}],
T air temperature [°C],
exp[..] 2.7183 (base of natural logarithm) raised to the power [..].

Values of slope Δ for different air temperatures are given in Annex 2 (Table 2.4). In the FAO Penman-Monteith equation, where Δ occurs in the numerator and denominator, the slope of the vapour pressure curve is calculated using mean air temperature (Equation 9).

Actual vapour pressure (e_a) derived from dewpoint temperature

As the dewpoint temperature is the temperature to which the air needs to be cooled to make the air saturated, the actual vapour pressure (e_a) is the saturation vapour pressure at the dewpoint temperature (T_{dew}) [ºC], or:

$$e_a = e^o(T_{dew}) = 0.6108\ \exp\left[\frac{17.27\ T_{dew}}{T_{dew}+237.3}\right] \qquad (14)$$

Actual vapour pressure (e_a) derived from psychrometric data

The actual vapour pressure can be determined from the difference between the dry and wet bulb temperatures, the so-called wet bulb depression. The relationship is expressed by the following equation:

$$e_a = e^o(T_{wet}) - \gamma_{psy}(T_{dry} - T_{wet}) \qquad (15)$$

where e_a actual vapour pressure [kPa],
$e°(T_{wet})$ saturation vapour pressure at wet bulb temperature [kPa],
γ_{psy} psychrometric constant of the instrument [kPa °C^{-1}],
T_{dry}-T_{wet} wet bulb depression, with T_{dry} the dry bulb and T_{wet} the wet bulb temperature [°C].

The psychrometric constant of the instrument is given by:

$$\gamma_{psy} = a_{psy}\ P \qquad (16)$$

where a_{psy} is a coefficient depending on the type of ventilation of the wet bulb [°C^{-1}], and P is the atmospheric pressure [kPa]. The coefficient a_{psy} depends mainly on the design of the psychrometer and rate of ventilation around the wet bulb. The following values are used:

a_{psy} = 0.000662 for ventilated (Asmann type) psychrometers, with an air movement of some 5 m/s,
0.000800 for natural ventilated psychrometers (about 1 m/s),
0.001200 for non-ventilated psychrometers installed indoors.

EXAMPLE 4
Determination of actual vapour pressure from psychrometric readings

Determine the vapour pressure from the readings of an aspirated psychrometer in a location at an elevation of 1 200 m. The temperatures measured by the dry and wet bulb thermometers are 25.6 and 19.5°C respectively.

From Eq. 7 (Table 2.1), at:	z=	1 200	m
Then:	P =	87.9	kPa
From Eq. 11 (Table 2.3), for	T_{wet} =	19.5	°C
Then:	$e°(T_{wet})$ =	2.267	kPa
Ventilated psychrometer	a_{psy} =	0.000662	°C^{-1}
From Eq. 15:	e_a = 2.267 - 0.000662 (87.9) (25.6 - 19.5)=	1.91	kPa
The actual vapour pressure is 1.91 kPa.			

Actual vapour pressure (e_a) derived from relative humidity data

The actual vapour pressure can also be calculated from the relative humidity. Depending on the availability of the humidity data, different equations should be used.

• For RH_{max} and RH_{min}:

$$e_a = \frac{e^o(T_{min})\frac{RH_{max}}{100} + e^o(T_{max})\frac{RH_{min}}{100}}{2} \qquad (17)$$

where e_a actual vapour pressure [kPa],
$e°(T_{min})$ saturation vapour pressure at daily minimum temperature [kPa],
$e°(T_{max})$ saturation vapour pressure at daily maximum temperature [kPa],
RH_{max} maximum relative humidity [%],
RH_{min} minimum relative humidity [%].

For periods of a week, ten days or a month, RH_{max} and RH_{min} are obtained by dividing the sum of the daily values by the number of days in that period.

• For RH_{max}:

When using equipment where errors in estimating RH_{min} can be large, or when RH data integrity are in doubt, then one should use only RH_{max}:

$$e_a = e^o(T_{min})\frac{RH_{max}}{100} \qquad (18)$$

• For RH_{mean}:

In the absence of RH_{max} and RH_{min}, another equation can be used to estimate e_a:

$$e_a = \frac{RH_{mean}}{100}\left[\frac{e^o(T_{max}) + e^o(T_{min})}{2}\right] \qquad (19)$$

where RH_{mean} is the mean relative humidity, defined as the average between RH_{max} and RH_{min}. However, Equation 19 is less desirable than are Equations 17 or 18.

EXAMPLE 5
Determination of actual vapour pressure from relative humidity

Given the following daily minimum and maximum air temperature and the corresponding relative humidity data:
T_{min} = 18°C and RH_{max} = 82%
T_{max} = 25°C and RH_{min} = 54%
Determine the actual vapour pressure.

From Eq. 11 (Table 2.3), at:	T_{min} =	18	°C
Then:	$e°(T_{min})$ =	2.064	kPa
From Eq. 11 (Table 2.3), at:	T_{max} =	25	°C
Then:	$e°(T_{max})$ =	3.168	kPa
From Eq. 17:	e_a = [2.064 (82/100) + 3.168 (54/100)] =	1.70	kPa
Note that when using Eq. 19:	e_a =	1.78	kPa

Vapour pressure deficit (e_s - e_a)

The vapour pressure deficit is the difference between the saturation (e_s) and actual vapour pressure (e_a) for a given time period. For time periods such as a week, ten days or a month e_s is computed from Equation 12 using the T_{max} and T_{min} averaged over the time period and similarly the e_a is computed with one of the equations 4 to 19, using avrage measurements over the period. As stated above, using mean air temperature and not T_{max} and T_{min} in Equation 12 results in a lower estimate of e_s, thus in a lower vapour pressure deficit and hence an underestimation of the ET_o (see Box 7). When desired, e_s and e_a for long time periods cal also be calculated as averages of values computed for each day of the period.

EXAMPLE 6
Determination of vapour pressure deficit

Determine the vapour pressure deficit with the data of the previous example (Example 5).

From Example 5:	$e°(T_{min})$ =	2.064	kPa
	$e°(T_{max})$ =	3.168	kPa
	e_a =	1.70	kPa
	e_s - e_a = (2.064 + 3.168)/2 - 1.70 =	0.91	kPa

The vapour pressure deficit is 0.91 kPa.

BOX 7
Calculation sheet for vapour pressure deficit (e_s - e_a)

Saturation vapour pressure: e_s (Eq. 11 or Table 2.3)

T_{max}		°C	$e^o(T_{max}) = 0.6108 \exp\left[\frac{17.27\ T_{max}}{T_{max} + 237.3}\right]$		kPa
T_{min}		°C	$e^o(T_{min}) = 0.6108 \exp\left[\frac{17.27\ T_{min}}{T_{min} + 237.3}\right]$		kPa
saturation vapour pressure $e_s = [e°(T_{max})+e°(T_{min})]/2$ Eq.12					kPa

Actual vapour pressure: e_a

1. e_a derived from dewpoint temperature (Eq. 14 or Table 2.3)

T_{dew}		°C	$e_a = 0.6108 \exp\left[\frac{17.27\ T_{dew}}{T_{dew} + 237.3}\right]$		kPa

OR 2. e_a derived from maximum and minimum relative humidity

RH_{max}		%	$e^o(T_{min})\frac{RH_{max}}{100}$		kPa
RH_{min}		%	$e^o(T_{max})\frac{RH_{min}}{100}$		kPa
$e_a = [e°(T_{min})\ RH_{max}/100 + e°(T_{max})\ RH_{min}/100] / 2$ Eq. 17					kPa

OR 3. e_a derived from maximum relative humidity (errors in RH_{min})

RH_{max}		%	$e_a = e°(T_{min})\ RH_{max}/100$ Eq. 18		kPa

OR 4. e_a derived from mean relative humidity (less recommended)

RH_{mean}		%	$e_a = e_s\ (RH_{mean})/100$ Eq. 19		kPa

Vapour pressure deficit: (e_s - e_a) kPa

RADIATION

Concepts

Extraterrestrial radiation (R_a)

The radiation striking a surface perpendicular to the sun's rays at the top of the earth's atmosphere, called the solar constant, is about 0.082 MJ m^{-2} min^{-1}. The local intensity of radiation is, however, determined by the angle between the direction of the sun's rays and the normal to the surface of the atmosphere. This angle will change during the day and will be different at different latitudes and in different seasons. The solar radiation received at the top of the earth's atmosphere on a horizontal surface is called the extraterrestrial (solar) radiation, R_a.

If the sun is directly overhead, the angle of incidence is zero and the extraterrestrial radiation is 0.0820 MJ m^{-2} min^{-1}. As seasons change, the position of the sun, the length of the day and, hence, R_a change as well. Extraterrestrial radiation is thus a function of latitude, date and time of day. Daily values of R_a throughout the year for different latitudes are plotted in Figure 13.

FIGURE 13
Annual variation in extraterrestrial radiation (R_a) at the equator, 20 and 40° north and south

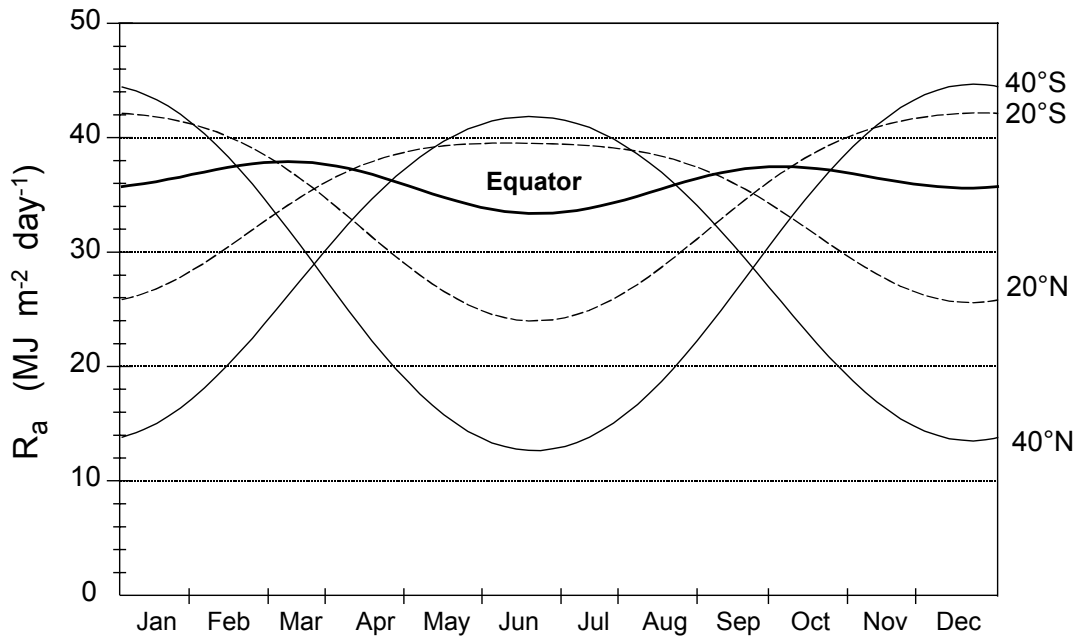

Solar or shortwave radiation (R_S)

As the radiation penetrates the atmosphere, some of the radiation is scattered, reflected or absorbed by the atmospheric gases, clouds and dust. The amount of radiation reaching a horizontal plane is known as the solar radiation, R_S. Because the sun emits energy by means of electromagnetic waves characterized by short wavelengths, solar radiation is also referred to as shortwave radiation.

FIGURE 14
Annual variation of the daylight hours (N) at the equator, 20 and 40° north and south

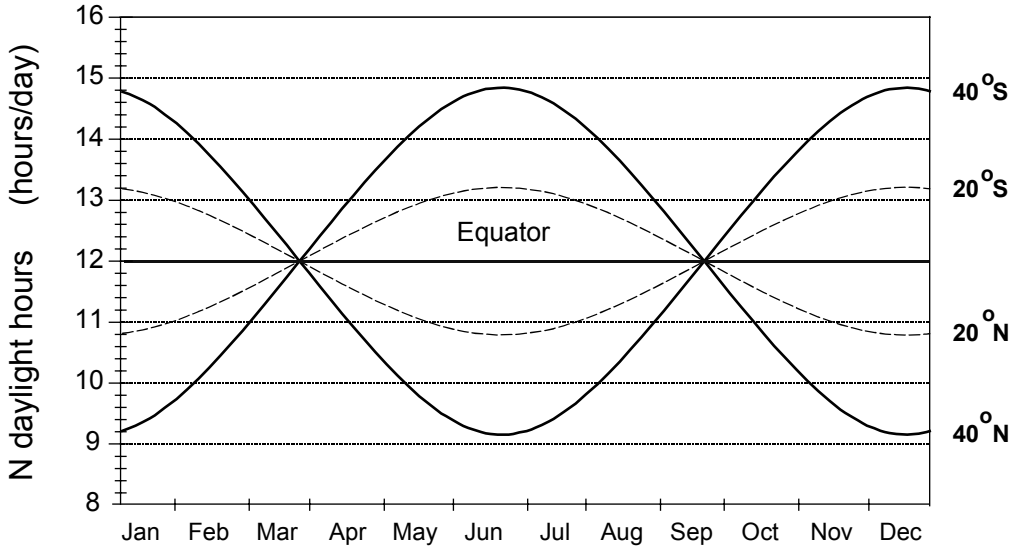

For a cloudless day, R_S is roughly 75% of extraterrestrial radiation. On a cloudy day, the radiation is scattered in the atmosphere, but even with extremely dense cloud cover, about 25% of the extraterrestrial radiation may still reach the earth's surface mainly as diffuse sky radiation. Solar radiation is also known as global radiation, meaning that it is the sum of direct shortwave radiation from the sun and diffuse sky radiation from all upward angles.

Relative shortwave radiation (R_S/R_{SO})

The relative shortwave radiation is the ratio of the solar radiation (R_S) to the clear-sky solar radiation (R_{SO}). R_S is the solar radiation that actually reaches the earth's surface in a given period, while R_{SO} is the solar radiation that would reach the same surface during the same period but under cloudless conditions.

The relative shortwave radiation is a way to express the cloudiness of the atmosphere; the cloudier the sky the smaller the ratio. The ratio varies between about 0.33 (dense cloud cover) and 1 (clear sky). In the absence of a direct measurement of R_n, the relative shortwave radiation is used in the computation of the net longwave radiation.

Relative sunshine duration (n/N)

The relative sunshine duration is another ratio that expresses the cloudiness of the atmosphere. It is the ratio of the actual duration of sunshine, n, to the maximum possible duration of sunshine or daylight hours N. In the absence of any clouds, the actual duration of sunshine is equal to the daylight hours (n = N) and the ratio is one, while on cloudy days n and consequently the ratio may be zero. In the absence of a direct measurement of R_S, the relative sunshine duration, n/N, is often used to derive solar radiation from extraterrestrial radiation.

As with extraterrestrial radiation, the daylength N depends on the position of the sun and is hence a function of latitude and date. Daily values of N throughout the year for different latitudes are plotted in Figure 14.

Albedo (α) and net solar radiation (R_{ns})

A considerable amount of solar radiation reaching the earth's surface is reflected. The fraction, α, of the solar radiation reflected by the surface is known as the albedo. The albedo is highly variable for different surfaces and for the angle of incidence or slope of the ground surface. It may be as large as 0.95 for freshly fallen snow and as small as 0.05 for a wet bare soil. A green vegetation cover has an albedo of about 0.20-0.25. For the green grass reference crop, α is assumed to have a value of 0.23.

The net solar radiation, R_{ns}, is the fraction of the solar radiation R_s that is not reflected from the surface. Its value is $(1-\alpha)R_s$.

Net longwave radiation (R_{nl})

The solar radiation absorbed by the earth is converted to heat energy. By several processes, including emission of radiation, the earth loses this energy. The earth, which is at a much lower temperature than the sun, emits radiative energy with wavelengths longer than those from the sun. Therefore, the terrestrial radiation is referred to as longwave radiation. The emitted longwave radiation ($R_{l,up}$) is absorbed by the atmosphere or is lost into space. The longwave radiation received by the atmosphere ($R_{l,down}$) increases its temperature and, as a consequence, the atmosphere radiates energy of its own, as illustrated in Figure 15. Part of the radiation finds it way back to the earth's surface. Consequently, the earth's surface both emits and receives longwave radiation. The difference between outgoing and incoming longwave radiation is called the net longwave radiation, R_{nl}. As the outgoing longwave radiation is almost always greater than the incoming longwave radiation, R_{nl} represents an energy loss.

Net radiation (R_n)

The net radiation, R_n, is the difference between incoming and outgoing radiation of both short and long wavelengths. It is the balance between the energy absorbed, reflected and emitted by the earth's surface or the difference between the incoming net shortwave (R_{ns}) and the net outgoing longwave (R_{nl}) radiation (Figure 15). R_n is normally positive during the daytime and negative during the nighttime. The total daily value for R_n is almost always positive over a period of 24 hours, except in extreme conditions at high latitudes.

Soil heat flux (G)

In making estimates of evapotranspiration, all terms of the energy balance (Equation 1) should be considered. The soil heat flux, G, is the energy that is utilized in heating the soil. G is positive when the soil is warming and negative when the soil is cooling. Although the soil heat flux is small compared to R_n and may often be ignored, the amount of energy gained or lost by the soil in this process should theoretically be subtracted or added to R_n when estimating evapotranspiration.

Units

The standard unit used in this handbook to express energy received on a unit surface per unit time is megajoules per square metre per day (MJ m^{-2} day^{-1}). In meteorological bulletins other units might be used or radiation might even be expressed in units no longer accepted as standard S.I. units, such as calories cm^{-2} day^{-1}.

FIGURE 15
Various components of radiation

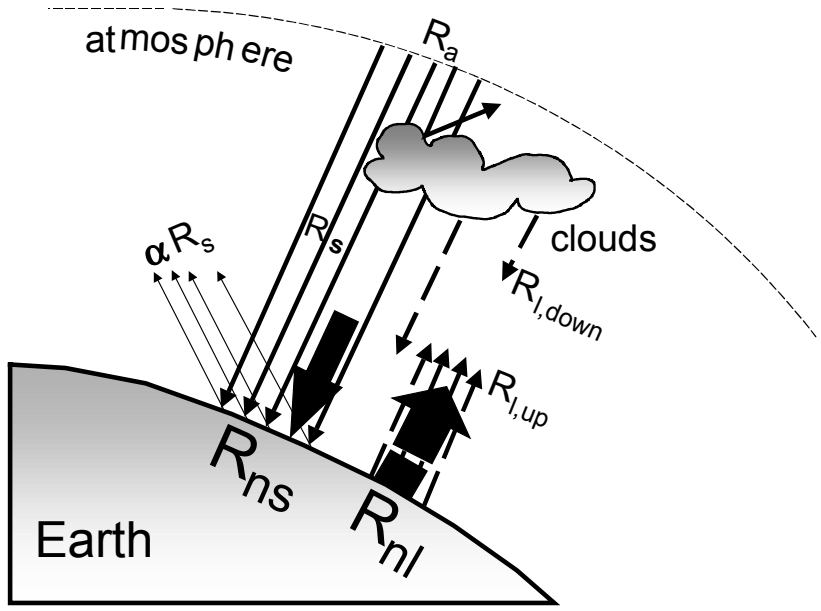

In the FAO Penman-Monteith equation (Equation 6), radiation expressed in MJ m^{-2} day^{-1} is converted (Box 8) to equivalent evaporation in mm day^{-1} by using a conversion factor equal to the inverse of the latent heat heat of vaporization ($1/\lambda = 0.408$):

$$\text{equivalent evaporation } \left[\text{mm day}^{-1}\right] = 0.408 \text{ x Radiation } \left[\text{MJ m}^{-2} \text{ day}^{-1}\right] \qquad (20)$$

BOX 8
Conversion from energy values to equivalent evaporation

The conversion from energy values to depths of water or vice versa is given by:

$$\text{Radiation } [\text{depth of water}] = \frac{\text{Radiation } [\text{energy / surface}]}{\lambda \, \rho_w}$$

where λ latent heat of vaporization [MJ kg^{-1}],
ρ_w density of water, i.e., 1 000 kg m^{-3},
[depth of water] is expressed in m,
[energy/surface] is expressed in MJ m^{-2}.

By using a single value of 2.45 MJ kg^{-1} for λ (see section on atmospheric parameters and Annex 3) and multiplying the above equation by 1 000 to obtain mm:

$$\text{Radiation } \left[\text{mm day}^{-1}\right] \approx \frac{\text{Radiation } \left[\text{MJ m}^{-2} \text{ day}^{-1}\right]}{2.45} = 0.408 \text{ x Radiation } \left[\text{MJ m}^{-2} \text{ day}^{-1}\right]$$

Common units used to express energy received on a unit surface per unit time, and conversion factors are summarized in Table 3.

TABLE 3
Conversion factors for radiation

	multiplier to obtain energy received on a unit surface per unit time				equivalent evaporation
	MJ m^{-2} day^{-1}	**J cm^{-2} day^{-1}**	**cal cm^{-2} day^{-1}**	**W m^{-2}**	**mm day^{-1}**
1 MJ m^{-2} day^{-1}	1	100	23.9	11.6	0.408
1 cal cm^{-2} day^{-1}	4.1868 10^{-2}	4.1868	1	0.485	0.0171
1 W m^{-2}	0.0864	8.64	2.06	1	0.035
1 mm day^{-1}	2.45	245	58.5	28.4	1

Measurement

Solar radiation can be measured with pyranometers, radiometers or solarimeters. The instruments contain a sensor installed on a horizontal surface that measures the intensity of the total solar radiation, i.e., both direct and diffuse radiation from cloudy conditions. The sensor is often protected and kept in a dry atmosphere by a glass dome that should be regularly wiped clean.

Net longwave and net shortwave radiation can be measured by recording the difference in output between sensors facing upward and downward. In a net radiometer, the glass domes are replaced by polyethylene domes that have a transmission range for both shortwave and longwave radiation.

Where pyranometers are not available, solar radiation is usually estimated from the duration of bright sunshine. The actual duration of sunshine, n, is measured with a Campbell-Stokes sunshine recorder. This instrument records periods of bright sunshine by using a glass globe that acts as a lens. The sun rays are concentrated at a focal point that burns a hole in a specially treated card mounted concentrically with the sphere. The movement of the sun changes the focal point throughout the day and a trace is drawn on the card. If the sun is obscured, the trace is interrupted. The hours of bright sunshine are indicated by the lengths of the line segments.

The quantity of heat conducted into the soil, G, can be measured with systems of soil heat flux plates and thermocouples or thermisters.

Calculation procedures

Extraterrestrial radiation for daily periods (R_a)

The extraterrestrial radiation, R_a, for each day of the year and for different latitudes can be estimated from the solar constant, the solar declination and the time of the year by:

$$R_a = \frac{24\ (60)}{\pi} G_{sc}\, d_r\, [\omega_s\ \sin(\varphi)\ \sin(\delta) + \cos(\varphi)\ \cos(\delta) \sin(\omega_s)] \qquad (21)$$

where
R_a extraterrestrial radiation [MJ m^{-2} day^{-1}],
G_{sc} solar constant = 0.0820 MJ m^{-2} min^{-1},
d_r inverse relative distance Earth-Sun (Equation 23),
ω_s sunset hour angle (Equation 25 or 26) [rad],
φ latitude [rad] (Equation 22),
δ solar declination (Equation 24) [rad].

R_a is expressed in the above equation in MJ m^{-2} day^{-1}. The corresponding equivalent evaporation in mm day^{-1} is obtained by multiplying R_a by 0.408 (Equation 20). The latitude, φ, expressed in radians is positive for the northern hemisphere and negative for the southern hemisphere (Example 7). The conversion from decimal degrees to radians is given by:

$$[\text{Radians}] = \frac{\pi}{180}\ [\text{decimal degrees}] \qquad (22)$$

EXAMPLE 7
Conversion of latitude in degrees and minutes to radians

Express the latitudes of Bangkok (Thailand) at 13°44'N and Rio de Janeiro (Brazil) at 22°54'S in radians.

Latitude	Bangkok (northern hemisphere)	Rio de Janeiro (southern hemisphere)
degrees & minutes	13°44'N	22°54'S
decimal degrees	13 + 44/60 = 13.73	(-22) + (-54/60) = - 22.90
radians	(π/180) 13.73 = + 0.240	(π/180) (-22.90) = - 0.400

The latitudes of Bangkok and Rio de Janeiro are respectively + 0.240 and - 0.400 radians.

The inverse relative distance Earth-Sun, d_r, and the solar declination, δ, are given by:

$$d_r = 1 + 0.033 \cos\left(\frac{2\pi}{365} J\right) \qquad (23)$$

$$\delta = 0.409 \sin\left(\frac{2\pi}{365} J - 1.39\right) \qquad (24)$$

where J is the number of the day in the year between 1 (1 January) and 365 or 366 (31 December). Values for J for all days of the year and an equation for estimating J are given in Annex 2 (Table 2.5).

The sunset hour angle, ω_s, is given by:

$$\omega_s = \arccos\left[-\tan(\varphi)\tan(\delta)\right] \qquad (25)$$

As the arccos function is not available in all computer languages, the sunset hour angle can also be computed using the arctan function:

$$\omega_s = \frac{\pi}{2} - \arctan\left[\frac{-\tan(\varphi)\tan(\delta)}{X^{0.5}}\right] \qquad (26)$$

where

$$X = 1 - [\tan(\varphi)]^2 [\tan(\delta)]^2 \qquad (27)$$

and $X = 0.00001$ if $X \leq 0$

Values for R_a for different latitudes are given in Annex 2 (Table 2.6). These values represent R_a on the 15th day of each month. These values deviate from values that are averaged over each day of the month by less than 1% for all latitudes during non-frozen periods and are included for simplicity of calculation. These values deviate slightly from the values in the Smithsonian Tables. For the winter months in latitudes greater than 55° (N or S), the equations for R_a have limited validity. Reference should be made to the Smithsonian Tables to assess possible deviations.

EXAMPLE 8
Determination of extraterrestrial radiation

Determine the extraterrestrial radiation (R_a) for 3 September at 20°S.

From Eq. 22	20°S or $\varphi = (\pi/180)(-20)$ =	- 0.35	rad
	(the value is negative for the southern hemisphere)		
From Table 2.5:	The number of day in the year, J =	246	days
From Eq. 23	$d_r = 1 + 0.033 \cos(2\pi(246)/365)$ =	0.985	rad
From Eq. 24	$\delta = 0.409 \sin(2\pi(246)/365-1.39)$ =	0.120	rad
From Eq. 25:	ω_s = arccos[-tan(-0.35)tan(0.120)] =	1.527	rad
Then:	sin(φ)sin(δ) =	-0.041	-
and:	cos(φ)cos(δ) =	0.933	-
From Eq. 21	$R_a = 24(60)/\pi\ (0.0820)(0.985)[1.527$ (-0.041)+0.933sin(1.527)] =	32.2	MJ m^{-2} d^{-1}
From Eq. 20	expressed as equivalent evaporation = 0.408 (32.2)=	13.1	mm/day

The extraterrestrial radiation is 32.2 MJ m^{-2} day^{-1}.

Extraterrestrial radiation for hourly or shorter periods (R_a)

For hourly or shorter periods the solar time angle at the beginning and end of the period should be considered when calculating R_a:

$$R_a = \frac{12\ (60)}{\pi} G_{sc}\, d_r \left[(\omega_2 - \omega_1)\sin(\varphi)\sin(\delta) + \cos(\varphi)\cos(\delta)(\sin(\omega_2) - \sin(\omega_1))\right] \qquad (28)$$

where
- R_a extraterrestrial radiation in the hour (or shorter) period [MJ m^{-2} hour^{-1}],
- G_{sc} solar constant = 0.0820 MJ m^{-2} min^{-1},
- d_r inverse relative distance Earth-Sun (Equation 23),
- δ solar declination [rad] (Equation 24),
- φ latitude [rad] (Equation 22),
- ω_1 solar time angle at beginning of period [rad] (Equation 29),
- ω_2 solar time angle at end of period [rad] (Equation 30).

The solar time angles at the beginning and end of the period are given by:

$$\omega_1 = \omega - \frac{\pi t_1}{24} \tag{29}$$

$$\omega_2 = \omega + \frac{\pi t_1}{24} \tag{30}$$

where ω solar time angle at midpoint of hourly or shorter period [rad],
t_1 length of the calculation period [hour]: i.e., 1 for hourly period or 0.5 for a 30-minute period.

The solar time angle at midpoint of the period is:

$$\omega = \frac{\pi}{12}\left[(t + 0.06667(L_z - L_m) + S_c) - 12\right] \tag{31}$$

where t standard clock time at the midpoint of the period [hour]. For example for a period between 14.00 and 15.00 hours, t = 14.5,
L_z longitude of the centre of the local time zone [degrees west of Greenwich]. For example, L_z = 75, 90, 105 and 120° for the Eastern, Central, Rocky Mountain and Pacific time zones (United States) and L_z = 0° for Greenwich, 330° for Cairo (Egypt), and 255° for Bangkok (Thailand),
L_m longitude of the measurement site [degrees west of Greenwich],
S_c seasonal correction for solar time [hour].

Of course, $\omega < -\omega_s$ or $\omega > \omega_s$ from Equation 31 indicates that the sun is below the horizon so that, by definition, R_a is zero.

The seasonal correction for solar time is:

$$S_c = 0.1645 \sin(2b) - 0.1255 \cos(b) - 0.025 \sin(b) \tag{32}$$

$$b = \frac{2\pi (J - 81)}{364} \tag{33}$$

where J is the number of the day in the year.

Daylight hours (N)

The daylight hours, N, are given by:

$$N = \frac{24}{\pi} \omega_s \tag{34}$$

where ω_s is the sunset hour angle in radians given by Equation 25 or 26. Mean values for N (15th day of each month) for different latitudes are given in Annex 2, Table 2.7.

EXAMPLE 9
Determination of daylight hours

Determine the daylight hours (N) for 3 September at 20°S.

From Example 8:	ω_s = arccos[-tan(-0.35)tan(0.120)] =	1.527	rad
From Eq. 34:	N = 24/π (1.527) =	11.7	hour
The number of daylight hours is 11.7 hours.			

BOX 9
Calculation sheet for extraterrestrial radiation (R_a) and daylight hours (N)

Latitude Degrees and minutes are
+ positive for northern hemisphere
- negative for southern hemisphere

Degrees		°	---------->		°
Minutes		'	---------- / 60 ---------->		°
Decimal degrees = Sum(degrees+minutes/60)					°
$\varphi = \pi/180$ * [decimal degrees]			Eq. 22		rad

Day of the year

Day					
Month			J Table 2.5 (Annex 2)		
$d_r = 1+0.033 \cos(2\pi J/365)$			Eq. 23		
$\delta = 0.409 \sin(2\pi J/365 - 1.39)$			Eq. 24		rad
$\sin(\varphi)\sin(\delta)$					
$\cos(\varphi)\cos(\delta)$					
ω_s = arccos[-tan(φ)tan(δ)]			Eq. 25		rad
(24 (60)/π) G_{sc}				**37.59**	MJ $m^{-2}day^{-1}$

Extraterrestrial radiation: R_a

$$R_a = \frac{24\,(60)}{\pi} G_{sc}\, d_r \left[\omega_s \sin(\varphi)\sin(\delta) + \cos(\varphi)\cos(\delta)\sin(\omega_s)\right]$$ Eq.21

MJ $m^{-2}day^{-1}$

Daylight hours: N

$$N = \frac{24}{\pi}\omega_s$$ Eq. 34

hour/day

Solar radiation (R_S)

If the solar radiation, R_S, is not measured, it can be calculated with the Angstrom formula, which relates solar radiation to extraterrestrial radiation and relative sunshine duration:

$$R_s = \left(a_s + b_s \frac{n}{N} \right) R_a \qquad (35)$$

where
- R_S solar or shortwave radiation [MJ m^{-2} day^{-1}],
- n actual duration of sunshine [hour],
- N maximum possible duration of sunshine or daylight hours [hour],
- n/N relative sunshine duration [-],
- R_a extraterrestrial radiation [MJ m^{-2} day^{-1}],
- a_S regression constant, expressing the fraction of extraterrestrial radiation reaching the earth on overcast days (n = 0),
- a_S+b_S fraction of extraterrestrial radiation reaching the earth on clear days (n = N).

R_S is expressed in the above equation in MJ m^{-2} day^{-1}. The corresponding equivalent evaporation in mm day^{-1} is obtained by multiplying R_S by 0.408 (Equation 20). Depending on atmospheric conditions (humidity, dust) and solar declination (latitude and month), the Angstrom values a_S and b_S will vary. Where no actual solar radiation data are available and no calibration has been carried out for improved a_S and b_S parameters, the values $a_S = 0.25$ and $b_S = 0.50$ are recommended.

The extraterrestrial radiation, R_a, and the daylight hours or maximum possible duration of sunshine, N, are given by Equations 21 and 34. Values for R_a and N for different latitudes are also listed in Annex 2 (Tables 2.6 and 2.7). The actual duration of sunshine, n, is recorded with a Campbell Stokes sunshine recorder.

EXAMPLE 10
Determination of solar radiation from measured duration of sunshine

In Rio de Janeiro (Brazil) at a latitude of 22°54'S, 220 hours of sunshine were recorded in May. Determine the solar radiation.

From Eq. 22:	latitude = 22°54'S = 22.90°S or π/180 (-22.90) =	 -0.40	 rad
From Table 2.5:	for 15 May, the day in the year (J) =	135	--
From Eq. 21 or Table 2.6:	R_a =	25.1	MJ m^{-2} day^{-1}
From Eq. 34 or Table 2.7	N = n = 220 hours / 31 days =	10.9 7.1	hours day^{-1} hours day^{-1}
From Eq. 35:	R_s = [0.25 + 0.50 (7.1/10.9)] R_a = = 0.58 R_a = 0.58 (25.1) =	 14.5	 MJ m^{-2} day^{-1}
From Eq. 20:	expressed as equivalent evaporation = 0.408 (14.5) =	 5.9	 mm/day

The estimated solar radiation is 14.5 MJ m^{-2} day^{-1}.

Clear-sky solar radiation (R_{so})

The calculation of the clear-sky radiation, R_{so}, when n = N, is required for computing net longwave radiation.

• For near sea level or when calibrated values for a_s and b_s are available:

$$R_{so} = (a_s + b_s) R_a \quad (36)$$

where R_{so} clear-sky solar radiation [MJ m^{-2} day^{-1}],
a_s+b_s fraction of extraterrestrial radiation reaching the earth on clear-sky days (n = N).

• When calibrated values for a_s and b_s are not available:

$$R_{so} = \left(0.75 + 2\ 10^{-5}\ z\right) R_a \quad (37)$$

where z station elevation above sea level [m].

Other more complex estimates for R_{so}, which include turbidity and water vapour effects, are discussed in Annex 3 (Equations 3.14 to 20).

Net solar or net shortwave radiation (R_{ns})

The net shortwave radiation resulting from the balance between incoming and reflected solar radiation is given by:

$$R_{ns} = (1 - \alpha) R_s \quad (38)$$

where R_{ns} net solar or shortwave radiation [MJ m^{-2} day^{-1}],
α albedo or canopy reflection coefficient, which is 0.23 for the hypothetical grass reference crop [dimensionless],
R_s the incoming solar radiation [MJ m^{-2} day^{-1}].

R_{ns} is expressed in the above equation in MJ m^{-2} day^{-1}.

Net longwave radiation (R_{nl})

The rate of longwave energy emission is proportional to the absolute temperature of the surface raised to the fourth power. This relation is expressed quantitatively by the Stefan-Boltzmann law. The net energy flux leaving the earth's surface is, however, less than that emitted and given by the Stefan-Boltzmann law due to the absorption and downward radiation from the sky. Water vapour, clouds, carbon dioxide and dust are absorbers and emitters of longwave radiation. Their concentrations should be known when assessing the net outgoing flux. As humidity and cloudiness play an important role, the Stefan-Boltzmann law is corrected by these two factors when estimating the net outgoing flux of longwave radiation. It is thereby assumed that the concentrations of the other absorbers are constant:

$$R_{nl} = \sigma \left[\frac{T_{max,K}^4 + T_{min,K}^4}{2} \right] \left(0.34 - 0.14 \sqrt{e_a} \right) \left(1.35 \frac{R_s}{R_{so}} - 0.35 \right) \quad (39)$$

where R_{nl} net outgoing longwave radiation [MJ m^{-2} day^{-1}],
σ Stefan-Boltzmann constant [4.903 10^{-9} MJ K^{-4} m^{-2} day^{-1}],
$T_{max,K}$ maximum absolute temperature during the 24-hour period [K = °C + 273.16],
$T_{min,K}$ minimum absolute temperature during the 24-hour period [K = °C + 273.16],
e_a actual vapour pressure [kPa],
R_s/R_{so} relative shortwave radiation (limited to ≤ 1.0),
R_s measured or calculated (Equation 35) solar radiation [MJ m^{-2} day^{-1}],
R_{so} calculated (Equation 36 or 37) clear-sky radiation [MJ m^{-2} day^{-1}].

An average of the maximum air temperature to the fourth power and the minimum air temperature to the fourth power is commonly used in the Stefan-Boltzmann equation for 24-hour time steps. The term (0.34-0.14$\sqrt{e_a}$) expresses the correction for air humidity, and will be smaller if the humidity increases. The effect of cloudiness is expressed by (1.35 R_s/R_{so} - 0.35). The term becomes smaller if the cloudiness increases and hence R_s decreases. The smaller the correction terms, the smaller the net outgoing flux of longwave radiation. Note that the R_s/R_{so} term in Equation 39 must be limited so that $R_s/R_{so} \leq 1.0$.

Where measurements of incoming and outgoing short and longwave radiation during bright sunny and overcast hours are available, calibration of the coefficients in Equation 39 can be carried out.

Annex 2 (Table 2.8) lists values for σT_K^4 for different air temperatures.

EXAMPLE 11
Determination of net longwave radiation

In Rio de Janeiro (Brazil) at a latitude of 22°54'S (= -22.70°), 220 hours of bright sunshine, a mean monthly daily maximum and minimum air temperature of 25.1 and 19.1°C and a vapour pressure of 2.1 kPa were recorded in May. Determine the net longwave radiation.

From Example 10: From Eq. 36:	R_s = $R_{so} = 0.75\ R_a = 0.75\ .\ 25.1$ =	14.5 18.8	MJ m^{-2} day^{-1} MJ m^{-2} day^{-1}
From Table 2.8 or for: Then: and:	σ = T_{max} = 25.1°C = $\sigma T_{max,K}^4$ =	4.903 10^{-9} 298.3 38.8	MJ K^{-4} m^{-2} day^{-1} K MJ m^{-2} day^{-1}
and: and:	T_{min} = 19.1°C = $\sigma\ T_{min,K}^4$ = 35.8 MJ m^{-2} day^{-1}	292.3 35.8	K MJ m^{-2} day^{-1}
and: and: and: -	e_a = 0.34 - 0.14 $\sqrt{e_a}$ = R_s/R_{so} = (14.5)/(18.8) 1.35(0.77)-0.35 =	2.1 0.14 0.77 0.69	kPa - - -
From Eq. 39:	R_{nl} = [(38.7 + 35.7)/2] (0.14) (0.69) =	3.5	MJ m^{-2} day^{-1}
From Eq. 20:	expressed as equivalent evaporation = 0.408 (3.5) =	 1.4	 mm/day

The net longwave radiation is 3.5 MJ m^{-2} day^{-1}.

Net radiation (R_n)

The net radiation (R_n) is the difference between the incoming net shortwave radiation (R_{ns}) and the outgoing net longwave radiation (R_{nl}):

$$R_n = R_{ns} - R_{nl} \qquad (40)$$

EXAMPLE 12
Determination of net radiation

Determine the net radiation in Rio de Janeiro in May with the data from previous examples.

From Example 10:	R_s =	14.5	MJ m^{-2} day^{-1}
From Eq. 39:	$R_{ns} = (1 - 0.23)\ R_s$ =	11.1	MJ m^{-2} day^{-1}
From Example 11:	R_{nl} =	3.5	MJ m^{-2} day^{-1}
From Eq. 40:	R_n = 11.1 - 3.5 =	7.6	MJ m^{-2} day^{-1}
From Eq. 20:	expressed as equivalent evaporation = 0.408 (7.7) =	3.1	mm/day

The net radiation is 7.6 MJ m^{-2} day^{-1}.

BOX 10
Calculation sheet for net radiation (R_n)

Latitude		°			
Day			R_a (Box 9 or Table 2.6)		MJ m^{-2} d^{-1}
Month			N (Box 9 or Table 2.7)		hours
n		hours	(in absence of Rs) n/N		
Net solar radiation: R_{ns}					
If n is measured instead of R_s: $R_s = (0.25+0.50\ n/N)\ R_a$			Eq. 35		MJ m^{-2} d^{-1}
$R_{so} = [0.75 + 2\ (Altitude)/\ 100\ 000]\ R_a$			Eq. 37		MJ m^{-2} d^{-1}
R_s / R_{so}			(≤ 1.0)		
$R_{ns} = 0.77\ R_s$			Eq. 38		MJ m^{-2} d^{-1}
Net longwave radiation: R_{nl} with σ = 4.903 10^{-9} MJ K^{-4} m^{-2} day^{-1} and $T_K = T[°C] + 273.16$					
T_{max}		°C	$T_{max,K} = T_{max} + 273.16$		K
T_{min}		°C	$T_{min,K} = T_{min} + 273.16$		K
			$\sigma T_{max,K}^4$ (Table 2.8)		MJ m^{-2} d^{-1}
			$\sigma T_{min,K}^4$ (Table 2.8)		MJ m^{-2} d^{-1}
$(\sigma T_{max,K}^4 + \sigma T_{min,K}^4)/2$					MJ m^{-2} d^{-1}
e_a		kPa	$(0.34-0.14\sqrt{e_a})$		
R_s/R_{so}			$(1.35\ R_s/R_{so}-0.35)$		
$R_{nl} = (\sigma T_{max,K}^4 + \sigma T_{min,K}^4)/2\ (0.34-0.14\sqrt{e_a})(1.35R_s/R_{so}-0.35)$ Eq. 39					MJ m^{-2} d^{-1}
Net radiation: R_n					
$R_n = R_{ns} - R_{nl}$			Eq. 40		MJ m^{-2} d^{-1}

Soil heat flux (G)

Complex models are available to describe soil heat flux. Because soil heat flux is small compared to R_n, particularly when the surface is covered by vegetation and calculation time steps are 24 hours or longer, a simple calculation procedure is presented here for long time steps, based on the idea that the soil temperature follows air temperature:

$$G = c_s \frac{T_i + T_{i-1}}{\Delta t} \Delta z \qquad (41)$$

where
- G soil heat flux [MJ m^{-2} day^{-1}],
- c_s soil heat capacity [MJ m^{-3} $°C^{-1}$],
- T_i air temperature at time i [°C],
- T_{i-1} air temperature at time i-1 [°C],
- Δt length of time interval [day],
- Δz effective soil depth [m].

As the soil temperature lags air temperature, the average temperature for a period should be considered when assessing the daily soil heat flux, i.e., Δt should exceed one day. The depth of penetration of the temperature wave is determined by the length of the time interval. The effective soil depth, Δz, is only 0.10-0.20 m for a time interval of one or a few days but might be 2 m or more for monthly periods. The soil heat capacity is related to its mineral composition and water content.

• For day and ten-day periods:
As the magnitude of the day or ten-day soil heat flux beneath the grass reference surface is relatively small, it may be ignored and thus:

$$G_{day} \approx 0 \qquad (42)$$

• For monthly periods:
When assuming a constant soil heat capacity of 2.1 MJ m^{-3} $°C^{-1}$ and an appropriate soil depth, Equation 41 can be used to derive G for monthly periods:

$$G_{month,i} = 0.07 \, (T_{month,i+1} - T_{month,i-1}) \qquad (43)$$

or, if $T_{month,i+1}$ is unknown:

$$G_{month,i} = 0.14 \, (T_{month,i} - T_{month,i-1}) \qquad (44)$$

where
- $T_{month,i}$ mean air temperature of month i [°C],
- $T_{month,i-1}$ mean air temperature of previous month [°C],
- $T_{month,i+1}$ mean air temperature of next month [°C].

• For hourly or shorter periods:
For hourly (or shorter) calculations, G beneath a dense cover of grass does not correlate well with air temperature. Hourly G can be approximated during daylight periods as:

$$G_{hr} = 0.1\ R_n \qquad (45)$$

and during nighttime periods as:

$$G_{hr} = 0.5\ R_n \qquad (46)$$

Where the soil is warming, the soil heat flux G is positive. The amount of energy required for this process is subtracted from R_n when estimating evapotranspiration.

EXAMPLE 13
Determination of soil heat flux for monthly periods

Determine the soil heat flux in April in Algiers (Algeria) when the soil is warming. The mean monthly temperatures of March, April and May are 14.1, 16.1, and 18.8°C respectively.

From Eq. 43	for the month of April: G_{month} = 0.07 (18.8 - 14.1) =	0.33	MJ m^{-2} day^{-1}
From Eq. 20	expressed as equivalent evaporation = 0.408(0.33) =	0.13	mm/day
The soil heat flux is 0.33 MJ m^{-2} day^{-1}.			

WIND SPEED

Measurement

Wind is characterized by its direction and velocity. Wind direction refers to the direction from which the wind is blowing. For the computation of evapotranspiration, wind speed is the relevant variable. As wind speed at a given location varies with time, it is necessary to express it as an average over a given time interval. Wind speed is given in metres per second (m s^{-1}) or kilometres per day (km day^{-1}).

Wind speed is measured with anemometers. The anemometers commonly used in weather stations are composed of cups or propellers which are turned by the force of the wind. By counting the number of revolutions over a given time period, the average wind speed over the measuring period is computed.

Wind profile relationship

Wind speeds measured at different heights above the soil surface are different. Surface friction tends to slow down wind passing over it. Wind speed is slowest at the surface and increases with height. For this reason anemometers are placed at a chosen standard height, i.e., 10 m in meteorology and 2 or 3 m in agrometeorology. For the calculation of evapotranspiration, wind speed measured at 2 m above the surface is required. To adjust wind speed data obtained from instruments placed at elevations other than the standard height of 2 m, a logarithmic wind speed profile may be used for measurements above a short grassed surface:

$$u_2 = u_z \frac{4.87}{\ln(67.8\, z - 5.42)} \qquad (47)$$

where u_2 wind speed at 2 m above ground surface [m s^{-1}],
u_z measured wind speed at z m above ground surface [m s^{-1}],
z height of measurement above ground surface [m].

The corresponding multipliers or conversion factors are given in Annex 2 (Table 2.9) and are plotted in Figure 16.

FIGURE 16
Conversion factor to convert wind speed measured at a certain height above ground level to wind speed at the standard height (2 m)

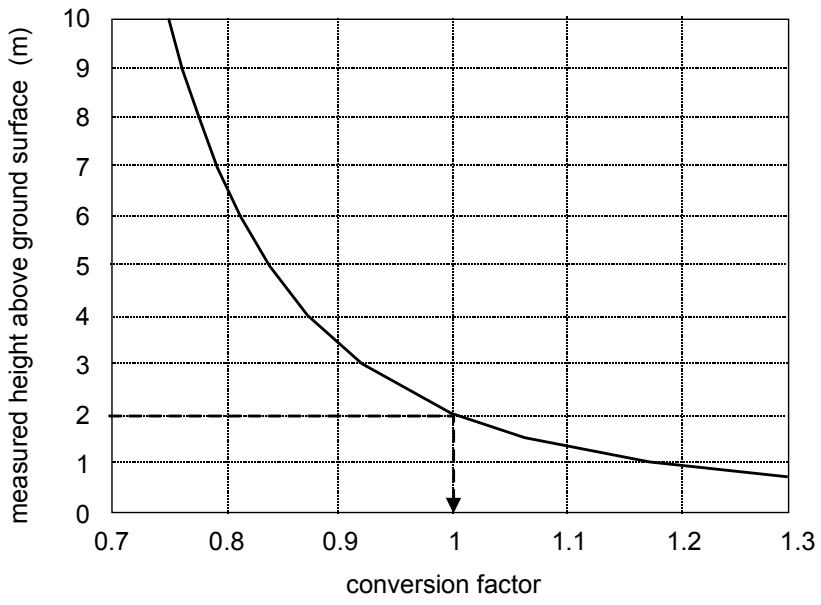

EXAMPLE 14
Adjusting wind speed data to standard height

Determine the wind speed at the standard height of 2 m, from a measured wind speed of 3.2 m/s at 10 m above the soil surface.

For:	u_z =	3.2	m/s
And:	z =	10	m
Then:	Conversion factor = 4.87 / ln(67.8 (10) - 5.42) =	0.75	-
From Eq. 47:	u_2 = 3.2 (0.75) =	2.4	m/s

The wind speed at 2 m above the soil surface is 2.4 m/s.

CLIMATIC DATA ACQUISITION

Weather stations

Meteorological data are recorded at various types of weather stations. Agrometeorological stations are sited in cropped areas where instruments are exposed to atmospheric conditions similar to those for the surrounding crops. In these stations, air temperature and humidity, wind speed and sunshine duration are typically measured at 2 m above an extensive surface of grass or short crop. Where needed and feasible, the cover of the station is irrigated. Guidelines for the establishment and maintenance of agrometeorological stations are given in the FAO Irrigation and Drainage Paper No. 27. This handbook also describes the different types of instruments, their installation and reliability.

Data collected at stations other than agrometeorological stations require a careful analysis of their validity before their use. For example, in aeronautic stations, data relevant for aviation are measured. As airports are often situated near urban conditions, temperatures may be higher than those found in rural agricultural areas. Wind speed is commonly measured at 10 m height above the ground surface.

The country's national meteorological service should be contacted for information on the climatic data collected at various types of weather stations in the country. National services commonly publish meteorological bulletins listing processed climatic data from the various stations.

The annexes list procedures for the statistical analysis, assessment, correction and completion of partial or missing weather data:

Annex 4: Statistical analysis of weather data sets;
Annex 5: Measuring and assessing integrity of weather data;
Annex 6: Correction of weather data observed at non-reference sites for computing ET_o.

Agroclimatic monthly databases

Starting in 1984, FAO has published mean monthly agroclimatic data from 2 300 stations in the FAO Plant Production and Protection Series. Several volumes exist:

No. 22: Volume 1: data for Africa, countries north of the equator (1984),
Volume 2: data for Africa, countries south of the equator (1984);
No. 24: Agroclimatic data for Latin America and the Caribbean (1985);
No. 25: Volume 1: Agroclimatic data for Asia (A-J) (1987),
Volume 2: Agroclimatic data for Asia (K-Z) (1987).

CLIMWAT for CROPWAT (FAO Irrigation and Drainage Paper No. 46) contains monthly data from 3 262 climatic stations contained on five separate diskettes. The stations are grouped by country and by continent. Monthly averages of maximum and minimum temperatures, mean relative humidity, wind speed, sunshine hours, radiation data as well as rainfall and ET_o calculated with the FAO Penman-Monteith method are listed on the diskettes for mean long-term conditions.

FAOCLIM provides a user friendly interface on compact disc to the agroclimatic database of the Agrometeorology Group in FAO. The data presented are an extension of the previously published FAO Plant Production and Protection Series and the number of stations has been increased from 2 300 to about 19 000, with an improved world wide coverage. However, values for all principal weather parameters are not available for all stations. Many contain air temperature and precipitation only.

These databases can be consulted in order to verify the consistency of the actual database or to estimate missing climatic parameters. However, they should only be used for preliminary studies as they contain mean monthly data only. FAOCLIM provides monthly time series for only a few stations. The information in these databases should never replace actual data.

Other electronic databases for portions of the globe have been published by the International Water Management Institute (IWMI). These databases include daily and monthly air temperature, precipitation and ET_o predicted using the Hargreaves ET_o equation that is based on differences between daily maximum and minimum air temperature.

ESTIMATING MISSING CLIMATIC DATA

The assessment of the reference evapotranspiration ET_o with the Penman-Monteith method is developed in Chapter 4. The calculation requires mean daily, ten-day or monthly maximum and minimum air temperature (T_{max} and T_{min}), actual vapour pressure (e_a), net radiation (R_n) and wind speed measured at 2 m (u_2). If some of the required weather data are missing or cannot be calculated, it is strongly recommended that the user estimate the missing climatic data with one of the following procedures and use the FAO Penman-Monteith method for the calculation of ET_o. The use of an alternative ET_o calculation procedure, requiring only limited meteorological parameters, is less recommended. Procedures to estimate missing humidity, radiation and wind speed data are given in this section.

Estimating missing humidity data

Where humidity data are lacking or are of questionable quality, an estimate of actual vapour pressure, e_a, can be obtained by assuming that dewpoint temperature (T_{dew}) is near the daily minimum temperature (T_{min}). This statement implicitly assumes that at sunrise, when the air temperature is close to T_{min}, that the air is nearly saturated with water vapour and the relative humidity is nearly 100%. If T_{min} is used to represent T_{dew} then:

$$e_a = e^o(T_{min}) = 0.611 \exp\left[\frac{17.27\ T_{min}}{T_{min} + 237.3}\right] \quad (48)$$

The relationship $T_{dew} \approx T_{min}$ holds for locations where the cover crop of the station is well watered. However, particularly for arid regions, the air might not be saturated when its temperature is at its minimum. Hence, T_{min} might be greater than T_{dew} and a further calibration may be required to estimate dewpoint temperatures. In these situations, "T_{min}" in the above equation may be better approximated by subtracting 2-3°C from T_{min}. Appropriate correction procedures are given in Annex 6. In humid and subhumid climates, T_{min} and T_{dew} measured in early morning may be less than T_{dew} measured during the daytime because of condensation of dew during the night. After sunrise, evaporation of the dew will once again

humidify the air and will increase the value measured for T_{dew} during the daytime. This phenomenon is demonstrated in Figure 5.4 of Annex 5. However, it is standard practice in 24-hour calculations of ET_o to use T_{dew} measured or calculated durin early morning.

The estimate for e_a from T_{min} should be checked. When the prediction by Equation 48 is validated for a region, it can be used for daily estimates of e_a.

Estimating missing radiation data

Net radiation measuring devices, requiring professional control, have rarely been installed in agrometeorological stations. In the absence of a direct measurement, longwave and net radiation can be derived from more commonly observed weather parameters, i.e., solar radiation or sunshine hours, air temperature and vapour pressure. Where solar radiation is not measured, it can perhaps be estimated from measured hours of bright sunshine. However, where daily sunshine hours (n) are not available, solar radiation data cannot be computed with the calculation procedures previously presented. This section presents various methods to estimate solar radiation data with an alternative methodology.

Solar Radiation data from a nearby weather station

This method relies on the fact that for the same month and often for the same day, the variables affecting incoming solar radiation, R_s, and sunshine duration, n, are similar throughout a given region. This implies that: (i) the size of the region is small; (ii) the air masses governing rainfall and cloudiness are nearly identical within parts of the region; and (iii) the physiography of the region is almost homogenous. Differences in relief should be negligible as they strongly influence the movement of air masses. Under such conditions, radiation data observed at nearby stations can be used.

Caution should be used when applying this method to mountainous and coastal areas where differences in exposure and altitude could be important or where rainfall is variable due to convective conditions. Moreover, data from a station located nearby but situated on the other side of a mountain may not be transferable as conditions governing radiation are different. The user should observe climatic conditions in both locations and obtain information from local persons concerning general differences in cloud cover and type.

Where the north-south distance to a weather station within the same homogeneous region exceeds 50 km so that the value for R_a changes, the R_s measurement should be adjusted using the ratio of the solar to extraterrestrial radiation, R_s/R_a:

$$R_s = \frac{R_{s,reg}}{R_{a,reg}} R_a \qquad (49)$$

where $R_{s,reg}$ solar radiation at the regional location [MJ m^{-2} day^{-1}],
$R_{a,reg}$ extraterrestrial radiation at the regional location [MJ m^{-2} day^{-1}].

Once the solar radiation has been derived from the radiation data of a nearby station, the net longwave radiation (Equation 39) and the net radiation (Equation 40) can be calculated.

The estimation method of Equation 49 is recommended for monthly calculations of ET_o. If using the method for daily estimates of ET_o, a more careful analysis of weather data in the importing and exporting meteorological stations has to be performed to verify whether both

stations are in the same homogeneous climatic region and are close enough to experience similar conditions within the same day. The analysis should include the comparison of daily weather data from both stations, particularly the maximum and minimum air temperature and humidity. In fact, similar cloudiness and sunshine durations are related to similarities in temperature and humidity trends.

Generally, daily calculations of ET_o with estimated radiation data are justified when utilized as a sum or an average over a several-day period. This is the case for the computation of the mean evapotranspiration demand between successive irrigations or when planning irrigation schedules. Under these conditions, the relative error for one day often counterbalances the error for another day of the averaging period. Daily estimates should not be utilized as true daily estimates but only in averages over the period under consideration.

Solar Radiation data derived from air temperature differences

The difference between the maximum and minimum air temperature is related to the degree of cloud cover in a location. Clear-sky conditions result in high temperatures during the day (T_{max}) because the atmosphere is transparent to the incoming solar radiation and in low temperatures during the night (T_{min}) because less outgoing longwave radiation is absorbed by the atmosphere. On the other hand, in overcast conditions, T_{max} is relatively smaller because a significant part of the incoming solar radiation never reaches the earth's surface and is absorbed and reflected by the clouds. Similarly, T_{min} will be relatively higher as the cloud cover acts as a blanket and decreases the net outgoing longwave radiation. Therefore, the difference between the maximum and minimum air temperature (T_{max} - T_{min}) can be used as an indicator of the fraction of extraterrestrial radiation that reaches the earth's surface. This principle has been utilized by Hargreaves and Samani to develop estimates of ET_o using only air temperature data.

The Hargreaves' radiation formula, adjusted and validated at several weather stations in a variety of climate conditions, becomes:

$$R_s = k_{Rs} \sqrt{(T_{max} - T_{min})}\ R_a \qquad (50)$$

where R_a extraterrestrial radiation [MJ m^{-2} d^{-1}],
T_{max} maximum air temperature [°C],
T_{min} minimum air temperature [°C],
k_{Rs} adjustment coefficient (0.16 .. 0.19) [$°C^{-0.5}$].

The square root of the temperature difference is closely related to the existing daily solar radiation in a given location. The adjustment coefficient k_{RS} is empirical and differs for 'interior' or 'coastal' regions:

- for 'interior' locations, where land mass dominates and air masses are not strongly influenced by a large water body, $k_{RS} \cong 0.16$;
- for 'coastal' locations, situated on or adjacent to the coast of a large land mass and where air masses are influenced by a nearby water body, $k_{RS} \cong 0.19$.

The relationship between R_S/R_a and the temperature difference is plotted in Figure 17 for interior and coastal locations. The fraction of extraterrestrial radiation that reaches the earth's surface, R_S/R_a, ranges from about 0.25 on a day with dense cloud cover to about 0.75 on a

FIGURE 17
Relationship between the fraction of extraterrestrial radiation that reaches the earth's surface, R_s/R_a, and the air temperature difference T_{max} - T_{min} for interior (k_{Rs} = 0.16) and coastal (k_{Rs} = 0.19) regions

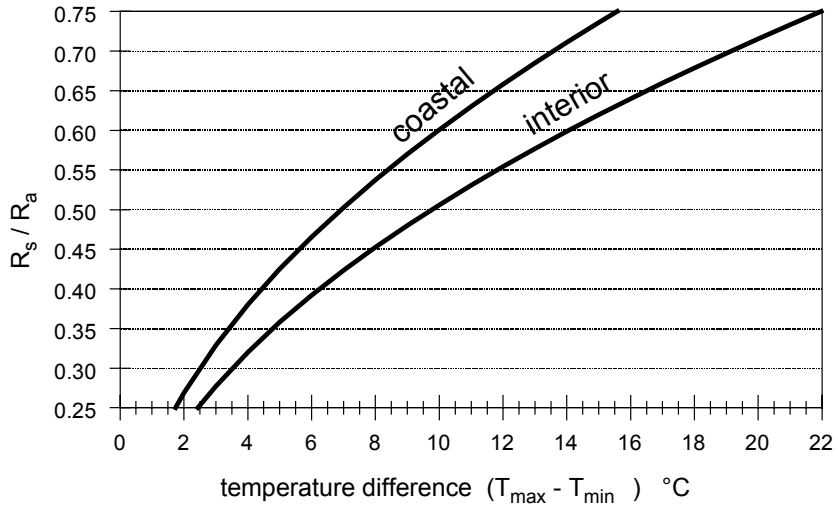

cloudless day with clear sky. R_S predicted by Equation 50 should be limited to ≤ R_{SO} from Equation 36 or 37.

The temperature difference method is recommended for locations where it is not appropriate to import radiation data from a regional station, either because homogeneous climate conditions do not occur, or because data for the region are lacking. For island conditions, the methodology of Equation 50 is not appropriate due to moderating effects of the surrounding water body.

Caution is required when daily computations of ET_O are needed. The advice given for Equation 49 fully applies. It is recommended that daily estimates of ET_O that are based on estimated R_S be summed or averaged over a several-day period, such as a week, decade or month to reduce prediction error.

EXAMPLE 15
Determination of solar radiation from temperature data

Determine the solar radiation from the temperature data of July in Lyon (France) at a latitude of 45°43'N and at 200 m above sea level. In July, the mean monthly maximum and minimum air temperatures are 26.6 and 14.8°C respectively.

From Table 2.5:	latitude = 45°43' = +45.72° decimal degrees =	0.80	radian
	The day of the year for 15 July is	196	-
From Eq. 21 or Annex 2 Table 2.6):	R_a =	40.6	MJ m^{-2} day^{-1}
From Eq. 50 (same latitude):	R_s = 0.16 [√(26.6-14.8)] R_a = 0.55 (40.6) =	22.3	MJ m^{-2} day^{-1}
From Eq. 20 (same latitude):	equivalent evaporation = 0.408 (22.3) =	9.1	mm/day
In July, the estimated solar radiation, R_s, is 22.3 MJ m^{-2} day^{-1}			

EXAMPLE 16
Determination of net radiation in the absence of radiation data

Calculate the net radiation for Bangkok (13°44'N) by using T_{max} and T_{min}. The station is located at the coast at 2 m above sea level. In April, the monthly average of the daily maximum temperature, daily minimum temperature and daily vapour pressure are 34.8°C, 25.6°C and 2.85 kPa respectively.

For Latitude 13°44'N = +13.73° decimal degrees = -0.24 radian
and for 15 April, J =105:

From Eq. 21 or Table 2.6:	R_a =	38.1	MJ m^{-2} day^{-1}
	(in coastal location) k_{Rs} =	0.19	
	$(T_{max} - T_{min})$ = (34.8 - 25.6) =	9.2°C	°C
From Eq. 50:	$R_s = 0.19 \sqrt{(9.2)}\ R_a$	21.9	MJ m^{-2} day^{-1}
From Eq. 36:	$R_{so} = 0.75\ R_a$	28.5	MJ m^{-2} day^{-1}
From Eq. 38:	$R_{ns} = 0.77\ R_s$	16.9	MJ m^{-2} day^{-1}
	σ =	$4.903\ 10^{-9}$	MJ K^{-4} m^{-2} day-1
	T_{max} =	34.8	°C
	$\sigma T_{max,K}^4$ =	44.1	MJ m^{-2} day^{-1}
	T_{min}	25.6	°C
	$\sigma T_{min,K}^4$ =	39.1	MJ m^{-2} day^{-1}
	$(\sigma T_{max,K}^4 + \sigma T_{min,K}^4)/2$ = (44.1 + 39.1)/2 =	41.6	MJ m^{-2} day^{-1}
For:	e_a = 2.85 kPa	2.85	kPa
	$(0.34-0.14\sqrt{e_a})$ =	0.10	-
For:	R_s/R_{so} =	0.77	-
Then:	$(1.35(R_s/R_{so})-0.35)$ =	0.69	-
From Eq. 39:	R_{nl} = 41.6 (0.10) 0.69 =	3.0	MJ m^{-2} day^{-1}
From Eq. 40:	R_n = (16.9 - 2.9) =	13.9	MJ m^{-2} day^{-1}
From Eq. 20:	equivalent evaporation = 0.408 (13.9) =	5.7	mm/day

The estimated net radiation is 13.9 MJ m^{-2} day^{-1}.

Empirical methodology for island locations

For island locations, where the land mass has a width perpendicular to the coastline of 20 km or less, the air masses influencing the atmospheric conditions are dominated by the adjacent water body in all directions. The temperature method is not appropriate for this situation. Where radiation data from another location on the island are not available, a first estimate of the monthly solar average can be obtained from the empirical relation:

$$R_s = 0.7\ R_a - b \qquad (51)$$

where R_S solar radiation [MJ m^{-2} day^{-1}],
R_a extraterrestrial radiation [MJ m^{-2} day^{-1}],
b empirical constant, equal to 4 MJ m^{-2} day^{-1}.

This relationship is only applicable for low altitudes (from 0 to 100 m). The empirical constant represents the fact that in island locations some clouds are usually present, thus making the mean solar radiation 4 MJ m^{-2} day^{-1} below the nearly clear sky envelope (0.7 R_a). Local adjustment of the empirical constant may improve the estimation.

The method is only appropriate for monthly calculations. The constant relation between R_S and R_a does not yield accurate daily estimates.

Missing wind speed data

Wind speed data from a nearby weather station

Importing wind speed data from a nearby station, as for radiation data, relies on the fact that the air flow above a 'homogeneous' region may have relatively large variations through the course of a day but small variations when referring to longer periods or the total for the day. Data from a nearby station may be imported where air masses are of the same origin or where the same fronts govern air flows in the region and where the relief is similar.

When importing wind speed data from another station, the regional climate, trends in variation of other meteorological parameters and relief should be compared. Strong winds are often associated with low relative humidity and light winds are common with high relative humidity. Thus, trends in variation of daily maximum and minimum relative humidities should be similar in both locations. In mountainous areas, data should not necessarily be imported from the nearest station but from nearby stations with similar elevation and exposure to the dominant winds. The paired stations may even vary from one season to another, depending on the dominant winds.

Imported wind speed data can be used when making monthly estimates of evapotranspiration. Daily calculations are justified when utilized as a sum or average over a several-day period, such as a week or decade.

Empirical estimates of monthly wind speed

As the variation in wind speed average over monthly periods is relatively small and fluctuates around average values, monthly values of wind speed may be estimated. The 'average' wind speed estimates may be selected from information available for the regional climate, but should take seasonal changes into account. General values are suggested in Table 4.

TABLE 4
General classes of monthly wind speed data

Description	mean monthly wind speed at 2 m
light wind	... ≤ 1.0 m/s
light to moderate wind	1 – 3 m/s
moderate to strong wind	3 – 5 m/s
strong wind	... ≥ 5.0 m/s

Where no wind data are available within the region, a value of 2 m/s can be used as a temporary estimate. This value is the average over 2 000 weather stations around the globe.

In general, wind speed at 2 m, u_2, should be limited to about $u_2 \geq 0.5$ m/s when used in the ET_o equation (Equation 6). This is necessary to account for the effects of boundary layer instability and bouyancy of air in promoting exchange of vapour at the surface when air is calm. This effect occurs when the wind speed is small and buoyancy of warm air induces air exchange at the surface. Limiting $u_2 \geq 0.5$ m/s in the ET_o equation improves the estimation accuracy under the conditions of very low wind speed.

Minimum data requirements

This section has shown how solar radiation, vapour pressure and wind data can be estimated when missing. Many of the suggested procedures rely upon maximum and minimum air temperature measurements. Unfortunately, there is no dependable way to estimate air temperature when it is missing. Therefore it is suggested that maximum and minimum daily air temperature data are the minimum data requirements necessary to apply the FAO Penman-Monteith method.

An alternative equation for ET_o when weather data are missing

When solar radiation data, relative humidity data and/or wind speed data are missing, they should be estimated using the procedures presented in this section. As an alternative, ET_o can be estimated using the Hargreaves ET_o equation where:

$$ET_o = 0.0023 (T_{mean} + 17.8) (T_{max} - T_{min})^{0.5} R_a \qquad (52)$$

where all parameters have been previously defined. Units for both ET_o and R_a in Equation 52 are mm day^{-1}. Equation 52 should be verified in each new region by comparing with estimates by the FAO Penman-Monteith equation (Equation 6) at weather stations where solar radiation, air temperature, humidity, and wind speed are measured. If necessary, Equation 52 can be calibrated on a monthly or annual basis by determining empirical coefficients where $ET_o = a + b\ ET_{o\ Eq.52}$, where the "Eq. 52" subscript refers to ET_o predicted using Equation 52. The coefficients a and b can be determined by regression analyses or by visual fitting. In general, estimating solar radiation, vapor pressure and wind speed as described in Equations 48 to 51 and Table 4 and then utilizing these estimates in Equation 6 (the FAO Penman-Monteith equation) will provide somewhat more accurate estimates as compared to estimating ET_o directly using Equation 52. This is due to the ability of the estimation equations to incorporate general climatic characteristics such as high or low wind speed or high or low relative humidity into the ET_o estimate made using Equation 6.

Equation 52 has a tendency to underpredict under high wind conditions (u_2 > 3 m/s) and to overpredict under conditions of high relative humidity.

Chapter 4

Determination of ET_o

This chapter demonstrates how the crop reference evapotranspiration (ET_o) is determined either from meteorological data or from pan evaporation.

The FAO Penman-Monteith method is maintained as the sole standard method for the computation of ET_o from meteorological data. The method itself is introduced in Chapter 2, and the computation of all data required for the calculation of ET_o is discussed in Chapter 3. This chapter presents guidelines to calculate ET_o with different time steps, ranging from hours to months, and with missing climatic data. The ET_o calculation can be done by hand with the help of a calculation sheet, or by means of a computer.

ET_o can also be estimated from the evaporation loss from a water surface. The procedure to obtain ET_o from pan evaporation and the coefficients for different types of pans are presented in this chapter.

PENMAN-MONTEITH EQUATION

From the original Penman-Monteith equation and the equations of the aerodynamic and canopy resistance, the FAO Penman-Monteith equation has been derived in Chapter 2:

$$ET_o = \frac{0.408\,\Delta\,(R_n - G) + \gamma \dfrac{900}{T + 273} u_2\,(e_s - e_a)}{\Delta + \gamma\,(1 + 0.34\,u_2)} \qquad (6)$$

where

ET_o	reference evapotranspiration [mm day^{-1}],
R_n	net radiation at the crop surface [MJ m^{-2} day^{-1}],
G	soil heat flux density [MJ m^{-2} day^{-1}],
T	air temperature at 2 m height [°C],
u_2	wind speed at 2 m height [m s^{-1}],
e_s	saturation vapour pressure [kPa],
e_a	actual vapour pressure [kPa],
e_s-e_a	saturation vapour pressure deficit [kPa],
Δ	slope vapour pressure curve [kPa $°C^{-1}$],
γ	psychrometric constant [kPa $°C^{-1}$].

The FAO Penman-Monteith equation determines the evapotranspiration from the hypothetical grass reference surface and provides a standard to which evapotranspiration in

different periods of the year or in other regions can be compared and to which the evapotranspiration from other crops can be related.

Calculation procedure

Calculation sheet

ET_o can be estimated by means of the calculation sheet presented in Box 11. The calculation sheet refers to tables in Annex II for the determination of some of the climatic parameters. The calculation procedure consists of the following steps:

1. Derivation of some climatic parameters from the daily maximum (T_{max}) and minimum (T_{min}) air temperature, altitude (z) and mean wind speed (u_2).
2. Calculation of the vapour pressure deficit (e_s-e_a). The saturation vapour pressure (e_s) is derived from T_{max} and T_{min}, while the actual vapour pressure (e_a) can be derived from the dewpoint temperature (T_{dew}), from maximum (RH_{max}) and minimum (RH_{min}) relative humidity, from the maximum (RH_{max}), or from mean relative humidity (RH_{mean}).
3. Determination of the net radiation (R_n) as the difference between the net shortwave radiation (R_{ns}) and the net longwave radiation (R_{nl}). In the calculation sheet, the effect of soil heat flux (G) is ignored for daily calculations as the magnitude of the flux in this case is relatively small. The net radiation, expressed in MJ m^{-2} day^{-1}, is converted to mm/day (equivalent evaporation) in the FAO Penman-Monteith equation by using 0.408 as the conversion factor within the equation.
4. ET_o is obtained by combining the results of the previous steps.

Examples 17 and 20 present typical examples using the calculation sheet.

Computerized calculations

Calculations of the reference crop evapotranspiration ET_o are often computerized. The calculation procedures of all data required for the calculation of ET_o by means of the FAO Penman-Monteith equation are presented in Chapter 3. Typical sequences in which the calculations can be executed are given in the calculation sheets. The procedures presented in Boxes 7 (vapour pressure deficit), 9 (extraterrestrial radiation and daylight hours), 10 (net radiation) and 11 (ET_o) can be used when developing a spreadsheet or computer program to calculate ET_o.

Many software packages already use the FAO Penman-Monteith equation to assess the reference evapotranspiration. As an example, the output of CROPWAT, the FAO software for irrigation scheduling, is presented in Figure 18.

ET_o calculated with different time steps

The selection of the time step with which ET_o is calculated depends on the purpose of the calculation, the accuracy required and the time step of the climatic data available.

BOX 11
Calculation sheet for ET_o (FAO Penman-Monteith) using meteorological tables of Annex 2

Parameters

T_{max}		°C			
T_{min}		°C	$T_{mean} = (T_{max}+T_{min})/2$		°C
T_{mean}		°C	Δ (Table 2.4 of Annex 2)		kPa/°C
Altitude		m	γ (Table 2.2 of Annex 2)		kPa/°C
u_2		m/s	$(1 + 0.34\ u_2)$		
$\Delta\ /\ [\Delta\ +\ \gamma\ (1 + 0.34\ u_2)]$					
$\gamma\ /\ [\Delta\ +\ \gamma\ (1 + 0.34\ u_2)]$					
$[\ 900\ /\ (T_{mean}\ +\ 273)\ ]\ u_2$					

Vapour pressure deficit

T_{max}		°C	$e°(T_{max})$ (Table 2.3)		kPa
T_{min}		°C	$e°(T_{min})$ (Table 2.3)		kPa
Saturation vapour pressure			$e_s = [(e°(T_{max}) + e°(T_{min})]/2$		kPa
e_a derived from dewpoint temperature:					
T_{dew}		°C	$e_a = e°(T_{dew})$ (Table 2.3)		kPa
OR e_a derived from maximum and minimum relative humidity:					
RH_{max}		%	$e°(T_{min})\ RH_{max}/100$		kPa
RH_{min}		%	$e°(T_{max})\ RH_{min}/100$		kPa
			e_a: (average)		kPa
OR e_a derived from maximum relative humidity: (recommended if there are errors in RH_{min})					
RH_{max}		%	$e_a = e°(T_{min})\ RH_{max}/100$		kPa
OR e_a derived from mean relative humidity: (less recommended due to non-linearities)					
RH_{mean}		%	$e_a = e_s\ RH_{mean}/100$		kPa
Vapour pressure deficit			**$(e_s - e_a)$**		kPa

Radiation

Latitude		°			
Day			R_a (Table 2.6)		MJ m^{-2} d^{-1}
Month			N (Table 2.7)		hours
n		hours	n/N		
If no R_s data available: $R_s = (0.25 + 0.50\ n/N)\ R_a$					MJ m^{-2} d^{-1}
$R_{so} = [0.75 + 2\ (Altitude)/\ 100\ 000]\ R_a$					MJ m^{-2} d^{-1}
R_s / R_{so}					
$R_{ns} = 0.77\ R_s$					MJ m^{-2} d^{-1}
T_{max}			$\sigma\ T_{max,K}^4$ (Table 2.8)		MJ m^{-2} d^{-1}
T_{min}			$\sigma\ T_{min,K}^4$ (Table 2.8)		MJ m^{-2} d^{-1}
$(\sigma T_{max,K}^4 + \sigma T_{min,K}^4)/2$					MJ m^{-2} d^{-1}
e_a		kPa	$(0.34 - 0.14\ \sqrt{e_a})$		
R_s/R_{so}			$(1.35\ R_s/R_{so} - 0.35)$		
$R_{nl} = (\sigma T_{max,K}^4 + \sigma T_{min,K}^4)/2\ \ (0.34 - 0.14\ \sqrt{e_a})\ \ (1.35\ R_s/R_{so} - 0.35)$					MJ m^{-2} d^{-1}
$R_n = R_{ns} - R_{nl}$					MJ m^{-2} d^{-1}
T_{month}		°C	G_{day} (assume)	**0**	MJ m^{-2} d^{-1}
$T_{month-1}$		°C	$G_{month} = 0.14\ (T_{month} - T_{month-1})$		MJ m^{-2} d^{-1}
$R_n - G$					MJ m^{-2} d^{-1}
$0.408\ (R_n - G)$					mm/day

Grass reference evapotranspiration

$\left[\frac{\Delta}{\Delta + \gamma\,(1 + 0.34\,u_2)}\right]\ [0.408\ (R_n - G)]$		mm/day
$\left[\frac{\gamma}{\Delta + \gamma\,(1 + 0.34\,u_2)}\right]\left[\frac{900}{T + 273}\right]\ u_2\ [(e_s - e_a)]$		mm/day
$ET_o = \frac{0.408\Delta\ (R_n - G) + \gamma\ \frac{900}{T + 273}\ u_2\ (e_s - e_a)}{\Delta + \gamma\,(1 + 0.34\,u_2)}$		mm/day

FIGURE 18
ET_o computed by CROPWAT

MONTHLY REFERENCE EVAPOTRANSPIRATION PENMAN MONTEITH

Meteostation: CABINDA Country: Angola
Altitude: 20 m. Coordinates: -5.33 South 12.11 East

Month	MinTemp °C	MaxTemp °C	Humid. %	Wind km/day	Sunshine Hours	Radiation MJ/m²/day	ETo-PenMon mm/day
January	22.8	29.6	81	78	4.0	15.7	3.4
February	22.7	30.3	82	69	4.6	16.9	3.7
March	23.0	30.6	80	78	5.1	17.4	3.8
April	23.0	30.2	82	69	5.0	16.4	3.5
May	22.0	28.6	84	69	3.8	13.5	2.9
June	19.2	26.5	81	69	3.3	12.2	2.6
July	17.6	25.1	78	78	3.2	12.3	2.6
August	18.6	25.3	78	78	2.6	12.4	2.6
September	20.5	26.5	78	104	2.0	12.4	2.8
October	22.5	28.0	79	130	2.2	12.9	3.1
November	23.0	28.7	80	104	3.2	14.4	3.3
December	23.0	29.1	82	95	3.8	15.2	3.4
Year	21.5	28.2	80	85	3.6	14.3	3.1

CROPWAT 7.0 Climate file: C:\PROF-P~1\CROPWAT\CROPWAT\CLI\CABINDA.PEN 03/07/98

Ten-day or monthly time step

Notwithstanding the non-linearity in the Penman-Monteith equation and some weather parameter methods, mean ten-day or monthly weather data can be used to compute the mean ten-day or monthly values for the reference evapotranspiration. The value of the reference evapotranspiration calculated with mean monthly weather data is indeed very similar to the average of the daily ET_o values calculated with daily average weather data for that month.

The meteorological data consist of:

- Air temperature: ten-day or monthly average daily maximum (T_{max}) and average daily minimum temperature (T_{min}).
- Air humidity: ten-day or monthly average of the daily actual vapour pressure (e_a) derived from psychrometric, dewpoint or relative humidity data.
- Wind speed: ten-day or monthly average of daily wind speed data measured at 2 m height (u_2).
- Radiation: ten-day or monthly average of daily net radiation (R_n) computed from the mean ten-day or monthly measured shortwave radiation or from actual duration of daily sunshine hours (n). The extraterrestrial radiation (R_a) and daylight hours (N) for a specific day of the month can be computed using Equations 21 and 34 or can be selected from Tables 2.5 and 2.6 in Annex 2.

When the soil is warming (spring) or cooling (autumn), the soil heat flux (G) for monthly periods may become significant relative to the mean monthly R_n. In these cases G cannot be ignored and its value should be determined from the mean monthly air temperatures of the previous and next month. Chapter 3 outlines the calculation procedure (Equations 43 and 44).

EXAMPLE 17
Determination of ET_o with mean monthly data

Given the monthly average climatic data of April of Bangkok (Thailand) located at 13 °44'N and at an elevation of 2 m:

-	Monthly average daily maximum temperature (T_{max}) =	34.8	°C
-	Monthly average daily minimum temperature (T_{min}) =	25.6	°C
-	Monthly average daily vapour pressure (e_a) =	2.85	kPa
Measured at 2 m	Monthly average daily wind speed (u_2) =	2	m/s
-	Monthly average sunshine duration (n) =	8.5	hours/day
For April	Mean monthly average temperature ($T_{month,i}$) =	30.2	°C
For March	Mean monthly average temperature ($T_{month,i-1}$) =	29.2	°C

Determination according to outline of Box 11 (calculation sheet ET_o)

Parameters			
- From Table 2.4 or Eq. 13:	T_{mean} = [(T_{max} = 34.8) + (T_{min} = 25.6)]/2 = Δ =	30.2 0.246	°C kPa/°C
From Table 2.1 and Table 2.2 or Eq. 7 and Eq. 8:	Altitude = P = γ =	2 101.3 0.0674	m kPa kPa/°C
-	(1 + 0.34 u_2) =	1.68	-
-	$\Delta/[\Delta+\gamma(1+0.34u_2)]$ =0.246/[(0.246 + 0.0674 (1.68)] =	0.685	-
-	$\gamma/[\Delta+\gamma(1+0.34u_2)]$ = 0.0667/[0.246 + 0.0674 (1.68)] =	0.188	-
-	900/(T_{mean}+273) u_2 =	5.94	-

Vapour pressure deficit

From Table 2.3 or Eq. 11:	T_{max} = e°(T_{max}) =	34.8 5.56	°C kPa
From Table 2.3 or Eq. 11:	T_{min} = e°(T_{min}) =	25.6 3.28	°C kPa
- Given	e_s = (5.56 + 3.28)/2 = e_a =	4.42 2.85	kPa kPa
-	Vapour pressure deficit (e_s-e_a) = (4.42 - 2.85) =	1.57	kPa

Radiation (for month = April)			
From Table 2.6 or 2.5 or Eq. 21:	J = (for 15 April) Latitude = 13°44'N = (13 + 44/60)= R_a =	105 13.73 38.06	- °N MJ m^{-2} day^{-1}
N (Table 2.7 or Eq. 34):	Daylength N =	12.31	hours
-	n/N = (8.5/12.31) =	0.69	-
-	R_s = [0.25 + 0.50 (0.69)] 38.06 =	22.65	MJ m^{-2} day^{-1}
-	R_{so} = (0.75 + 2 (2)/100 000) 38.06 =	28.54	MJ m^{-2} day^{-1}
-	R_s/R_{so} = (22.65/28.54) =	0.79	-
-	R_{ns} = 0.77 (22.65) =	17.44	MJ m^{-2} day^{-1}
From Table 2.8:	T_{max} = $\sigma T_{max,K}^4$ =	34.8 44.10	°C MJ m^{-2} day^{-1}
From Table 2.8:	T_{min} = $\sigma T_{min,K}^4$ =	25.6 39.06	°C MJ m^{-2} day^{-1}
-	$(\sigma T_{max,K}^4 + \sigma T_{min,K}^4)/2$ = (44.10 + 39.06)/2 =	41.58	MJ m^{-2} day^{-1}
For: Then:	e_a = $(0.34-0.14\sqrt{e_a})$ =	2.85 0.10	kPa -
For: Then:	R_s/R_{so} = $(1.35\ R_s/R_{so} - 0.35)$ =	0.79 0.72	- -
- - - - -	R_{nl} = 41.58 (0.10) 0.72 = R_n = (17.44 - 3.11) = G = 0.14 (30.2 - 29.2) = $(R_n - G)$ = (14.33 - 0.14) = 0.408 $(R_n - G)$ =	3.11 14.33 0.14 14.19 5.79	MJ m^{-2} day^{-1} MJ m^{-2} day^{-1} MJ m^{-2} day^{-1} MJ m^{-2} day^{-1} mm/day
Grass reference evapotranspiration			
- - - - -	0.408 (R_n-G) $\Delta/[\Delta+\gamma(1+0.34u_2)]$ = (5.79) 0.685 = $900u_2/(T+273)$ (e_s-e_a) $\gamma/[\Delta+\gamma(1+0.34u_2)]$ = 5.94(1.57)0.188 = ET_o = (3.97 + 1.75) =	 3.97 1.75 5.72	 mm/day mm/day mm/day
The grass reference evapotranspiration is 5.7 mm/day.			

Daily time step

Calculation of ET_o with the Penman-Monteith equation on 24-hour time scales will generally provide accurate results. The required meteorological data consist of:

- Air temperature: maximum (T_{max}) and minimum (T_{min}) daily air temperatures.
- Air humidity: mean daily actual vapour pressure (e_a) derived from psychrometric, dewpoint temperature or relative humidity data.
- Wind speed: daily average for 24 hours of wind speed measured at 2 m height (u_2).
- Radiation: net radiation (R_n) measured or computed from solar and longwave radiation or from the actual duration of sunshine (n). The extraterrestrial radiation (R_a) and daylight hours (N) for a specific day of the month should be computed using Equations 21 and 34. As the magnitude of daily soil heat flux (G) beneath the reference grass surface is relatively small, it may be ignored for 24-hour time steps.

EXAMPLE 18
Determination of ET_o with daily data

Given the meteorological data as measured on 6 July in Uccle (Brussels, Belgium) located at 50°48'N and at 100 m above sea level:

-	Maximum air temperature (T_{max}) =	21.5	°C
-	Minimum air temperature (T_{min}) =	12.3	°C
-	Maximum relative humidity (RH_{max}) =	84	%
-	Minimum relative humidity (RH_{min}) =	63	%
-	Wind speed measured at 10 m height =	10	km/h
-	Actual hours of sunshine (n) =	9.25	hours
Conversion of wind speed			
At 10 m height	Wind speed = 10 km/h or u_z =	2.78	m/s
From Eq. 47, with z = 10 m:	At standard height, $u_2 = 0.748\ (2.78)$ =	2.078	m/s
Parameters			
From Eq. 7, for:	altitude = P =	100 100.1	m kPa
-	$T_{mean} = (21.5 + 12.3)/2$ =	16.9	°C
From Eq. 13, for:	T_{mean} = Δ =	16.9 0.122	°C kPa/°C
From Eq. 8, for:	P = γ =	100.1 0.0666	kPa kPa/°C
-	$(1 + 0.34\ u_2)$ =	1.71	-
- -	$\Delta/[\Delta+\gamma(1+0.34u_2)]$ = $0.122/[(0.122 + 0.0666\ (1.71)]$ =	0.518	-
- -	$\gamma/[\Delta+\gamma(1+0.34u_2)]$ = $0.0666/[0.122 + 0.0666\ (1.71)]$ =	0.282	-
-	$900/(T_{mean}+273)\ u_2$ =	6.450	-

Vapour pressure deficit			
From Eq. 11, for: Then:	T_{max} = $e°(T_{max})$ =	21.5 2.564	°C kPa
From Eq. 11, for: Then:	T_{min} = $e°(T_{min})$ =	12.3 1.431	°C kPa
-	e_s = (2.564 + 1.431) =	1.997	kPa
Given relative humidity data	RH_{max} = RH_{min} =	84 63	% %
From Eq. 17:	e_a = [1.431 (0.84) + 2.564 (0.63)]/2 =	1.409	kPa
-	Vapour pressure deficit (e_s-e_a) = (1.997 - 1.409) =	0.589	kPa
Radiation			
From Table 2.5:	Month 7, Day = 6 J =	 187	 -
From Eq. 21:	Latitude = 50°48'N = J = R_a =	50.80 187 41.09	°N - MJ m^{-2} day^{-1}
From Eq. 34:	Latitude = 50°48'N = J = N = 16.1 n/N = 9.25/16.3 =	50.80 187 16.1 0.57	°N - hours -
From Eq. 35 From Eq. 37 - From Eq. 38	R_s = [0.25 + 0.50 (0.57)] 41.09 R_{so} = (0.75 + 2 (100)/100 000) 41.09 = R_s/R_{so} = R_{ns} = 0.77 (22.07) =	22.07 30.90 0.71 17.00	MJ m^{-2} day^{-1} MJ m^{-2} day^{-1} - MJ m^{-2} day^{-1}
For: Then: For: Then: - -	T_{max} = $T_{max,K}$ = 21.5 + 273.16 = $\sigma T_{max,K}^4$ = T_{min} = $T_{min,K}$ = 12.3 + 273.16 = $\sigma T_{min,K}^4$ = $(\sigma T_{max,K}^4 + \sigma T_{min,K}^4)/2$ = (36.96 + 32.56)/2 = (0.34-0.14$\sqrt{e_a}$) =	21.5 294.7 36.96 12.3 285.5 32.56 34.76 0.17	°C K MJ m^{-2} day^{-1} °C K MJ m^{-2} day^{-1} MJ m^{-2} day^{-1} -
- From Eq. 39 From Eq. 40 From Eq. 42 - -	(1.35(R_s/R_{so})-0.35) = R_{nl} = 34.76 (0.17) 0.61 = R_n = (17.00 - 3.71) = G = (R_n - G) = (13.28 - 0) = 0.408 (R_n-G) =	0.61 3.71 13.28 0 13.28 5.42	- MJ m^{-2} day^{-1} MJ m^{-2} day^{-1} MJ m^{-2} day^{-1} MJ m^{-2} day^{-1} mm/day
Grass reference evapotranspiration			
- - - -	0.408 (R_n-G) $\Delta/[\Delta+\gamma(1+0.34u_2)]$ = 900/(T+273) u_2 (e_s-e_a) $\gamma/[\Delta+\gamma(1+0.34u_2)]$ = ET_o (Eq. 6) = 2.81 + 1.07 = 3.88 ≈	2.81 1.07 3.9	mm/day mm/day mm/day
The grass reference evapotranspiration is 3.9 mm/day.			

Hourly time step

In areas where substantial changes in wind speed, dewpoint or cloudiness occur during the day, calculation of the ET_o equation using hourly time steps is generally better than using 24-hour calculation time steps. Such weather changes can cause 24-hour means to misrepresent evaporative power of the environment during parts of the day and may introduce error into the calculations. However, under most conditions, application of the FAO Penman-Monteith equation with 24-hour data produces accurate results.

With the advent of electronic, automated weather stations, weather data are increasingly reported for hourly or shorter periods. Therefore, in situations where calculations are computerized, the FAO Penman-Monteith equation can be applied on an hourly basis with good results. When applying the FAO Penman-Monteith equation on an hourly or shorter time scale, the equation and some of the procedures for calculating meteorological data should be adjusted for the smaller time step. The FAO Penman-Monteith equation for hourly time steps is:

$$ET_o = \frac{0.408\Delta(R_n - G) + \gamma \frac{37}{T_{hr} + 273} u_2 (e^o(T_{hr}) - e_a)}{\Delta + \gamma(1 + 0.34\, u_2)} \qquad (53)$$

where
- ET_o reference evapotranspiration [mm $hour^{-1}$],
- R_n net radiation at the grass surface [MJ m^{-2} $hour^{-1}$] (Equation 40),
- G soil heat flux density [MJ m^{-2} $hour^{-1}$] (Equations 45 and 46),
- T_{hr} mean hourly air temperature [°C],
- Δ saturation slope vapour pressure curve at T_{hr} [kPa $°C^{-1}$] (Equation 13),
- γ psychrometric constant [kPa $°C^{-1}$] (Equation 8),
- $e°(T_{hr})$ saturation vapour pressure at air temperature T_{hr} [kPa] (Equation 11),
- e_a average hourly actual vapour pressure [kPa] (Equation 54),
- u_2 average hourly wind speed [m s^{-1}].

Given relative humidity measurements, the actual vapour pressure is determined as:

$$e_a = e^o(T_{hr}) \frac{RH_{hr}}{100} \qquad (54)$$

where
- e_a average hourly actual vapour pressure [kPa],
- $e°(T_{hr})$ saturation vapour pressure at air temperature T_{hr} [kPa] (Equation 11),
- RH_{hr} average hourly relative humidity [%].

The net radiation is the difference between the net shortwave radiation (R_{ns}) and the net longwave radiation (R_{nl}) at the hourly time steps. Consequently:

- If R_{ns} and R_{nl} need to be calculated, the extraterrestrial radiation value (R_a) for the hourly period (Equation 28) should be used.
- In the computation of R_{nl} by means of Equation 39, $(\sigma T_{max,K}^4 + \sigma T_{min,K}^4)/2$ is replaced by $\sigma T_{hr,K}^4$ and the Stefan-Boltzman constant becomes:
  $\sigma = (4.903/24)\ 10^{-9} = 2.043\ 10^{-10}$ MJ m^{-2} $hour^{-1}$.

Since the ratio R_s/R_{so} is used to represent cloud cover, when calculating R_{nl} for hourly periods during the nighttime, the ratio R_s/R_{so} can be set equal to the R_s/R_{so} calculated for a time period occurring 2-3 hours before sunset, before the sun angle becomes small. This will generally serve as a good approximation of cloudiness occurring during the subsequent nighttime. The hourly period that is 2 to 3 hours before sunset can be identified during computation of R_a as the period where ω, calculated from Equation 31, is within the range $(\omega_s - 0.79) \leq \omega \leq (\omega_s - 0.52)$, where ω_s is calculated using Equation 25. As a more approximate alternative, one can assume $R_s/R_{so} = 0.4$ to 0.6 during nighttime periods in humid and subhumid climates and $R_s/R_{so} = 0.7$ to 0.8 in arid and semiarid climates. A value of $R_s/R_{so} = 0.3$ presumes total cloud cover.

Soil heat flux is important for hourly calculations. Equations 45 and 46 can be used to derive G for the hourly periods.

The required meteorological data consist of:

- Air temperature: mean hourly temperature (T_{hr}).
- Air humidity: average hourly relative humidity (RH_{hr}).
- Wind speed: average hourly wind speed data measured at 2 m height (u_2).
- Radiation: total hourly solar (R_s) or net radiation (R_n).

Because of the need for standardization, the constants in Equation 53 presume a constant surface resistance (r_s) of 70 s/m during all periods. This constant resistance may cause some underprediction of hourly ET_o during some daytime periods when actual r_s may be somewhat lower. The constant resistance may cause some overprediction of hourly ET_o during evening periods when actual r_s may be somewhat higher. However, when the calculations of hourly ET_o from Equation 53 are summed over 24 hour periods to produce an equivalent 24-hour ET_o, the hourly differences tend to compensate one another and the results are generally equivalent to calculations of ET_o made on a 24-hour time step. Precise estimates of ET_o for specific hourly periods may require the use of aerodynamic stability functions and functions for modifying the value for r_s based on levels of radiation, humidity and temperature. Application of these functions are not normally required when hourly calculations are to be summed to 24-hour totals. Therefore, these functions are not described here.

EXAMPLE 19
Determination of ET_o with hourly data

Given mean average hourly data between 02.00 and 03.00 hours and 14.00 and 15.00 hours on 1 October in N'Diaye (Senegal) at 16°13'N and 16°15'W and 8 m above sea level. In the absence of calibrated coefficients, indicative values for a_s and b_s (Eq. 35 Angstrom formula) and for the coefficients of the net longwave radiation (Eq. 39) are used.

Measured climatic data		02.00-03.00 h	14.00-15.00 h	Units
T_{hr}: mean hourly temperature =		28	38	°C
RH_{hr}: mean hourly relative humidity =		90	52	%
u_2: mean hourly wind speed =		1.9	3.3	m/s
R_s: total solar radiation =		-	2.450	MJ m^{-2} $hour^{-1}$
Parameters				
From Eq. 13	Δ =	0.220	0.358	kPa $°C^{-1}$
From Eq. 8	γ =	0.0673	0.0673	kPa $°C^{-1}$
Vapour pressure deficit				
From Eq. 11	$e°(T)$ =	3.780	6.625	kPa
From Eq. 54	e_a =	3.402	3.445	kPa
-	$e_s - e_a$ =	0.378	3.180	kPa

Extraterrestrial radiation		02.00-03.00 h	14.00-15.00 h	Units
From Table 2.5 for 1 October:	J = 274			-
From Eq. 22:	$\varphi = \pi/180$ (16.22) = 0.2830			rad
From Eq. 23:	d_r = 1.0001			-
From Eq. 24:	δ = - 0.0753			rad
From Eq. 33:	b = 3.3315			-
From Eq. 32:	S_c = 0.1889			hour
-	L_z = 15			degrees
-	L_m = 16.25			degrees
-	t =	2.5	14.5	hour
From Eq. 31:	ω =	-2.46	0.682	rad
-	t_l =	1	1	hour
From Eq. 29:	ω_1 =	-	0.5512	rad
From Eq. 30:	ω_2 =	-	0.8130	rad
From Eq. 28:	R_a =	0	3.543	MJ m^{-2} $hour^{-1}$
Radiation				
Given	R_s =	0	2.450	MJ m^{-2} $hour^{-1}$
From Eq. 37:	R_{so} =	0	2.658	MJ m^{-2} $hour^{-1}$
From Eq. 38:	R_{ns} =	0	1.887	MJ m^{-2} $hour^{-1}$
-	σT_K^4 =	1.681	1.915	MJ m^{-2} $hour^{-1}$
-	(0.34-0.14 $\sqrt{e_a}$) =	0.082	0.080	-
-	R_s/R_{so} =	0.8 (assumed)	0.922	-
-	(1.35 R_s/R_{so} - 0.35) =	0.730	0.894	-
From Eq. 39:	R_{nl} =	0.100	0.137	MJ m^{-2} $hour^{-1}$
From Eq. 40:	R_n =	-0.100	1.749	MJ m^{-2} $hour^{-1}$
From Eq. 46, 45:	G =	-0.050	0.175	MJ m^{-2} $hour^{-1}$
-	(R_n - G) =	-0.050	1.574	MJ m^{-2} $hour^{-1}$
-	0.408(R_n - G) =	-0.020	0.642	mm/hour
Grass reference evapotranspiration				
-	0.408(R_n-G)			
-	$\Delta/[\Delta+\gamma(1+0.34u_2)]$ =	-0.01	0.46	mm/hour
	37/(T+273) u_2 (e_s-e_a)			
From Eq. 53:	$\gamma/[\Delta+\gamma(1 +0.34u_2)$=	0.01	0.17	mm/hour
	ET_o =	0.00	0.63	mm/hour
The grass reference evapotranspiration is 0.00 mm/hour between 02.00 and 03.00 hours and 0.63 mm/hour between 14.00 and 15.00 hours.				

CALCULATION PROCEDURES WITH MISSING DATA

The meteorological data, required to estimate ET_o by means of the FAO Penman-Monteith equation, consist of air temperature, air humidity, wind speed and radiation. Where some of these data are missing or cannot be calculated, it is strongly recommended that the user estimate the missing climatic data with one of the procedures presented in Chapter 3 and that the FAO Penman-Monteith method be used for the calculation of ET_o. The use of an alternative ET_o calculation procedure, requiring only limited meteorological parameters, is less recommended.

Example 20 illustrates the estimation of monthly ET_o with the FAO Penman-Monteith for a data set containing only maximum and minimum air temperature. The procedures given in Chapter 3 to estimate missing humidity, radiation and wind speed data should be validated by comparing ET_o calculated with full and with limited data sets for weather stations in the region with complete data sets.

EXAMPLE 20
Determination of ET_o with missing data

Given the monthly average daily maximum and average daily minimum air temperature of July from a station near Lyon, France (45°43' N, altitude 200 m). No other climatic data were recorded.

-	Monthly average daily maximum temperature (T_{max}) =	26.6	°C
-	Monthly average daily minimum temperature (T_{min}) =	14.8	°C

Determination according to Box 11 (calculation sheet ET_o)

Estimation of wind speed:
2 m/s is used as a temporary estimate. Due to the relatively small crop height of 0.12 m of the reference crop and the appearance of u_2 in both the nominator and denominator of the FAO Penman-Monteith equation, ET_o is not highly sensitive to normal ranges of wind speed.

Parameters:

-	T_{mean} = (26.6 + 14.8)/2 =	20.7	°C
From Table 2.4 or Eq. 13:	T_{mean} =	20.7	°C
	Δ =	0.150	kPa/°C
From Table 2.2 or Eq. 8:	Altitude =	200	m
	γ =	0.066	kPa/°C
-	(1 + 0.34 u_2) = (1 + 0.34 (2)) =	1.68	-
-	$\Delta/[\Delta+\gamma(1+0.34u_2)]$ =0.150/[(0.150 + 0.066 (1.68)] =	0.576	-
-	$\gamma/[\Delta+\gamma(1+0.34u_2)]$ = 0.0658/[0.150 + 0.066 (1.68)] =	0.252	-
-	900/(T_{mean}+273) u_2 =	6.13	-

Estimation of humidity data:

Assume (Eq. 48):	$T_{dew} \approx T_{min}$ =	14.8	°C
Consequently (Eq. 14 or Table 2.3) for:	T_{dew} =	14.8	°C
Then	e_a =	1.68	kPa
From Table 2.3 or Eq. 11, for:	T_{max} =	26.6	°C
Then:	$e°(T_{max})$ =	3.48	kPa
From Table 2.3 or Eq. 11, for: Then:	T_{min} =	14.8	°C
	$e°(T_{min})$ =	1.68	kPa
-	e_s = (3.48 + 1.68)/2 =	2.58	kPa
-	(e_s-e_a) = (2.58 - 1.68) =	0.90	kPa
This corresponds with:			
-	RH_{max} = 100 $e_a/e°(T_{min})$ =	100	%
-	RH_{min} = 100 $e_a/e°(T_{max})$ = 100 (1.68/3.48) =	48	%
-	RH_{mean} = (RH_{max} + RH_{min})/2 =	74	%

Estimation of radiation data:

R_s can be derived from the difference between T_{max} and T_{min}:

From Eq. 50	$R_s = 0.16 \sqrt{(26.6-14.8)}\ R_a$	-	MJ m^{-2} day^{-1}
-	$R_s = 0.55\ R_a$	-	MJ m^{-2} day^{-1}
Table 2.6 or Eq. 21, for:	For Day 15, Month = July, J =	196	-
	Latitude = 45°43'N =	45.72	°N
Then:	R_a =	40.55	MJ m^{-2} day^{-1}
-	$R_s = 0.55\ R_a = 0.55\ (40.55)$ =	22.29	MJ m^{-2} day^{-1}
-	$R_{so} = (0.75 + 2\ (200)/100\ 000)\ 40.55$ =	30.58	MJ m^{-2} day^{-1}
-	R_s/R_{so} =	0.73	-
-	$R_{ns} = 0.77\ (22.29)$ =	17.16	MJ m^{-2} day^{-1}
Table 2.8, for:	T_{max} = 26.6°C	26.6	°C
	$T_{max,K} = 26.6 + 273.16$ =	299.76	K
Then:	$\sigma T_{max,K}^4$	39.59	MJ m^{-2} day^{-1}
Table 2.8, for:	T_{min} = 14.8°C	14.8	°C
	$T_{min,K} = 14.8 + 273.16$	287.96	K
Then:	$\sigma T_{min,K}^4$	33.71	MJ m^{-2} day^{-1}
-	$(\sigma T_{max,K}^4 + \sigma T_{min,K}^4)/2 = (39.59 + 33.71)/2$ =	36.65	MJ m^{-2} day^{-1}
For:	e_a =	1.68	kPa
Then:	$(0.34-0.14\sqrt{e_a})$ =	0.16	-
For:	R_s/R_{so} =	0.73	-
Then:	$(1.35\ R_s/R_{so} - 0.35)$ =	0.63	-
-	$R_{nl} = 36.65\ (0.16)\ 0.63$ =	3.68	MJ m^{-2} day^{-1}
-	$R_n = (17.16 - 3.68)$ =	13.48	MJ m^{-2} day^{-1}
Assume:	G =	0	MJ m^{-2} day^{-1}
-	$(R_n - G) = (13.48 - 0)$ =	13.48	MJ m^{-2} day^{-1}
-	$0.408\ (R_n - G)$ =	5.50	mm/day
Grass reference evapotranspiration:			
-	$0.408\ (R_n-G)\ \Delta/[\Delta+\gamma(1+0.34u_2)]$ =	3.17	mm/day
-	$900/(T+273)\ u_2\ (e_s-e_a)\ \gamma/[\Delta+\gamma(1+0.34u_2)]$ =	1.39	mm/day
-	$ET_o = (3.17 + 1.39)$ =	4.56	mm/day
The estimated grass reference evapotranspiration is 4.6 mm/day. If instead of 2 m/s, the wind speed is estimated as 1 or 3 m/s, ET_o would have been 7% lower (4.2 mm/day) or 6% higher (4.8 mm/day) respectively. In comparison, the Hargreaves equation (Equation 52) predicts ET_o = 5.0 mm/day			

PAN EVAPORATION METHOD

Pan evaporation

The evaporation rate from pans filled with water is easily obtained. In the absence of rain, the amount of water evaporated during a period (mm/day) corresponds with the decrease in water depth in that period. Pans provide a measurement of the integrated effect of radiation, wind, temperature and humidity on the evaporation from an open water surface. Although the pan responds in a similar fashion to the same climatic factors affecting crop transpiration, several factors produce significant differences in loss of water from a water surface and from a cropped surface. Reflection of solar radiation from water in the shallow pan might be different from the assumed 23% for the grass reference surface. Storage of heat within the pan can be appreciable and may cause significant evaporation during the night while most crops transpire only during the daytime. There are also differences in turbulence, temperature and humidity of the air immediately above the respective surfaces. Heat transfer through the sides of the pan occurs and affects the energy balance.

Notwithstanding the difference between pan-evaporation and the evapotranspiration of cropped surfaces, the use of pans to predict ETo for periods of 10 days or longer may be warranted. The pan evaporation is related to the reference evapotranspiration by an empirically derived pan coefficient:

$$ET_o = K_p \, E_{pan} \qquad (55)$$

where ET_o reference evapotranspiration [mm/day],
K_p pan coefficient [-],
E_{pan} pan evaporation [mm/day].

Pan coefficient (K_p)

Pan types and environment

Different types of pans exist. Descriptions of Class A and Colorado sunken pans are given in Boxes 12 and 13. As the colour, size, and position of the pan have a significant influence on the measured results, the pan coefficients are pan specific.

In selecting the appropriate pan coefficient, not only the pan type, but also the ground cover in the station, its surroundings as well as the general wind and humidity conditions, should be checked. The siting of the pan and the pan environment also influence the results. This is particularly so where the pan is placed in fallow rather than cropped fields. Two cases are commonly considered: Case A where the pan is sited on a short green (grass) cover and surrounded by fallow soil; and Case B where the pan is sited on fallow soil and surrounded by a green crop (Figure 19).

FIGURE 19
Two cases of evaporation pan siting and their environment

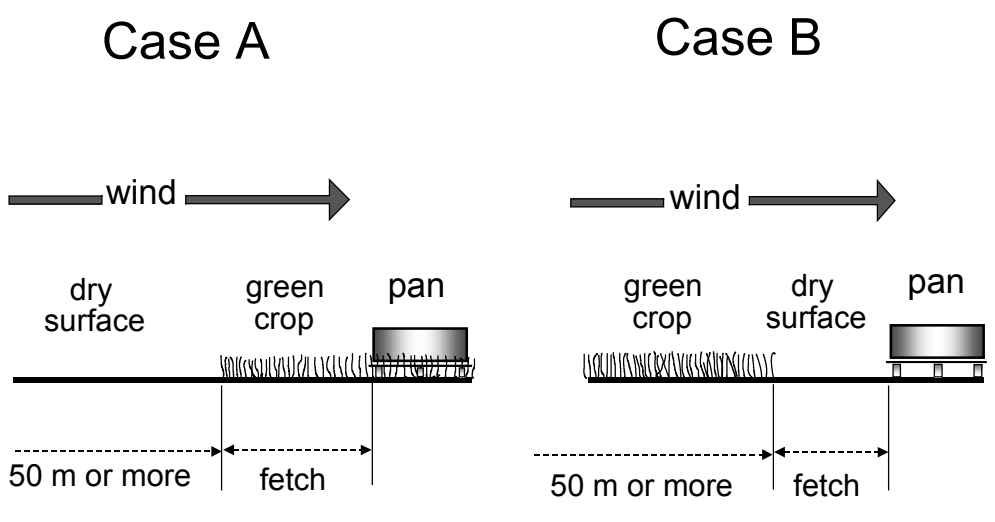

Pan coefficients

Depending on the type of pan and the size and state of the upwind buffer zone (fetch), pan coefficients will differ. The larger the upwind buffer zone, the more the air moving over the pan will be in equilibrium with the buffer zone. At equilibrium with a large fetch, the air contains more water vapour and less heat in Case A than in Case B. Pan coefficients for the Class A pan and for the Colorado sunken pan for different ground cover, fetch and climatic conditions are presented in Tables 5 and 6. Regression equations derived from the tables are presented in Table 7. Where measured data from other types of sunken pans are available, such data should first be related to Colorado sunken pan data or to the FAO Penman-Monteith equation to develop K_p. Ratios between evaporation from sunken pans and from the Colorado sunken pan for different climatic conditions and pan environment are given in Table 8.

Where data are missing, wind speed can be estimated by taking a global value of $u_2 = 2$ m s^{-1} or as indicated in Table 4 (page 63). RH_{mean} can be approximated from air temperature as $RH_{mean} = 50\ e^o(T_{min})/e^o(T_{max}) + 50$.

Adjustments

Under some conditions not accounted for in the tables, the presented K_p coefficients may need some adjustment. This is the case in areas with no agricultural development, or where the pans are enclosed by tall crops. Not maintaining the standard colour of the pan or installing screens can affect the pan readings and will require some adjustment of the pan coefficient.

In areas with no agricultural development and extensive areas of bare soils (large fetch, Case B), as found under desert or semi-desert conditions, the listed values for K_p given for arid, windy areas may need to be reduced by up to 20%; for areas with moderate levels of wind, temperature and relative humidity, the listed values may need to be reduced by 5-10%; no or little reduction in K_p is needed in humid, cool conditions.

Where pans are placed in a small enclosure but surrounded by tall crops, for example 2.5 m high maize, the listed pan coefficients will need to be increased by up to 30% for dry windy climates whereas only a 5-10% increase is required for calm, humid conditions.

Painting the pans may affect the pan evaporation. The pan coefficients presented apply to galvanized pans annually painted with aluminium and to stainless steel pans. Little difference in E_{pan} will occur where the inside and outside surfaces of the pan are painted white. An increase in E_{pan} of up to 10% may occur when they are painted black. The material from which the pan is made may account for variations of only a few percent.

The level at which the water is maintained in the pan is important; resulting errors may be up to 15% when water levels in the Class A pan fall 10 cm below the accepted standard of between 5 and 7.5 cm below the rim. Screens mounted over pans will reduce E_{pan} by up to 10%. In an attempt to avoid pans being used by birds for drinking, pans filled to the rim with water can be placed near the Class A pan; birds may prefer to use the fully filled pan. The evaporation pan should be placed in a large, secure, wire enclosure to prevent animals from entering and drinking. The turbidity of the water in the pan usually does not affect E_{pan} by more than 5%. The overall variation in E_{pan} is not constant with time because of ageing, deterioration and repainting.

TABLE 5
Pan coefficients (K_p) for Class A pan for different pan siting and environment and different levels of mean relative humidity and wind speed (FAO Irrigation and Drainage Paper No. 24)

Class A pan	Case A: Pan placed in short green cropped area				Case B: Pan placed in dry fallow area			
RH mean (%) →		low < 40	medium 40 -70	high > 70		low < 40	medium 40 -70	high > 70
Wind speed (m s^{-1})	Windward side distance of green crop (m)				Windward side distance of dry fallow (m)			
Light	1	.55	.65	.75	1	.7	.8	.85
< 2	10	.65	.75	.85	10	.6	.7	.8
	100	.7	.8	.85	100	.55	.65	.75
	1 000	.75	.85	.85	1 000	.5	.6	.7
Moderate	1	.5	.6	.65	1	.65	.75	.8
2-5	10	.6	.7	.75	10	.55	.65	.7
	100	.65	.75	.8	100	.5	.6	.65
	1 000	.7	.8	.8	1 000	.45	.55	.6
Strong	1	.45	.5	.6	1	.6	.65	.7
5-8	10	.55	.6	.65	10	.5	.55	.65
	100	.6	.65	.7	100	.45	.5	.6
	1 000	.65	.7	.75	1 000	.4	.45	.55
Very strong	1	.4	.45	.5	1	.5	.6	.65
> 8	10	.45	.55	.6	10	.45	.5	.55
	100	.5	.6	.65	100	.4	.45	.5
	1 000	.55	.6	.65	1 000	.35	.4	.45

TABLE 6
Pan coefficients (K_p) for Colorado sunken pan for different pan siting and environment and different levels of mean relative humidity and wind speed (FAO Irrigation and Drainage Paper No. 24)

Sunken Colorado	Case A: Pan placed in short green cropped area				Case B: Pan placed in dry fallow area (1)			
RH mean (%) →		low < 40	medium 40 -70	high > 70		low < 40	medium 40 -70	high > 70
Wind speed (m s^{-1})	Windward side distance of green crop (m)				Windward side distance of dry fallow (m)			
Light	1	.75	.75	.8	1	1.1	1.1	1.1
< 2	10	1.0	1.0	1.0	10	.85	.85	.85
	≥ 100	1.1	1.1	1.1	100	.75	.75	.8
					1 000	.7	.7	.75
Moderate	1	.65	.7	.7	1	.95	.95	.95
2-5	10	.85	.85	.9	10	.75	.75	.75
	≥ 100	.95	.95	.95	100	.65	.65	.7
					1 000	.6	.6	.65
Strong	1	.55	.6	.65	1	.8	.8	.8
5-8	10	.75	.75	.75	10	.65	.65	.65
	≥ 100	.8	.8	.8	100	.55	.6	.65
					1 000	.5	.55	.6
Very strong	1	.5	.55	.6	1	.7	.75	.75
> 8	10	.65	.7	.7	10	.55	.6	.65
	≥ 100	.7	.75	.75	100	.5	.55	.6
					1 000	.45	.5	.55

(1) For extensive areas of bare-fallow soils and no agricultural development, reduce K_{pan} by 20% under hot, windy conditions; by 5-10% for moderate wind, temperature and humidity conditions.

TABLE 7
Pan coefficients (K_p): regression equations derived from Tables 5 and 6

Class A pan with green fetch	$K_p = 0.108 - 0.0286\, u_2 + 0.0422 \ln(FET) + 0.1434 \ln(RH_{mean}) - 0.000631 [\ln(FET)]^2 \ln(RH_{mean})$
Class A pan with dry fetch	$K_p = 0.61 + 0.00341\, RH_{mean} - 0.000162\, u_2 RH_{mean} - 0.00000959\, u_2 FET + 0.00327\, u_2 \ln(FET) - 0.00289\, u_2 \ln(86.4\, u_2) - 0.0106 \ln(86.4\, u_2) \ln(FET) + 0.00063 [\ln(FET)]^2 \ln(86.4\, u_2)$
Colorado sunken pan with green fetch	$K_p = 0.87 + 0.119 \ln(FET) - 0.0157 [\ln(86.4\, u_2)]^2 - 0.0019 [\ln(FET)]^2 \ln(86.4\, u_2) + 0.013 \ln(86.4\, u_2) \ln(RH_{mean}) - 0.000053 \ln(86.4\, u_2) \ln(FET) RH_{mean}$
Colorado sunken pan with dry fetch	$K_p = 1.145 - 0.080 u_2 + 0.000903 (u_2)^2 \ln(RH_{mean}) - 0.0964 \ln(FET) + 0.0031 u_2 \ln(FET) + 0.0015 [\ln(FET)]^2 \ln(RH_{mean})$
Coefficients and parameters	K_p pan coefficient [ ] u_2 average daily wind speed at 2 m height (m s^{-1}) RH_{mean} average daily relative humidity [%] = (RH_{max} + RH_{min})/2 FET fetch, or distance of the identified surface type (grass or short green agricultural crop for case A, dry crop or bare soil for case B upwind of the evaporation pan)
Range for variables	1 m ≤ FET ≤ 1 000 m (these limits must be observed) 30% ≤ RH_{mean} ≤ 84% 1 m s^{-1} ≤ u_2 ≤ 8 m s^{-1}

Recommendations

The above considerations and adjustments indicate that the use of tables or the corresponding equations may not be sufficient to consider all local environmental factors influencing K_p and that local adjustment may be required. To do so, an appropriate calibration of E_{pan} against ET_o computed with the Penman-Monteith method is recommended.

It is recommended that the pan should be installed inside a short green cropped area with a size of a square of at least 15 by 15 m. The pan should not be installed in the centre but at a distance of at least 10 m from the green crop edge in the general upwind direction.

Where observations of wind speed and relative humidity, required for the computation of K_p, are not available at the site, estimates of the weather variables from a nearby station have to be utilized. It is then recommended that these variables be averaged for the computation period and that E_{pan} be averaged for the same period.

Equation 1 in Table 7 yields $K_p = 0.83$ for data in Example 21 as shown in Example 22.

TABLE 8
Ratios between the evaporation from sunken pans and a Colorado sunken pan for different climatic conditions and environments (FAO Irrigation and Drainage Paper No. 24)

		Ratio E_{pan} mentioned and E_{pan} Colorado			
Climate		Humid-temperate climate		Arid to semi-arid (dry season)	
Ground cover surrounding pan (50 m or more)		Short green cover	Dry fallow	Short green cover	Dry fallow
	Pan area (m^2)				
GGI 20 diameter 5 m, depth 2 m (former Soviet Union)	19.6	1.0	1.1	1.05	1.25
Sunken pan diameter 12 ft (3.66 m) depth 3.3 ft (Israel)	10.5				
BPI diameter 6 ft (1.83 m), depth 2 ft (0.61 m) (USA)	2.6				
Kenya pan diameter 4 ft (1.22 m) depth 14 in (0.356 m)	1.2				
Australian pan diameter 3 ft (0.91 m) depth 3 ft (0.91 m)	0.7		1.0		1.0
Symmons pan 6 ft^2 (0.56 m^2) depth 2 ft (0.61 m)	0.6				
Aslyng pan 0.33 m^2, depth 1 m (Denmark)	0.3			1.0	
GGI 3000 diameter 0.618 cm, depth 60-80 cm (former Soviet Union)	0.3				
Sunken pan diameter 50 cm, depth 25 cm (Netherlands)	0.2	1.0	0.95	1.0	0.95

EXAMPLE 21
Determination of ET_o from pan evaporation using tables

Given the daily evaporation data for the first week of July for a Class A pan installed in a green area surrounded by short irrigated field crops: 8.2, 7.5, 7.6, 6.8, 7.6, 8.9 and 8.5 mm/day. In that period the mean wind speed is 1.9 m/s and the daily mean relative humidity is 73%. Determine the 7-day average reference evapotranspiration.

Pan is installed on a green surface: Case A

Pan is surrounded by irrigated crops: Wind speed is light: Relative humidity is high:	$fetch_{max}$ = u < RH_{mean} >	1 000 2 70	m m/s %
From Table 5 (for above conditions):	K_p =	0.85	-
- From Eq. 55:	E_{pan} = (8.2+7.5+7.6+6.8+7.6+8.9+8.5)/7 = ET_o = 0.85 (7.9) =	7.9 6.7	mm/day mm/day

The 7-day average of the crop reference evapotranspiration is 6.7 mm/day

BOX 12
Description of Class A pan

The Class A Evaporation pan is circular, 120.7 cm in diameter and 25 cm deep. It is made of galvanized iron (22 gauge) or Monel metal (0.8 mm). The pan is mounted on a wooden open frame platform which is 15 cm above ground level. The soil is built up to within 5 cm of the bottom of the pan. The pan must be level. It is filled with water to 5 cm below the rim, and the water level should not be allowed to drop to more than 7.5 cm below the rim. The water should be regularly renewed, at least weekly, to eliminate extreme turbidity. The pan, if galvanized, is painted annually with aluminium paint. Screens over the pan are not a standard requirement and should preferably not be used. Pans should be protected by fences to keep animals from drinking.

The site should preferably be under grass, 20 by 20 m, open on all sides to permit free circulation of the air. It is preferable that stations be located in the centre or on the leeward side of large cropped fields.

Pan readings are taken daily in the early morning at the same time that precipitation is measured. Measurements are made in a stilling well that is situated in the pan near one edge. The stilling well is a metal cylinder of about 10 cm in diameter and some 20 cm deep with a small hole at the bottom.

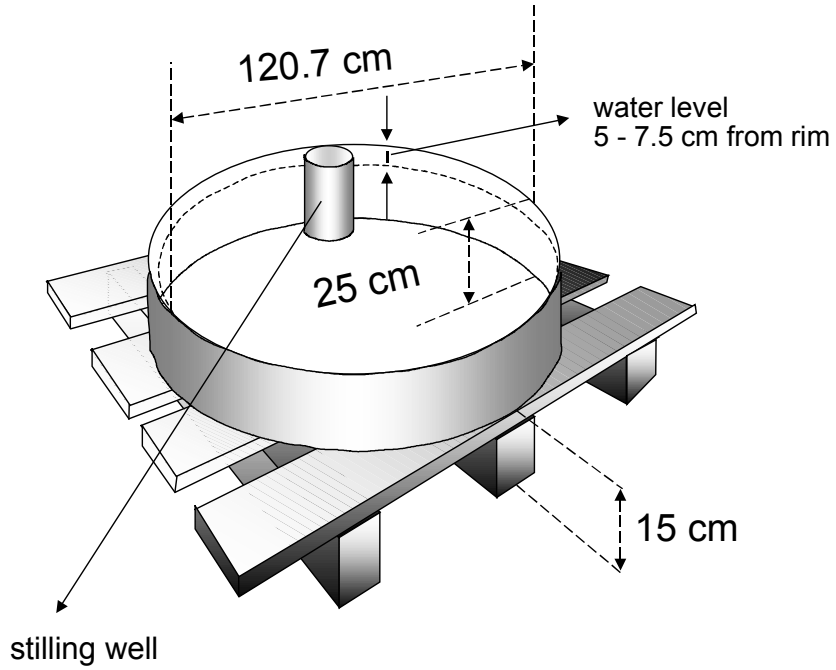

BOX 13
Description of Colorado sunken pan

The Colorado sunken pan is 92 cm (3 ft) square and 46 cm (18 in) deep, made of 3 mm thick iron, placed in the ground with the rim 5 cm (2 in) above the soil level. Also, the dimensions 1 m square and 0.5 m deep are frequently used. The pan is painted with black tar paint. The water level is maintained at or slightly below ground level, i.e., 5-7.5 cm below the rim.

Measurements are taken similarly to those for the Class A pan. Siting and environment requirements are also similar to those for the Class A pan.

Sunken Colorado pans are sometimes preferred in crop water requirements studies, as these pans give a better direct estimation of the reference evapotranspiration than does the Class A pan. The disadvantage is that maintenance is more difficult and leaks are not visible.

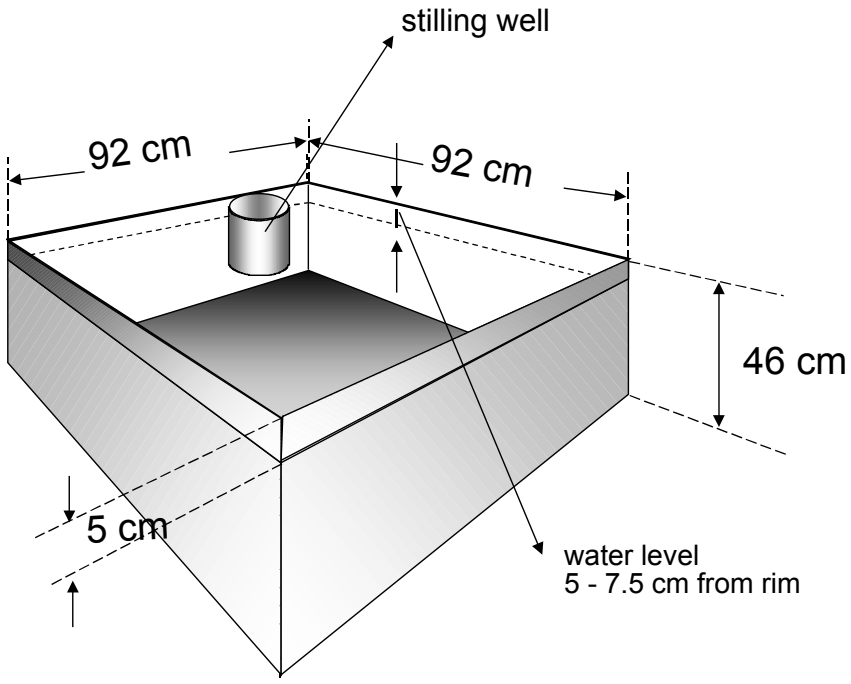

EXAMPLE 22
Determination of ET_o from pan evaporation using equations

Given the 7-day average evaporation measurement from Example 21, estimate the ET_o for the two types of pans and two types of fetch conditions represented by equations in Table 7. Assume that fetch is 1000 m in both fetch cases (green and dry).

	Fetch = u_2 = RH_{mean} =		1000 1.9 73	m m/s %
Class A pan with green fetch	$K_p = 0.108 - 0.0286\,u_2 + 0.0422\ln(FET) + 0.1434\ln(RH_{mean}) - 0.000631[\ln(FET)]^2\ln(RH_{mean})$ E_{pan} = ET_o =	$K_p = 0.108 - 0.0286\,(1.9) + 0.0422\ln(1000) + 0.1434\ln(73) - 0.000631[\ln(1000)]^2\ln(73)$ $ET_o = 0.83\,(7.9)$	0.83 7.9 6.6	- mm/day mm/day
Class A pan with dry fetch	$K_p = 0.61 + 0.00341\,RH_{mean} - 0.000162\,u_2\,RH_{mean} - 0.00000959\,u_2\,FET + 0.00327\,u_2\ln(FET) - 0.00289\,u_2\ln(86.4\,u_2) - 0.0106\ln(86.4\,u_2)\ln(FET) + 0.00063\,[\ln(FET)]^2\ln(86.4\,u_2)$ E_{pan} = ET_o =	$K_p = 0.61 + 0.00341\,(73) - 0.000162\,(1.9)\,(73) - 0.00000959\,(1.9)\,(1000) + 0.00327\,(1.9)\ln(1000) - 0.00289\,(1.9)\ln(86.4\,(1.9)) - 0.0106\ln(86.4\,(1.9))\ln(1000) + 0.00063\,[\ln(1000)]^2\ln(86.4\,(1.9))$ $ET_o = 0.61\,(7.9)$	0.61 7.9 4.8	- mm/day mm/day
Colorado sunken pan with green fetch	$K_p = 0.87 + 0.119\ln(FET) - 0.0157[\ln(86.4\,u_2)]^2 - 0.0019[\ln(FET)]^2\ln(86.4\,u_2) + 0.013\ln(86.4\,u_2)\ln(RH_{mean}) - 0.000053\ln(86.4\,u_2)\ln(FET)RH_{mean}$ E_{pan} = ET_o =	$K_p = 0.87 + 0.119\ln(100) - 0.0157[\ln(86.4\,(1.9))]^2 - 0.0019[\ln(1000)]^2\ln(86.4\,(1.9)) + 0.013\ln(86.4\,(1.9))\ln(73) - 0.000053\ln(86.4\,(1.9))\ln(1000)\,(73)$ $ET_o = 0.97\,(7.9)$	0.97 7.9 7.7	- mm/day mm/day
Colorado sunken pan with dry fetch	$K_p = 1.145 - 0.080\,u_2 + 0.000903(u_2)^2\ln(RH_{mean}) - 0.0964\ln(FET) + 0.0031\,u_2\ln(FET) + 0.0015\,[\ln(FET)]^2\ln(RH_{mean})$ E_{pan} = ET_o =	$K_p = 1.145 - 0.080\,(1.9) + 0.000903(1.9)^2\ln(73) - 0.0964\ln(1000) + 0.0031\,(1.9)\ln(1000) + 0.0015\,[\ln(1000)]^2\ln(73)$ $ET_o = 0.69\,(7.9)$	0.69 7.9 5.4	- mm/day mm/day
The 7-day average of the crop reference evapotranspiration for the four pan/fetch conditions is 6.6, 4.8, 7.7, and 5.4 mm/day				

Part B

Crop evapotranspiration under standard conditions

This part examines crop evapotranspiration under standard conditions (ET_c). This is the evapotranspiration from disease-free, well-fertilized crops, grown in large fields, under optimum soil water conditions and achieving full production under the given climatic conditions.

The effects of various weather conditions on evapotranspiration are incorporated into ET_o (Part A). The effects of characteristics that distinguish the cropped surface from the reference surface are integrated into the crop coefficient. By multiplying ET_o by the crop coefficient, ET_c is determined.

Typical crop coefficients, calculation procedures for adjusting the crop coefficients and for calculating ET_c are presented in this part. Two calculation approaches are outlined: the single and the dual crop coefficient approach. In the single crop coefficient approach, the difference in evapotranspiration between the cropped and reference grass is combined into one single coefficient. In the dual crop coefficient approach, the crop coefficient is split into two factors describing separately the differences in evaporation and transpiration between the crop and reference surface.

As discussed in Chapter 5 and summarized in Table 10, the single crop coefficient approach is used for most applications related to irrigation planning, design, and management. The dual crop coefficient approach is relevant in calculations where detailed estimates of soil water evaporation are required, such as in real time irrigation scheduling applications, water quality modelling, and in research.

Chapter 5

Introduction to crop evapotranspiration (ET_c)

This chapter outlines the crop coefficient approach for calculating the crop evapotranspiration under standard conditions (ET_c). The standard conditions refer to crops grown in large fields under excellent agronomic and soil water conditions. The crop evapotranspiration differs distinctly from the reference evapotranspiration (ET_o) as the ground cover, canopy properties and aerodynamic resistance of the crop are different from grass. The effects of characteristics that distinguish field crops from grass are integrated into the crop coefficient (K_c). In the crop coefficient approach, crop evapotranspiration is calculated by multiplying ET_o by K_c.

Differences in evaporation and transpiration between field crops and the reference grass surface can be integrated in a single crop coefficient (K_c) or separated into two coefficients: a basal crop (K_{cb}) and a soil evaporation coefficient (K_e), i.e., $K_c = K_{cb} + K_e$. The approach to follow should be selected as a function of the purpose of the calculation, the accuracy required and the data available.

CALCULATION PROCEDURES

Direct calculation

The evapotranspiration rate from a cropped surface can be directly measured by the mass transfer or the energy balance method. It can also be derived from studies of the soil water balance determined from cropped fields or from lysimeters.

Crop evapotranspiration can also be derived from meteorological and crop data by means of the Penman-Monteith equation (Eq. 3). By adjusting the albedo and the aerodynamic and canopy surface resistances to the growing characteristics of the specific crop, the evapotranspiration rate can be directly estimated. The albedo and resistances are, however, difficult to estimate accurately as they may vary continually during the growing season as climatic conditions change, as the crop develops, and with wetness of the soil surface. The canopy resistance will further be influenced by the soil water availability, and it increases strongly if the crop is subjected to water stress.

As there is still a considerable lack of consolidated information on the aerodynamic and canopy resistances for the various cropped surfaces, the FAO Penman-Monteith method is used in this handbook only for estimating ET_o, the evapotranspiration from a well-watered hypothetical grass surface having fixed crop height, albedo and surface resistance.

Crop coefficient approach

In the crop coefficient approach the crop evapotranspiration, ET_c, is calculated by multiplying the reference crop evapotranspiration, ET_o, by a crop coefficient, K_c:

$$ET_c = K_c \, ET_o \qquad (56)$$

where ET_c crop evapotranspiration [mm d^{-1}],
K_c crop coefficient [dimensionless],
ET_o reference crop evapotranspiration [mm d^{-1}].

Most of the effects of the various weather conditions are incorporated into the ET_o estimate. Therefore, as ET_o represents an index of climatic demand, K_c varies predominately with the specific crop characteristics and only to a limited extent with climate. This enables the transfer of standard values for K_c between locations and between climates. This has been a primary reason for the global acceptance and usefulness of the crop coefficient approach and the K_c factors developed in past studies.

The reference ET_o is defined and calculated using the FAO Penman-Monteith equation (Chapter 4). The crop coefficient, K_c, is basically the ratio of the crop ET_c to the reference ET_o, and it represents an integration of the effects of four primary characteristics that distinguish the crop from reference grass. These characteristics are:

- Crop height. The crop height influences the aerodynamic resistance term, r_a, of the FAO Penman-Monteith equation and the turbulent transfer of vapour from the crop into the atmosphere. The r_a term appears twice in the full form of the FAO Penman-Monteith equation.
- Albedo (reflectance) of the crop-soil surface. The albedo is affected by the fraction of ground covered by vegetation and by the soil surface wetness. The albedo of the crop-soil surface influences the net radiation of the surface, R_n, which is the primary source of the energy exchange for the evaporation process.
- Canopy resistance. The resistance of the crop to vapour transfer is affected by leaf area (number of stomata), leaf age and condition, and the degree of stomatal control. The canopy resistance influences the surface resistance, r_s.
- Evaporation from soil, especially exposed soil.

The soil surface wetness and the fraction of ground covered by vegetation influence the surface resistance, r_s. Following soil wetting, the vapour transfer rate from the soil is high, especially for crops having incomplete ground cover. The combined surface resistance of the canopy and of the soil determines the (bulk) surface resistance, r_s. The surface resistance term in the Penman-Monteith equation represents the resistance to vapour flow from within plant leaves and from beneath the soil surface.

The K_c in Equation 56 predicts ET_c under standard conditions. This represents the upper envelope of crop evapotranspiration and represents conditions where no limitations are placed on crop growth or evapotranspiration due to water shortage, crop density, or disease, weed, insect or salinity pressures. The ET_c predicted by K_c is adjusted if necessary to non-standard

conditions, $ET_{c\ adj}$, where any environmental condition or characteristic is known to have an impact on or to limit ET_c. Factors for correcting ET_c to $ET_{c\ adj}$ are described in Part C.

FACTORS DETERMINING THE CROP COEFFICIENT

The crop coefficient integrates the effect of characteristics that distinguish a typical field crop from the grass reference, which has a constant appearance and a complete ground cover. Consequently, different crops will have different K_c coefficients. The changing characteristics of the crop over the growing season also affect the K_c coefficient. Finally, as evaporation is an integrated part of crop evapotranspiration, conditions affecting soil evaporation will also have an effect on K_c.

Crop type

Due to differences in albedo, crop height, aerodynamic properties, and leaf and stomata properties, the evapotranspiration from full grown, well-watered crops differs from ET_o.

The close spacings of plants and taller canopy height and roughness of many full grown agricultural crops cause these crops to have K_c factors that are larger than 1. The K_c factor is often 5-10% higher than the reference (where $K_c = 1.0$), and even 15-20% greater for some tall crops such as maize, sorghum or sugar cane (Figure 20). Typical values for the crop coefficient for full grown crops ($K_{c\ mid}$) are listed in Table 12.

Crops such as pineapples, that close their stomata during the day, have very small crop coefficients. In most species, however, the stomata open as irradiance increases. In addition to the stomatal response to environment, the position and number of the stomata and the resistance of the cuticula to vapour transfer determine the water loss from the crop. Species with stomata on only the lower side of the leaf and/or large leaf resistances will have relatively smaller K_c values. This is the case for citrus and most deciduous fruit trees. Transpiration control and spacing of the trees, providing only 70% ground cover for mature trees, may cause the K_c of those trees, if cultivated without a ground cover crop, to be smaller than one (Figure 20).

Climate

The K_c values of Table 12 are typical values expected for average K_c under a standard climatic condition, which is defined as a sub-humid climate with average daytime minimum relative humidity (RH_{min}) ≈ 45% and having calm to moderate wind speeds averaging 2 m/s.

Variations in wind alter the aerodynamic resistance of the crops and hence their crop coefficients, especially for those crops that are substantially taller than the hypothetical grass reference. The effect of the difference in aerodynamic properties between the grass reference surface and agricultural crops is not only crop specific. It also varies with the climatic conditions and crop height. Because aerodynamic properties are greater for many agricultural crops as compared to the grass reference, the ratio of ET_c to ET_o (i.e., K_c) for many crops increases as wind speed increases and as relative humidity decreases. More arid climates and conditions of greater wind speed will have higher values for K_c. More humid climates and conditions of lower wind speed will have lower values for K_c.

FIGURE 20
Typical K_c for different types of full grown crops

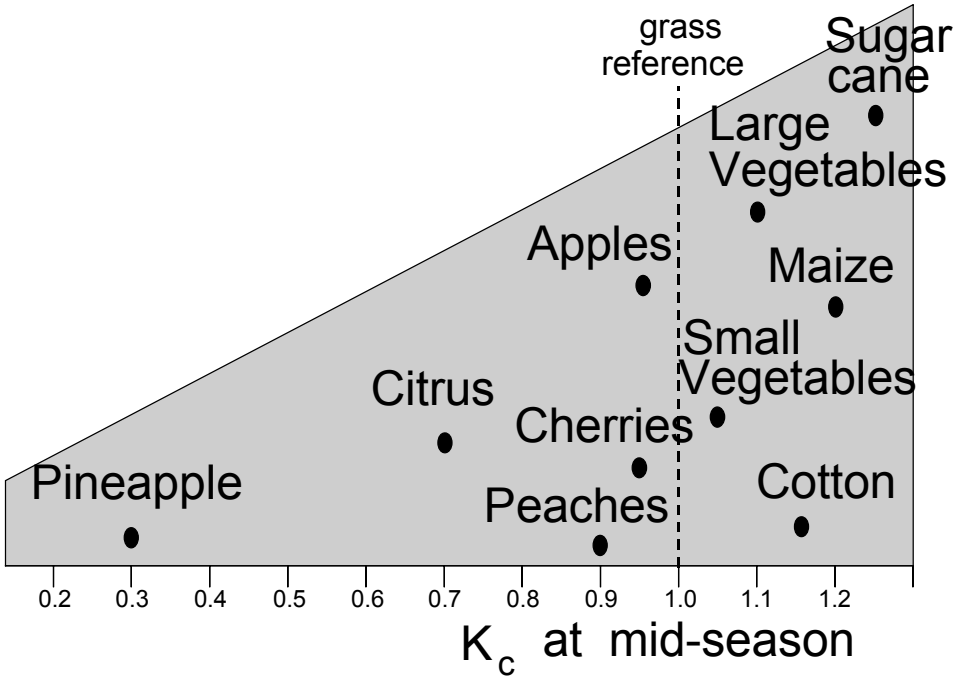

FIGURE 21
Extreme ranges expected in K_c for full grown crops as climate and weather change

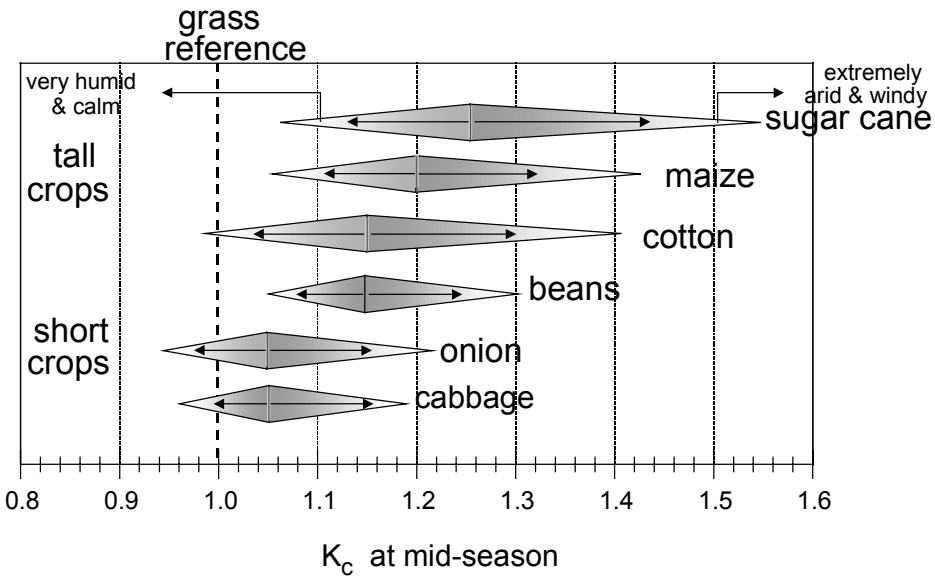

The relative impact of the climate on K_c for full grown crops is illustrated in Figure 21. The upper bounds represent extremely arid and windy conditions, while the lower bounds are valid under very humid and calm weather conditions. The ranges expected in K_c as climate and weather conditions change are quite small for short crops but are large for tall crops. Guidelines for the adjustment of K_c to the climatic conditions as a function of crop height are given in Chapter 6.

Under humid and calm wind conditions, K_c becomes less dependent on the differences between the aerodynamic components of ET_c and ET_o and the K_c values for 'full-cover' agricultural crops do not exceed 1.0 by more than about 0.05. This is because full-cover agricultural crops and the reference crop of clipped grass both provide for nearly maximum absorption of shortwave radiation, which is the primary energy source for evaporation under humid and calm conditions. Generally, the albedos, α, are similar over a wide range of full-cover agricultural crops, including the reference crop. Because the vapour pressure deficit (e_s - e_a) is small under humid conditions, differences in ET caused by differences in aerodynamic resistance, r_a, between the agricultural crop and the reference crop are also small, especially with low to moderate wind speed.

Under arid conditions, the effect of differences in r_a between the agricultural crop and the grass reference crop on ET_c become more pronounced because the (e_s - e_a) term may be relatively large. The larger magnitudes of (e_s - e_a) amplify differences in the aerodynamic term in the numerator of the Penman-Monteith equation (Equation 3) for both the crop and the reference crop. Hence, K_c will be larger under arid conditions when the agricultural crop has a leaf area and roughness height that are greater than that of the grass reference.

Because the $1/r_a$ term in the numerator of the Penman-Monteith equation (Equation 3) is multiplied by the vapour pressure deficit (e_s - e_a), the ET from tall crops increases proportionately more relative to ET_o than does ET from short crops when relative humidity is low. The K_c for tall crops, such as those 2-3 m in height, can be as much as 30% higher in a windy, arid climate as compared with a calm, humid climate. The increase in K_c is due to the influence of the larger aerodynamic roughness of the tall crop relative to grass on the transport of water vapour from the surface.

Soil evaporation

Differences in soil evaporation and crop transpiration between field crops and the reference surface are integrated within the crop coefficient. The K_c coefficient for full-cover crops primarily reflects differences in transpiration as the contribution of soil evaporation is relatively small. After rainfall or irrigation, the effect of evaporation is predominant when the crop is small and scarcely shades the ground. For such low-cover conditions, the K_c coefficient is determined largely by the frequency with which the soil surface is wetted. Where the soil is wet for most of the time from irrigation or rain, the evaporation from the soil surface will be considerable and K_c may exceed 1. On the other hand, where the soil surface is dry, evaporation is restricted and K_c will be small and might even drop to as low as 0.1 (Figure 22).

Differences in soil evaporation between the field crop and the reference surface can be forecast more precisely by using a dual crop coefficient.

FIGURE 22
The effect of evaporation on K_c. The horizontal line represents K_c when the soil surface is kept continuously wet. The curved line corresponds to K_c when the soil surface is kept dry but the crop receives sufficient water to sustain full transpiration

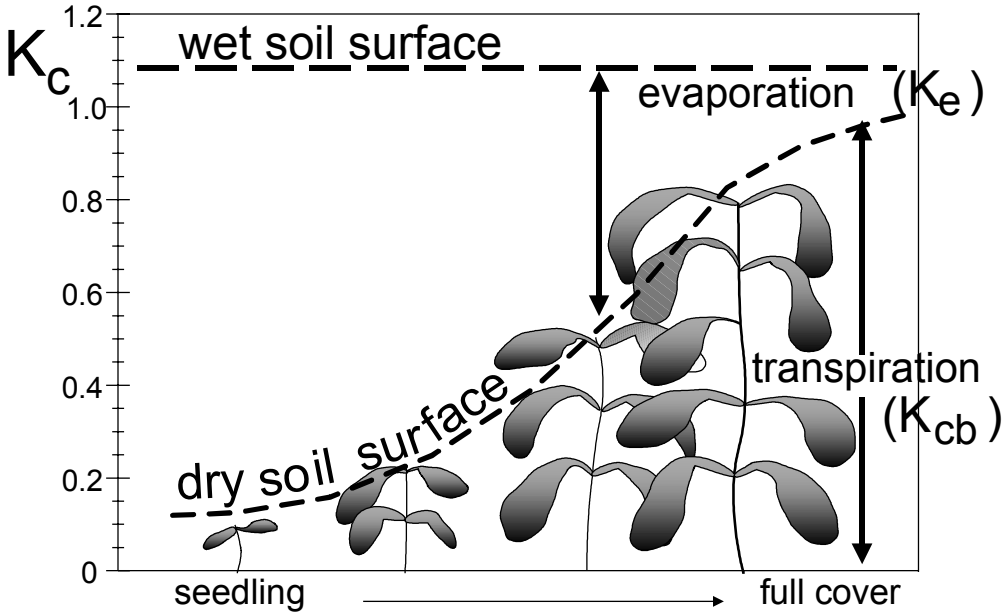

FIGURE 23
Crop growth stages for different types of crops

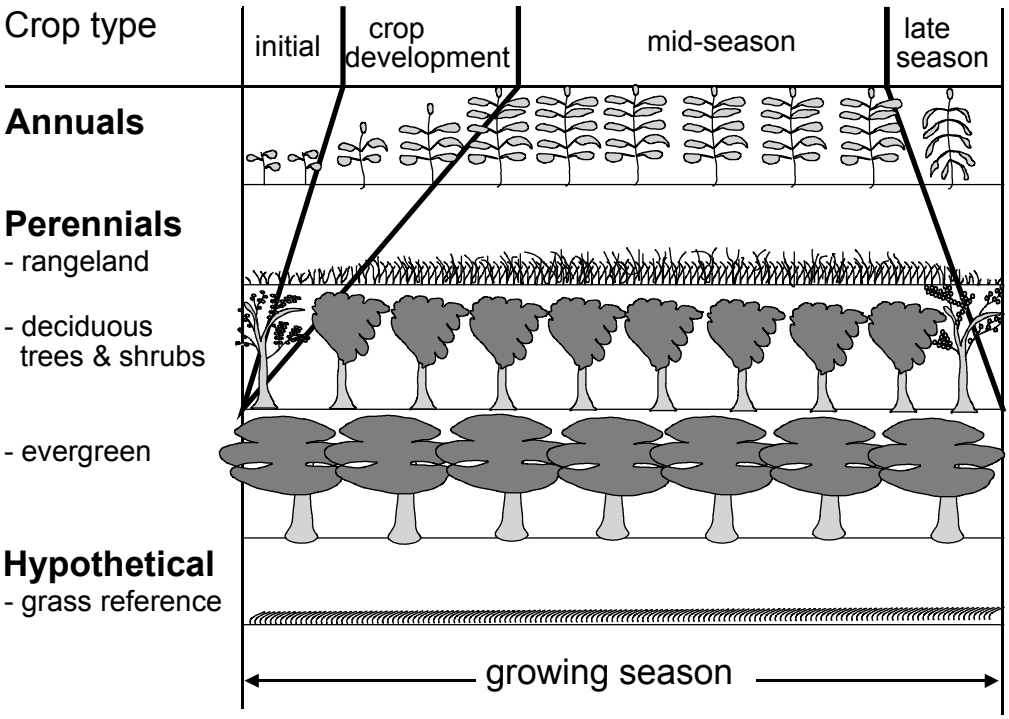

Crop growth stages

As the crop develops, the ground cover, crop height and the leaf area change. Due to differences in evapotranspiration during the various growth stages, the K_c for a given crop will vary over the growing period. The growing period can be divided into four distinct growth stages: initial, crop development, mid-season and late season. Figure 23 illustrates the general sequence and proportion of these stages for different types of crops.

Initial stage

The initial stage runs from planting date to approximately 10% ground cover. The length of the initial period is highly dependent on the crop, the crop variety, the planting date and the climate. The end of the initial period is determined as the time when approximately 10% of the ground surface is covered by green vegetation. For perennial crops, the planting date is replaced by the 'greenup' date, i.e., the time when the initiation of new leaves occurs.

During the initial period, the leaf area is small, and evapotranspiration is predominately in the form of soil evaporation. Therefore, the K_c during the initial period ($K_{c\ ini}$) is large when the soil is wet from irrigation and rainfall and is low when the soil surface is dry. The time for the soil surface to dry is determined by the time interval between wetting events, the evaporation power of the atmosphere (ET_o) and the importance of the wetting event. General estimates for $K_{c\ ini}$ as a function of the frequency of wetting and ET_o are given in Table 9. The data assume a medium textured soil. The procedure for estimating $K_{c\ ini}$ is presented in Chapter 6.

TABLE 9
Approximate values for $K_{c\ ini}$ for medium wetting events (10-40 mm) and a medium textured soil

wetting interval	evaporating power of the atmosphere (ET_o)			
	low 1 - 3 mm/day	**moderate 3 - 5 mm/day**	**high 5 - 7 mm/day**	**very high > 7 mm/day**
less than weekly	1.2 - 0.8	1.1 - 0.6	1.0 - 0.4	0.9 - 0.3
weekly	0.8	0.6	0.4	0.3
longer than once per week	0.7 - 0.4	0.4 - 0.2*	0.3 - 0.2*	0.2* - 0.1*

Values derived from Figures 29 and 30
(*) Note that irrigation intervals may be too large to sustain full transpiration for some young annual crops.

Crop development stage

The crop development stage runs from 10% ground cover to effective full cover. Effective full cover for many crops occurs at the initiation of flowering. For row crops where rows commonly interlock leaves such as beans, sugar beets, potatoes and corn, effective cover can be defined as the time when some leaves of plants in adjacent rows begin to intermingle so that soil shading becomes nearly complete, or when plants reach nearly full size if no intermingling occurs. For some crops, especially those taller than 0.5 m, the average fraction of the ground surface covered by vegetation (f_c) at the start of effective full cover is about 0.7-0.8. Fractions of sunlit

and shaded soil and leaves do not change significantly with further growth of the crop beyond $f_c \approx 0.7$ to 0.8. It is understood that the crop or plant can continue to grow in both height and leaf area after the time of effective full cover. Because it is difficult to visually determine when densely sown vegetation such as winter and spring cereals and some grasses reach effective full cover, the more easily detectable stage of heading (flowering) is generally used for these types of crops.

For dense grasses, effective full cover may occur at about 0.10-0.15 m height. For thin stands of grass (dry rangeland), grass height may approach 0.3-0.5 m before effective full cover is reached. Densely planted forages such as alfalfa and clover reach effective full cover at about 0.3-0.4 m.

Another way to estimate the occurrence of effective full cover is when the leaf area index (LAI) reaches three. LAI is defined as the average total area of leaves (one side) per unit area of ground surface.

As the crop develops and shades more and more of the ground, evaporation becomes more restricted and transpiration gradually becomes the major process. During the crop development stage, the K_c value corresponds to amounts of ground cover and plant development. Typically, if the soil surface is dry, $K_c = 0.5$ corresponds to about 25-40% of the ground surface covered by vegetation due to the effects of shading and due to microscale transport of sensible heat from the soil into the vegetation. A $K_c = 0.7$ often corresponds to about 40-60% ground cover. These values will vary, depending on the crop, frequency of wetting and whether the crop uses more water than the reference crop at full ground cover (e.g., depending on its canopy architecture and crop height relative to clipped grass).

Mid-season stage

The mid-season stage runs from effective full cover to the start of maturity. The start of maturity is often indicated by the beginning of the ageing, yellowing or senescence of leaves, leaf drop, or the browning of fruit to the degree that the crop evapotranspiration is reduced relative to the reference ET_o. The mid-season stage is the longest stage for perennials and for many annuals, but it may be relatively short for vegetable crops that are harvested fresh for their green vegetation.

At the mid-season stage the K_c reaches its maximum value. The value for K_c ($K_{c\ mid}$) is relatively constant for most growing and cultural conditions. Deviation of the $K_{c\ mid}$ from the reference value '1' is primarily due to differences in crop height and resistance between the grass reference surface and the agricultural crop and weather conditions.

Late season stage

The late season stage runs from the start of maturity to harvest or full senescence. The calculation for K_c and ET_c is presumed to end when the crop is harvested, dries out naturally, reaches full senescence, or experiences leaf drop.

For some perennial vegetation in frost free climates, crops may grow year round so that the date of termination may be taken as the same as the date of ‘planting’.

FIGURE 24
Typical ranges expected in K_c for the four growth stages

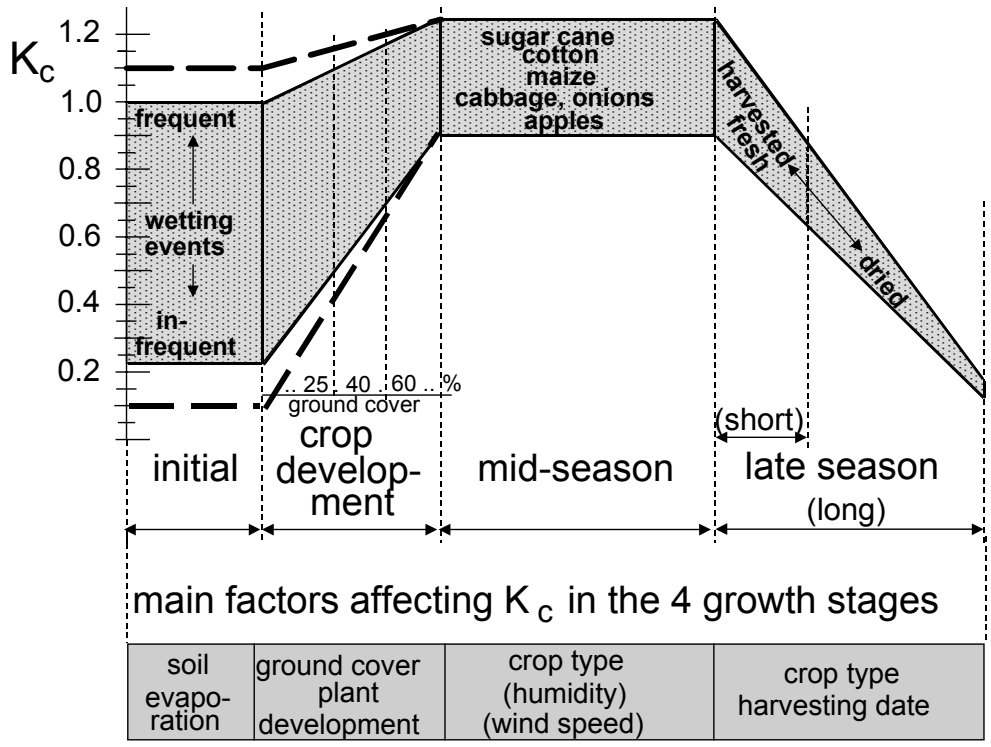

The K_c value at the end of the late season stage ($K_{c\ end}$) reflects crop and water management practices. The $K_{c\ end}$ value is high if the crop is frequently irrigated until harvested fresh. If the crop is allowed to senesce and to dry out in the field before harvest, the $K_{c\ end}$ value will be small. Senescence is usually associated with less efficient stomatal conductance of leaf surfaces due to the effects of ageing, thereby causing a reduction in K_c.

Figure 24 illustrates the variation in K_c for different crops as influenced by weather factors and crop development.

CROP EVAPOTRANSPIRATION (ET_C)

Crop evapotranspiration is calculated by multiplying ET_o by K_c, a coefficient expressing the difference in evapotranspiration between the cropped and reference grass surface. The difference can be combined into one single coefficient, or it can be split into two factors describing separately the differences in evaporation and transpiration between both surfaces. The selection of the approach depends on the purpose of the calculation, the accuracy required, the climatic data available and the time step with which the calculations are executed. Table 10 presents the general selection criteria.

TABLE 10
General selection criteria for the single and dual crop coefficient approaches

	Single crop coefficient K_c	**Dual crop coefficient $K_{cb} + K_e$**
Purpose of calculation	- irrigation planning and design - irrigation management - basic irrigation schedules - real time irrigation scheduling for non-frequent water applications (surface and sprinkler irrigation)	- research - real time irrigation scheduling - irrigation scheduling for high frequency water application (microirrigation and automated sprinkler irrigation) - supplemental irrigation - detailed soil and hydrologic water balance studies
Time step	daily, 10-day, monthly (data and calculation)	daily (data and calculation)
Solution method	graphical pocket calculator computer	computer

Single and dual crop coefficient approaches

Single crop coefficient approach (K_c)

In the single crop coefficient approach, the effect of crop transpiration and soil evaporation are combined into a single K_c coefficient. The coefficient integrates differences in the soil evaporation and crop transpiration rate between the crop and the grass reference surface. As soil evaporation may fluctuate daily as a result of rainfall or irrigation, the single crop coefficient expresses only the time-averaged (multi-day) effects of crop evapotranspiration.

As the single K_c coefficient averages soil evaporation and transpiration, the approach is used to compute ET_c for weekly or longer time periods, although calculations may proceed on a daily time step. The time-averaged single K_c is used for planning studies and irrigation system design where the averaged effects of soil wetting are acceptable and relevant. This is the case for surface irrigation and set sprinkler systems where the time interval between successive irrigation is of several days, often ten days or more. For typical irrigation management, the time-averaged single K_c is valid.

Dual crop coefficient approach ($K_{cb} + K_e$)

In the dual crop coefficient approach, the effects of crop transpiration and soil evaporation are determined separately. Two coefficients are used: the basal crop coefficient (K_{cb}) to describe plant transpiration, and the soil water evaporation coefficient (K_e) to describe evaporation from the soil surface. The single K_c coefficient is replaced by:

$$K_c = K_{cb} + K_e \qquad (57)$$

where K_{cb} basal crop coefficient,
K_e soil water evaporation coefficient.

The basal crop coefficient, K_{cb}, is defined as the ratio of ET_c to ET_o when the soil surface layer is dry but where the average soil water content of the root zone is adequate to sustain full plant transpiration. The K_{cb} represents the baseline potential K_c in the absence of the additional effects of soil wetting by irrigation or precipitation. The soil evaporation coefficient, K_e, describes the evaporation component from the soil surface. If the soil is wet following rain or irrigation, K_e may be large. However, the sum of K_{cb} and K_e can never exceed a maximum value, $K_{c\ max}$, determined by the energy available for evapotranspiration at the soil surface. As the soil surface becomes drier, K_e becomes smaller and falls to zero when no water is left for evaporation. The estimation of K_e requires a daily water balance computation for the calculation of the soil water content remaining in the upper topsoil.

The dual coefficient approach requires more numerical calculations than the procedure using the single time-averaged K_c coefficient. The dual procedure is best for real time irrigation scheduling, for soil water balance computations, and for research studies where effects of day-to-day variations in soil surface wetness and the resulting impacts on daily ET_c, the soil water profile, and deep percolation fluxes are important. This is the case for high frequency irrigation with microirrigation systems or lateral move systems such as centre pivots and linear move systems.

Crop coefficient curve

After the selection of the calculation approach, the determination of the lengths for the crop growth stages and the corresponding crop coefficients, a crop coefficient curve can be constructed. The curve represents the changes in the crop coefficient over the length of the growing season. The shape of the curve represents the changes in the vegetation and ground cover during plant development and maturation that affect the ratio of ET_c to ET_o. From the curve, the K_c factor and hence ET_c can be derived for any period within the growing season.

Single crop coefficient

The generalized crop coefficient curve is shown in Figure 25. Shortly after the planting of annuals or shortly after the initiation of new leaves for perennials, the value for K_c is small, often less than 0.4. The K_c begins to increase from the initial K_c value, $K_{c\ ini}$, at the beginning of rapid plant development and reaches a maximum value, $K_{c\ mid}$, at the time of maximum or near maximum plant development. During the late season period, as leaves begin to age and senesce due to natural or cultural practices, the K_c begins to decrease until it reaches a lower value at the end of the growing period equal to $K_{c\ end}$.

Dual crop coefficient

The single 'time-averaged' K_c curve in Figure 25 incorporates averaged wetting effects into the K_c factor. The value for $K_{c\ mid}$ is relatively constant for most growing and cultural conditions. However, the values for $K_{c\ ini}$ and $K_{c\ end}$ can vary considerably on a daily basis, depending on the frequency of wetting by irrigation and rainfall. The dual crop coefficient approach calculates the actual increases in K_c for each day as a function of plant development and the wetness of the soil surface.

As the single K_c coefficient includes averaged effects of evaporation from the soil, the basal crop coefficient, K_{cb} d escribing only plant transpiration, lies below the K_c value (Figure

FIGURE 25
Generalized crop coefficient curve for the single crop coefficient approach

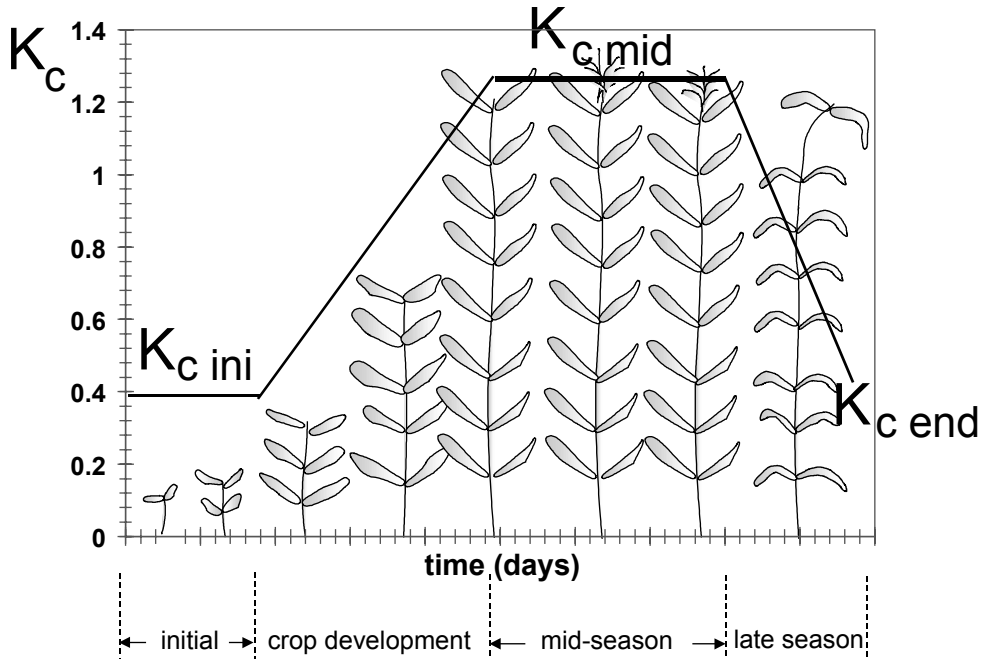

FIGURE 26
Crop coefficient curves showing the basal K_{cb} (thick line), soil evaporation K_e (thin line) and the corresponding single $K_c = K_{cb} + K_e$ curve (dashed line)

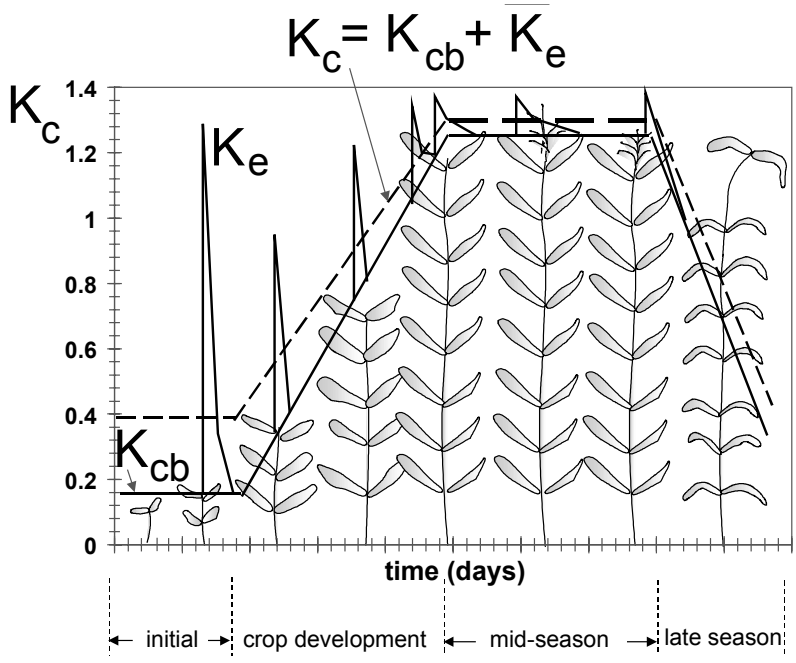

26). The largest difference between K_c and K_{cb} is found in the initial growth stage where evapotranspiration is predominantly in the form of soil evaporation and crop transpiration is still small. Because crop canopies are near or at full ground cover during the mid-season stage, soil evaporation beneath the canopy has less effect on crop evapotranspiration and the value for K_{cb} in the mid-season stage will be nearly the same as K_c. Depending on the ground cover, the basal crop coefficient during the mid-season may be only 0.05-0.10 lower than the K_c value. Depending on the frequency with which the crop is irrigated during the late season stage, K_{cb} will be similar to (if infrequently irrigated) or less than the K_c value.

Figure 26 presents typical shapes for the K_{cb}, K_e and single K_c curves. The K_{cb} curve in the figure represents the minimum K_c for conditions of adequate soil water and dry soil surface. The K_e 'spikes' in the figure represent increased evaporation when precipitation or irrigation has wetted the soil surface and has temporarily increased total ET_c. These wet soil evaporation spikes decrease as the soil surface layer dries. The spikes generally reach a maximum value of 1.0-1.2, depending on the climate, the magnitude of the wetting event and the portion of soil surface wetted.

Summed together, the values for K_{cb} and for K_e represent the single crop coefficient, K_c. The total K_c curve, shown as the dashed line in Figure 26, illustrates the effect of averaging $K_{cb} + K_e$ over time and is displayed as a 'smoothed' curve. It is this smoothed curve that is represented by the single K_c calculation procedure. The K_c curve lies above the K_{cb} curve, with potentially large differences during the initial and development stages, depending on the frequency of soil wetting.

FLOW CHART OF THE CALCULATIONS

The calculation procedures required for the crop coefficient approaches are developed in the following chapters. In Chapter 6, a single time-averaged crop coefficient is used to calculate ET_c. The approach using two coefficients to describe the effects of crop and soil separately is outlined in Chapter 7. Figure 27 presents the general calculation procedures.

FIGURE 27
General procedure for calculating ET_c

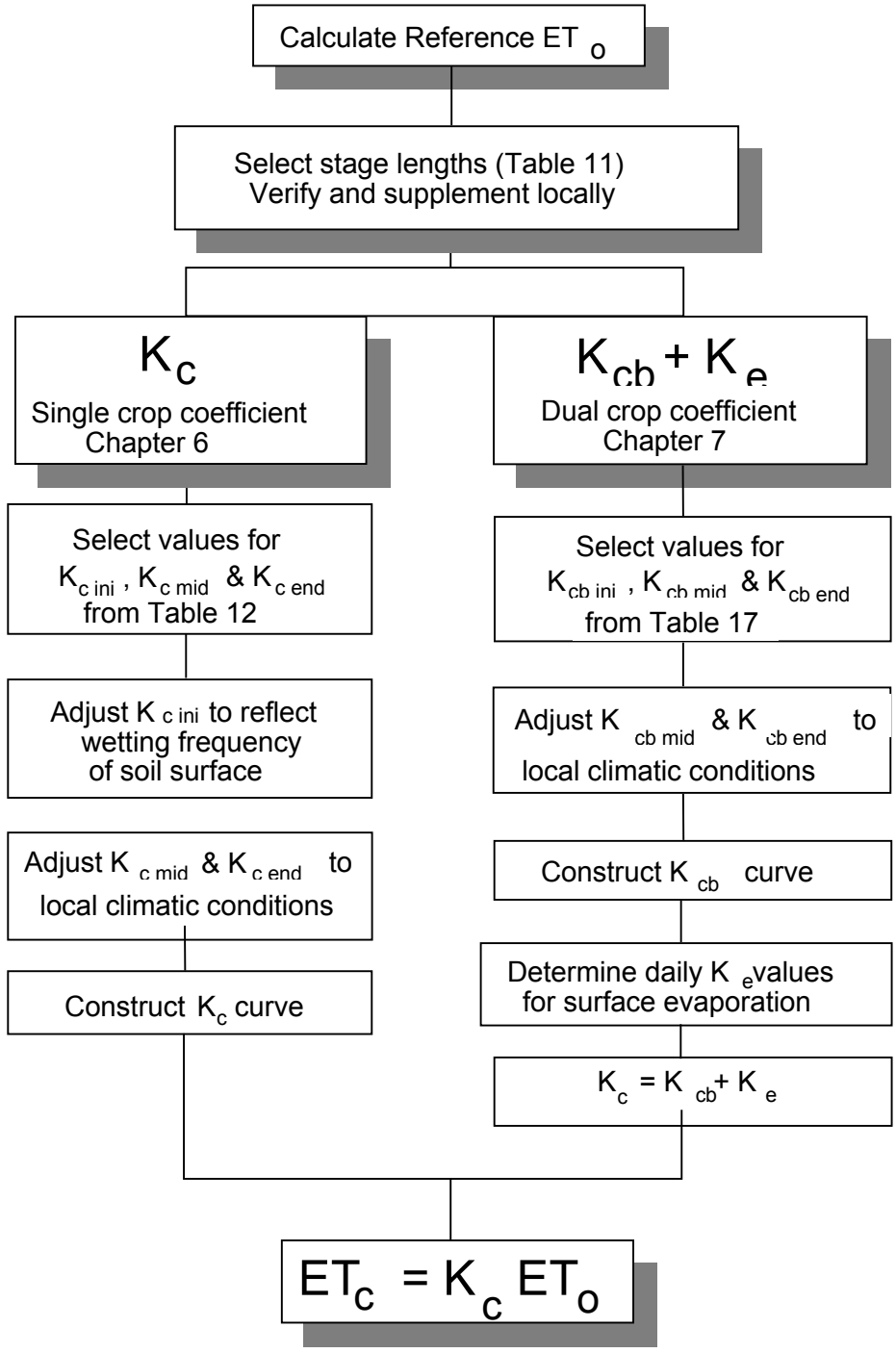

Chapter 6

ET_c – single crop coefficient (K_c)

This chapter deals with the calculation of crop evapotranspiration (ET_c) under standard conditions. No limitations are placed on crop growth or evapotranspiration from soil water and salinity stress, crop density, pests and diseases, weed infestation or low fertility. ET_c is determined by the crop coefficient approach whereby the effect of the various weather conditions are incorporated into ET_o and the crop characteristics into the K_c coefficient:

$$ET_c = K_c \, ET_o \qquad (58)$$

The effect of both crop transpiration and soil evaporation are integrated into a single crop coefficient. The K_c coefficient incorporates crop characteristics and averaged effects of evaporation from the soil. For normal irrigation planning and management purposes, for the development of basic irrigation schedules, and for most hydrologic water balance studies, average crop coefficients are relevant and more convenient than the K_c computed on a daily time step using a separate crop and soil coefficient (Chapter 7). Only when values for K_c are needed on a daily basis for specific fields of crops and for specific years, must a separate transpiration and evaporation coefficient ($K_{cb} + K_e$) be considered.

The calculation procedure for crop evapotranspiration, ET_c, consists of:

1. identifying the crop growth stages, determining their lengths, and selecting the corresponding K_c coefficients;
2. adjusting the selected K_c coefficients for frequency of wetting or climatic conditions during the stage;
3. constructing the crop coefficient curve (allowing one to determine K_c values for any period during the growing period); and
4. calculating ET_c as the product of ET_o and K_c.

LENGTH OF GROWTH STAGES

FAO Irrigation and Drainage Paper No. 24 provides general lengths for the four distinct growth stages and the total growing period for various types of climates and locations. This information has been supplemented from other sources and is summarized in Table 11.

In some situations, the time of emergence of vegetation and the time of effective full cover can be predicted using cumulative degree-based regression equations or by more sophisticated plant growth models. These types of models should be verified or validated for the local area or for a specific crop variety using local observations.

TABLE 11
Lengths of crop development stages* for various planting periods and climatic regions (days)

Crop	Init. (L_{ini})	Dev. (L_{dev})	Mid (L_{mid})	Late (L_{late})	Total	Plant Date	Region
a. Small Vegetables							
Broccoli	35	45	40	15	135	Sept	Calif. Desert, USA
Cabbage	40	60	50	15	165	Sept	Calif. Desert, USA
Carrots	20	30	50/30	20	100	Oct/Jan	Arid climate
	30	40	60	20	150	Feb/Mar	Mediterranean
	30	50	90	30	200	Oct	Calif. Desert, USA
Cauliflower	35	50	40	15	140	Sept	Calif. Desert, USA
Celery	25	40	95	20	180	Oct	(Semi)Arid
	25	40	45	15	125	April	Mediterranean
	30	55	105	20	210	Jan	(Semi)Arid
Crucifers[1]	20	30	20	10	80	April	Mediterranean
	25	35	25	10	95	February	Mediterranean
	30	35	90	40	195	Oct/Nov	Mediterranean
Lettuce	20	30	15	10	75	April	Mediterranean
	30	40	25	10	105	Nov/Jan	Mediterranean
	25	35	30	10	100	Oct/Nov	Arid Region
	35	50	45	10	140	Feb	Mediterranean
Onion (dry)	15	25	70	40	150	April	Mediterranean
	20	35	110	45	210	Oct; Jan.	Arid Region; Calif.
Onion (green)	25	30	10	5	70	April/May	Mediterranean
	20	45	20	10	95	October	Arid Region
	30	55	55	40	180	March	Calif., USA
Onion (seed)	20	45	165	45	275	Sept	Calif. Desert, USA
Spinach	20	20	15/25	5	60/70	Apr; Sep/Oct	Mediterranean
	20	30	40	10	100	November	Arid Region
Radish	5	10	15	5	35	Mar/Apr	Medit.; Europe
	10	10	15	5	40	Winter	Arid Region
b. Vegetables – Solanum Family *(Solanaceae)*							
Egg plant	30	40	40	20	130\14	October	Arid Region
	30	45	40	25	0	May/June	Mediterranean
Sweet peppers	25/30	35	40	20	125	April/June	Europe and Medit.
(bell)	30	40	110	30	210	October	Arid Region
Tomato	30	40	40	25	135	January	Arid Region
	35	40	50	30	155	Apr/May	Calif., USA
	25	40	60	30	155	Jan	Calif. Desert, USA
	35	45	70	30	180	Oct/Nov	Arid Region
	30	40	45	30	145	April/May	Mediterranean
c. Vegetables - Cucumber Family *(Cucurbitaceae)*							
Cantaloupe	30	45	35	10	120	Jan	Calif., USA
	10	60	25	25	120	Aug	Calif., USA
Cucumber	20	30	40	15	105	June/Aug	Arid Region
	25	35	50	20	130	Nov; Feb	Arid Region
Pumpkin,	20	30	30	20	100	Mar, Aug	Mediterranean
Winter squash	25	35	35	25	120	June	Europe
Squash,	25	35	25	15	100	Apr; Dec.	Medit.; Arid Reg.
Zucchini	20	30	25	15	90	May/June	Medit.; Europe

continued…

* Lengths of crop development stages provided in this table are indicative of general conditions, but may vary substantially from region to region, with climate and cropping conditions, and with crop variety. The user is strongly encouraged to obtain appropriate local information.

1 Crucifers include cabbage, cauliflower, broccoli, and Brussel sprouts. The wide range in lengths of seasons is due to varietal and species differences.

Table 11 continued

Crop	Init. (L_{ini})	Dev. (L_{dev})	Mid (L_{mid})	Late (L_{late})	Total	Plant Date	Region
Sweet melons	25	35	40	20	120	May	Mediterranean
	30	30	50	30	140	March	Calif., USA
	15	40	65	15	135	Aug	Calif. Desert, USA
	30	45	65	20	160	Dec/Jan	Arid Region
Water melons	20	30	30	30	110	April	Italy
	10	20	20	30	80	Mat/Aug	Near East (desert)
d. Roots and Tubers							
Beets, table	15	25	20	10	70	Apr/May	Mediterranean
	25	30	25	10	90	Feb/Mar	Mediterranean & Arid
Cassava: year 1	20	40	90	60	210	Rainy	Tropical regions
year 2	150	40	110	60	360	season	
Potato	25	30	30/45	30	115/130	Jan/Nov	(Semi)Arid Climate
	25	30	45	30	130	May	Continental Climate
	30	35	50	30	145	April	Europe
	45	30	70	20	165	Apr/May	Idaho, USA
	30	35	50	25	140	Dec	Calif. Desert, USA
Sweet potato	20	30	60	40	150	April	Mediterranean
	15	30	50	30	125	Rainy seas.	Tropical regions
Sugarbeet	30	45	90	15	180	March	Calif., USA
	25	30	90	10	155	June	Calif., USA
	25	65	100	65	255	Sept	Calif. Desert, USA
	50	40	50	40	180	April	Idaho, USA
	25	35	50	50	160	May	Mediterranean
	45	75	80	30	230	November	Mediterranean
	35	60	70	40	205	November	Arid Regions
e. Legumes (*Leguminosae*)							
Beans (green)	20	30	30	10	90	Feb/Mar	Calif., Mediterranean
	15	25	25	10	75	Aug/Sep	Calif., Egypt, Lebanon
Beans (dry)	20	30	40	20	110	May/June	Continental Climates
	15	25	35	20	95	June	Pakistan, Calif.
	25	25	30	20	100	June	Idaho, USA
Faba bean,	15	25	35	15	90	May	Europe
broad bean	20	30	35	15	100	Mar/Apr	Mediterranean
- dry	90	45	40	60	235	Nov	Europe
- green	90	45	40	0	175	Nov	Europe
Green gram, cowpeas	20	30	30	20	110	March	Mediterranean
Groundnut	25	35	45	25	130	Dry season	West Africa
	35	35	35	35	140	May	High Latitudes
	35	45	35	25	140	May/June	Mediterranean
Lentil	20	30	60	40	150	April	Europe
	25	35	70	40	170	Oct/Nov	Arid Region
Peas	15	25	35	15	90	May	Europe
	20	30	35	15	100	Mar/Apr	Mediterranean
	35	25	30	20	110	April	Idaho, USA
Soybeans	15	15	40	15	85	Dec	Tropics
	20	30/35	60	25	140	May	Central USA
	20	25	75	30	150	June	Japan

continued...

Table 11 continued.

Crop	Init. (L_{ini})	Dev. (L_{dev})	Mid (L_{mid})	Late (L_{late})	Total	Plant Date	Region
f. Perennial Vegetables (with winter dormancy and initially bare or mulched soil)							
Artichoke	40	40	250	30	360	Apr (1st yr)	California
	20	25	250	30	325	May (2nd yr)	(cut in May)
Asparagus	50	30	100	50	230	Feb	Warm Winter
	90	30	200	45	365	Feb	Mediterranean
g. Fibre Crops							
Cotton	30	50	60	55	195	Mar-May	Egypt; Pakistan; Calif.
	45	90	45	45	225	Mar	Calif. Desert, USA
	30	50	60	55	195	Sept	Yemen
	30	50	55	45	180	April	Texas
Flax	25	35	50	40	150	April	Europe
	30	40	100	50	220	October	Arizona
h. Oil Crops							
Castor beans	25	40	65	50	180	March	(Semi)Arid Climates
	20	40	50	25	135	Nov.	Indonesia
Safflower	20	35	45	25	125	April	California, USA
	25	35	55	30	145	Mar	High Latitudes
	35	55	60	40	190	Oct/Nov	Arid Region
Sesame	20	30	40	20	100	June	China
Sunflower	25	35	45	25	130	April/May	Medit.; California
i. Cereals							
Barley/Oats/	15	25	50	30	120	November	Central India
Wheat	20	25	60	30	135	March/Apr	35-45 ^oL
	15	30	65	40	150	July	East Africa
	40	30	40	20	130	Apr	
	40	60	60	40	200	Nov	
	20	50	60	30	160	Dec	Calif. Desert, USA
Winter Wheat	20[2]	60[2]	70	30	180	December	Calif., USA
	30	140	40	30	240	November	Mediterranean
	160	75	75	25	335	October	Idaho, USA
Grains (small)	20	30	60	40	150	April	Mediterranean
	25	35	65	40	165	Oct/Nov	Pakistan; Arid Reg.
Maize (grain)	30	50	60	40	180	April	East Africa (alt.)
	25	40	45	30	140	Dec/Jan	Arid Climate
	20	35	40	30	125	June	Nigeria (humid)
	20	35	40	30	125	October	India (dry, cool)
	30	40	50	30	150	April	Spain (spr, sum.); Calif.
	30	40	50	50	170	April	Idaho, USA
Maize (sweet)	20	20	30	10	80	March	Philippines
	20	25	25	10	80	May/June	Mediterranean
	20	30	50/30	10	90	Oct/Dec	Arid Climate
	30	30	30	10[3]	110	April	Idaho, USA
	20	40	70	10	140	Jan	Calif. Desert, USA
Millet	15	25	40	25	105	June	Pakistan
	20	30	55	35	140	April	Central USA

continued...

[2] These periods for winter wheat will lengthen in frozen climates according to days having zero growth potential and wheat dormancy . Under general conditions and in the absence of local data, fall planting of winter wheat can be presumed to occur in northern temperate climates when the 10-day running average of mean daily air temperature decreases to 17^o C or December 1, whichever comes first. Planting of spring wheat can be presumed to occur when the 10-day running average of mean daily air temperature increases to 5^o C. Spring planting of maize-grain can be presumed to occur when the 10-day running average of mean daily air temperature increases to 13^o C.

[3] The late season for sweet maize will be about 35 days if the grain is allowed to mature and dry.

Table 11 continued

Crop	Init. (L_{ini})	Dev. (L_{dev})	Mid (L_{mid})	Late (L_{late})	Total	Plant Date	Region
Sorghum	20 20	35 35	40 45	30 30	130 140	May/June Mar/April	USA, Pakis., Med. Arid Region
Rice	30 30	30 30	60 80	30 40	150 180	Dec; May May	Tropics; Mediterranean Tropics
j. Forages							
Alfalfa, total season[4]	10	30	var.	var.	var.		last -4°C in spring until first -4°C in fall
Alfalfa[4] 1st cutting cycle	10 10	20 30	20 25	10 10	60 75	Jan Apr (last -4° C)	Calif., USA. Idaho, USA.
Alfalfa[4], other cutting cycles	5 5	10 20	10 10	5 10	30 45	Mar Jun	Calif., USA. Idaho, USA.
Bermuda for seed	10	25	35	35	105	March	Calif. Desert, USA
Bermuda for hay (several cuttings)	10	15	75	35	135	---	Calif. Desert, USA
Grass Pasture[4]	10	20	--	--	--		7 days before last -4°C in spring until 7 days after first -4°C in fall
Sudan, 1st cutting cycle	25	25	15	10	75	Apr	Calif. Desert, USA
Sudan, other cutting cycles	3	15	12	7	37	June	Calif. Desert, USA
k. Sugar Cane							
Sugarcane, virgin	35 50 75	60 70 105	190 220 330	120 140 210	405 480 720		Low Latitudes Tropics Hawaii, USA
Sugarcane, ratoon	25 30 35	70 50 105	135 180 210	50 60 70	280 320 420		Low Latitudes Tropics Hawaii, USA
l. Tropical Fruits and Trees							
Banana, 1st yr	120	90	120	60	390	Mar	Mediterranean
Banana, 2nd yr	120	60	180	5	365	Feb	Mediterranean
Pineapple	60	120	600	10	790		Hawaii, USA
m. Grapes and Berries							
Grapes	20 20 20 30	40 50 50 60	120 75 90 40	60 60 20 80	240 205 180 210	April Mar May April	Low Latitudes Calif., USA High Latitudes Mid Latitudes (wine)
Hops	25	40	80	10	155	April	Idaho, USA
n. Fruit Trees							
Citrus	60	90	120	95	365	Jan	Mediterranean
Deciduous Orchard	20 20 30	70 70 50	90 120 130	30 60 30	210 270 240	March March March	High Latitudes Low Latitudes Calif., USA

continued...

[4] In climates having killing frosts, growing seasons can be estimated for alfalfa and grass as:
alfalfa: last -4°C in spring until first -4°C in fall (Everson, D.O., M. Faubion and D.E. Amos 1978. "Freezing temperatures and growing seasons in Idaho." Univ. Idaho Agric. Exp. station bulletin 494. 18 p.)
grass: 7 days before last -4°C in spring and 7 days after last -4°C in fall (Kruse E.G. and Haise, H.R. 1974. "Water use by native grasses in high altitude Colorado meadows." USDA Agric. Res. Service, Western Region report ARS-W-6-1974. 60 pages)

Table 11 continued

Crop	Init. (L_{ini})	Dev. (L_{dev})	Mid (L_{mid})	Late (L_{late})	Total	Plant Date	Region
Olives	30	90	60	90	270[5]	March	Mediterranean
Pistachios	20	60	30	40	150	Feb	Mediterranean
Walnuts	20	10	130	30	190	April	Utah, USA
o. Wetlands - Temperate Climate							
Wetlands (Cattails, Bulrush)	10 180	30 60	80 90	20 35	140 365	May November	Utah, USA; killing frost Florida, USA
Wetlands (short veg.)	180	60	90	35	365	November	frost-free climate

5 Olive trees gain new leaves in March. See footnote 24 of Table 12 for additional information, where the K_C continues outside of the "growing period".

Primary source: FAO Irrigation and Drainage Paper 24 (Doorenbos and Pruitt, 1977), Table 22.

The lengths of the initial and development periods may be relatively short for deciduous trees and shrubs that can develop new leaves in the spring at relatively fast rates (Figure 23).

The rate at which vegetation cover develops and the time at which it attains effective full cover are affected by weather conditions in general and by mean daily air temperature in particular. Therefore, the length of time between planting and effective full cover will vary with climate, latitude, elevation and planting date. It will also vary with cultivar (crop variety). Generally, once the effective full cover for a plant canopy has been reached, the rate of further phenological development (flowering, seed development, ripening, and senescence) is more dependent on plant genotype and less dependent on weather. As an example, Figure 28 presents the variation in length of the growing period for one cultivar of rice for one region and for various planting dates.

The end of the mid-season and beginning of the late season is usually marked by senescence of leaves, often beginning with the lower leaves of plants. The length of the late season period may be relatively short (less than 10 days) for vegetation killed by frost (for example, maize at high elevations in latitudes > 40°N) or for agricultural crops that are harvested fresh (for example, table beets and small vegetables).

High temperatures may accelerate the ripening and senescence of crops. Long duration of high air temperature (> 35°C) can cause some crops such as turf grass to go into dormancy. If severely high air temperatures are coupled with moisture stress, the dormancy of grass can be permanent for the remainder of the growing season. Moisture stress or other environmental stresses will usually accelerate the rate of crop maturation and can shorten the mid and late season growing periods.

The values in Table 11 are useful only as a general guide and for comparison purposes. The listed lengths of growth stages are average lengths for the regions and periods specified and are intended to serve only as examples. Local observations of the specific plant stage development should be used, wherever possible, to incorporate effects of plant variety, climate and cultural practices. Local information can be obtained by interviewing farmers, ranchers, agricultural extension agents and local researchers, by conducting local surveys, or by remote sensing. When determining stage dates from local observations, the guidelines and visual descriptions may be helpful.

FIGURE 28
Variation in the length of the growing period of rice (cultivar: Jaya) sown during various months of the year at different locations along the Senegal River (Africa)

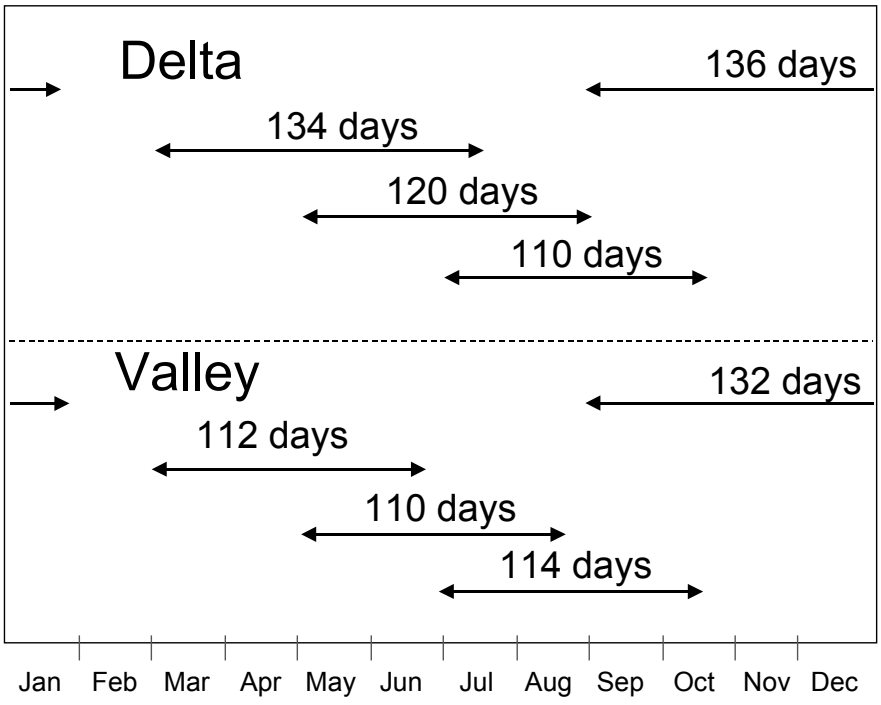

CROP COEFFICIENTS

Changes in vegetation and ground cover mean that the crop coefficient K_c varies during the growing period. The trends in K_c during the growing period are represented in the crop coefficient curve. Only three values for K_c are required to describe and construct the crop coefficient curve: those during the initial stage ($K_{c\ ini}$), the mid-season stage ($K_{c\ mid}$) and at the end of the late season stage ($K_{c\ end}$).

Tabulated K_c values

Table 12 lists typical values for $K_{c\ ini}$, $K_{c\ mid}$, and $K_{c\ end}$ for various agricultural crops. The coefficients presented are organized by group type (i.e., small vegetables, legumes, cereals, etc.) to assist in locating the crop in the table and to aid in comparing crops within the same group. There is usually close similarity in the coefficients among the members of the same crop group, as the plant height, leaf area, ground coverage and water management are normally similar.

The coefficients in Table 12 integrate the effects of both transpiration and evaporation over time. The effects of the integration over time represent an average wetting frequency for a 'standard' crop under typical growing conditions in an irrigated setting. The values for K_c during the initial and crop development stages are subject to the effects of large variations in wetting frequencies and therefore refinements to the value used for $K_{c\ ini}$ should always be made. For frequent wettings such as with high frequency sprinkler irrigation or rainfall, the values for $K_{c\ ini}$ may increase substantially.

TABLE 12
Single (time-averaged) crop coefficients, K_c, and mean maximum plant heights for non stressed, well-managed crops in subhumid climates (RH_{min} ≈ 45%, u_2 ≈ 2 m/s) for use with the FAO Penman-Monteith ET_o.

Crop	$K_{c\ ini}$ [1]	$K_{c\ mid}$	$K_{c\ end}$	Maximum Crop Height (h) (m)
a. Small Vegetables	**0.7**	**1.05**	**0.95**	
Broccoli		1.05	0.95	0.3
Brussel Sprouts		1.05	0.95	0.4
Cabbage		1.05	0.95	0.4
Carrots		1.05	0.95	0.3
Cauliflower		1.05	0.95	0.4
Celery		1.05	1.00	0.6
Garlic		1.00	0.70	0.3
Lettuce		1.00	0.95	0.3
Onions - dry		1.05	0.75	0.4
- green		1.00	1.00	0.3
- seed		1.05	0.80	0.5
Spinach		1.00	0.95	0.3
Radish		0.90	0.85	0.3
b. Vegetables – Solanum Family (*Solanaceae*)	**0.6**	**1.15**	**0.80**	
Egg Plant		1.05	0.90	0.8
Sweet Peppers (bell)		1.05[2]	0.90	0.7
Tomato		1.15[2]	0.70-0.90	0.6
c. Vegetables – Cucumber Family (*Cucurbitaceae*)	**0.5**	**1.00**	**0.80**	
Cantaloupe	0.5	0.85	0.60	0.3
Cucumber – Fresh Market	0.6	1.00[2]	0.75	0.3
– Machine harvest	0.5	1.00	0.90	0.3
Pumpkin, Winter Squash		1.00	0.80	0.4
Squash, Zucchini		0.95	0.75	0.3
Sweet Melons		1.05	0.75	0.4
Watermelon	0.4	1.00	0.75	0.4
d. Roots and Tubers	**0.5**	**1.10**	**0.95**	
Beets, table		1.05	0.95	0.4
Cassava – year 1	0.3	0.80[3]	0.30	1.0
– year 2	0.3	1.10	0.50	1.5
Parsnip	0.5	1.05	0.95	0.4
Potato		1.15	0.75[4]	0.6
Sweet Potato		1.15	0.65	0.4
Turnip (and Rutabaga)		1.10	0.95	0.6
Sugar Beet	0.35	1.20	0.70[5]	0.5

continued…

1 These are general values for $K_{c\ ini}$ under typical irrigation management and soil wetting. For frequent wettings such as with high frequency sprinkle irrigation or daily rainfall, these values may increase substantially and may approach 1.0 to 1.2. $K_{c\ ini}$ is a function of wetting interval and potential evaporation rate during the initial and development periods and is more accurately estimated using Figures 29 and 30, or Equation 7-3 in Annex 7, or using the dual $K_{cb\ ini} + K_e$.

2 Beans, Peas, Legumes, Tomatoes, Peppers and Cucumbers are sometimes grown on stalks reaching 1.5 to 2 meters in height. In such cases, increased K_c values need to be taken. For green beans, peppers and cucumbers, 1.15 can be taken, and for tomatoes, dry beans and peas, 1.20. Under these conditions h should be increased also.

3 The midseason values for cassava assume non-stressed conditions during or following the rainy season. The $K_{c\ end}$ values account for dormancy during the dry season.

4 The $K_{c\ end}$ value for potatoes is about 0.40 for long season potatoes with vine kill.

5 This $K_{c\ end}$ value is for no irrigation during the last month of the growing season. The $K_{c\ end}$ value for sugar beets is higher, up to 1.0, when irrigation or significant rain occurs during the last month.

Table 12 continued

Crop	$K_{c\ ini}$ [1]	$K_{c\ mid}$	$K_{c\ end}$	Maximum Crop Height (h) (m)
e. Legumes (*Leguminosae*)	**0.4**	**1.15**	**0.55**	
Beans, green	0.5	1.05[2]	0.90	0.4
Beans, dry and Pulses	0.4	1.15[2]	0.35	0.4
Chick pea		1.00	0.35	0.4
Fababean (broad bean) – Fresh	0.5	1.15[2]	1.10	0.8
– Dry/Seed	0.5	1.15[2]	0.30	0.8
Grabanzo	0.4	1.15	0.35	0.8
Green Gram and Cowpeas		1.05	0.60-0.35[6]	0.4
Groundnut (Peanut)		1.15	0.60	0.4
Lentil		1.10	0.30	0.5
Peas – Fresh	0.5	1.15[2]	1.10	0.5
– Dry/Seed		1.15	0.30	0.5
Soybeans		1.15	0.50	0.5-1.0
f. Perennial Vegetables (with winter dormancy and initially bare or mulched soil)	**0.5**	1.00	0.80	
Artichokes	0.5	1.00	0.95	0.7
Asparagus	0.5	0.95[7]	0.30	0.2-0.8
Mint	0.60	1.15	1.10	0.6-0.8
Strawberries	0.40	0.85	0.75	0.2
g. Fibre Crops	**0.35**			
Cotton		1.15-1.20	0.70-0.50	1.2-1.5
Flax		1.10	0.25	1.2
Sisal[8]		0.4-0.7	0.4-0.7	1.5
h. Oil Crops	**0.35**	**1.15**	**0.35**	
Castorbean (*Ricinus*)		1.15	0.55	0.3
Rapeseed, Canola		1.0-1.15[9]	0.35	0.6
Safflower		1.0-1.15[9]	0.25	0.8
Sesame		1.10	0.25	1.0
Sunflower		1.0-1.15[9]	0.35	2.0
i. Cereals	**0.3**	**1.15**	**0.4**	
Barley		1.15	0.25	1
Oats		1.15	0.25	1
Spring Wheat		1.15	0.25-0.4[10]	1
Winter Wheat - with frozen soils	0.4	1.15	0.25-0.4[10]	1
- with non-frozen soils	0.7	1.15	0.25-0.4[10]	
Maize, Field (grain) *(field corn)*		1.20	0.60,0.35[11]	2
Maize, Sweet *(sweet corn)*		1.15	1.05[12]	1.5
Millet		1.00	0.30	1.5
Sorghum – grain		1.00-1.10	0.55	1-2
– sweet		1.20	1.05	2-4
Rice	1.05	1.20	0.90-0.60	1

continued…

6 The first $K_{c\ end}$ is for harvested fresh. The second value is for harvested dry.

7 The K_c for asparagus usually remains at $K_{c\ ini}$ during harvest of the spears, due to sparse ground cover. The $K_{c\ mid}$ value is for following regrowth of plant vegetation following termination of harvest of spears.

8 K_c for sisal depends on the planting density and water management (e.g., intentional moisture stress).

9 The lower values are for rainfed crops having less dense plant populations.

10 The higher value is for hand-harvested crops.

11 The first $K_{c\ end}$ value is for harvest at high grain moisture. The second $K_{c\ end}$ value is for harvest after complete field drying of the grain (to about 18% moisture, wet mass basis).

12 If harvested fresh for human consumption. Use $K_{c\ end}$ for field maize if the sweet maize is allowed to mature and dry in the field.

Table 12 continued

Crop	$K_{c\ ini}$[1]	$K_{c\ mid}$	$K_{c\ end}$	Maximum Crop Height (h) (m)
j. Forages				
Alfalfa Hay – averaged cutting effects	0.40	0.95[13]	0.90	0.7
– individual cutting periods	0.40[14]	1.20[14]	1.15[14]	0.7
– for seed	0.40	0.50	0.50	0.7
Bermuda hay – averaged cutting effects	0.55	1.00[13]	0.85	0.35
– Spring crop for seed	0.35	0.90	0.65	0.4
Clover hay, Berseem – averaged cutting effects	0.40	0.90[13]	0.85	0.6
– individual cutting periods	0.40[14]	1.15[14]	1.10[14]	0.6
Rye Grass hay – averaged cutting effects	0.95	1.05	1.00	0.3
Sudan Grass hay (annual) – averaged cutting effects	0.50	0.90[14]	0.85	1.2
– individual cutting periods	0.50[14]	1.15[14]	1.10[14]	1.2
Grazing Pasture - Rotated Grazing	0.40	0.85-1.05	0.85	0.15-0.30
- Extensive Grazing	0.30	0.75	0.75	0.10
Turf grass - cool season[15]	0.90	0.95	0.95	0.10
- warm season[15]	0.80	0.85	0.85	0.10
k. Sugar Cane	0.40	1.25	0.75	3
l. Tropical Fruits and Trees				
Banana – 1st year	0.50	1.10	1.00	3
– 2nd year	1.00	1.20	1.10	4
Cacao	1.00	1.05	1.05	3
Coffee – bare ground cover	0.90	0.95	0.95	2-3
– with weeds	1.05	1.10	1.10	2-3
Date Palms	0.90	0.95	0.95	8
Palm Trees	0.95	1.00	1.00	8
Pineapple[16] – bare soil	0.50	0.30	0.30	0.6-1.2
– with grass cover	0.50	0.50	0.50	0.6-1.2
Rubber Trees	0.95	1.00	1.00	10
Tea – non-shaded	0.95	1.00	1.00	1.5
– shaded[17]	1.10	1.15	1.15	2
m. Grapes and Berries				
Berries (bushes)	0.30	1.05	0.50	1.5
Grapes – Table or Raisin	0.30	0.85	0.45	2
– Wine	0.30	0.70	0.45	1.5-2
Hops	0.3	1.05	0.85	5

continued…

[13] This $K_{c\ mid}$ coefficient for hay crops is an overall average $K_{c\ mid}$ coefficient that averages K_c for both before and following cuttings. It is applied to the period following the first development period until the beginning of the last late season period of the growing season.

[14] These K_c coefficients for hay crops represent immediately following cutting; at full cover; and immediately before cutting, respectively. The growing season is described as a series of individual cutting periods (Figure 35).

[15] Cool season grass varieties include dense stands of bluegrass, ryegrass, and fescue. Warm season varieties include bermuda grass and St. Augustine grass. The 0.95 values for cool season grass represent a 0.06 to 0.08 m mowing height under general turf conditions. Where careful water management is practiced and rapid growth is not required, K_c's for turf can be reduced by 0.10.

[16] The pineapple plant has very low transpiration because it closes its stomates during the day and opens them during the night. Therefore, the majority of ET_c from pineapple is evaporation from the soil. The $K_{c\ mid} < K_{c\ ini}$ since $K_{c\ mid}$ occurs during full ground cover so that soil evaporation is less. Values given assume that 50% of the ground surface is covered by black plastic mulch and that irrigation is by sprinkler. For drip irrigation beneath the plastic mulch, K_c's given can be reduced by 0.10.

[17] Includes the water requirements of the shade trees.

Table 12 continued

Crop	$K_{c\ ini}$[1]	$K_{c\ mid}$	$K_{c\ end}$	Maximum Crop Height (h) (m)
n. Fruit Trees				
Almonds, no ground cover	0.40	0.90	0.65[18]	5
Apples, Cherries, Pears[19]				
- no ground cover, killing frost	0.45	0.95	0.70[18]	4
- no ground cover, no frosts	0.60	0.95	0.75[18]	4
- active ground cover, killing frost	0.50	1.20	0.95[18]	4
- active ground cover, no frosts	0.80	1.20	0.85[18]	4
Apricots, Peaches, Stone Fruit[19, 20]				
- no ground cover, killing frost	0.45	0.90	0.65[18]	3
- no ground cover, no frosts	0.55	0.90	0.65[18]	3
- active ground cover, killing frost	0.50	1.15	0.90[18]	3
- active ground cover, no frosts	0.80	1.15	0.85[18]	3
Avocado, no ground cover	0.60	0.85	0.75	3
Citrus, no ground cover[21]				
- 70% canopy	0.70	0.65	0.70	4
- 50% canopy	0.65	0.60	0.65	3
- 20% canopy	0.50	0.45	0.55	2
Citrus, with active ground cover or weeds[22]				
- 70% canopy	0.75	0.70	0.75	4
- 50% canopy	0.80	0.80	0.80	3
- 20% canopy	0.85	0.85	0.85	2
Conifer Trees[23]	1.00	1.00	1.00	10
Kiwi	0.40	1.05	1.05	3
Olives (40 to 60% ground coverage by canopy)[24]	0.65	0.70	0.70	3-5
Pistachios, no ground cover	0.40	1.10	0.45	3-5
Walnut Orchard[19]	0.50	1.10	0.65[18]	4-5

continued…

18 These $K_{c\ end}$ values represent K_c prior to leaf drop. After leaf drop, $K_{c\ end} \approx 0.20$ for bare, dry soil or dead ground cover and $K_{c\ end} \approx 0.50$ to 0.80 for actively growing ground cover (consult Chapter 11).

19 Refer to Eq. 94, 97 or 98 and footnotes 21 and 22 for estimating K_c for immature stands.

20 Stone fruit category applies to peaches, apricots, pears, plums and pecans.

21 These K_c values can be calculated from Eq. 98 for $K_{c\ min} = 0.15$ and $K_{c\ full} = 0.75$, 0.70 and 0.75 for the initial, mid season and end of season periods, and $f_{c\ eff} = f_c$ where f_c = fraction of ground covered by tree canopy (e.g., the sun is presumed to be directly overhead). The values listed correspond with those in Doorenbos and Pruitt (1977) and with more recent measurements. The midseason value is lower than initial and ending values due to the effects of stomatal closure during periods of peak ET. For humid and subhumid climates where there is less stomatal control by citrus, values for $K_{c\ ini}$, $K_{c\ mid}$, and $K_{c\ end}$ can be increased by 0.1 - 0.2, following Rogers et al. (1983).

22 These K_c values can be calculated as $K_c = f_c\ K_{c\ ngc} + (1 - f_c)\ K_{c\ cover}$ where $K_{c\ ngc}$ is the K_c of citrus with no active ground cover (calculated as in footnote 21), $K_{c\ cover}$ is the K_c for the active ground cover (0.95), and f_c is defined in footnote 21. The values listed correspond with those in Doorenbos and Pruitt (1977) and with more recent measurements. Alternatively, K_c for citrus with active ground cover can be estimated directly from Eq. 98 by setting $K_{c\ min} = K_{c\ cover}$. For humid and subhumid climates where there is less stomatal control by citrus, values for $K_{c\ ini}$, $K_{c\ mid}$, and $K_{c\ end}$ can be increased by 0.1 - 0.2, following Rogers et al. (1983).

For non-active or only moderately active ground cover (active indicates green and growing ground cover with LAI > about 2 to 3) , K_c should be weighted between K_c for no ground cover and K_c for active ground cover, with the weighting based on the "greenness" and approximate leaf area of the ground cover.

23 Confers exhibit substantial stomatal control due to reduced aerodynamic resistance. The K_c can easily reduce below the values presented, which represent well-watered conditions for large forests.

Table 12 continued

Crop	$K_{c\ ini}$[1]	$K_{c\ mid}$	$K_{c\ end}$	Maximum Crop Height (h) (m)
o. Wetlands – temperate climate				
Cattails, Bulrushes, killing frost	0.30	1.20	0.30	2
Cattails, Bulrushes, no frost	0.60	1.20	0.60	2
Short Veg., no frost	1.05	1.10	1.10	0.3
Reed Swamp, standing water	1.00	1.20	1.00	1-3
Reed Swamp, moist soil	0.90	1.20	0.70	1-3
p. Special				
Open Water, < 2 m depth or in subhumid climates or tropics		1.05	1.05	
Open Water, > 5 m depth, clear of turbidity, temperate climate		0.65[25]	1.25[25]	

[24] These coefficients represent about 40 to 60% ground cover. Refer to Eq. 98 and footnotes 21 and 22 for estimating K_c for immature stands. In Spain, Pastor and Orgaz (1994) have found the following monthly K_c's for olive orchards having 60% ground cover: 0.50, 0.50, 0.65, 0.60, 0.55, 0.50, 0.45, 0.45, 0.55, 0.60, 0.65, 0.50 for months January through December. These coefficients can be invoked by using $K_{c\ ini}$ = 0.65, $K_{c\ mid}$ = 0.45, and $K_{c\ end}$ = 0.65, with stage lengths = 30, 90, 60 and 90 days, respectively for initial, development, midseason and late season periods, and using K_c during the winter ("off season") in December to February = 0.50.

[25] These K_c's are for deep water in temperate latitudes where large temperature changes in the water body occur during the year, and initial and peak period evaporation is low as radiation energy is absorbed into the deep water body. During fall and winter periods ($K_{c\ end}$), heat is released from the water body that increases the evaporation above that for grass. Therefore, $K_{c\ mid}$ corresponds to the period when the water body is gaining thermal energy and $K_{c\ end}$ when releasing thermal energy. These K_c's should be used with caution.

Primary sources: **$K_{c\ ini}$: Doorenbos and Kassam (1979)**
$K_{c\ mid}$ and $K_{c\ end}$: Doorenbos and Pruitt (1977); Pruitt (1986); Wright (1981, 1982), Snyder et al., (1989)

The values for $K_{c\ mid}$ and $K_{c\ end}$ in Table 12 represent those for a sub-humid climate with an average daytime minimum relative humidity (RH_{min}) of about 45% and with calm to moderate wind speeds averaging 2 m/s. For more humid or arid conditions, or for more or less windy conditions, the K_c coefficients for the mid-season and end of late season stage should be modified as described in this chapter.

The values for K_c in Table 12 are values for non-stressed crops cultivated under excellent agronomic and water management conditions and achieving maximum crop yield (standard conditions). Where stand density, height or leaf area are less than that attained under such conditions, the value for $K_{c\ mid}$ and, for most crops, for $K_{c\ end}$ will need to be modified (Part C, Chapters 8, 9 and 10).

Crop coefficient for the initial stage ($K_{c\ ini}$)

Calculation procedure

The values for $K_{c\ ini}$ in Table 12 are only approximations and should only be used for estimating ET_c during preliminary or planning studies. For several group types only one value

for $K_{c\ ini}$ is listed and it is considered to be representative of the whole group for a typical irrigation water management. More accurate estimates of $K_{c\ ini}$ can be obtained by considering:

Time interval between wetting events

Evapotranspiration during the initial stage for annual crops is predominately in the form of evaporation. Therefore, accurate estimates for $K_{c\ ini}$ should consider the frequency with which the soil surface is wetted during the initial period. Where the soil is frequently wet from irrigation or rain, the evaporation from the soil surface can be considerable and $K_{c\ ini}$ will be large. On the other hand, where the soil surface is dry, evaporation is restricted and the $K_{c\ ini}$ will be small (Table 9).

Evaporation power of the atmosphere

The value of $K_{c\ ini}$ is affected by the evaporating power of the atmosphere, i.e., ET_o. The higher the evaporation power of the atmosphere, the quicker the soil will dry between water applications and the smaller the time-averaged K_c will be for any particular period.

Magnitude of the wetting event

As the amount of water available in the topsoil for evaporation and hence the time for the soil surface to dry is a function of the magnitude of the wetting event, $K_{c\ ini}$ will be smaller for light wetting events than for large wettings.

Depending on the time interval between wetting events, the magnitude of the wetting event, and the evaporation power of the atmosphere, $K_{c\ ini}$ can vary between 0.1 and 1.15. A numerical procedure to compute $K_{c\ ini}$ is provided in Annex 7.

Time interval between wetting events

In general, the mean time interval between wetting events is estimated by counting all rainfall and irrigation events occurring during the initial period that are greater than a few millimetres. Wetting events occurring on adjacent days can be counted as one event. The mean wetting interval is estimated by dividing the length of the initial period by the number of events.

Where only monthly rainfall values are available without any information on the number of rainy days, the number of events within the month can be estimated by dividing the monthly rainfall depth by the depth of a typical rain event. The typical depth, if it exists, can vary widely from climate to climate, region to region and from season to season. Table 13 presents some information on the range of rainfall depths. After deciding what rainfall is typical for the region and time of the year, the number of rainy days and the mean wetting interval can be estimated.

TABLE 13
Classification of rainfall depths

rain event	depth
Very light (drizzle)	≤ 3 mm
Light (light showers)	5 mm
Medium (showers)	≥ 10 mm
Heavy (rainstorms)	≥ 40 mm

Where rainfall is insufficient, irrigation is needed to keep the crop well watered. Even where irrigation is not yet developed, the mean interval between the future irrigations should be

estimated to obtain the required frequency of wetting necessary to keep the crop stress free. The interval might be as small as a few days for small vegetables, but up to a week or longer for cereals depending on the climatic conditions. Where no estimate of the interval can be made, the user may refer to the values for $K_{c\ ini}$ of Table 12.

EXAMPLE 23
Estimation of interval between wetting events

Estimate, from mean monthly rainfall data, the interval between rains during the rainy season for a station in a temperate climate (Paris, France: 50 mm/month), dry climate (Gafsa, Tunisia: 20 mm/month) and tropical climate (Calcutta, India: 300 mm/month).

Station	monthly rain (mm/month)	typical rainfall (mm)	number of rainy days	interval between rains
Paris	50	3	17	~ 2 days
Gafsa	20	5	4	weekly
Calcutta	300	20	15	~ 2 days

Determination of $K_{c\ ini}$

The crop coefficient for the initial growth stage can be derived from Figures 29 and 30 which provide estimates for $K_{c\ ini}$ as a function of the average interval between wetting events, the evaporation power ET_o, and the importance of the wetting event.

Light wetting events (infiltration depths of 10 mm or less): rainfall and high frequency irrigation systems

Figure 29 is used for all soil types when wetting events are light. When wetting during the initial period is only by precipitation, one will usually use Figure 29 to determine $K_{c\ ini}$. The graph can also be used when irrigation is by high frequency systems such as microirrigation and centre pivot and light applications of about 10 mm or less per wetting event are applied.

EXAMPLE 24
Graphical determination of $K_{c\ ini}$

A silt loam soil receives irrigation every two days during the initial growth stage via a centre pivot irrigation system. The average depth applied by the centre pivot system is about 12 mm per event and the average ET_o during the initial stage is 4 mm/day. Estimate the crop evapotranspiration during that stage.

From Fig. 29 using the 2-day interval curve:	$K_{c\ ini}$ =	0.85	-
-	$ET_c = K_c\ ET_o$ = 0.85 (4.0) =	3.4	mm/day
The average crop evapotranspiration during the initial growth stage is 3.4 mm/day			

Heavy wetting events (infiltration depths of 40 mm or more): surface and sprinkler irrigation

Figure 30 is used for heavy wetting events when infiltration depths are greater than 40 mm, such as for when wetting is primarily by periodic irrigation such as by sprinkler or surface irrigation. Following a wetting event, the amount of water available in the topsoil for evaporation is considerable, and the time for the soil surface to dry might be significantly increased. Consequently, the average K_c factor is larger than for light wetting events. As the time for the soil surface to dry is, apart from the evaporation power and the frequency of wetting, also determined by the water storage capacity of the topsoil, a distinction is made between soil types.

FIGURE 29
Average $K_{c\ ini}$ as related to the level of ET_o and the interval between irrigations and/or significant rain during the initial growth stage for all soil types when wetting events are light to medium (3-10 mm per event)

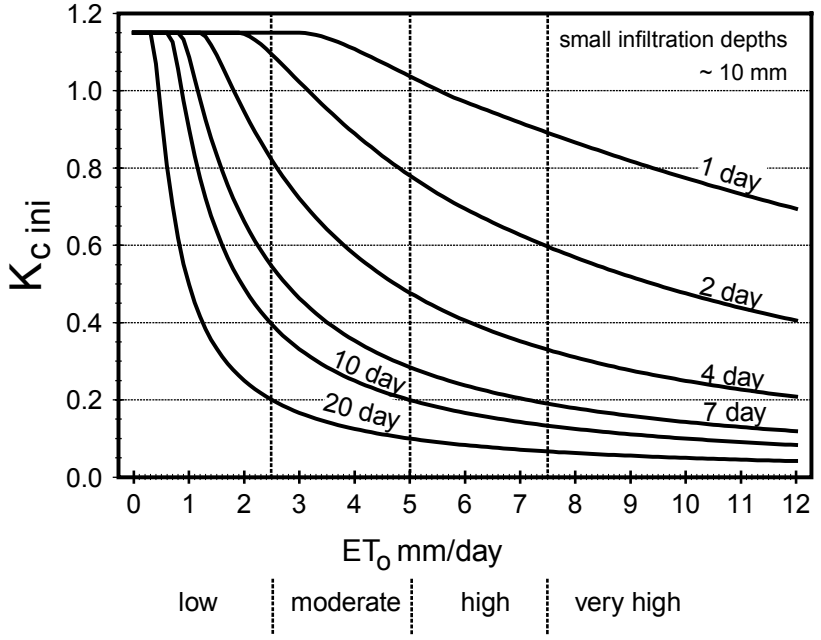

Figure 30a is used for coarse textured soils and Figure 30b is used for fine and medium textured soils. Coarse textured soils include sands and loamy sand textured soils. Medium textured soils include sandy loam, loam, silt loam and silt textured soils. Fine textured soils include silty clay loam, silty clay and clay textured soils.

Average wetting events (infiltration depths between 10 and 40 mm):

Where average infiltration depths are between 10 and 40 mm, the value for $K_{c\ ini}$ can be estimated from Figures 29 and 30:

$$K_{c\ ini} = K_{c\ ini\ (Fig.\ 29)} + \frac{(I-10)}{(40-10)}\left[K_{c\ ini\ (Fig.\ 30)} - K_{c\ ini\ (Fig.\ 29)}\right] \qquad (59)$$

where $K_{c\ ini\ (Fig.29)}$ value for $K_{c\ ini}$ from Figure 29,
$K_{c\ ini\ (Fig.30)}$ value for $K_{c\ ini}$ from Figure 30,
I average infiltration depth [mm].

The values 10 and 40 in Equation 59 are the average depths of infiltration (millimetres) upon which Figures 29 and 30 are based.

FIGURE 30
Average $K_{c\ ini}$ as related to the level of ET_o and the interval between irrigations greater than or equal to 40 mm per wetting event, during the initial growth stage for a) coarse textured soils; b) medium and fine textured soils

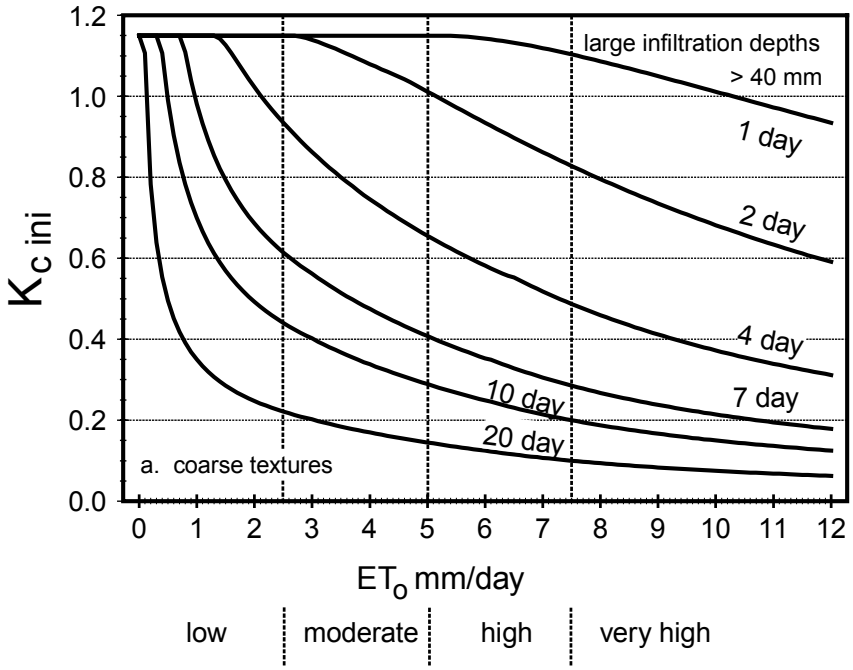

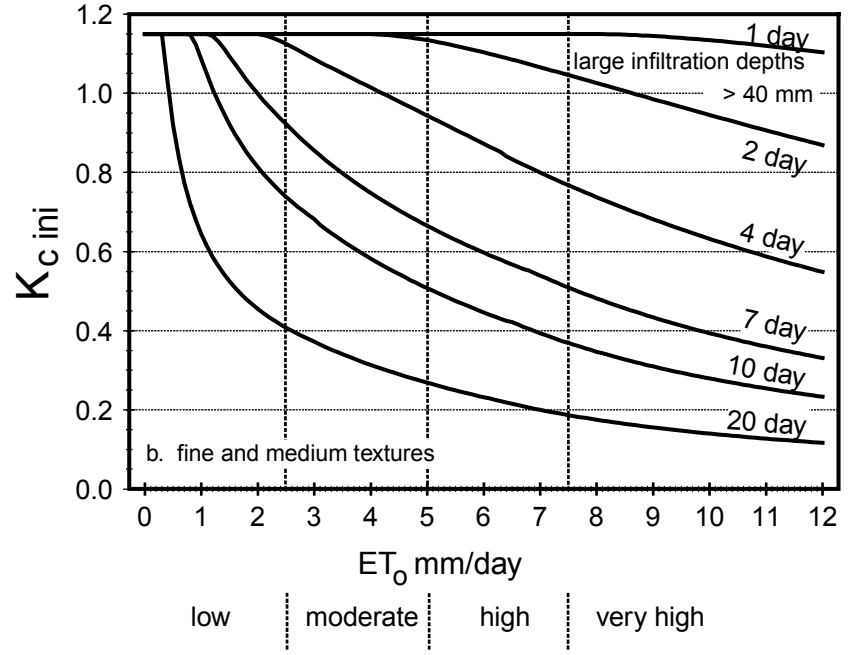

EXAMPLE 25
Interpolation between light and heavy wetting events

Small vegetables cultivated in a dry area on a coarse textured soil receive 20 mm of water twice a week by means of a sprinkler irrigation system. The average ET_o during the initial stage is 5 mm/day. Estimate the crop evapotranspiration during that stage.

For:	7/2 = ET_o = and a coarse textured soil	3.5 5	day interval mm/day
From Fig. 29:	$K_{c\ ini(Fig.\ 29)} \approx$	0.55	-
From Fig. 30.a:	$K_{c\ ini(Fig.\ 30a)} \approx$	0.7	-
For: From Eq. 59: From Eq. 58:	I = $K_{c\ ini}$ = 0.55 + [(20-10)/(40-10)] (0.7-0.55) = 0.55+0.33(0.15)= ET_c = 0.60 (5) =	20 0.60 3.0	mm - mm/day
The average crop evapotranspiration during the initial growth stage for the small vegetables is 3.0 mm/day.			

Adjustment for partial wetting by irrigation

Many types of irrigation systems wet only a fraction of the soil surface. For example, for a trickle irrigation system, the fraction of the surface wetted, f_w, may be only 0.4. For furrow irrigation systems, the fraction of the surface wetted may range from 0.3 to 0.8. Common values for the fraction of the soil surface wetted by irrigation or precipitation are given in Table 20. When only a fraction of the soil surface is wetted, the value for $K_{c\ ini}$ obtained from Table 12 or from Figures 29 or 30 should be multiplied by the fraction of the surface wetted to adjust for the partial wetting:

$$K_{c\ ini} = f_w\ K_{c\ ini\,(Tab,\ Fig)} \qquad (60)$$

where f_w the fraction of surfaced wetted by irrigation or rain [0 - 1],
$K_{c\ ini\ (Tab,Fig)}$ the value for $K_{c\ ini}$ from Table 12 or Figure 29 or 30.

In addition, in selecting which figure to use (i.e., Figure 29 or 30), the average infiltrated depth, expressed in millimetres over the entire field surface, should be divided by f_w to represent the true infiltrated depth of water for the part of the surface that is wetted (Figure 31):

$$I_w = \frac{I}{f_w} \qquad (61)$$

where I_w irrigation depth for the part of the surface that is wetted [mm],
f_w fraction of surface wetted by irrigation,
I the irrigation depth for the field [mm].

When irrigation of part of the soil surface and precipitation over the entire soil surface both occur during the initial period, f_w should represent the average of f_w for each type of wetting, weighted according to the total infiltration depth received by each type.

FIGURE 31
Partial wetting by irrigation

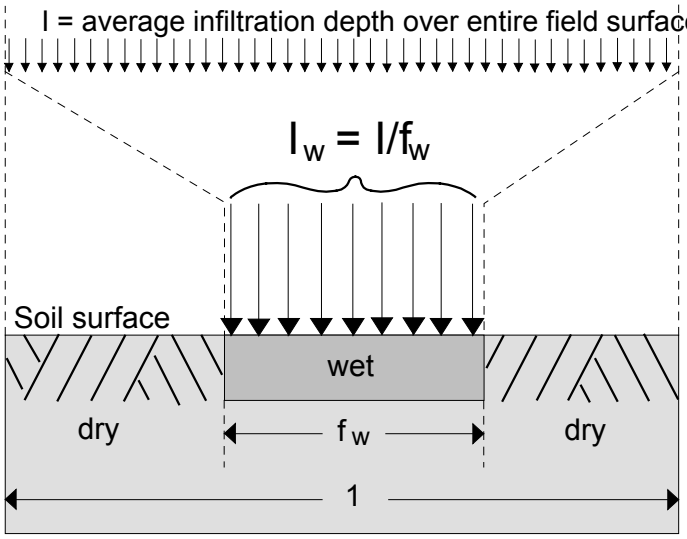

EXAMPLE 26
Determination of $K_{c\ ini}$ for partial wetting of the soil surface

Determine the evapotranspiration of the crop in Example 24 if it had been irrigated using a trickle system every two days (with 12 mm each application expressed as an equivalent depth over the field area), and where the average fraction of surface wet was 0.4, and where little or no precipitation occurred during the initial period.

The average depth of infiltration per event in the wetted fraction of the surface:

From Eq. 61:	$I_w = I / f_w$ = 12 mm / 0.4 =	30	mm

Therefore, one can interpolate between Fig. 29 representing light wetting events (~10 mm per event) and Fig. 30.b representing medium textured soil and large wetting events (~40 mm per event).

For:	ET_o = 4 mm/day	4	mm/day
and:	a 2 day wetting interval:	-	-
Fig. 29 produces:	$K_{c\ ini}$ = 0.85	0.85	-
Fig. 30.b produces	$K_{c\ ini}$ = 1.15	1.15	-
From Eq. 59:	$K_{c\ ini}$ = 0.85 + [(30 - 10)/(40 - 10)] (1.15 - 0.85) =	1.05	-

Because the fraction of soil surface wetted by the trickle system is 0.4, the actual $K_{c\ ini}$ for the trickle irrigation is calculated as:

From Eq. 60:	$K_{c\ ini} = f_w K_{c\ ini\ Fig}$ = 0.4 (1.05) =	0.42	-
	This value (0.42) represents the $K_{c\ ini}$ as applied over the entire field area.		
-	$ET_c = K_{c\ ini}\ ET_o$ = 0.42 (4) =	1.7	mm/day

The average crop evapotranspiration during the initial growth stage for this trickle irrigated crop is 1.7 mm/day.

$K_{c\ ini}$ for trees and shrubs

$K_{c\ ini}$ for trees and shrubs should reflect the ground condition prior to leaf emergence or initiation in case of deciduous trees or shrubs, and the ground condition during the dormancy or low active period for evergreen trees and shrubs. The $K_{c\ ini}$ depends upon the amount of grass or weed cover, frequency of soil wetting, tree density and mulch density. For a deciduous orchard in frost-free climates, the $K_{c\ ini}$ can be as high as 0.8 or 0.9, where grass ground cover exists, and as low as 0.3 or 0.4 when the soil surface is kept bare and wetting is infrequent. The $K_{c\ ini}$ for an evergreen orchard (having no concerted leaf drop) with a dormant period has less variation from $K_{c\ mid}$, as exemplified for citrus in Table 12, footnotes 21 and 22. For 50% canopy or less, the $K_{c\ ini}$ also reflects ground cover conditions (bare soil, mulch or active grass or weed cover).

$K_{c\ ini}$ for paddy rice

For rice growing in paddy fields with a water depth of 0.10-0.20 m, the ET_c during the initial stage mainly consists of evaporation from the standing water. The $K_{c\ ini}$ in Table 12 is 1.05 for a sub-humid climate with calm to moderate wind speeds. The $K_{c\ ini}$ should be adjusted for the local climate as indicated in Table 14.

TABLE 14
$K_{c\ ini}$ for rice for various climatic conditions

Humidity	Wind speed		
	light	moderate	strong
arid - semi-arid	1.10	1.15	1.20
sub-humid - humid	1.05	1.10	1.15
very humid	1.00	1.05	1.10

Crop coefficient for the mid-season stage ($K_{c\ mid}$)

Illustration of the climatic effect

Typical values for the crop coefficient for the mid-season growth stage, $K_{c\ mid}$, are listed in Table 12 for various agricultural crops.

As discussed in Chapter 5, the effect of the difference in aerodynamic properties between the grass reference surface and agricultural crops is not only crop specific but also varies with the climatic conditions and crop height (Figure 21). More arid climates and conditions of greater wind speed will have higher values for $K_{c\ mid}$. More humid climates and conditions of lower wind speed will have lower values for $K_{c\ mid}$.

The relative impact of climate on $K_{c\ mid}$ is illustrated in Figure 32 where the adjustments to the values from Table 12 are shown for various types of climates, mean daily wind speeds and various crop heights. As an example, expected variations for $K_{c\ mid}$ for tomatoes in response to regional climatic conditions are presented in Box 14.

Determination of $K_{c\ mid}$

For specific adjustment in climates where RH_{min} differs from 45% or where u_2 is larger or smaller than 2.0 m/s, the $K_{c\ mid}$ values from Table 12 are adjusted as:

$$K_{c\ mid} = K_{c\ mid\ (Tab)} + [0.04(u_2 - 2) - 0.004(RH_{min} - 45)]\left(\frac{h}{3}\right)^{0.3} \qquad (62)$$

FIGURE 32
Adjustment (additive) to the $K_{c\ mid}$ values from Table 12 for different crop heights and mean daily wind speeds (u_2) for different humidity conditions

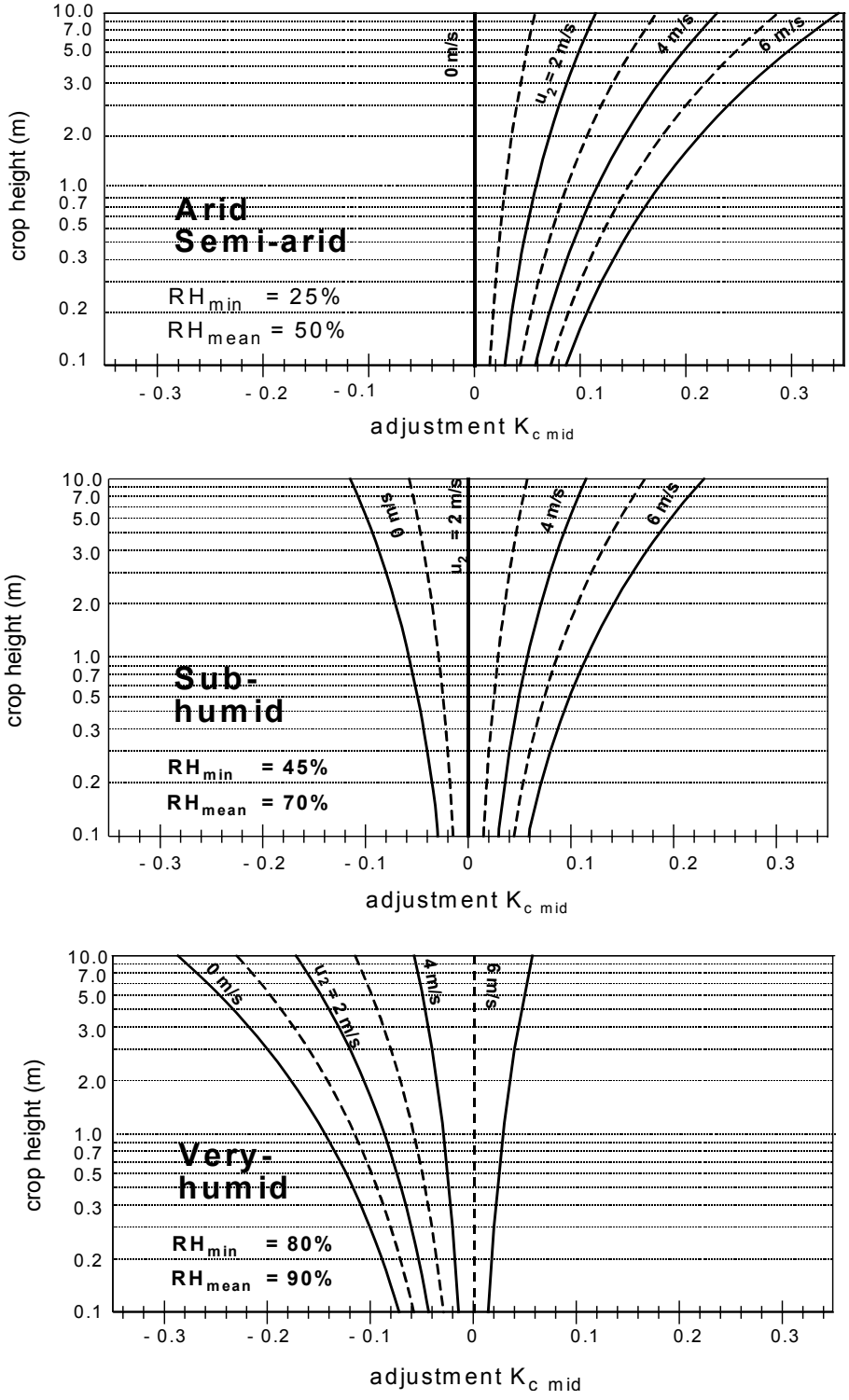

where $K_{c\ mid\ (Tab)}$ value for $K_{c\ mid}$ taken from Table 12,
u_2 mean value for daily wind speed at 2 m height over grass during the mid-season growth stage [m s^{-1}], for 1 m $s^{-1} \leq u_2 \leq 6$ m s^{-1},
RH_{min} mean value for daily minimum relative humidity during the mid-season growth stage [%], for $20\% \leq RH_{min} \leq 80\%$,
h mean plant height during the mid-season stage [m] for 0.1 m < h < 10 m.

The $K_{c\ mid}$ values determined with equations 62 and 65 are average adjustments for the midseason and late season periods. The values for parameters u_2 and RH_{min} should be accordingly taken as averages for these periods (see example, Annex 8). The limits expressed for parameters u_2, RH_{min} and h should be observed.

BOX 14
Demonstration of effect of climate on $K_{c\ mid}$ for wheat crop grown under field conditions

From Table 12 for wheat: $K_{c\ mid}$ = 1.15 and h = 1.0 m

For semi-arid to arid conditions
- for strong wind (4 m/s) $K_{c\ mid}$ = 1.15 + 0.10 = 1.25
- for moderate wind (2 m/s) $K_{c\ mid}$ = 1.15 + 0.05 = 1.20
- for calm wind (1 m/s) $K_{c\ mid}$ = 1.15 + 0.00 = 1.17

For sub-humid conditions
- for strong wind (4 m/s) $K_{c\ mid}$ = 1.15 + 0.05 = 1.20
- for moderate wind (2 m/s) $K_{c\ mid}$ = 1.15 + 0.00 = 1.15
- for calm wind (1 m/s) $K_{c\ mid}$ = 1.15 - 0.05 = 1.12

For humid and very humid conditions
- for strong wind (4 m/s) $K_{c\ mid}$ = 1.15 - 0.05 = 1.10
- for moderate wind (2 m/s) $K_{c\ mid}$ = 1.15 - 0.10 = 1.05
- for calm wind (1 m/s) $K_{c\ mid}$ = 1.15 - 0.15 = 1.02

Depending on the aridity of the climate and the wind conditions, the crop coefficient for wheat during the mid-season stage ranges from 1.02 (humid and calm wind) to 1.25 (arid and strong wind).

Where the user does not have access to a calculator with an exponential function, the solution of the $(h/3)^{0.3}$ expression can be approximated as $[(h/3)^{0.5}]^{0.5}$ where the square root key is used.

RH_{min} is used rather than RH_{mean} because it is easier to approximate RH_{min} from T_{max} where relative humidity data are unavailable. Moreover, under the common condition where T_{min} approaches T_{dew} (i.e., $RH_{max} \approx 100\%$), the vapour pressure deficit (e_s - e_a), with e_s from Equation 12 and e_a from Equation 17, becomes $[(100\text{-}RH_{min})/200]\ e°(T_{max})$, where $e°(T_{max})$ is saturation vapour pressure at maximum daily air temperature. This indicates that RH_{min} better reflects the impact of vapour pressure deficit on K_c than does RH_{mean}.

RH_{min} is calculated on a daily or average monthly basis as:

$$RH_{min} = \frac{e^o(T_{dew})}{e^o(T_{max})} 100 \qquad (63)$$

where T_{dew} is mean dewpoint temperature and T_{max} is mean daily maximum air temperature during the mid-season growth stage. Where dewpoint temperature or other hygrometric data are

not available or are of questionable quality, RH_{min} can be estimated by substituting mean daily minimum air temperature, T_{min}, for T_{dew}[1]. Then:

$$RH_{min} = \frac{e^o(T_{min})}{e^o(T_{max})} 100 \quad (64)$$

The values for u_2 and RH_{min} need only be approximate for the mid-season growth stage. This is because Equation 62 is not strongly sensitive to these values, changing 0.04 per 1 m/s change in u_2 and per 10% change in RH_{min} for a 3 m tall crop. Measurements, calculation and estimation of missing wind and humidity data are provided in Chapter 3. Wind speed measured at other than 2 m height should be adjusted to reflect values for wind speed at 2 m over grass using Equation 47. Where no data on u_2 or RH_{min} are available, the general classification for wind speed and humidity data given in Tables 15 and 16 can be used.

TABLE 15
Empirical estimates of monthly wind speed data

description	mean monthly wind speed at 2 m
light wind	...≤ 1.0 m/s
light to moderate wind	2.0 m/s
moderate to strong wind	4.0 m/s
strong wind	... ≥ 5.0 m/s
general global conditions	**2 m/s**

TABLE 16
Typical values for RH_{min} compared with RH_{mean} for general climatic classifications

Climatic classification	RH_{min} (%)	RH_{mean} (%)
Arid	20	45
Semi-arid	30	55
Sub-humid	45	70
Humid	70	85
Very humid	80	90

Equation 62 is valid for mean plant heights up to 10 m. For plant heights smaller than 0.1 m, vegetation will behave aerodynamically similar to grass reference and eq. 62 should not be applied. Example values for h are listed in Table 12 for various crops. However, the mean plant height will greatly vary with crop variety and with cultural practices. Therefore, wherever possible, h should be obtained from general field observations. However, the presence of the 0.3 exponent in Equation 62 makes these equations relatively insensitive to small errors in the value used for h. Generally, a single value for h is used to represent the mid-season period.

Adjustment for frequency of wetting

$K_{c\ mid}$ is less affected by wetting frequency than is $K_{c\ ini}$, as vegetation during this stage is generally near full ground cover so that the effects of surface evaporation on K_c are smaller. For frequent irrigation of crops (more frequently than every 3 days) and where the $K_{c\ mid}$ of Table 12 is less than 1.0, the value can be replaced by approximately 1.1-1.3 to account for the combined effects of continuously wet soil, evaporation due to interception (sprinkler irrigation) and roughness of the vegetation, especially where the irrigation system moistens an important fraction of the soil surface ($f_w > 0.3$).

[1] In the case of arid and semi-arid climates, T_{min} in equation (64) should be adjusted as indicated in Annex 6 (equation 6-6) by subtracting 2°C from the average value of T_{min} to better approximate T_{dew}.

EXAMPLE 27
Determination of $K_{c\ mid}$

Calculate $K_{c\ mid}$ for maize crops near Taipei, Taiwan and near Mocha, Yemen. The average mean daily wind speed (u_2) during the mid-season stage at Taipei is about 1.3 m/s and the minimum relative humidity (RH_{min}) during this stage averages 75%. The average u_2 during the mid-season near Mocha is 4.6 m/s and the RH_{min} during this stage averages 44%.

From Table 12, the value for $K_{c\ mid}$ is 1.20 for maize. The value for h from Table 12 is 2 m. Using Eq. 62

For Taipei (humid climate):

$$K_{c\ mid} = 1.20 + [0.04(1.3-2) - 0.004(75-45)]\left(\frac{2}{3}\right)^{0.3} = 1.07$$

For Mocha (arid climate):

$$K_{c\ mid} = 1.20 + [0.04(4.6-2) - 0.004(44-45)]\left(\frac{2}{3}\right)^{0.3} = 1.30$$

The average crop coefficient predicted during the mid-season stage is 1.07 for Taipei and 1.30 for Mocha.

Crop coefficient for the end of the late season stage ($K_{c\ end}$)

Typical values for the crop coefficient at the end of the late season growth stage, $K_{c\ end}$, are listed in Table 12 for various agricultural crops. The values given for $K_{c\ end}$ reflect crop and water management practices particular to those crops. If the crop is irrigated frequently until harvested fresh, the topsoil remains wet and the $K_{c\ end}$ value will be relatively high. On the other hand, crops that are allowed to senesce and dry out in the field before harvest receive less frequent irrigation or no irrigation at all during the late season stage. Consequently, both the soil surface and vegetation are dry and the value for $K_{c\ end}$ will be relatively small (Figure 33).

Where the local water management and harvest timing practices are known to deviate from the typical values presented in Table 12, then the user should make some adjustments to the values for $K_{c\ end}$. Some guidance on adjustment of K_c values for wetting frequency is provided in Chapter 7. For premature harvest, the user can construct a K_c curve using the $K_{c\ end}$ value provided in Table 12 and a late season length typical of a normal harvest date; but can then terminate the application of the constructed curve early, corresponding to the time of the early harvest.

The $K_{c\ end}$ values in Table 12 are typical values expected for average $K_{c\ end}$ under the standard climatic conditions. More arid climates and conditions of greater wind speed will have higher values for $K_{c\ end}$. More humid climates and conditions of lower wind speed will have lower values for $K_{c\ end}$. For specific adjustment in climates where RH_{min} differs from 45% or where u_2 is larger or smaller than 2.0 m/s, Equation 65 can be used:

$$K_{c\ end} = K_{c\ end\ (Tab)} + [0.04(u_2 - 2) - 0.004(RH_{min} - 45)]\left(\frac{h}{3}\right)^{0.3} \quad (65)$$

FIGURE 33
Ranges expected for $K_{c\ end}$

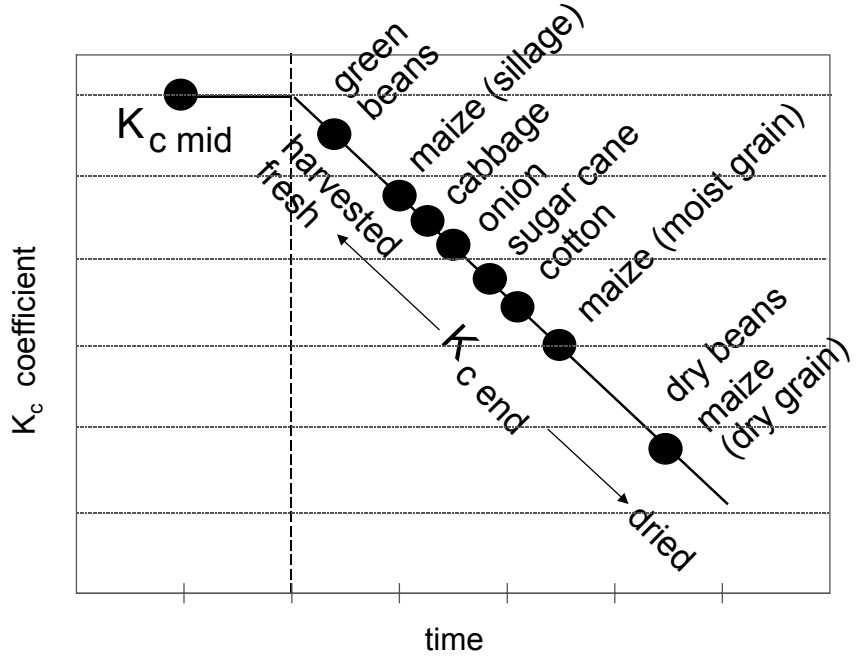

FIGURE 34
Crop coefficient curve

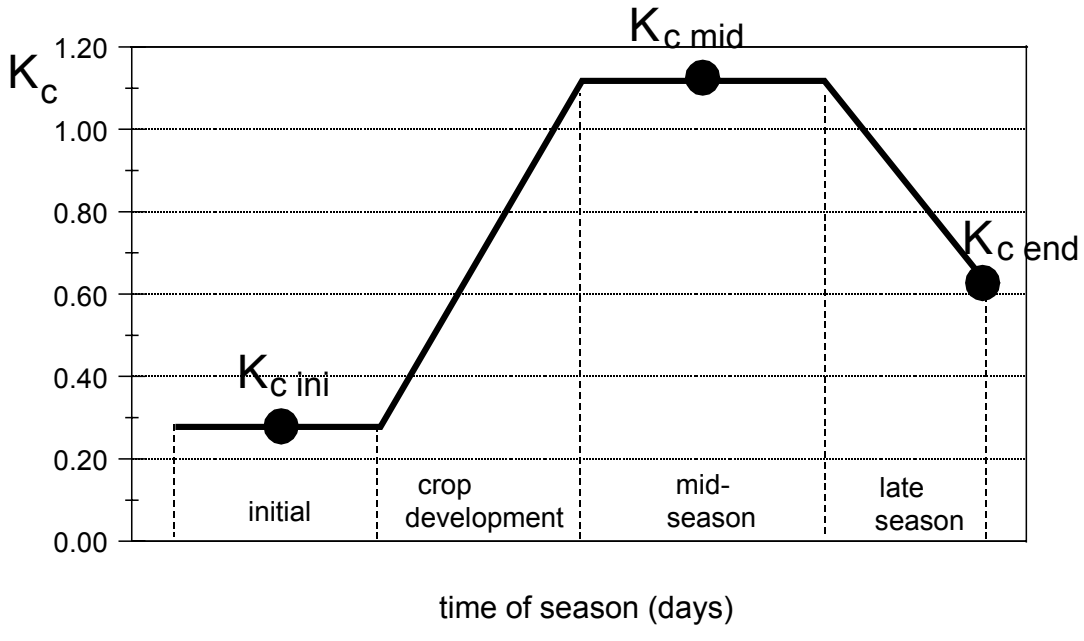

where $K_{c\ end\ (Tab)}$ value for $K_{c\ end}$ taken from Table 12,

u_2 mean value for daily wind speed at 2 m height over grass during the late season growth stage [m s^{-1}], for 1 m $s^{-1} \leq u_2 \leq 6$ m s^{-1},

RH_{min} mean value for daily minimum relative humidity during the late season stage [%],for $20\% \leq RH_{min} \leq 80\%$,

h mean plant height during the late season stage [m], for 0.1 m ≤ h ≤ 10 m.

Equation 65 is only applied when the tabulated values for $K_{c\ end}$ exceed 0.45. The equation reduces the $K_{c\ end}$ with increasing RH_{min}. This reduction in $K_{c\ end}$ is characteristic of crops that are harvested 'green' or before becoming completely dead and dry (i.e., $K_{c\ end} \geq 0.45$).

No adjustment is made when $K_{c\ end\ (Table)} < 0.45$ (i.e., $K_{c\ end} = K_{c\ end\ (Tab)}$). When crops are allowed to senesce and dry in the field (as evidenced by $K_{c\ end} < 0.45$), u_2 and RH_{min} have less effect on $K_{c\ end}$ and no adjustment is necessary. In fact, $K_{c\ end}$ may decrease with decreasing RH_{min} for crops that are ripe and dry at the time of harvest, as lower relative humidity accelerates the drying process.

CONSTRUCTION OF THE K_c CURVE

Annual crops

Only three point values for K_c are required to describe and to construct the K_c curve. The curve such as that shown in Figure 34 is constructed using the following three steps:

1. Divide the growing period into four general growth stages that describe crop phenology or development (initial, crop development, mid-season, and late season stage), determine the lengths of the growth stages, and identify the three K_c values that correspond to $K_{c\ ini}$, $K_{c\ mid}$ and $K_{c\ end}$ from Table 12.
2. Adjust the K_c values to the frequency of wetting and/or climatic conditions of the growth stages as outlined in the previous section.
3. Construct a curve by connecting straight line segments through each of the four growth stages. Horizontal lines are drawn through $K_{c\ ini}$ in the initial stage and through $K_{c\ mid}$ in the mid-season stage. Diagonal lines are drawn from $K_{c\ ini}$ to $K_{c\ mid}$ within the course of the crop development stage and from $K_{c\ mid}$ to $K_{c\ end}$ within the course of the late season stage.

K_c curves for forage crops

Many crops grown for forage or hay are harvested several times during the growing season. Each harvest essentially terminates a 'sub' growing season and associated K_c curve and initiates a new 'sub' growing season and associated K_c curve. The resulting K_c curve for the entire growing season is the aggregation of a series of K_c curves associated with each sub-cycle. Figure 35 presents a K_c curve for the entire growing season constructed for alfalfa grown for hay in southern Idaho.

FIGURE 35
Constructed curve for K_c for alfalfa hay in southern Idaho, the United States using values from Tables 11 and 12 and adjusted using Equations 62 and 65 (data from Wright, 1990)

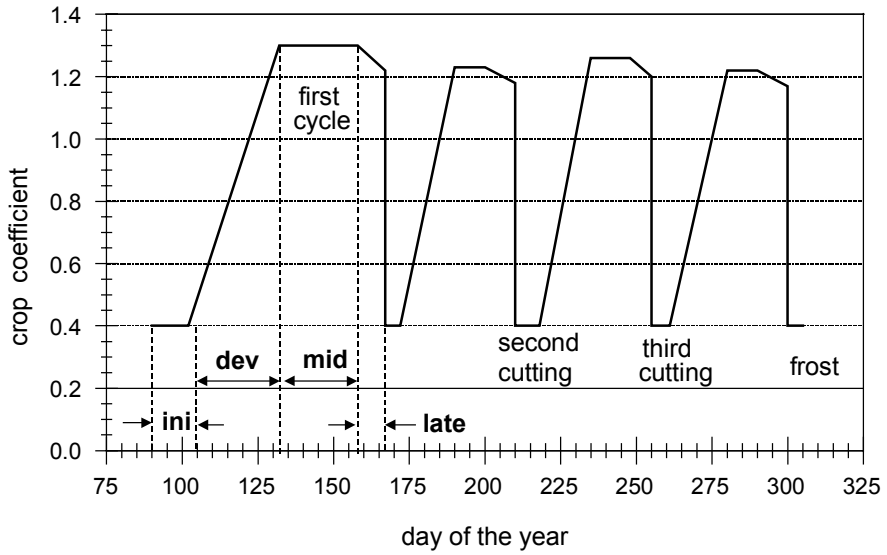

In the southern Idaho climate, greenup (leaf initiation) begins in the spring on about day 90 of the year. The crop is usually harvested (cut) for hay three or four times during the growing season. Therefore, Figure 35 shows four K_c sub-cycles or cutting cycles: sub-cycle 1 follows greenup in the spring and the three additional K_c sub-cycles follow cuttings. Cuttings create a ground surface with less than 10% vegetation cover. Cutting cycle 1 is longer in duration than cycles 2, 3 and 4 due to lower air and soil temperatures during this period that reduce crop growth rates. The lengths for cutting cycle 1 were taken from the first entry for alfalfa ("1st cutting cycle") in Table 11 for Idaho, the United States (10/30/25/10). The lengths for cutting cycles 2, 3 and 4 were taken from the entry for alfalfa in Table 11 for "individual cutting periods" for Idaho, the United States (5/20/10/10). These lengths were based on observations. In the southern Idaho climate, frosts terminate the growing season sometime in the fall, usually around day 280-290 of the year (early to mid-October).

The magnitudes of the K_c values during the mid-season periods of each cutting cycle shown in Figure 35 vary from cycle to cycle due to the effects of adjusting the values for $K_{c\ mid}$ and $K_{c\ end}$ for each cutting cycle period using Equations 62 and 65. In applying these two adjustment equations, the u_2 and RH_{min} values were averages for the mid-season and late season stages within each cutting cycle. Basal K_{cb} curves similar to Figure 35 can be constructed for forage or hay crops, following procedures presented in Chapter 7.

$K_{c\ mid}$ when effects of individual cutting periods are averaged

Under some conditions, the user may wish to average the effects of cuttings for a forage crop over the course of the growing season. When cutting effects are averaged, then only a single value for $K_{c\ mid}$ and a only single K_c curve need to be employed for the whole growing

season. When this is the case, a "normal" K_c curve is constructed as in Figure 25, where only one midseason period is shown for the forage crop. The $K_{c\ mid}$ for this total midseason period must average the effects of occasional cuttings or harvesting. The value that is used for $K_{c\ mid}$ is therefore an average of the K_c curve for the time period starting at the first attainment of full cover and ending at the beginning of the final late season period near dormancy or frost. The value used for $K_{c\ mid}$ under these averaged conditions may be only about 80% of the K_c value that represents full ground cover. These averaged, full-season $K_{c\ mid}$ values are listed in Table 12. For example, for alfalfa hay, the averaged, full-season $K_{c\ mid}$ is 1.05, whereas, the $K_{c\ mid}$ for an individual cutting period is 1.20.

Fruit trees

Values for the crop coefficient during the mid-season and end of late season stages are given in Table 12. As mentioned before, the K_c values listed are typical values for standard climatic conditions and need to be adjusted by using Equations 62 and 65 where RH_{min} or u_2 differ. As the mid and late season stages of deciduous trees are quite long, the specific adjustment of K_c to RH_{min} and u_2 should take into account the varying climatic conditions throughout the season. Therefore, several adjustments of K_c are often required if the mid and late seasons cover several climatic seasons, e.g., spring, summer and autumn or wet and dry seasons. The $K_{c\ ini}$ and $K_{c\ end}$ for evergreen non dormant trees and shrubs are often not different, where climatic conditions do not vary much, as happens in tropical climates. Under these conditions, seasonal adjustments for climate may therefore not be required since variations in ET_c depend mostly on variations in ET_o.

CALCULATING ET_C

From the crop coefficient curve the K_c value for any period during the growing period can be graphically or numerically determined. Once the K_c values have been derived, the crop evapotranspiration, ET_c, can be calculated by multiplying the K_c values by the corresponding ET_o values.

Graphical determination of K_c

Weekly, ten-day or monthly values for K_c are necessary when ET_c calculations are made on weekly, ten-day or monthly time steps. A general procedure is to construct the K_c curve, overlay the curve with the lengths of the weeks, decade or months, and to derive graphically from the curve the K_c value for the period under consideration (Figure 36). Assuming that all decades have a duration of 10 days facilitates the derivation of K_c and introduces little error into the calculation of ET_c.

The constructed K_c curve in Box 15 was used to construct the curve in Figure 36. This curve has been overlaid with the lengths of the decades. K_c values of 0.15, 1.19 and 0.35 and the actual lengths for growth stages equal to 25, 25, 30 and 20 days were used. The crop was planted at the beginning of the last decade of May and was harvested 100 days later at the end of August.

For all decades the K_c values can be derived directly from the curve. The value at the middle of the decade is considered to be the average K_c of that 10 day period. Only the second decade of June, where the K_c value changes abruptly, requires some calculation.

BOX 15
Case study of a dry bean crop at Kimberly, Idaho, the United States (single crop coefficient)

An example application for using the K_c procedure under average soil wetness conditions is presented for a dry bean crop planted on 23 May 1974 at Kimberly, Idaho, the United States (latitude = 42.4°N). The initial, development, mid-season and late season stage lengths are taken from Table 11 for a continental climate as 20, 30, 40 and 20 days (the stage lengths listed for southern Idaho were not used in this example in order to demonstrate the only approximate accuracy of values provided in Table 11 when values for the specific location are not available). Initial values for $K_{c\ ini}$, $K_{c\ mid}$ and $K_{c\ end}$ are selected from Table 12 as 0.4, 1.15, and 0.35.

The mean RH_{min} and u_2 during both the mid-season and late season growth stages were 30% and 2.2 m/s. The maximum height suggested in Table 12 for dry beans is 0.4 m. Therefore, $K_{c\ mid}$ is adjusted using Eq. 62 as:

$$K_{c\ mid} = 1.15 + [0.04\,(2.2-2) - 0.004\,(30-45)]\left(\frac{0.4}{3}\right)^{0.3} = 1.19$$

As $K_{c\ end}$ = 0.35 is less than 0.45, no adjustment is made to $K_{c\ end}$. The value for $K_{c\ mid}$ is not significantly different from that in Table 12 as $u_2 \approx 2$ m/s, RH_{min} is just 15% lower than the 45% represented in Table 12, and the height of the beans is relatively short. The initial K_c curve for dry beans in Idaho can be drawn, for initial, planning purposes, as shown in the graph (dotted line), where $K_{c\ ini}$, $K_{c\ mid}$ and $K_{c\ end}$ are 0.4, 1.19, and 0.35 and the four lengths of growth stages are 20, 30, 40 and 20 days. Note that the $K_{c\ ini}$ = 0.4 taken from Table 12 serves only as an initial, approximate estimate for $K_{c\ ini}$.

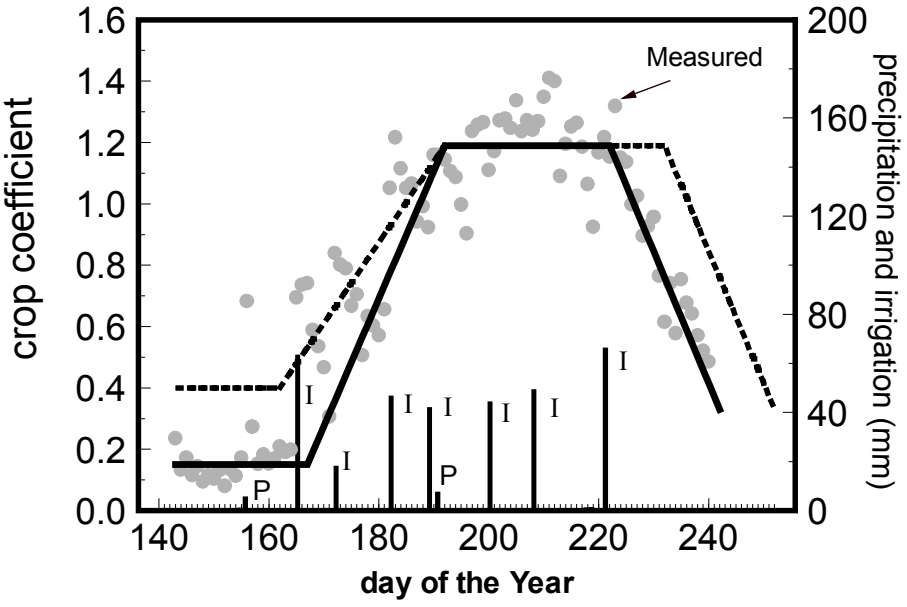

Constructed K_c curves using values from Tables 11 and 12 directly (dotted line) and modified using $K_{c\ ini}$ from Fig. 29 and L_{ini} = 25, L_{dev} = 25, L_{mid} = 30, and L_{late} = 20 days (heavy line) for dry beans at Kimberly, Idaho. Also shown are daily measured K_c (lysimeter data from Wright, 1990).

$K_{c\ ini}$ can be more accurately estimated using the approach described in this chapter. ET_o during the initial period at Kimberly (late May - early June, 1974) averaged 5.3 mm/day, and the wetting interval during this period was approximately 14 days (2 rainfall events occurred averaging 5 mm per event). Therefore, as the wetting events were light (< 10 mm each), Fig. 29 is used. The soil texture at Kimberly, Idaho is silt loam. From Fig. 29, $K_{c\ ini}$ for the 14 day wetting interval and ET_o = 5.3 mm/day is about 0.15. This value is substantially less than the general 0.4 value suggested by Table 12, and emphasizes the need to utilize local, actual precipitation and irrigation data when determining $K_{c\ ini}$.

Comparison of constructed curves with measurements

Because the ET_c data for the dry bean crop at Kimberly, Idaho were measured using a precision lysimeter system during 1974 by Wright (1990), the actual K_c measurements can be compared with the constructed K_c curves, where actual K_c was calculated by dividing lysimeter measurements of ET_c by daily ET_o estimated using the FAO Penman-Monteith equation.

As illustrated in the graph, the mid-season length as taken from Table 11 for the general, continental climate overestimated the true mid-season length for dry beans in southern Idaho, which averaged only about 30 days rather than 40 days as suggested by Table 11. This illustrates the importance of using the local observation of 30 days for mid-season period length rather than the general value from Table 11.

The final, best estimate for the K_c curve for the dry bean crop in southern Idaho is plotted (lower curve in graph) using K_c values of 0.15, 1.19, and 0.35 and the actual observed lengths of growth stages equal to 25, 25, 30 and 20 days. Note the impact that the error in estimating mid-season length has on the area under the K_c curve. This supports the need to obtain local observations of growth stage dates and lengths.

The value calculated for $K_{c\ mid}$ (1.19) appears to have underestimated the measured value for K_c during portions of the mid-season period at Kimberly. Some of this effect was due to effects of increased soil water evaporation following four irrigations during the 1974 mid-season which increased the effective K_c. This is illustrated in Box 16, where the basal K_{cb} + K_e approach is introduced and demonstrated for this same example.

The 0.15 value calculated for $K_{c\ ini}$ using Fig. 29 agrees closely with measured K_c during the initial period. Measured K_c during the development period exceeded the final K_c curve during days on or following wetting events. The day to day variation in the lysimeter measured K_c is normal and is caused by day to day variations in weather, in wind direction, by errors in prediction of R_n and ET_o, and by some random errors in the lysimeter measurements and weather measurements.

FIGURE 36
K_c curve and ten-day values for K_c and ET_c derived from the graph for the dry bean crop example (Box 15)

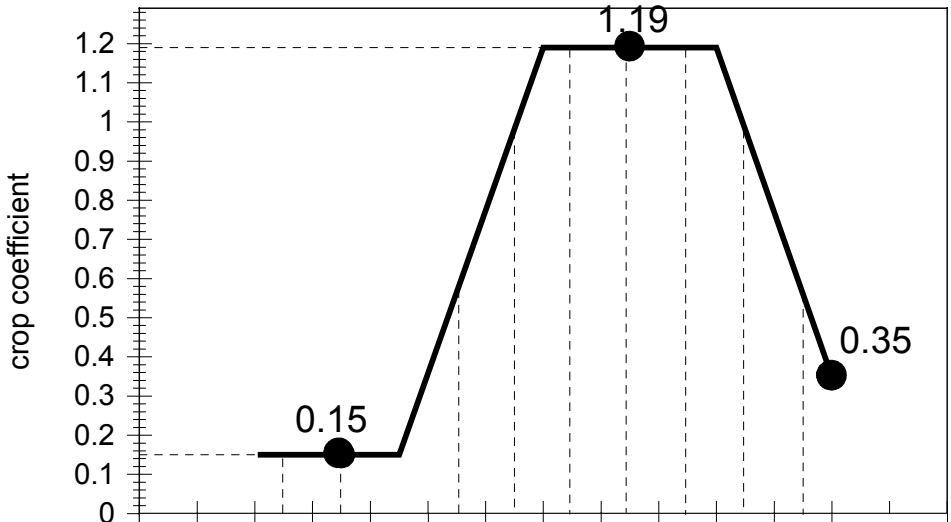

1	2	3	1	2	3	1	2	3	1	2	3	
May			June			July			August			
K_c	0.15	0.15	0.20	0.57	0.98	1.19	1.19	1.19	0.98	0.56	
ET_o	3.0	3.4	4.0	4.2	4.5	5.1	5.6	6.0	5.5	5.2	mm/day
ET_c	0.5	0.5	0.8	2.4	4.4	6.1	6.7	7.1	5.4	2.9	mm/day

During the first five days of that decade, $K_c = 0.15$, while during the second part of the decade K_c varies from 0.15 to 0.36 at the end of day 10. The K_c for that decade is consequently: 5/10 (0.15) + 5/10 (0.15+0.36)/2 = 0.20.

Numerical determination of K_c

The K_c coefficient for any period of the growing season can be derived by considering that during the initial and mid-season stages K_c is constant and equal to the K_c value of the growth stage under consideration. During the crop development and late season stage, K_c varies linearly between the K_c at the end of the previous stage ($K_{c\ prev}$) and the K_c at the beginning of the next stage ($K_{c\ next}$), which is $K_{c\ end}$ in the case of the late season stage:

$$K_{c\,i} = K_{c\,prev} + \left[\frac{i - \Sigma(L_{prev})}{L_{stage}}\right]\left(K_{c\,next} - K_{c\,prev}\right) \qquad (66)$$

where
- i day number within the growing season [1 .. length of the growing season],
- $K_{c\,i}$ crop coefficient on day i,
- L_{stage} length of the stage under consideration [days],
- $\Sigma(L_{prev})$ sum of the lengths of all previous stages [days].

Equation 66 applies to all four stages.

EXAMPLE 28
Numerical determination of K_c

Determine K_c at day 20, 40, 70 and 95 for the dry bean crop (Figure 36).

Crop growth stage	Length (days)	K_c
initial	25	$K_{c\ ini}$ = 0.15
crop development	25	0.15 ... 1.19
mid-season	30	$K_{c\ mid}$ = 1.19
late season	20	1.19 .. $K_{c\ end}$ = 0.35

At i = 20:	initial stage, $K_c = K_{c\ ini}$ =	0.15	-
At i = 40	Crop development stage,		
For:	$\Sigma(L_{prev}) = L_{ini}$ =	25	days
and:	$L_{stage} = L_{dev}$ =	25	days
From Eq. 66:	K_c = 0.15+[(40-25)/25](1.19-0.15)=	0.77	-
At i = 70:	mid-season stage, $K_c = K_{c\ mid}$ =	1.19	-
At i = 95	late season stage,		
For:	$\Sigma(L_{prev}) = L_{ini} + L_{dev} + L_{mid}$ = (25+25+30)=	80	days
and:	$L_{stage} = L_{late}$ =	20	days
From Eq. 66:	K_c = 1.19+[(95-80)/20](0.35-1.19)=	0.56	-

The crop coefficients at day 20, 40, 70 and 95 for the dry bean crop are 0.15, 0.77, 1.19 and 0.56 respectively.

ALFALFA-BASED CROP COEFFICIENTS

As two reference crop definitions (grass and alfalfa) are in use in various parts of the world, two families of K_c curves for agricultural crops have been developed. These are the alfalfa-based K_c curves by Wright (1981; 1982) and grass-based curves by Pruitt (Doorenbos and Pruitt 1977; Jensen *et al*. 1990) and those reported in this paper. The user must exercise caution to avoid mixing grass-based K_c values with alfalfa reference ET and vice versa. Usually, a K_c based on the alfalfa reference can be 'converted' for use with a grass reference by multiplying by a factor ranging from about 1.0 to 1.3, depending on the climate (1.05 for humid, calm conditions, and 1.2 for semi-arid, moderately windy conditions, and 1.35 for arid, windy conditions):

$$K_{c\ (grass)} = K_{ratio}\ K_{c\ (alfalfa)} \qquad (67)$$

where $K_{c\ (grass)}$ grass-based K_c (this handbook),
$K_{c\ (alfalfa)}$ alfalfa-based K_c,
K_{ratio} conversion factor (1.0 ... 1.3).

A reference conversion ratio can be established for any climate by using the $K_{c\ mid}$ = 1.20 listed for alfalfa in Table 12 and then adjusting this $K_{c\ mid}$ for the climate using Equation 62. For example, at Kimberly, Idaho, the United States, where RH_{min} = 30% and u_2 = 2.2 m/s are average values during the summer months, a reference conversion ratio between alfalfa and grass references using Equation 62 is approximately:

$$K_{ratio} = 1.2 + [0.04(2.2-2) - 0.004(30-45)]\left(\frac{0.5}{3}\right)^{0.3} = 1.24 \quad (68)$$

where h = 0.5 m is the standard height for the alfalfa reference.

TRANSFERABILITY OF PREVIOUS K_C VALUES

The values for $K_{c\ mid}$ and $K_{c\ end}$ listed in Table 12 are for a large part based on the original values presented in FAO Irrigation and Drainage Papers No. 24 and 33 (FAO-24 and FAO-33), with some adjustment and revisions to reflect recent findings. Similarly adjustments in $K_{c\ mid}$ to compensate for differences in aerodynamic roughness and leaf area, as introduced in Equation 62 are derived from the K_c values given for different wind and RH_{min} conditions in the concerned Kc table in FAO-24, with some upward adjustment to better reflect increased ET_{crop} values under high wind and low RH_{min} when applied with the FAO Penman-Monteith equation.

The K_c's from FAO-24 were based primarily on a living grass reference crop. The FAO Penman-Monteith equation presented in this publication similarly represents the same standardized grass reference. For that reason K_c values are in general not very different between these publications except under high wind and low RH_{min}.

The No. 24 modified Penman was found frequently to overestimate ET_o even up to 25 % under high wind and low evaporative conditions and required often substantial local calibration (see chapter 2). K_c values derived from crop water use studies which used the FAO-24 Penman equation to compute grass reference crop evapotranspiration, can therefore not be used and need to be adjusted using ETo values estimated from the FAO Penman-Monteith equation. Similarly crop water requirement estimates based on the FAO-24 Modified Penman equation will need to be reassessed in view of the found differences between the FAO-24 Penman and the FAO Penman-Monteith reference equations.

Chapter 7

ET_c – dual crop coefficient ($K_c = K_{cb} + K_e$)

Like Chapter 6, this chapter also deals with the calculation of crop evapotranspiration (ET_c) under standard conditions where no limitations are placed on crop growth or evapotranspiration. This chapter presents the procedure for predicting the effects of specific wetting events on the value for the crop coefficient K_c. The solution consists of splitting K_c into two separate coefficients, one for crop transpiration, i.e., the basal crop coefficient (K_{cb}), and one for soil evaporation (K_e):

$$ET_c = (K_{cb} + K_e)\ ET_o \qquad (69)$$

The dual crop coefficient approach is more complicated and more computationally intensive than the single crop coefficient approach (K_c) of Chapter 6. The procedure is conducted on a daily basis and is intended for applications using computers. It is recommended that the approach be followed when improved estimates for K_c are needed, for example to schedule irrigations for individual fields on a daily basis.

The calculation procedure for crop evapotranspiration, ET_c, consists of:

1. identifying the lengths of crop growth stages, and selecting the corresponding K_{cb} coefficients;

2. adjusting the selected K_{cb} coefficients for climatic conditions during the stage;

3. constructing the basal crop coefficient curve (allowing one to determine K_{cb} values for any period during the growing period);

4. determining daily K_e values for surface evaporation; and

5. calculating ET_c as the product of ET_o and ($K_{cb} + K_e$).

TRANSPIRATION COMPONENT ($K_{cb}\ ET_o$)

Basal crop coefficient (K_{cb})

The basal crop coefficient (K_{cb}) is defined as the ratio of the crop evapotranspiration over the reference evapotranspiration (ET_c/ET_o) when the soil surface is dry but transpiration is occurring at a potential rate, i.e., water is not limiting transpiration (Figure 22). Therefore, '$K_{cb}\ ET_o$' represents primarily the transpiration component of ET_c. The $K_{cb}\ ET_o$ does include a residual diffusive evaporation component supplied by soil water below the dry surface and by soil water from beneath dense vegetation.

As the K_c values of Chapter 6 include averaged effects of evaporation from the soil surface, the K_{cb} values lie below the K_c values as illustrated in Figure 26 and a separate table for K_{cb} is required. Recommended values for K_{cb} are listed in Table 17 for the same crops listed in Table 12. As with Table 12, the values for K_{cb} in the table represent K_{cb} for a sub-humid climate and with moderate wind speed. For specific adjustment in climates where RH_{min} differs from 45% or where the wind speed is larger or smaller than 2 m/s, the $K_{cb\ mid}$ and $K_{cb\ end}$ values larger than 0.45 must be adjusted using the following equation:

$$K_{cb} = K_{cb\,(Tab)} + [0.04(u_2 - 2) - 0.004(RH_{min} - 45)]\left(\frac{h}{3}\right)^{0.3} \qquad (70)$$

where $K_{cb\,(Tab)}$ the value for $K_{cb\ mid}$ or $K_{cb\ end}$ (if ≥ 0.45) taken from Table 17,

u_2 the mean value for daily wind speed at 2 m height over grass during the mid or late season growth stage [m s^{-1}] for 1 m $s^{-1} \le u_2 \le 6$ m s^{-1},

RH_{min} the mean value for daily minimum relative humidity during the mid- or late season growth stage [%] for $20\% \le RH_{min} \le 80\%$,

h the mean plant height during the mid or late season stage [m] (from Table 12) for $20\% \le RH_{min} \le 80\%$.

For a full discussion on the impact of the climatic correction, and the numerical determination of $K_{cb\ mid}$ and $K_{cb\ end}$, the user is referred to the discussions on $K_{c\ mid}$ and $K_{c\ end}$ in Chapter 6.

Table 18 summarizes the general guidelines that were used in deriving K_{cb} values from the K_c values listed in Table 17. Where local research results are available, values for K_{cb} from Table 17 can be modified to reflect effects of local conditions, cultural practices or crop varieties on K_{cb}. However, local values for K_{cb} should not be expected to deviate by more than 0.2 from the values in Table 17. A greater deviation should signal the need to investigate or evaluate the local research technique, equipment and cultural practices. Where local K_{cb} values are used, no adjustment for climate using Equation 70 is necessary.

EXAMPLE 29
Selection and adjustment of basal crop coefficients, K_{cb}

Select $K_{cb\ ini}$, $K_{cb\ mid}$ and $K_{cb\ end}$ for the dry bean crop of Box 15.

$K_{cb\ ini}$, $K_{cb\ mid}$ and $K_{cb\ end}$ can be selected directly from Table 17 for dry beans as 0.15, 1.10 and 0.25. When adjusted for climate using Eq. 70:

$K_{cb\ ini} = 0.15$
$K_{cb\ mid} = 1.10 + (0.04\,(2.2\text{-}2) - 0.004\,(30\text{-}45))(0.4/3)^{0.3} = 1.14$
$K_{cb\ end} = 0.25$ (as $K_{cb} < 0.45$)

Height for beans was taken from Table 12 as 0.4 m.

The corresponding K_{cb} curve is shown in Figure 37.

TABLE 17
Basal crop coefficients, K_c, for non stressed, well-managed crops in subhumid climates ($RH_{min} \approx 45\%$, $u_2 \approx 2$ m/s) for use with the FAO Penman-Monteith ET_o.

Crop	$K_{cb\ ini}$[1]	$K_{cb\ mid}$[1]	$K_{cb\ end}$[1]
a. Small Vegetables	**0.15**	**0.95**	**0.85**
Broccoli		0.95	0.85
Brussel Sprouts		0.95	0.85
Cabbage		0.95	0.85
Carrots		0.95	0.85
Cauliflower		0.95	0.85
Celery		0.95	0.90
Garlic		0.90	0.60
Lettuce		0.90	0.90
Onions - dry		0.95	0.65
- green		0.90	0.90
- seed		1.05	0.70
Spinach		0.90	0.85
Radishes		0.85	0.75
b. Vegetables – Solanum Family (*Solanaceae*)	**0.15**	**1.10**	**0.70**
EggPlant		1.00	0.80
Sweet Peppers (bell)		1.00[2]	0.80
Tomato		1.10[2]	0.60-0.80
c. Vegetables – Cucumber Family (*Cucurbitaceae*)	**0.15**	**0.95**	**0.70**
Cantaloupe		0.75	0.50
Cucumber – Fresh Market		0.95[2]	0.70
– Machine harvest		0.95	0.80
Pumpkin, Winter Squash		0.95	0.70
Squash, Zucchini		0.90	0.70
Sweet Melons		1.00	0.70
Watermelon		0.95	0.70
d. Roots and Tubers	**0.15**	**1.00**	**0.85**
Beets, table		0.95	0.85
Cassava – year 1		0.70[3]	0.20
– year 2		1.00	0.45
Parsnip		0.95	0.85
Potato		1.10	0.65[4]
Sweet Potato		1.10	0.55
Turnip (and Rutabaga)		1.00	0.85
Sugar Beet		1.15	0.50[5]

continued…

1 These are values for K_{cb} representing conditions having a dry soil surface. These values are intended for use with the dual $K_{cb\ ini} + K_e$ approach, only. Values for maximum crop height, h, are given in Table 12 for adjusting K_{cb} for climate.

2 Beans, Peas, Legumes, Tomatoes, Peppers and Cucumbers are sometimes grown on stalks reaching 1.5 to 2 meters in height. In such cases, increased K_{cb} values need to be taken. For green beans, peppers and cucumbers, 1.10 can be taken, and for tomatoes, dry beans and peas, 1.15. Under these conditions h should be increased also.

3 The misdseason values for cassava assume nonstressed conditions during or following the rainy season. The $K_{cb\ end}$ values account for domancy during the dry season.

4 The $K_{cb\ end}$ value for potatoes is about 0.35 for long season potatoes with vine kill.

5 This $K_{cb\ end}$ value is for no irrigation during the last month of the growing season. The $K_{cb\ end}$ value for sugar beets is higher, up to 0.9, when irrigation or significant rain occurs during the last month of the growing season.

Table 17 continued

Crop	$K_{cb\ ini}$[1]	$K_{cb\ mid}$[1]	$K_{cb\ end}$[1]
e. Lugumes (*Leguminosae*)	**0.15**	**1.10**	**0.50**
Beans, green		1.00[2]	0.80
Beans, dry and Pulses		1.10[2]	0.25
Chick pea		0.95	0.25
Fababean (broad bean) – Fresh – Dry/Seed		1.10[2] 1.10[2]	1.05 0.20
Grabanzo		1.05	0.25
Green Gram and Cowpeas		1.00	0.55-0.25[6]
Groundnut (Peanut)		1.10	0.50
Lentil		1.05	0.20
Peas – Fresh – Dry/Seed		1.10[2] 1.10	1.05 0.20
Soybeans		1.10	0.30
f. Perennial Vegetables (with winter dormancy and initially bare or mulched soil)			
Artichokes	0.15	0.95	0.90
Asparagus	0.15	0.90[7]	0.20
Mint	0.40	1.10	1.05
Strawberries	0.30	0.80	0.70
g. Fibre Crops	**0.15**		
Cotton		1.10-1.15	0.50-0.40
Flax		1.05	0.20
Sisal[8]		0.4-0.7	0.4-0.7
h. Oil Crops	**0.15**	**1.10**	**0.25**
Castorbean (*Ricinus*)		1.10	0.45
Rapeseed, Canola		0.95-1.10[9]	0.25
Safflower		0.95-1.10[9]	0.20
Sesame		1.05	0.20
Sunflower		0.95-1.10[9]	0.25
i. Cereals	**0.15**	**1.10**	**0.25**
Barley		1.10	0.15
Oats		1.10	0.15
Spring Wheat		1.10	0.15-0.3[10]
Winter Wheat	0.15-0.5[11]	1.10	0.15-0.3[10]
Maize - Field (grain) *(field corn)* - Sweet *(sweet corn)*	0.15	1.15 1.10	0.50,0.15[12] 1.00[13]
Millet		0.95	0.20
Sorghum – grain – sweet		0.95-1.05 1.15	0.35 1.00
Rice	1.00	1.15	0.70-0.45

continued…

6 The first $K_{cb\ end}$ is for harvested fresh. The second value is for harvested dry.

7 The K_{cb} for asparagus usually remains at $K_{cb\ ini}$ during harvest of the spears, due to sparse ground cover. The $K_{cb\ mid}$ value is for following regrowth of vegetation following termination of harvest of spears.

8 K_{cb} for sisal depends on the planting density and water management (e.g., intentional moisture stress).

9 The lower values are for rainfed crops having less dense plant populations.

10 The higher value is for hand-harvested crops.

11 The two $K_{cb\ ini}$ values for winter wheat are for less than 10% ground cover and for during the dormant, winter period, if the vegetation fully covers the ground, but conditions are nonfrozen.

12 The first $K_{cb\ end}$ value is for harvest at high grain moisture. The second $K_{cb\ end}$ value is for harvest after complete field drying of the grain (to about 18% moisture, wet mass basis).

13 If harvested fresh for human consumption. Use $K_{cb\ end}$ for field maize if the sweet maize is allowed to mature and dry in the field.

Table 17 continued.

Crop	$K_{cb\ ini}$[1]	$K_{cb\ mid}$[1]	$K_{cb\ end}$[1]
j. Forages			
Alfalfa Hay – individual cutting periods	0.30[14]	1.15[14]	1.10[14]
– for seed	0.30	0.45	0.45
Bermuda hay – averaged cutting effects	0.50	0.95[15]	0.80
– Spring crop for seed	0.15	0.85	0.60
Clover hay, Berseem – individual cutting periods	0.30[14]	1.10[14]	1.05[14]
Rye Grass hay – averaged cutting effects	0.85	1.00[15]	0.95
Sudan Grass hay (annual) – individual cutting periods	0.30[14]	1.10[14]	1.05[14]
Grazing Pasture - Rotated Grazing	0.30	0.80-1.00	0.80
- Extensive Grazing	0.30	0.70	0.70
Turf grass - cool season[16]	0.85	0.90	0.90
- warm season[16]	0.75	0.80	0.80
k. Sugar cane	0.15	1.20	0.70
l. Tropical Fruits and Trees			
Banana – 1st year	0.15	1.05	0.90
– 2nd year	0.60	1.10	1.05
Cacao	0.90	1.00	1.00
Coffee – bare ground cover	0.80	0.90	0.90
– with weeds	1.00	1.05	1.05
Date Palms	0.80	0.85	0.85
Palm Trees	0.85	0.90	0.90
Pineapple[17] (multiyear crop) – bare soil	0.15	0.25	0.25
– with grass cover	0.30	0.45	0.45
Rubber Trees	0.85	0.90	0.90
Tea – nonshaded	0.90	0.95	0.90
– shaded[18]	1.00	1.10	1.05
m. Grapes and Berries			
Berries (bushes)	0.20	1.00	0.40
Grapes – Table or Raisin	0.15	0.80	0.40
– Wine	0.15	0.65	0.40
Hops	0.15	1.00	0.80

continued…

14 These K_{cb} coefficients for hay crops represent immediately following cutting; at full cover; and immediately before cutting, respectively. The growing season is described as a series of individual cutting periods.

15 This $K_{cb\ mid}$ coefficient for bermuda and ryegrass hay crops is an overall average $K_{cb\ mid}$ coefficient that averages K_{cb} for both before and following cuttings. It is applied to the period following the first development period until the beginning of the last late season period of the growing season.

16 Cool season grass varieties include dense stands of bluegrass, ryegrass, and fescue. Warm season varieties include bermuda grass and St. Augustine grass. The 0.90 values for cool season grass represent a 0.06 to 0.08 m mowing height under general turf conditions. Where careful water management is practiced and rapid growth is not required, K_{cb}'s for turf can be reduced by 0.10.

17 The pineapple plant has very low transpiration because it closes its stomates during the day and opens them during the night. Therefore, the majority of ET_c from pineapple is evaporation from the soil.

18 Includes the water requirements of the shade trees.

Table 17 continued.

Crop	$K_{cb\ ini}$[1]	$K_{cb\ mid}$[1]	$K_{cb\ end}$[1]
n. Fruit Trees			
Almonds, no ground cover	0.20	0.85	0.60[19]
Apples, Cherries, Pears[20]			
- no ground cover, killing frost	0.35	0.90	0.65[19]
- no ground cover, no frosts	0.50	0.90	0.70[19]
- active ground cover, killing frost	0.45	1.15	0.90[19]
- active ground cover, no frosts	0.75	1.15	0.80[19]
Apricots, Peaches, Stone Fruit[20,21]			
- no ground cover, killing frost	0.35	0.85	0.60[19]
- no ground cover, no frosts	0.45	0.85	0.60[19]
- active ground cover, killing frost	0.45	1.10	0.85[19]
- active ground cover, no frosts	0.75	1.10	0.80[19]
Avocado, no ground cover	0.50	0.80	0.70
Citrus, no ground cover[22]			
70% canopy	0.65	0.60	0.65
50% canopy	0.60	0.55	0.60
20% canopy	0.45	0.40	0.50
Citrus, with active ground cover or weeds[23]			
70% canopy	0.75	0.70	0.75
50% canopy	0.75	0.75	0.75
20% canopy	0.80	0.80	0.85
Conifer Trees[24]	0.95	0.95	0.95
Kiwi	0.20	1.00	1.00
Olives (40 to 60% ground coverage by canopy)[25]	0.55	0.65	0.65
Pistachios, no ground cover	0.20	1.05	0.40
Walnut Orchard[20]	0.40	1.05	0.60[19]

19 These $K_{cb\ end}$ values represent K_{cb} prior to leaf drop. After leaf drop, $K_{cb\ end} \approx 0.15$ for bare, dry soil or dead ground cover and $K_{cb\ end} \approx 0.45$ to 0.75 for actively growing ground cover (consult Chapter 11).

20 Refer to Eq. 94, 97 or 98 and footnotes 22 and 23 for estimating K_{cb} for immature stands.

21 Stone fruit category applies to peaches, apricots, pears, plums and pecans.

22 These K_{cb} values can be calculated from Eq. 98 for $K_{c\ min} = 0.15$ and $K_{cb\ full} = 0.70$, 0.65 and 0.70 for the initial, mid season and end of season periods, and $f_{c\ eff} = f_c$ where f_c = fraction of ground covered by tree canopy (e.g., the sun is presumed to be directly overhead). The midseason value is lower than initial and ending values due to the effects of stomatal closure during periods of peak ET. For humid and subhumid climates where there is less stomatal control by citrus, values for $K_{cb\ ini}$, $K_{cb\ mid}$, and $K_{cb\ end}$ can be increased by 0.1 - 0.2, following Rogers et al. (1983).

23 These K_{cb} values can be calculated as $K_{cb} = f_c\ K_{cb\ ngc} + (1 - f_c)\ K_{cb\ cover}$ where $K_{cb\ ngc}$ is the K_{cb} of citrus with no active ground cover (calculated as in footnote 22), $K_{cb\ cover}$ is the K_{cb} for the active ground cover (0.90), and f_c is defined in footnote 22. Alternatively, K_{cb} for citrus with active ground cover can be estimated directly from Eq. 98 by setting $K_{c\ min} = K_{cb\ cover}$. For humid and subhumid climates where there is less stomatal control by citrus, values for $K_{cb\ ini}$, $K_{cb\ mid}$, and $K_{cb\ end}$ can be increased by 0.1 - 0.2, following Rogers et al. (1983).
For non-active or only moderately active ground cover (active indicates green and growing ground cover with LAI > about 2 to 3) , K_{cb} should be weighted between K_{cb} for no ground cover and K_{cb} for active ground cover, with the weighting based on the "greeness" and approximate leaf area of the ground cover.

24 Conifers exhibit substantial stomatal control due to reduced aerodynamic resistance. The K_{cb} can easily reduce below the values presented, which represent well-watered conditions for large forests.

25 These coefficients represent about 40 to 60% ground cover. Refer to Eq. 98, example 43, and footnotes 22 and 23 for estimating K_{cb} for immature stands.

Primary sources: $K_{cb\ ini}$: Doorenbos and Kassam (1979); $K_{cb\ mid}$ and $K_{cb\ end}$: Doorenbos and Pruitt (1977); Pruitt (1986); Wright (1981, 1982), Snyder *et al*. (1989)

TABLE 18
General guidelines to derive K_{cb} from the K_c values listed in Table 12

Growth stage	Ground condition, irrigation and cultural practices	K_{cb}	further adjustment
Initial	Annual crop - (nearly) bare soil surface	0.15	-
	Perennial crop - (nearly) bare soil surface	0.15 - 0.20	-
	Grasses, brush and trees - killing frost	0.30 - 0.40	-
	Perennial crop - some ground cover or leaf cover		
	- infrequently irrigated (olives, palm trees, fruit trees, ...)	$K_{c\ ini(Tab.12)}$ - 0.1	-
	- frequently irrigated (garden-type vegetables, ...)	$K_{c\ ini(Tab.12)}$ - 0.2	-
Mid-season	Ground cover more than 80%	$K_{c\ mid(Tab.12)}$ - 0.05	Climate (Eq. 70)
	Ground cover less than 80% (vegetables)	$K_{c\ mid(Tab.12)}$ - 0.10	Climate (Eq. 70)
At end of season	infrequently irrigated or wetted during late season	~ $K_{c\ end}$ - 0.05	-
	frequently irrigated or wetted during late season	$K_{c\ end}$ - 0.1	Climate (Eq. 70)

Climate: adjustment for climate using Eq. 70 where $K_{cb} > 0.45$

Determination of daily K_{cb} values

As outlined in Chapter 6, only three point values are required to describe and to construct the crop coefficient curve. After dividing the growing period into the four general growth stages and selecting and adjusting the K_{cb} values corresponding to the initial ($K_{cb\ ini}$), mid-season ($K_{cb\ mid}$) and end of the late season stages ($K_{cb\ end}$), the crop coefficient curve can be drawn (Figure 37) and the K_{cb} coefficients can be derived (Example 30).

EXAMPLE 30
Determination of daily values for K_{cb}

Calculate the basal crop coefficient for the dry beans (Example 29, Figure 37) at the middle of each of the four growth stages.

Initial stage (L_{ini} = 25 days), at day 12 of the growing period:
$K_{cb} = K_{cb\ ini} = 0.15$

Crop development stage (L_{dev} = 25 days), at day (25+25/2=) 37 of the growing period, using Eq. 66:
$K_{cb} = 0.15 + [(37 - 25)/25] (1.14 - 0.15) = 0.63$

Mid-season stage (L_{mid} = 30 days), at day (25+25+30/2=) 65 of the growing period:
$K_{cb} = K_{cb\ mid} = 1.14$

Late season stage (L_{late} = 20 days), at day (25+25+30+20/2=) 90 of the growing period, Eq. 66:
$K_{cb} = 1.14 + [(90-(25+25+30))/20] (0.25-1.14) = 0.70$

The basal crop coefficients, K_{cb}, at days 12, 37, 65 and 90 of the growing period are 0.15, 0.63, 1.14 and 0.70 respectively.

FIGURE 37
Constructed basal crop coefficient (K_{cb}) curve for a dry bean crop (Example 29) using growth stage lengths of 25, 25, 30 and 20 days

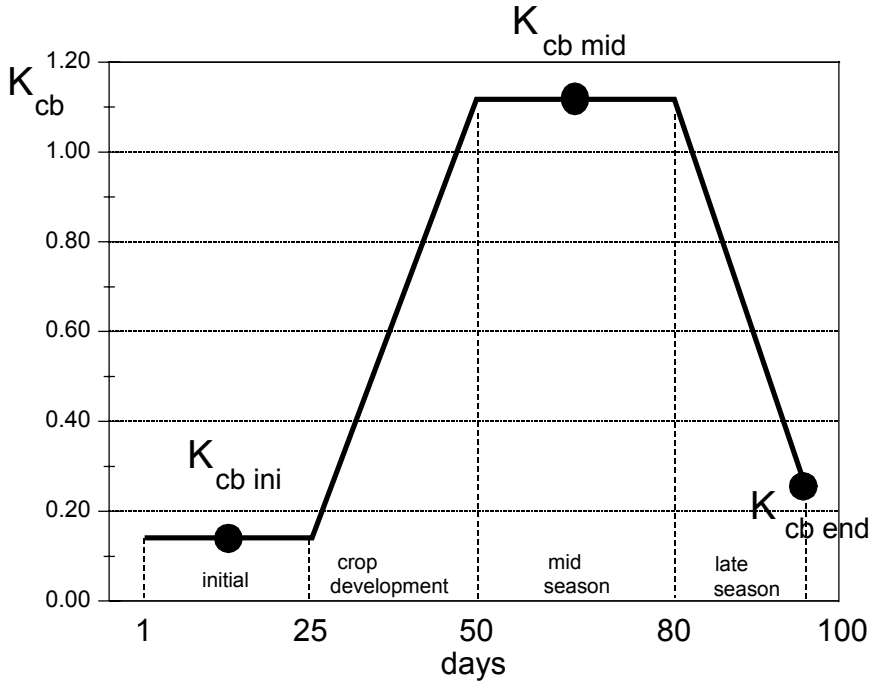

EVAPORATION COMPONENT (K_e ET_o)

The soil evaporation coefficient, K_e, describes the evaporation component of ET_c. Where the topsoil is wet, following rain or irrigation, K_e is maximal. Where the soil surface is dry, K_e is small and even zero when no water remains near the soil surface for evaporation.

Calculation procedure

Where the soil is wet, evaporation from the soil occurs at the maximum rate. However, the crop coefficient ($K_c = K_{cb} + K_e$) can never exceed a maximum value, $K_{c\ max}$. This value is determined by the energy available for evapotranspiration at the soil surface ($K_{cb} + K_e \leq K_{c\ max}$), or $K_e \leq (K_{c\ max} - K_{cb})$.

When the topsoil dries out, less water is available for evaporation and a reduction in evaporation begins to occur in proportion to the amount of water remaining in the surface soil layer, or:

$$K_e = K_r\ (K_{c\ max} - K_{cb}) \leq f_{ew}\ K_{c\ max} \qquad (71)$$

where
K_e soil evaporation coefficient,
K_{cb} basal crop coefficient,
$K_{c\ max}$ maximum value of K_c following rain or irrigation,
K_r dimensionless evaporation reduction coefficient dependent on the cumulative depth of water depleted (evaporated) from the topsoil,
f_{ew} fraction of the soil that is both exposed and wetted, i.e., the fraction of soil surface from which most evaporation occurs.

In computer programming terminology, Equation 71 is expressed as $K_e = \min(K_r (K_{c\ max} - K_{cb}), f_{ew} K_{c\ max})$.

Following rain or irrigation K_r is 1, and evaporation is only determined by the energy available for evaporation. As the soil surface dries, K_r becomes less than one and evaporation is reduced. K_r becomes zero when no water is left for evaporation in the upper soil layer.

Evaporation occurs predominantly from the exposed soil fraction. Hence, evaporation is restricted at any moment by the energy available at the exposed soil fraction, i.e., K_e cannot exceed $f_{ew} K_{c\ max}$, where f_{ew} is the fraction of soil from which most evaporation occurs, i.e., the fraction of the soil not covered by vegetation and that is wetted by irrigation or precipitation.

The calculation procedure consists in determining:

- the upper limit $K_{c\ max}$;
- the soil evaporation reduction coefficient K_r; and
- the exposed and wetted soil fraction f_{ew}.

The estimation of K_r requires a daily water balance computation for the surface soil layer.

Upper limit $K_{c\ max}$

$K_{c\ max}$ represents an upper limit on the evaporation and transpiration from any cropped surface and is imposed to reflect the natural constraints placed on available energy represented by the energy balance difference $R_n - G - H$ (Equation 1). $K_{c\ max}$ ranges from about 1.05 to 1.30 when using the grass reference ET_o:

$$K_{c\,max} = \max\left(\left\{1.2 + \left[0.04(u_2 - 2) - 0.004\,(RH_{min} - 45)\right]\left(\frac{h}{3}\right)^{0.3}\right\}, \{K_{cb} + 0.05\}\right) \qquad (72)$$

where
- h — mean maximum plant height during the period of calculation (initial, development, mid-season, or late-season) [m],
- K_{cb} — basal crop coefficient,
- max ( ) — maximum value of the parameters in braces { } that are separated by the comma.

Equation 72 ensures that $K_{c\ max}$ is always greater or equal to the sum K_{cb} + 0.05. This requirement suggests that wet soil will always increase the value for K_{cb} by 0.05 following complete wetting of the soil surface, even during periods of full ground cover. A value of 1.2 instead of 1 is used for $K_{c\ max}$ in Equation 72 because of the effect of increased aerodynamic roughness of surrounding crops during development, mid-season and late season growth stages which can increase the turbulent transfer of vapour from the exposed soil surface. The "1.2" coefficient also reflects the impact of the reduced albedo of wet soil and the contribution of heat stored in dry soil prior to the wetting event. All of these factors can contribute to increased evaporation relative to the reference.

The "1.2" coefficient in Equation 72 represents effects of wetting intervals that are greater than 3 or 4 days. If irrigation or precipitation events are more frequent, for example daily or each two days, then the soil has less opportunity to absorb heat between wettings, and the "1.2" coefficient in Equation 72 can be reduced to about 1.1. The time step to compute $K_{c\ max}$ may vary from daily to monthly.

Soil evaporation reduction coefficient (K_r)

Soil evaporation from the exposed soil can be assumed to take place in two stages: an energy limiting stage, and a falling rate stage. When the soil surface is wet, K_r is 1. When the water content in the upper soil becomes limiting, K_r decreases and becomes zero when the total amount of water that can be evaporated from the topsoil is depleted.

Maximum amount of water that can be evaporated

In the simple evaporation procedure, it is assumed that the water content of the evaporating layer of the soil is at field capacity, θ_{FC}, shortly following a major wetting event and that the soil can dry to a soil water content level that is halfway between oven dry (no water left) and wilting point, θ_{WP}. The amount of water that can be depleted by evaporation during a complete drying cycle can hence be estimated as:

$$TEW = 1000\ (\theta_{FC} - 0.5\theta_{WP})\ Z_e \qquad (73)$$

where
- TEW total evaporable water = maximum depth of water that can be evaporated from the soil when the topsoil has been initially completely wetted [mm],
- θ_{FC} soil water content at field capacity [$m^3\ m^{-3}$],
- θ_{WP} soil water content at wilting point [$m^3\ m^{-3}$],
- Z_e depth of the surface soil layer that is subject to drying by way of evaporation [0.10-0.15 m].

Where unknown, a value for Z_e, the effective depth of the soil evaporation layer, of 0.10-0.15 m is recommended. Typical values for θ_{FC}, θ_{WP} and TEW are given in Table 19.

TABLE 19
Typical soil water characteristics for different soil types

Soil type (USA Soil Texture Classification)	Soil water characteristics			Evaporation parameters	
	θ_{FC}	θ_{WP}	$(\theta_{FC}-\theta_{WP})$	Amount of water that can be depleted by evaporation	
				stage 1 REW	stages 1 and 2 TEW* (Z_e = 0.10 m)
	m^3/m^3	m^3/m^3	m^3/m^3	mm	mm
Sand	0.07 - 0.17	0.02 - 0.07	0.05 - 0.11	2 - 7	6 - 12
Loamy sand	0.11 - 0.19	0.03 - 0.10	0.06 - 0.12	4 - 8	9 - 14
Sandy loam	0.18 - 0.28	0.06 - 0.16	0.11 - 0.15	6 - 10	15 - 20
Loam	0.20 - 0.30	0.07 - 0.17	0.13 - 0.18	8 - 10	16 - 22
Silt loam	0.22 - 0.36	0.09 - 0.21	0.13 - 0.19	8 - 11	18 - 25
Silt	0.28 - 0.36	0.12 - 0.22	0.16 - 0.20	8 - 11	22 - 26
Silt clay loam	0.30 - 0.37	0.17 - 0.24	0.13 - 0.18	8 - 11	22 - 27
Silty clay	0.30 - 0.42	0.17 - 0.29	0.13 - 0.19	8 - 12	22 - 28
Clay	0.32 - 0.40	0.20 - 0.24	0.12 - 0.20	8 - 12	22 - 29

*$TEW = (\theta_{FC} - 0.5\ \theta_{WP})\ Z_e$

FIGURE 38
Soil evaporation reduction coefficient, K_r

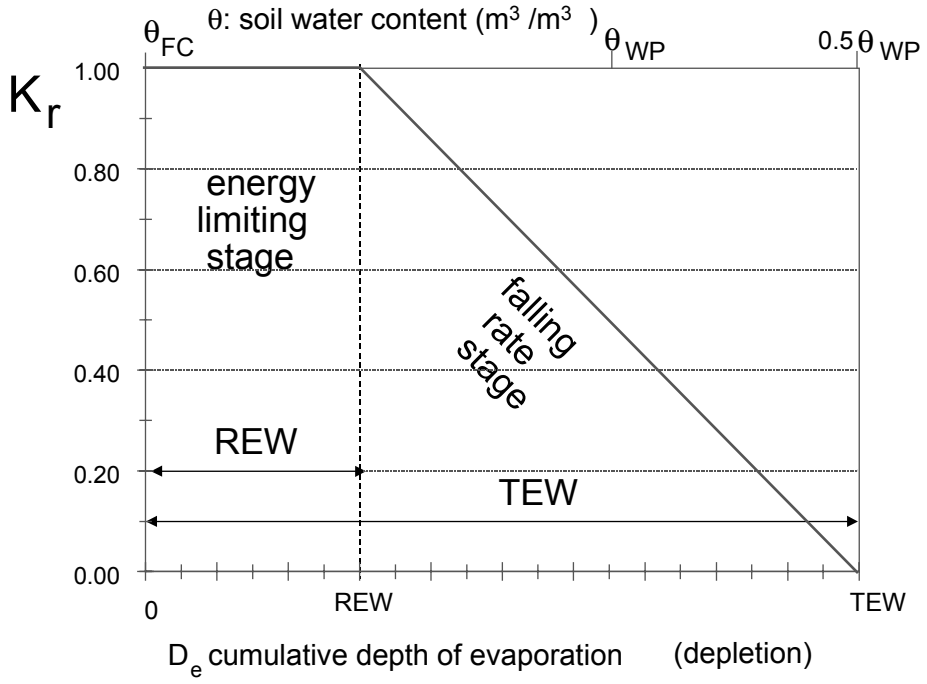

Stage 1: energy limiting stage

At the start of a drying cycle, following heavy rain or irrigation, the soil water content in the topsoil is at field capacity and the amount of water depleted by evaporation, D_e, is zero. During stage 1 of the drying process, the soil surface remains wet and it is assumed that evaporation from soil exposed to the atmosphere will occur at the maximum rate limited only by energy availability at the soil surface. This stage holds until the cumulative depth of evaporation, D_e, is such that the hydraulic properties of the upper soil become limiting and water cannot be transported to the soil surface at a rate that can supply the potential demand. During stage 1 drying, $K_r = 1$.

The cumulative depth of evaporation, D_e, at the end of stage 1 drying is REW (Readily evaporable water, which is the maximum depth of water that can be evaporated from the topsoil layer without restriction during stage1). The depth normally ranges from 5 to 12 mm and is generally highest for medium and fine textured soils. Typical values for REW are given in Table 19.

Stage 2: falling rate stage

The second stage (where the evaporation rate is reducing) is termed the 'falling rate stage' evaporation and starts when D_e exceeds REW. At this point, the soil surface is visibly dry, and the evaporation from the exposed soil decreases in proportion to the amount of water remaining in the surface soil layer:

$$K_r = \frac{TEW - D_{e,\,i-1}}{TEW - REW} \qquad \text{for } D_{e,i-1} > REW \qquad (74)$$

where K_r dimensionless evaporation reduction coefficient dependent on the soil water depletion (cumulative depth of evaporation) from the topsoil layer ($K_r = 1$ when $D_{e,i-1} \leq REW$),

$D_{e,i-1}$ cumulative depth of evaporation (depletion) from the soil surface layer at the end of day $_{i-1}$ (the previous day) [mm],

TEW maximum cumulative depth of evaporation (depletion) from the soil surface layer when $K_r = 0$ (TEW = total evaporable water) [mm],

REW cumulative depth of evaporation (depletion) at the end of stage 1 (REW = readily evaporable water) [mm].

EXAMPLE 31
Determination of the evapotranspiration from a bare soil

Determine the evapotranspiration from a bare loamy soil surface ($K_{cb} \approx 0.15$) for ten successive days following a heavy rain. The reference evapotranspiration during the drying period is $ET_o = 4.5$ mm/day, and the climate is subhumid with light wind.

From Table 19 For Loam: TEW ≈ 20 mm and REW ≈ 9 mm
For rain on bare soil $f_{ew} = 1$
From Eq. 72 $K_{c\,max} = 1.20$

(1) Day	(2) $D_{e\,start}$ mm	(3) Stage	(4) K_r	(5) K_e	(6) $K_e\,ET_o$ mm/day	(7) $D_{e\,end}$ mm	(8) ET_c mm/day
1	0.00	1	1	1.05	4.73	4.73	5.4
2	4.73	1	1	1.05	4.73	9.45	5.4
3	9.45	2	(20-9.45)/(20-9)=0.96	1.01	4.53	13.98	5.2
4	13.98	2	(20-13.98)/(20-9)=0.55	0.57	2.59	16.57	3.3
5	16.57	2	(20-16.57)/(20-9)=0.31	0.33	1.47	18.04	2.1
6	18.04	2	(20-18.04)/(20-9)=0.18	0.19	0.84	18.88	1.5
7	18.88	2	(20-18.88/(20-9)=0.10	0.11	0.48	19.36	1.2
8	19.36	2	(20-19.36)/(20-9)=0.06	0.06	0.27	19.64	0.9
9	19.64	2	(20-19.64)/(20-9)=0.03	0.03	0.16	19.79	0.8
10	19.79	2	(20-19.79)/(20-9)=0.02	0.02	0.09	19.88	0.8

(1) Day number.
(2) Depletion at beginning of the day (= depletion at end of previous day).
(3) Soil evaporation stage (stage 2 starts if D_e > REW = 9 mm).
(4) K_r ($K_r = 1$ for stage 1. Use Eq. 74 for stage 2).
(5) From Eq. 21: $K_e = K_r\,(K_{c\,max} - K_{cb}) = K_r\,(1.20\text{-}0.15) = 1.05\,K_r \leq 1.20$.
(6) Evaporation component: $K_e\,ET_o = K_e$ (4.5 mm/day).
(7) Depletion at end of day = (2) - (6).
(8) $ET_c = (K_{cb} + K_e)\,ET_o = (0.15 + K_e)\,ET_o = (0.15+K_e)$ 4.5 mm/day,
where $K_{cb}\,ET_o = (0.15\,ET_o) \approx 0.7$ mm/day is basal, "diffusive" evaporation from the soil, possibly from beneath the Z_e depth (~ 0.10 to 0.15 m). Since the soil in this situation is bare, one could set the K_{cb} equal to zero so that maximum K_e becomes $K_e = K_{c\,max} = 1.20$. Then all of the evaporation would be deducted from the surface soil layer.

The example demonstrates that the estimation of K_r requires a daily water balance calculation. This is further developed in the section on the daily calculation of K_e.

Exposed and wetted soil fraction (f_{ew})

f_{ew}: calculation procedure

In crops with incomplete ground cover, evaporation from the soil often does not occur uniformly over the entire surface, but is greater between plants where exposure to sunlight occurs and where more air ventilation is able to transport vapour from the soil surface to above the canopy. This is especially true where only part of the soil surface is wetted by irrigation.

It is recognized that both the location and the fraction of the soil surface exposed to sunlight change to some degree with the time of day and depending on row orientation. The procedure presented here predicts a general averaged fraction of the soil surface from which the majority of evaporation occurs. Diffusive evaporation from the soil beneath the crop canopy is assumed to be largely included in the basal K_{cb} coefficient.

Where the complete soil surface is wetted, as by precipitation or sprinkler, then the fraction of soil surface from which most evaporation occurs, f_{ew}, is essentially defined as ($1-f_c$), where f_c is the average fraction of soil surface covered by vegetation and ($1-f_c$) is the approximate fraction of soil surface that is exposed. However, for irrigation systems where only a fraction of the ground surface is wetted, f_{ew} must be limited to f_w, the fraction of the soil surface wetted by irrigation (Figure 39). Therefore, f_{ew} is calculated as:

$$f_{ew} = \min(1 - f_c , f_w) \qquad (75)$$

where $1-f_c$ average exposed soil fraction not covered (or shaded) by vegetation [0.01 - 1],
f_w average fraction of soil surface wetted by irrigation or precipitation [0.01 - 1].

The 'min()' function selects the lowest value of the '$1-f_c$' and 'f_w' values. Figure 39 illustrates the relation of f_{ew} to ($1-f_c$) and f_w.

The limitation imposed by Equation 75 assumes that the fraction of soil wetted by irrigation occurs within the fraction of soil exposed to sunlight and ventilation. This is generally the case, except perhaps with drip irrigation (Figure 39).

In the case of drip irrigation, where the majority of soil wetted by irrigation may be beneath the canopy and may therefore be shaded, more complex models of the soil surface and wetting patterns may be required to accurately estimate total evaporation from the soil. In this case, the value for f_w may need to be reduced to about one-half to one-third of that given in Table 20 to account for the effects of shading of emitters by the plant canopy on the evaporation rate from wetted soil (Example 34). A general approach could be to multiply f_w by $[1-(2/3)f_c]$ for drip irrigation.

f_w: fraction of soil surface wetted by irrigation or precipitation

Table 20 presents typical values for f_w. Where a mixture of irrigation and precipitation occur within the same drying period or on the same day, the value for f_w should be based on a weighted average of the f_w for precipitation ($f_w = 1$) and the f_w for the irrigation system. The weighting should be approximately proportional to the infiltration depths from each water source.

FIGURE 39
Determination of variable f_{ew} (cross-hatched areas) as a function of the fraction of ground surface coverage (f_c) and the fraction of the surface wetted (f_w)

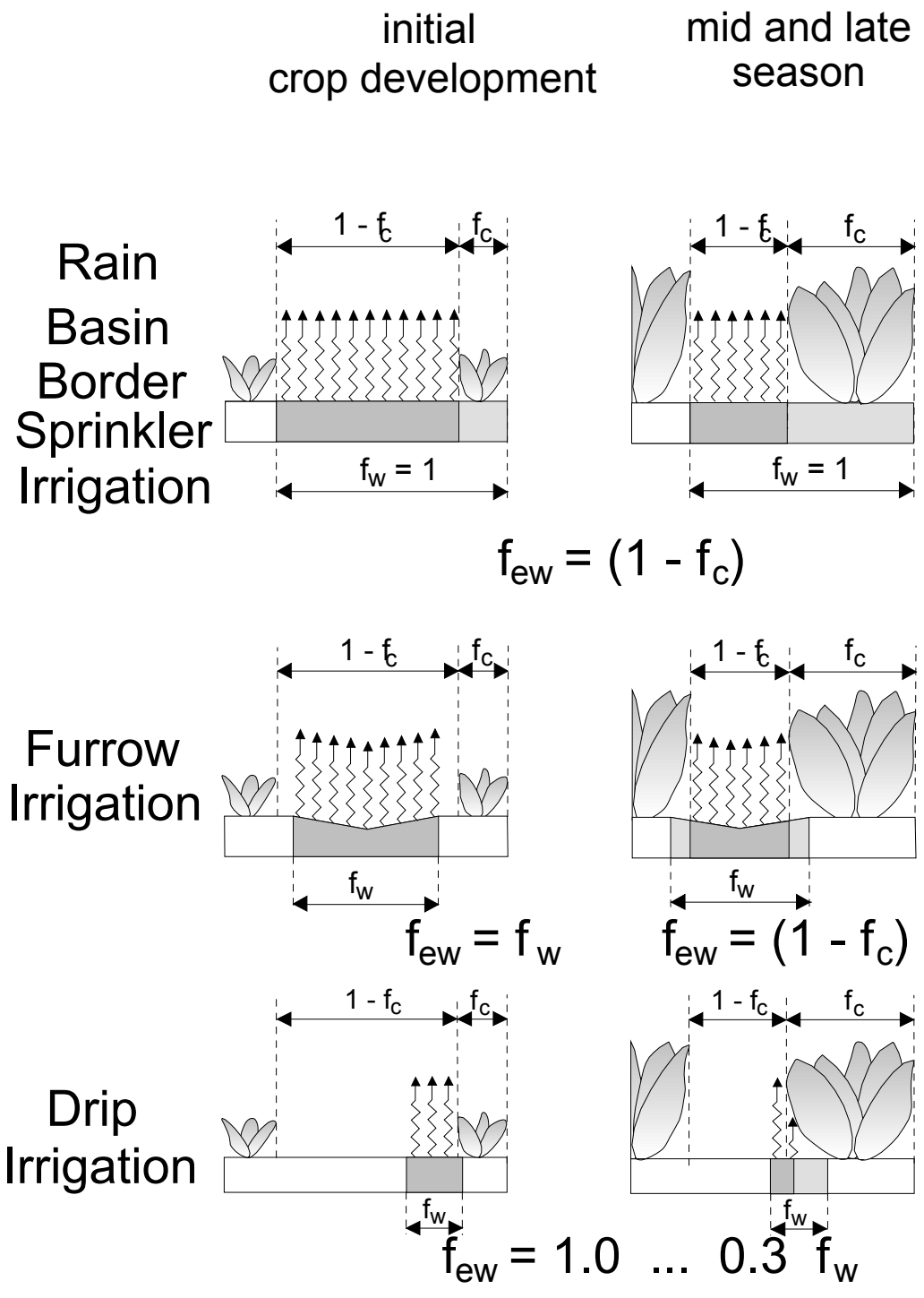

TABLE 20
Common values of fraction f_w of soil surface wetted by irrigation or precipitation

Wetting event	f_w
Precipitation	1.0
Sprinkler irrigation	1.0
Basin irrigation	1.0
Border irrigation	1.0
Furrow irrigation (every furrow), narrow bed	0.6 ... 1.0
Furrow irrigation (every furrow), wide bed	0.4 ... 0.6
Furrow irrigation (alternated furrows)	0.3 ... 0.5
Trickle irrigation	0.3 ... 0.4

Alternatively, on each day of the application, the following rules can be applied to determine f_w for that and subsequent days in a more simplified manner:

- Surface is wetted by irrigation and rain: f_w is the f_w for the irrigation system;
- Surface is wetted by irrigation: f_w is the f_w for the irrigation system;
- Surface is wetted by significant rain (i.e., > 3 to 4 mm) with no irrigation: $f_w = 1$;
- Where there is neither irrigation nor significant precipitation: f_w is the f_w of the previous day.

1-f_c: exposed soil fraction

The fraction of the soil surface that is covered by vegetation is termed f_c. Therefore, (1-f_c) represents the fraction of the soil that is exposed to sunlight and air ventilation and which serves as the site for the majority of evaporation from wet soil. The value for f_c is limited to < 0.99. The user should assume appropriate values for the various growth stages. Typical values for f_c and (1-f_c) are given in Table 21.

TABLE 21
Common values of fractions covered by vegetation (f_c) and exposed to sunlight (1-f_c)

Crop growth stage	f_c	1-f_c
Initial stage	0.0 - 0.1	1.0 - 0.9
Crop development stage	0.1 - 0.8	0.9 - 0.2
Mid-season stage	0.8 - 1.0	0.2 - 0.0
Late season stage	0.8 - 0.2	0.2 - 0.8

Where f_c is not measured, f_c can be estimated using the relationship:

$$f_c = \left(\frac{K_{cb} - K_{c\,min}}{K_{c\,max} - K_{c\,min}} \right)^{(1+0.5h)} \qquad (76)$$

where f_c the effective fraction of soil surface covered by vegetation [0-0.99],
K_{cb} the value for the basal crop coefficient for the particular day or period,
$K_{c\,min}$ the minimum K_c for dry bare soil with no ground cover [≈ 0.15 - 0.20],
$K_{c\,max}$ the maximum K_c immediately following wetting (Equation 72),
h mean plant height [m] .

This equation should be used with caution and validated from field observations. $K_{c\ min}$ is the minimum crop coefficient for dry bare soil when transpiration and evaporation from the soil are near baseline (diffusive) levels. $K_{c\ min} \approx 0.15$ - 0.20 is recommended. The value of $K_{c\ min}$ is an integral part of all K_{cb} coefficients. $K_{c\ min}$ ordinarily has the same value as the $K_{cb\ ini}$ used for annual crops under nearly bare soil conditions (0.15 - 0.20).

Equation 76 assumes that the value for K_{cb} is largely affected by the fraction of soil surface covered by vegetation. This is a good assumption for most vegetation and conditions. The '1+0.5h' exponent in the equation represents the effect of plant height on shading the soil surface and in increasing the value for K_{cb} given a specific value for f_c. The user should limit the difference K_{cb} - $K_{c\ min}$ to ≥ 0.01 for numerical stability. The value for f_c will change daily as K_{cb} changes. Therefore, the above equation is applied daily.

Application of Equation 76 predicts that f_c decreases during the late season period in proportion to K_{cb}, even though the ground may remain covered with senescing vegetation. This prediction helps to account for the local transport of sensible heat from senescing leaves to the soil surface below.

EXAMPLE 32
Calculation of the crop coefficient ($K_{cb} + K_e$) under sprinkler irrigation

A field of cotton has just been sprinkler irrigated. The K_{cb} for the specific day (during the development period) has been computed using Table 17 and Eq. 70 and then interpolated from the K_{cb} curve as 0.9. The ET_o = 7 mm/day, u_2 = 3 m/s and RH_{min} = 20%. Estimate the crop coefficient ($K_{cb} + K_e$).

Assuming h = 1 m, from Eq. 72, $K_{c\ max}$ for this arid climate is:

$$K_{c\ max} = \max\left(\left\{1.2 + [0.04(3-2) - 0.004\ (20-45)]\left(\frac{1}{3}\right)^{0.3}\right\}, \{0.9 + 0.05\}\right) = 1.30$$

From Eq. 76, where $K_{c\ min}$ = 0.15:

$$f_c = [(K_{cb} - K_{c\ min})/(K_{c\ max} - K_{c\ min})]^{(1\ +\ 0.5h)}$$
$$= [(0.9 - 0.15)/(1.3 - 0.15)]^{(1\ +\ 0.5(1))} = 0.53.$$

As the field was sprinkler irrigated, f_w = 1.0 and from Eq. 75:

$$f_{ew} = \min(1 - f_c, f_w)$$
$$= \min(1 - 0.53, 1.0) = 0.47.$$

Assuming that the irrigation was sufficient to fill the evaporating layer to field capacity,
so that $K_r = 1$, evaporation would be in stage 1.
From Eq. 71: $K_e = 1.00\ (1.30\text{-}0.90) = 0.40$

The value is compared against the upper limit $f_{ew}\ K_{c\ max}$ to ensure that it is less than the upper limit:
$f_{ew}\ K_{c\ max}$ = 0.47 (1.30) = 0.61, which is greater than the value for K_e. Therefore, the value for K_e can be used with no limitation.

The total K_c for the field, assuming no moisture stress due to a dry soil profile, is
$K_c = K_{cb} + K_e$
$= 0.9 + 0.40 = 1.30.$
This value is large because of the very wet soil surface, the relatively tall rough crop as compared to the grass reference, and the arid climate (u_2 = 3 m/s and RH_{min} = 20%). In this situation, K_c happens to equal $K_{c\ max}$, as the field has just been wetted by sprinkler irrigation.

EXAMPLE 33
Calculation of the crop coefficient ($K_{cb} + K_e$) under furrow irrigation

The cotton field in the previous example (Ex. 32) has been irrigated by furrow irrigation of alternate rows rather than by sprinkler, and the fraction of the field surface wetted by the irrigation is 0.3.

The f_{ew} in this case is calculated from Eq. 75 as:
$f_{ew} = \min(1-f_c, f_w) = \min(1 - 0.53, 0.3) = 0.3$.

Assuming that the irrigation was sufficient to fill the f_{ew} portion of the evaporating layer to field capacity, so that $K_r = 1$, evaporation would be in stage 1.
From Eq. 71: $K_e = 1.00\ (1.30 - 0.9) = 0.40$

The value is compared to the upper limit $f_{ew} K_{c\ max}$ which is 0.30 (1.30) = 0.39. Because 0.40 > 0.39, K_e from the f_{ew} surface area is constrained to 0.39.

The total K_c for the furrow irrigated field, assuming no moisture stress due to dry soil, is
$K_c = K_{cb} + K_e = 0.9 + 0.39 = 1.29$. This value is essentially the same as for the previous example (Ex. 32) because the procedure assumes that the soil between alternate rows is the portion that is wetted by the irrigation, so that the majority of the field surface has either vegetation cover or wet soil.

EXAMPLE 34
Calculation of the crop coefficient ($K_{cb} + K_e$) under drip irrigation

The cotton field in the previous example (Ex. 32) has been irrigated by drip irrigation, where the emitters are placed beneath the cotton canopy. The fraction of the field surface wetted by the irrigation is 0.3.

The f_{ew} in this case is calculated from Eq. 75 as $f_{ew} = \min(1-f_c, f_w)$. Because the emitters are beneath the canopy so that less energy is available for evaporation, the value for f_w is reduced by multiplying by $1 - (2/3)f_c$, so that:
$f_{ew} = \min[(1-f_c),(1 - 0.67\ f_c)\ f_w)] = \min[(1-0.53), (1 - 0.67(0.53))(0.3)] = 0.19$

Assuming that the irrigation was sufficient to fill the f_w portion of the evaporating layer to field capacity, so that $K_r = 1$, evaporation would be in stage 1.
From Eq. 71: $K_e = 1.00\ (1.30-0.90) = 0.40$.

The value is compared to the upper limit $f_{ew} K_{c\ max} = 0.19\ (1.30) = 0.25$. Because 0.25 < 0.40, K_e from the f_w fraction of the surface area is constrained by the available energy. Therefore $K_e = 0.25$.

The total K_c for the drip irrigated field, assuming no moisture stress due to dry soil, is:
$K_c = K_{cb} + K_e = 0.9 + 0.25 = 1.15$. This K_c value is less than that for sprinkler and furrow irrigation (Examples 32 and 33).

Daily calculation of K_e

Daily water balance

The estimation of K_e in the calculation procedure requires a daily water balance computation for the surface soil layer for the calculation of the cumulative evaporation or depletion from the wet condition. The daily soil water balance equation for the exposed and wetted soil fraction f_{ew} is (Figure 40):

FIGURE 40
Water balance of the topsoil layer

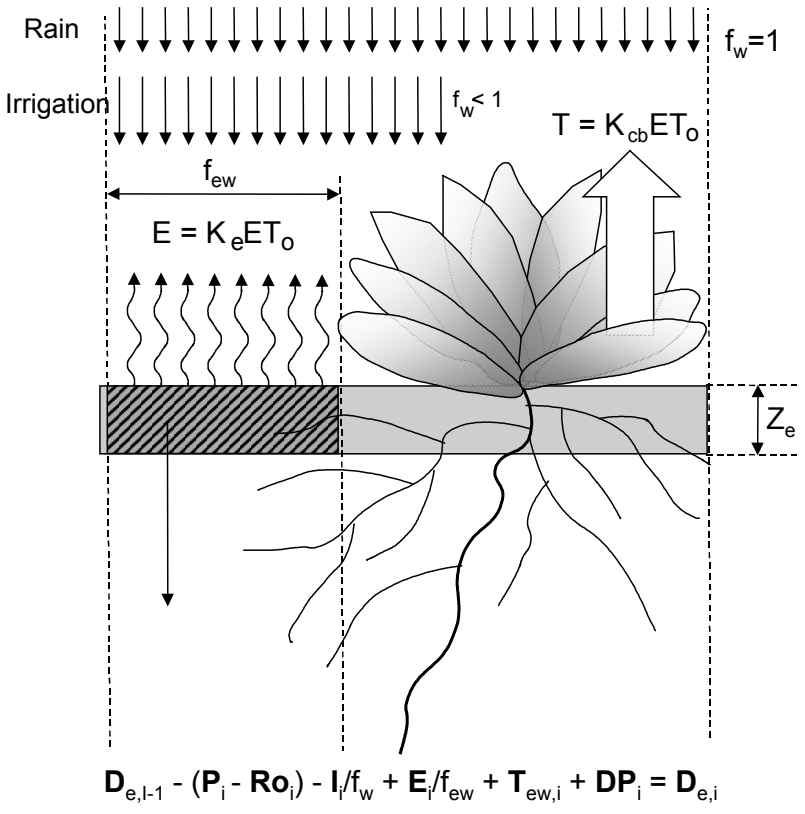

$$D_{e,i} = D_{e,i-1} - (P_i - RO_i) - \frac{I_i}{f_w} + \frac{E_i}{f_{ew}} + T_{ew,i} + DP_{e,i} \qquad (77)$$

where
- $D_{e,i-1}$ cumulative depth of evaporation following complete wetting from the exposed and wetted fraction of the topsoil at the end of day i-1 [mm],
- $D_{e,i}$ cumulative depth of evaporation (depletion) following complete wetting at the end of day i [mm],
- P_i precipitation on day i [mm],
- RO_i precipitation runoff from the soil surface on day i [mm],
- I_i irrigation depth on day i that infiltrates the soil [mm],
- E_i evaporation on day i (i.e., $E_i = K_e\ ET_o$) [mm],
- $T_{ew,i}$ depth of transpiration from the exposed and wetted fraction of the soil surface layer on day i [mm],
- $DP_{e,i}$ deep percolation loss from the topsoil layer on day i if soil water content exceeds field capacity [mm],
- f_w fraction of soil surface wetted by irrigation [0.01 - 1],
- f_{ew} exposed and wetted soil fraction [0.01 - 1].

Limits on $D_{e,\,i}$

By assuming that the topsoil is at field capacity following heavy rain or irrigation, the minimum value for the depletion $D_{e,i}$ is zero. As the soil surface dries, $D_{e,i}$ increases and in absence of any wetting event will steadily reach its maximum value TEW (Equation 73). At that moment no water is left for evaporation in the upper soil layer, K_r becomes zero, and the value for $D_{e,i}$ remains at TEW until the topsoil is wetted once again. The limits imposed on $D_{e,i}$ are consequently:

$$0 \leq D_{e,\,i} \leq TEW \qquad (78)$$

Initial depletion

To initiate the water balance for the evaporating layer, the user can assume that the topsoil is near field capacity following a heavy rain or irrigation, i.e., $D_{e,i-1} = 0$. Where a long period of time has elapsed since the last wetting, the user can assume that all evaporable water has been depleted from the evaporation layer at the beginning of calculations, i.e., $D_{e,\,i-1} = TEW = 1\,000\,(\theta_{FC} - 0.5\,\theta_{WP})\,Z_e$.

Precipitation and runoff

P_i is equivalent to daily precipitation. Daily precipitation in amounts less than about $0.2\,ET_o$ is normally entirely evaporated and can usually be ignored in the K_e and water balance calculations. The amount of rainfall lost by runoff depends on: the intensity of rainfall; the slope of land; the soil type, its hydraulic conditions and antecedent moisture content; and the land use and cover. For general situations, RO_i can be assumed to be zero or can be accounted for by considering only a certain percentage of P_i. This is especially true for the water balance of the topsoil layer, since almost all precipitation events that would have intensities or depths large enough to cause runoff would probably replenish the water content of the topsoil layer to field capacity. Therefore, the impact of the runoff component can be ignored. Light precipitation events will generally have little or no runoff.

Irrigation

I_i is generally expressed as a depth of water that is equivalent to the mean infiltrated irrigation depth distributed over the entire field. Therefore, the value I_i/f_w is used to describe the actual concentration of the irrigation volume over the fraction of the soil that is wetted (Figure 31).

Evaporation

Evaporation beneath the vegetation canopy is assumed to be included in K_{cb} and is therefore not explicitly quantified. The computed evaporation is fully concentrated in the exposed, wetted topsoil. The evaporation E_i is given by $K_e\,ET_o$. The E_i/f_{ew} provides for the actual concentration of the evaporation over the fraction of the soil that is both exposed and wetted.

Transpiration

Except for shallow rooted crops (i.e., where the depth of the maximum rooting zone is < 0.5 to 0.6 m), the amount of transpiration from the evaporating soil layer is small and can be ignored (i.e., $T_{ew} = 0$). In addition, for row crops, most of the water extracted by the roots may be extracted from beneath the vegetation canopy. Therefore, T_{ew} from the f_{ew} fraction of soil surface can be assumed to be zero in these cases.

EXAMPLE 35
Estimation of crop evapotranspiration with the dual crop coefficient approach

Estimate the crop evapotranspiration, ET_c, for ten successive days. It is assumed that:

- the soil is a sandy loam soil, characterized by θ_{FC} = 0.23 m^3 m^{-3} and θ_{WP} = 0.10 m^3 m^{-3},
- the depth of the surface soil layer that is subject to drying by way of evaporation, Z_e, is 0.1 m,
- during the period, the height of the vegetation h = 0.30 m, the average wind speed u_2 = 1.6 m s^{-1}, and RHmin = 35%,
- the K_{cb} on day 1 is 0.30 and increases to 0.40 by day 10,
- the exposed soil fraction, $(1-f_c)$, decreases from 0.92 on day 1 to 0.86 on day 10,
- all evaporable water has been depleted from the evaporation layer at the beginning of calculations ($D_{e,\ i-1}$ = TEW),
- irrigation occurs at the beginning of day 1 (I = 40 mm), and the fraction of soil surface wetted by irrigation, f_w = 0.8,
- a rain of 6 mm occurred at the beginning of day 6.

From Tab. 19 REW ≈ 8 mm
From Eq. 73 TEW = 1 000 (0.23 - 0.5(0.10)) 0.1 = 18 mm
From Eq. 72 $K_{c\ max} = 1.2 + [0.04(1.6-2) - 0.004(35-45)]\ (0.3/3)^{0.3} = 1.21$
All evaporable water has been depleted at the beginning of calculations, $D_{e,\ i-1}$ = TEW = 18 mm

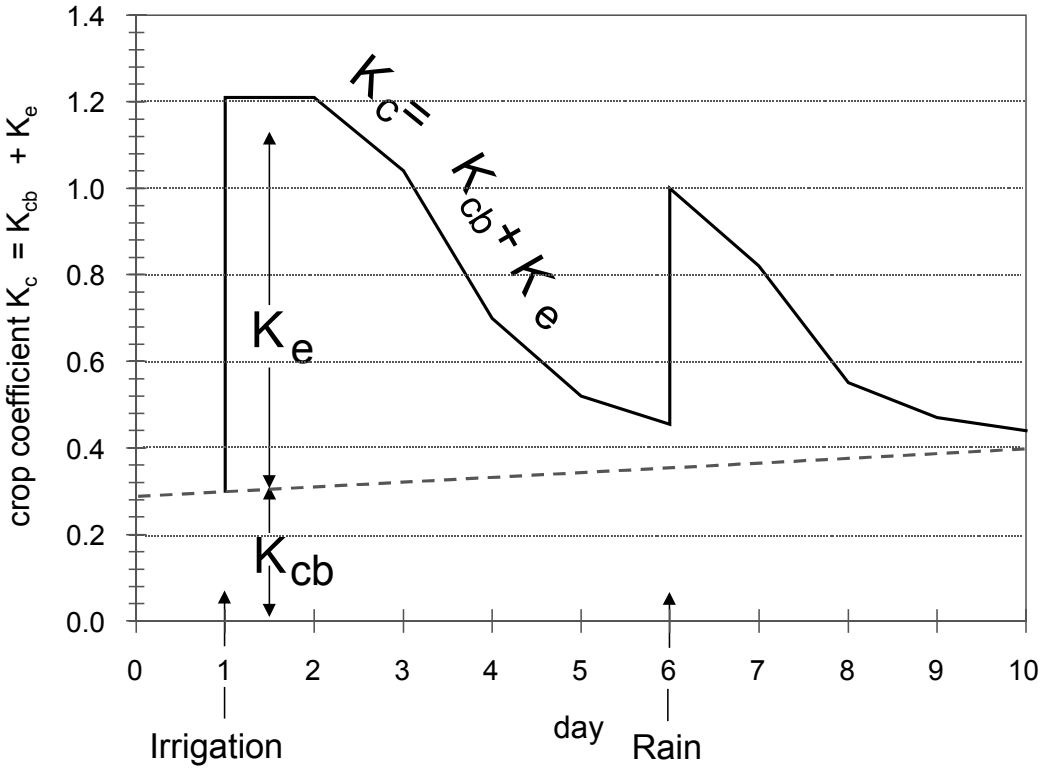

(1) Day	(2) ET_o	(3) P-RO	(4) I/f_w	(5) $1-f_c$	(6) f_w	(7) f_{ew}	(8) K_{cb}	(9) $D_{e,\,i\ start}$
	mm/d	mm	mm					mm
start	-	-	-	-	-	-	-	-
1	4.5	0	50	0.92	0.8	0.80	0.30	0
2	5.0	0	0	0.91	0.8	0.80	0.31	5
3	3.9	0	0	0.91	0.8	0.80	0.32	11
4	4.2	0	0	0.90	0.8	0.80	0.33	14
5	4.8	0	0	0.89	0.8	0.80	0.34	16
6	2.7	6	0	0.89	1	0.89	0.36	11
7	5.8	0	0	0.88	1	0.88	0.37	13
8	5.1	0	0	0.87	1	0.87	0.38	16
9	4.7	0	0	0.87	1	0.87	0.39	17
10	5.2	0	0	0.86	1	0.86	0.40	18

(10) K_r	(11) K_e	(12) E/f_{ew}	(13) DP_e	(14) $D_{e,i\ end}$	(15) E	(16) K_c	(17) ET_c
		mm	mm	mm	mm/d		mm/d
-	-	-	-	18	-	-	-
1.00	0.91	5.1	32	5	4.1	1.21	5.5
1.00	0.90	5.6	0	11	4.5	1.21	6.1
0.70	0.62	3.0	0	14	2.8	1.04	4.0
0.40	0.35	1.8	0	16	1.5	0.70	2.9
0.20	0.18	1.1	0	17	0.8	0.52	2.5
0.75	0.64	2.0	0	13	1.7	1.00	2.7
0.53	0.45	3.0	0	16	2.6	0.82	4.7
0.20	0.17	1.0	0	17	0.9	0.55	2.8
0.09	0.08	0.4	0	18	0.4	0.47	2.2
0.05	0.04	0.2	0	18	0.2	0.44	2.3

(1) Day number.

(2) ET_o is given. Note that ET_o would be forecast values in real time irrigation scheduling but are known values after the occurrence of the day, during an update of the calculations.

(3) (P-RO) are known values after the occurrence of the day, during an update of the calculations.

(4) Net irrigation depth for the part of the soil surface wetted by irrigation.

(5) $(1-f_c)$ is given (interpolated between 0.92 m on day 1 and 0.86 m on day 10).

(6) If significant rain: $f_{w,i} = 1.0$ (Tab. 20)
If irrigation: $f_{w,i} = 0.8$ (given),
otherwise: $f_{w,i} = f_{w,i-1}$.

(7) Eq. 75. Fraction of soil surface from which most evaporation occurs.

(8) K_{cb} is given (interpolated between 0.30 on day 1 and 0.40 on day 10).

(9) $D_{e,i\ start}$ (depletion at start of day)
If precipitation and irrigation occur early in the day then the status of depletion from the soil surface layer (at the start of the day) should be updated:
$= \text{Max}(D_{e,i-1} - I_{n,i}/f_{wi} - (\text{P-RO})_i$, or 0). where $D_{e,i-1}$ is taken from column 14 of previous day.
If precipitation and irrigation occur late in the day, then column 6 should be set equal to $D_{e,i-1}$ (column 14 of previous day).

(10) If $D_{e,i} \leq \text{REW}$ $K_r = 1$ If $D_{e,i} > \text{REW}$ $K_r =$ Eq. 74.

(11) Eq. 71 where $K_e = K_r\,(K_{c\,max} - K_{cb}) \leq f_{ew}\,K_{c\,max}$. (e.g., $K_e = \min(K_r\,(K_{c\,max} - K_{cb}), f_{ew}\,K_{c\,max})$.

(12) Evaporation from the wetted and exposed fraction of the soil surface $= (K_e\,ET_o)/f_{ew}$.

(13) Eq. 79 where $DP_e \geq 0$. (This is deep percolation from the evaporating layer).

(14) $D_{e,i}$ (depletion at end of day) is from Eq. 77 where $D_{e,i-1}$ is value in column 14 of previous day.

(15) Mean evaporation expressed as distributed over the entire field surface $= K_e\,ET_o$.

(16) $K_c = K_{cb} + K_e$.

(17) Eq. 69.

The daily water balance calculation for the surface layer, even for shallow rooted crops, is not usually sensitive to T_{ew}, as T_{ew} is a minor part of the flux from the Z_e depth for the first 3-5 days following a wetting event. T_{ew} can, therefore, generally be ignored. The effects of the reduction of the water content of the evaporating soil layer due to T_{ew} can be accounted for ulteriorly when it is assumed that $T_{ew} = 0$ by decreasing the value for Z_e, for example from 0.15 to 0.12 m or from 0.10 to 0.08 m.

Deep percolation

Following heavy rain or irrigation, the soil water content in the topsoil (Z_e layer) might exceed field capacity. However, in this simple procedure it is assumed that the soil water content is at θ_{FC} nearly immediately following a complete wetting event, so that the depletion $D_{e,i}$ in Equation 77 is zero. Following heavy rain or irrigation, downward drainage (percolation) of water from the topsoil layer is calculated as:

$$DP_{e,i} = (P_i - RO_i) + \frac{I_i}{f_w} - D_{e,i-1} \qquad \geq 0 \qquad (79)$$

As long as the soil water content in the evaporation layer is below field capacity (i.e., $D_{e,i} > 0$), the soil will not drain and $DP_{e,i} = 0$.

Order of calculation

In making calculations for the $K_{cb} + K_e$ procedure, for example when using a spreadsheet, the calculations should proceed in the following order: K_{cb}, h, $K_{c\ max}$, f_c, f_w, f_{ew}, K_r, K_e, E, DP_e, D_e, I, K_c, and ET_c.

CALCULATING ET_C

The calculation procedure lends itself to application by computer, either in the form of electronic spreadsheets (Example 35) or in the form of structured programming languages. The calculation procedure consists in determining:

a. Reference evaporation, ET_o:

Estimate ET_o: the procedure is given in Chapter 4.

b. Growth stages:

Determine the locally adjusted lengths of the four growth stages (for general information consult Table 11):

- Initial growth stage: L_{ini},
- Crop development stage: L_{dev},
- Mid-season stage: L_{mid},
- Late season stage: L_{late}.

c. Basal crop coefficient, K_{cb}:

Calculate basal crop coefficients for each day of the growing period:

- select $K_{cb\ ini}$, $K_{cb\ mid}$ and $K_{cb\ end}$ from Table 17;
- adjust $K_{cb\ mid}$ and $K_{cb\ end}$ to the local climatic conditions (Equation 70);
- determine the daily K_{cb} values
    - initial growth stage: $K_{cb} = K_{cb\ ini}$,
    - crop development stage: from $K_{cb\ ini}$ to $K_{cb\ mid}$ (Equation 66),
    - mid-season stage: $K_{cb} = K_{cb\ mid}$,
    - late season stage: from $K_{cb\ mid}$ to $K_{cb\ end}$ (Equation 66).

d. Evaporation coefficient, K_e:

Calculate the maximum value of K_c, i.e., the upper limit $K_{c\ max}$ (Equation 72), and Determine for each day of the growing period:

- the fraction of soil covered by vegetation, f_c (Table 21 or Equation 76),
- the fraction of soil surface wetted by irrigation or precipitation, f_w (Table 20),
- the fraction of soil surface from which most evaporation occurs, f_{ew} (Equation 75),
- the cumulative depletion from the evaporating soil layer, D_e, determined by means of a daily soil water balance of the topsoil (Equation 77),
- the corresponding evaporation reduction coefficient, K_r (Equation 74), and
- the soil evaporation coefficient, K_e (Equation 71).

e. Crop evapotranspiration, ET_c:

Calculate $ET_c = (K_{cb} + K_e)\ ET_o$ (Equation 69).

BOX 16
Case study of dry bean crop at Kimberly, Idaho, the United States (dual crop coefficient)

Results from applying the $K_{cb} + K_e$ procedure for a snap bean crop harvested as dry seed are shown in the figure below. This example uses the same data set that was used in the case study of Box 15. The measured ET_c data were measured using a precision lysimeter system at Kimberly, Idaho. Values for $K_{cb\ ini}$, $K_{cb\ mid}$, and $K_{cb\ end}$ were calculated in Example 29 as 0.15, 1.14, and 0.25. The lengths of growth stages were 25, 25, 30, and 20 days. The K_{cb} values are plotted in Fig. 37. The value for $K_{c\ max}$ from Eq. 72 for the mid-season period averaged 1.24, based on u_2 = 2.2 m/s and RH_{min} = 30% for Kimberly. The soil at Kimberly was a silt loam texture. Assuming that the depth of the evaporation soil layer, Z_e, was 0.1 m, values for TEW = 22 mm and REW = 9 mm, based on Eq. 73 and using soil data from Table 19.

The occurrence and magnitudes of individual wetting events are shown in the figure below. Nearly all wetting events were from irrigation. Because the irrigation was by furrow irrigation of alternate rows, the value for f_w was set equal to 0.5. Irrigation events occurred at about midday or during early afternoon.

The agreement between the estimated values for daily $K_{cb}+K_e$ (thin continuous line) and actual 24-hour measurements (symbols) is relatively good. Measured and predicted $K_{cb}+K_e$ was higher following wetting by rainfall or irrigation, as expected. The two wet soil evaporation 'spikes' occurring during the late initial period and early development period (between days 160 and 180) were less than $K_{c\ max}$, because this evaporation was from wetting by furrow irrigation where f_w = 0.5. The value for f_{ew} was constrained to f_w by Eq. 75 during these two events, because during this period, $f_w < 1\text{-}f_c$. Therefore, less than all of the 'potential energy' was converted into evaporation due to the limitation on maximum evaporation per unit surface area that was imposed by Eq. 71.

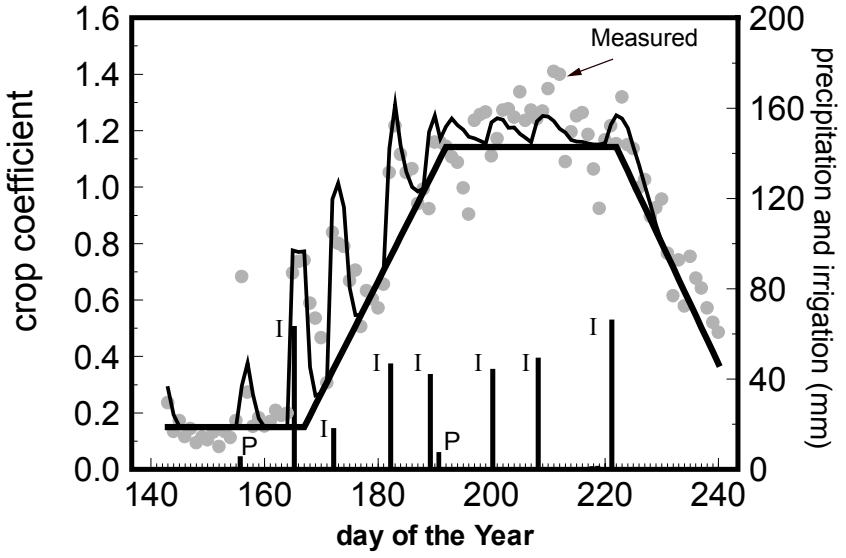

Measured (symbols) and predicted (thin line) daily coefficients ($K_{cb}+K_e$) and the basal crop curve (thick line) for a dry bean crop at Kimberly, Idaho. P in the figure denotes a precipitation event and I denotes an irrigation (data from Wright, 1990).

Part C

Crop evapotranspiration under non-standard conditions

In well-managed fields, the standard conditions are generally the actual field conditions. The ET_c calculated by means of the procedures described in Part B is the crop evapotranspiration under the standard field conditions.

Where the conditions encountered in the field differ from the standard conditions, a correction on ET_c is required. Low soil fertility, salt toxicity, soil waterlogging, pests, diseases and the presence of hard or impenetrable soil horizons in the root zone may result in scanty plant growth and lower evapotranspiration. Soil water shortage and soil salinity may reduce soil water uptake and limit crop evapotranspiration. The evapotranspiration from small isolated stands of plants or from fields where two different crops are grown together or where mulches are used to reduce evaporation may also deviate from the crop evapotranspiration under standard conditions.

This part discusses the effect on ET of management and environmental conditions that deviate from the standard conditions. The environmental effects are described by introducing stress coefficients and by adjusting K_c to the field conditions.

Chapter 8

ET_c under soil water stress conditions

Forces acting on the soil water decrease its potential energy and make it less available for plant root extraction. When the soil is wet, the water has a high potential energy, is relatively free to move and is easily taken up by the plant roots. In dry soils, the water has a low potential energy and is strongly bound by capillary and absorptive forces to the soil matrix, and is less easily extracted by the crop.

When the potential energy of the soil water drops below a threshold value, the crop is said to be water stressed. The effects of soil water stress are described by multiplying the basal crop coefficient by the water stress coefficient, K_S:

$$ET_{c\ adj} = (K_s\ K_{cb} + K_e)\ ET_o \qquad (80)$$

For soil water limiting conditions, $K_S < 1$. Where there is no soil water stress, $K_S = 1$.

K_S describes the effect of water stress on crop transpiration. Where the single crop coefficient is used, the effect of water stress is incorporated into K_c as:

$$ET_{c\ adj} = K_s\ K_c\ ET_o \qquad (81)$$

Because the water stress coefficient impacts only crop transpiration, rather than evaporation from soil, the application of K_s using Equation 80 is generally more valid than is application using Equation 81. However, in situations where evaporation from soil is not a large component of ET_c, use of Equation 81 will provide reasonable results.

SOIL WATER AVAILABILITY

Total available water (TAW)

Soil water availability refers to the capacity of a soil to retain water available to plants. After heavy rainfall or irrigation, the soil will drain until field capacity is reached. Field capacity is the amount of water that a well-drained soil should hold against gravitational forces, or the amount of water remaining when downward drainage has markedly decreased. In the absence of water supply, the water content in the root zone decreases as a result of water uptake by the crop. As water uptake progresses, the remaining water is held to the soil particles with greater force, lowering its potential energy and making it more difficult for the plant to extract it. Eventually, a point is reached where the crop can no longer extract the remaining water. The water uptake becomes zero when wilting point is reached. Wilting point is the water content at which plants will permanently wilt.

As the water content above field capacity cannot be held against the forces of gravity and will drain and as the water content below wilting point cannot be extracted by plant roots, the total available water in the root zone is the difference between the water content at field capacity and wilting point:

$$TAW = 1000\,(\theta_{FC} - \theta_{WP})\,Z_r \qquad (82)$$

where TAW the total available soil water in the root zone [mm],
θ_{FC} the water content at field capacity [$m^3\ m^{-3}$],
θ_{WP} the water content at wilting point [$m^3\ m^{-3}$],
Z_r the rooting depth [m].

TAW is the amount of water that a crop can extract from its root zone, and its magnitude depends on the type of soil and the rooting depth. Typical ranges for field capacity and wilting point are listed in Table 19 for various soil texture classes. Ranges of the maximum effective rooting depth for various crops are given in Table 22.

Readily available water (RAW)

Although water is theoretically available until wilting point, crop water uptake is reduced well before wilting point is reached. Where the soil is sufficiently wet, the soil supplies water fast enough to meet the atmospheric demand of the crop, and water uptake equals ET_c. As the soil water content decreases, water becomes more strongly bound to the soil matrix and is more difficult to extract. When the soil water content drops below a threshold value, soil water can no longer be transported quickly enough towards the roots to respond to the transpiration demand and the crop begins to experience stress. The fraction of TAW that a crop can extract from the root zone without suffering water stress is the readily available soil water:

$$RAW = p\ TAW \qquad (83)$$

where RAW the readily available soil water in the root zone [mm],
p average fraction of Total Available Soil Water (TAW) that can be depleted from the root zone before moisture stress (reduction in ET) occurs [0 - 1].

Values for p are listed in Table 22. The factor p differs from one crop to another. The factor p normally varies from 0.30 for shallow rooted plants at high rates of ET_c (> 8 mm d^{-1}) to 0.70 for deep rooted plants at low rates of ET_c (< 3 mm d^{-1}). A value of 0.50 for p is commonly used for many crops.

The fraction p is a function of the evaporation power of the atmosphere. At low rates of ET_c, the p values listed in Table 22 are higher than at high rates of ET_c. For hot dry weather conditions, where ET_c is high, p is 10-25% less than the values presented in Table 22, and the soil is still relatively wet when the stress starts to occur. When the crop evapotranspiration is low, p will be up to 20% more than the listed values. Often, a constant value is used for p for a specific growing period, rather than varying the value each day. A numerical approximation for adjusting p for ET_c rate is $p = p_{Table\ 22} + 0.04\ (5 - ET_c)$ where the adjusted p is limited to $0.1 \le p \le 0.8$ and ET_c is in mm/day. The influence of the numerical adjustment is shown in Figure 41.

TABLE 22
Ranges of maximum effective rooting depth (Z_r), and soil water depletion fraction for no stress (p), for common crops

Crop	Maximum Root Depth[1] (m)	Depletion Fraction[2] (for ET ≃ 5 mm/day) p
a. Small Vegetables		
Broccoli	0.4-0.6	0.45
Brussel Sprouts	0.4-0.6	0.45
Cabbage	0.5-0.8	0.45
Carrots	0.5-1.0	0.35
Cauliflower	0.4-0.7	0.45
Celery	0.3-0.5	0.20
Garlic	0.3-0.5	0.30
Lettuce	0.3-0.5	0.30
Onions - dry	0.3-0.6	0.30
- green	0.3-0.6	0.30
- seed	0.3-0.6	0.35
Spinach	0.3-0.5	0.20
Radishes	0.3-0.5	0.30
b. Vegetables – Solanum Family (*Solanaceae*)		
Egg Plant	0.7-1.2	0.45
Sweet Peppers (bell)	0.5-1.0	0.30
Tomato	0.7-1.5	0.40
c. Vegetables – Cucumber Family (*Cucurbitaceae*)		
Cantaloupe	0.9-1.5	0.45
Cucumber – Fresh Market	0.7-1.2	0.50
– Machine harvest	0.7-1.2	0.50
Pumpkin, Winter Squash	1.0-1.5	0.35
Squash, Zucchini	0.6-1.0	0.50
Sweet Melons	0.8-1.5	0.40
Watermelon	0.8-1.5	0.40
d. Roots and Tubers		
Beets, table	0.6-1.0	0.50
Cassava – year 1	0.5-0.8	0.35
– year 2	0.7-1.0	0.40
Parsnip	0.5-1.0	0.40
Potato	0.4-0.6	0.35
Sweet Potato	1.0-1.5	0.65
Turnip (and Rutabaga)	0.5-1.0	0.50
Sugar Beet	0.7-1.2	0.55[3]

continued…

1 The larger values for Z_r are for soils having no significant layering or other characteristics that can restrict rooting depth. The smaller values for Z_r may be used for irrigation scheduling and the larger values for modeling soil water stress or for rainfed conditions.

2 The values for p apply for $ET_c \approx 5$ mm/day. The value for p can be adjusted for different ET_c according to

$$p = p_{table\ 22} + 0.04\ (5 - ET_c)$$

where p is expressed as a fraction and ET_c as mm/day.

3 Sugar beets often experience late afternoon wilting in arid climates even at $p < 0.55$, with usually only minor impact on sugar yield.

Table 22 continued

Crop	Maximum Root Depth[1] (m)	Depletion Fraction[2] (for ET ≃ 5 mm/day) p
e. Lugumes (*Leguminosae*)		
Beans, green	0.5-0.7	0.45
Beans, dry and Pulses	0.6-0.9	0.45
Beans, lima, large vines	0.8-1.2	0.45
Chick pea	0.6-1.0	0.50
Fababean (broad bean) – Fresh	0.5-0.7	0.45
– Dry/Seed	0.5-0.7	0.45
Grabanzo	0.6-1.0	0.45
Green Gram and Cowpeas	0.6-1.0	0.45
Groundnut (Peanut)	0.5-1.0	0.50
Lentil	0.6-0.8	0.50
Peas – Fresh	0.6-1.0	0.35
– Dry/Seed	0.6-1.0	0.40
Soybeans	0.6-1.3	0.50
f. Perennial Vegetables (with winter dormancy and initially bare or mulched soil)		
Artichokes	0.6-0.9	0.45
Asparagus	1.2-1.8	0.45
Mint	0.4-0.8	0.40
Strawberries	0.2-0.3	0.20
g. Fibre Crops		
Cotton	1.0-1.7	0.65
Flax	1.0-1.5	0.50
Sisal	0.5-1.0	0.80
h. Oil Crops		
Castorbean (*Ricinus*)	1.0-2.0	0.50
Rapeseed, Canola	1.0-1.5	0.60
Safflower	1.0-2.0	0.60
Sesame	1.0-1.5	0.60
Sunflower	0.8-1.5	0.45
i. Cereals		
Barley	1.0-1.5	0.55
Oats	1.0-1.5	0.55
Spring Wheat	1.0-1.5	0.55
Winter Wheat	1.5-1.8	0.55
Maize, Field (grain) *(field corn)*	1.0-1.7	0.55
Maize, Sweet *(sweet corn)*	0.8-1.2	0.50
Millet	1.0-2.0	0.55
Sorghum – grain	1.0-2.0	0.55
– sweet	1.0-2.0	0.50
Rice	0.5-1.0	0.20[4]

continued...

[4] The value for p for rice is 0.20 of saturation.

Table 22 continued

Crop	Maximum Root Depth1 (m)	Depletion Fraction[2] (for ET ≃ 5 mm/day) p
j. Forages		
Alfalfa – for hay	1.0-2.0	0.55
– for seed	1.0-3.0	0.60
Bermuda – for hay	1.0-1.5	0.55
– Spring crop for seed	1.0-1.5	0.60
Clover hay, Berseem	0.6-0.9	0.50
Rye Grass hay	0.6-1.0	0.60
Sudan Grass hay (annual)	1.0-1.5	0.55
Grazing Pasture - Rotated Grazing	0.5-1.5	0.60
- Extensive Grazing	0.5-1.5	0.60
Turf grass - cool season[5]	0.5-1.0	0.40
- warm season[5]	0.5-1.0	0.50
k. Sugar Cane	1.2-2.0	0.65
l. Tropical Fruits and Trees		
Banana – 1st year	0.5-0.9	0.35
– 2nd year	0.5-0.9	0.35
Cacao	0.7-1.0	0.30
Coffee	0.9-1.5	0.40
Date Palms	1.5-2.5	0.50
Palm Trees	0.7-1.1	0.65
Pineapple	0.3-0.6	0.50
Rubber Trees	1.0-1.5	0.40
Tea – non-shaded	0.9-1.5	0.40
– shaded	0.9-1.5	0.45
m. Grapes and Berries		
Berries (bushes)	0.6-1.2	0.50
Grapes – Table or Raisin	1.0-2.0	0.35
– Wine	1.0-2.0	0.45
Hops	1.0-1.2	0.50
n. Fruit Trees		
Almonds	1.0-2.0	0.40
Apples, Cherries, Pears	1.0-2.0	0.50
Apricots, Peaches, Stone Fruit	1.0-2.0	0.50
Avocado	0.5-1.0	0.70
Citrus		
- 70% canopy	1.2-1.5	0.50
- 50% canopy	1.1-1.5	0.50
- 20% canopy	0.8-1.1	0.50
Conifer Trees	1.0-1.5	0.70
Kiwi	0.7-1.3	0.35
Olives (40 to 60% ground coverage by canopy)	1.2-1.7	0.65
Pistachios	1.0-1.5	0.40
Walnut Orchard	1.7-2.4	0.50

5 Cool season grass varieties include bluegrass, ryegrass and fescue. Warm season varieties include bermuda grass, buffalo grass and St. Augustine grass. Grasses are variable in rooting depth. Some root below 1.2 m while others have shallow rooting depths. The deeper rooting depths for grasses represent conditions where careful water management is practiced with higher depletion between irrigations to encourage the deeper root exploration.

FIGURE 41
Depletion factor for different levels of crop evapotranspiration

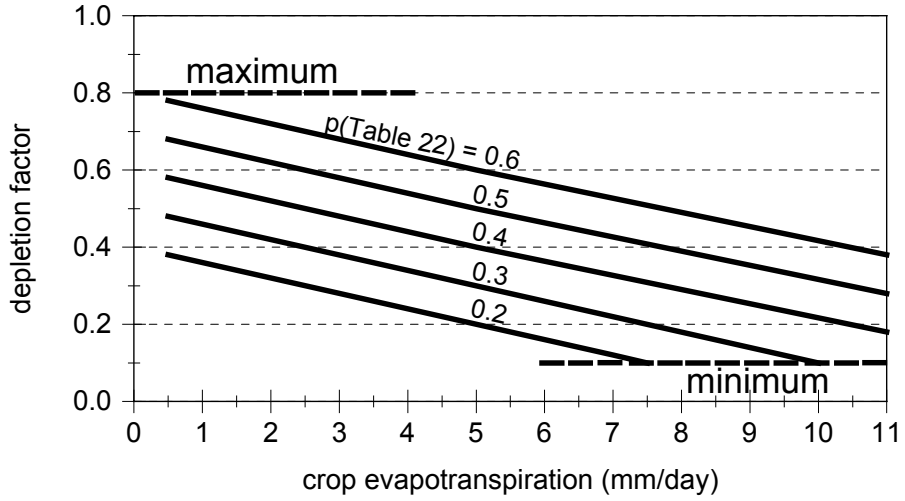

EXAMPLE 36
Determination of readily available soil water for various crops and soil types

Estimate RAW for a full-grown onion, tomato and maize crop. Assume that the crops are cultivated on loamy sand, silt and silty clay soils.

From Table 22
Onion $Z_r \approx 0.4$ m, p = 0.30
Tomato $Z_r \approx 0.8$ m, p = 0.40
Maize $Z_r \approx 1.2$ m, p = 0.55

From Table 19
Loamy sand $\theta_{FC} \approx 0.15$ m^3 m^{-3}, $\theta_{WP} \approx 0.06$ m^3 m^{-3}
1 000 (θ_{FC} - θ_{WP}) = 90 mm(water)/m(soil depth)

Silt $\theta_{FC} \approx 0.32$ m^3 m^{-3}, $\theta_{WP} \approx 0.15$ m^3 m^{-3}
1 000 (θ_{FC} - θ_{WP}) = 170 mm(water)/m(soil depth)

Silty clay $\theta_{FC} \approx 0.35$ m^3 m^{-3}, $\theta_{WP} \approx 0.23$ m^3 m^{-3}
1 000 (θ_{FC} - θ_{WP}) = 120 mm(water)/m(soil depth)

	Loamy sand		Silt		Silty clay	
	TAW (Eq. 82) mm	RAW (Eq. 83) mm	TAW (Eq. 82) mm	RAW (Eq. 83) mm	TAW (Eq. 82) mm	RAW (Eq. 83) mm
Onion	36	11	68	20	48	14
Tomato	72	29	136	54	96	38
Maize	108	59	204	112	144	79

To express the tolerance of crops to water stress as a function of the fraction (p) of TAW is not wholly correct. The rate of root water uptake is in fact influenced more directly by the potential energy level of the soil water (soil matric potential and the associated hydraulic conductivity) than by water content. As a certain soil matric potential corresponds in different soil types with different soil water contents, the value for p is also a function of the soil type. Generally, it can be stated that for fine textured soils (clay) the p values listed in Table 22 can be reduced by 5-10%, while for more coarse textured soils (sand), they can be increased by 5-10%.

RAW is similar to the term Management Allowed Depletion (MAD) introduced by Merriam. However, values for MAD are influenced by management and economic factors in addition to the physical factors influencing p. Generally, MAD < RAW where there is risk aversion or uncertainty, and MAD > RAW where plant moisture stress is an intentional part of soil water management.

WATER STRESS COEFFICIENT (K_S)

The effects of soil water stress on crop ET are described by reducing the value for the crop coefficient. This is accomplished by multiplying the crop coefficient by the water stress coefficient, K_S (Equations 80 and 81).

Water content in the root zone can also be expressed by root zone depletion, D_r, i.e., water shortage relative to field capacity. At field capacity, the root zone depletion is zero (D_r = 0). When soil water is extracted by evapotranspiration, the depletion increases and stress will be induced when D_r becomes equal to RAW. After the root zone depletion exceeds RAW (the water content drops below the threshold θ_t), the root zone depletion is high enough to limit evapotranspiration to less than potential values and the crop evapotranspiration begins to decrease in proportion to the amount of water remaining in the root zone (Figure 42).

FIGURE 42
Water stress coefficient, K_S

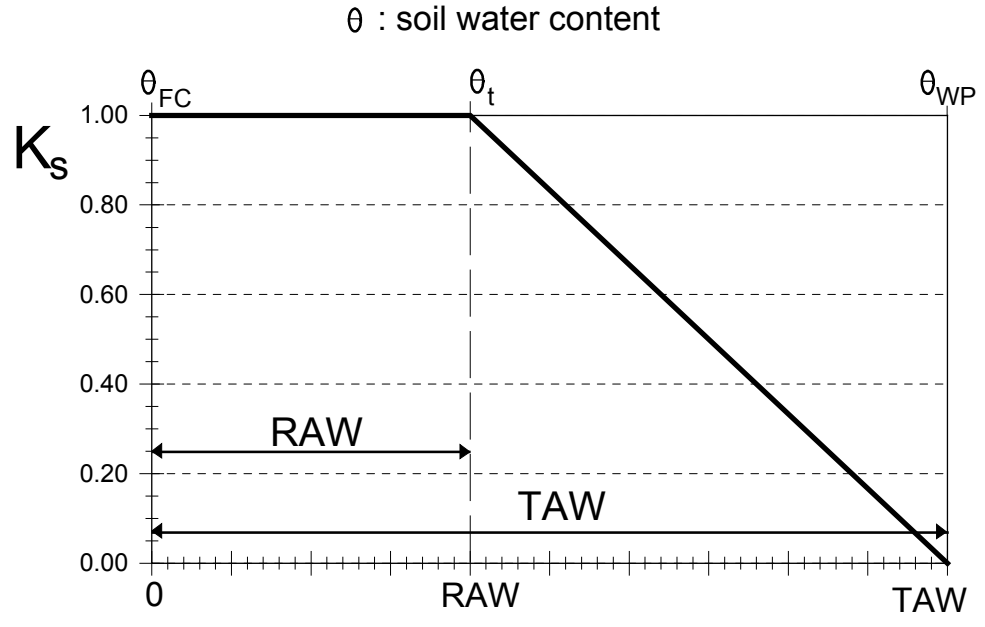

EXAMPLE 37
Effect of water stress on crop evapotranspiration

Estimate the effect of water stress on the evapotranspiration of a full grown tomato crop (Z_r = 0.8 m and p = 0.40) cultivated on a silty soil (θ_{FC} = 0.32 and θ_{WP} = 0.12 m^3 m^{-3}) for the coming 10 days when the initial root zone depletion is 55 mm and neither rain nor irrigations are either forecasted or planned. The expected ET_o for the coming decade is 5 mm/day and K_c = 1.2.

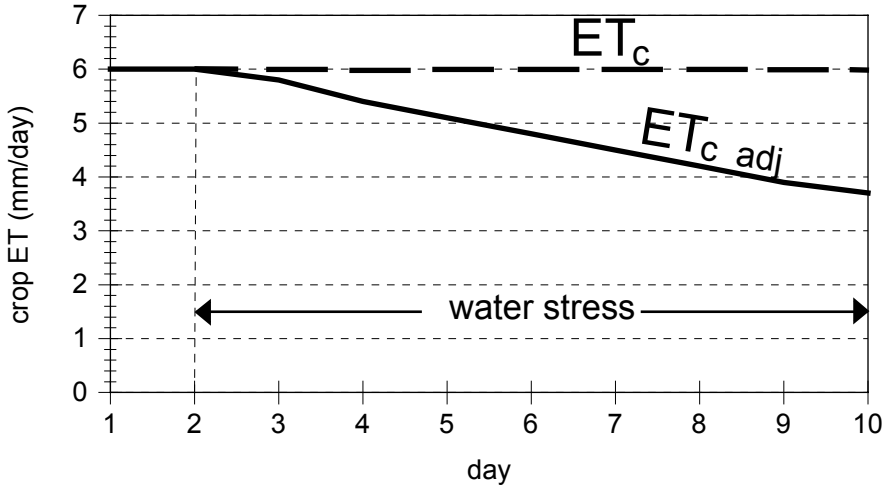

From Eq. 82 TAW = 1 000 (0.32-0.12) 0.8 = 160 mm
From Eq. 83 RAW = 0.40 (160) = 64 mm

(1) Day	(2) ET_o	(3) K_c	(4) ET_c	(5) $D_{r,i}$ start	(6) K_s	(7) $ET_{c\ adj}$	(8) $D_{r,i}$ end
	mm/day		mm/day	mm		mm/day	mm
start	-	-	-	-	-	-	55.0
1	5.0	1.2	6.0	55.0	1.00	6.0	61.0
2	5.0	1.2	6.0	61.0	1.00	6.0	67.0
3	5.0	1.2	6.0	67.0	0.97	5.8	72.8
4	5.0	1.2	6.0	72.8	0.91	5.4	78.3
5	5.0	1.2	6.0	78.3	0.85	5.1	83.4
6	5.0	1.2	6.0	83.4	0.80	4.8	88.2
7	5.0	1.2	6.0	88.2	0.75	4.5	92.6
8	5.0	1.2	6.0	92.6	0.70	4.2	96.9
9	5.0	1.2	6.0	96.9	0.66	3.9	100.8
10	5.0	1.2	6.0	100.8	0.62	3.7	104.5

(1) Day number.
(2) Reference crop evapotranspiration.
(3) Crop coefficient.
(4) Eq. 58, crop ET if no water stress.
(5) Root zone depletion at the beginning of the day (column 8 of previous day).
(6) Eq. 84 where K_s = 1 if $D_{r,i}$ < RAW.
(7) Eq. 81, crop ET under soil water stress conditions.
(8) Depletion at end of day .

The example demonstrates that the estimate of K_s requires a daily water balance calculation. This is developed further in the next section.

FIGURE 43
Water balance of the root zone

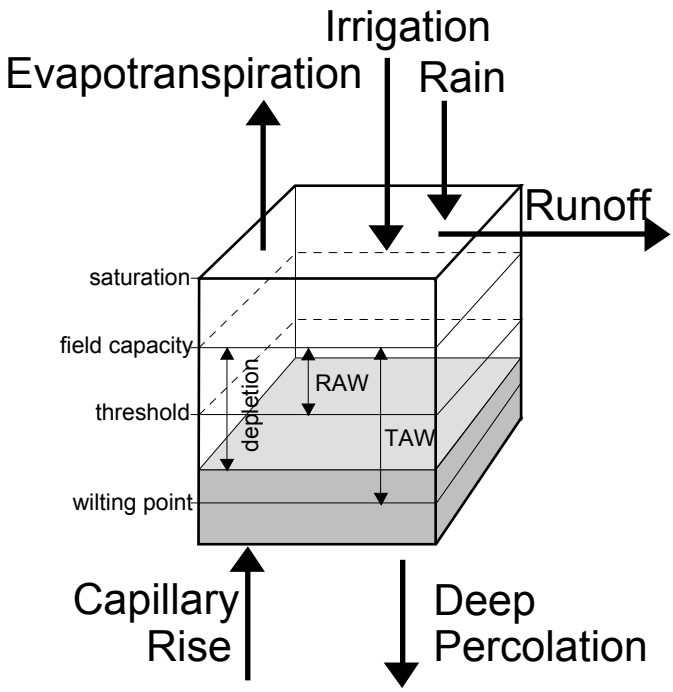

For $D_r > RAW$, K_S is given by:

$$K_s = \frac{TAW - D_r}{TAW - RAW} = \frac{TAW - D_r}{(1 - p)\ TAW} \qquad (84)$$

where K_S is a dimensionless transpiration reduction factor dependent on available soil water [0 - 1],
D_r root zone depletion [mm],
TAW total available soil water in the root zone [mm],
p fraction of TAW that a crop can extract from the root zone without suffering water stress [-].

After the computation of K_S, the adjusted evapotranspiration $ET_{c\ adj}$ is computed by means of Equation 80 or 81, depending on the coefficients used to describe crop evapotranspiration. When the root zone depletion is smaller than RAW, $K_S = 1$.

SOIL WATER BALANCE

The estimation of K_S requires a daily water balance computation for the root zone. Schematically (Figure 43), the root zone can be presented by means of a container in which the water content may fluctuate. To express the water content as root zone depletion is useful. It makes the adding and subtracting of losses and gains straightforward as the various parameters

of the soil water budget are usually expressed in terms of water depth. Rainfall, irrigation and capillary rise of groundwater towards the root zone add water to the root zone and decrease the root zone depletion. Soil evaporation, crop transpiration and percolation losses remove water from the root zone and increase the depletion. The daily water balance, expressed in terms of depletion at the end of the day is:

$$D_{r,i} = D_{r,i-1} - (P - RO)_i - I_i - CR_i + ET_{c,i} + DP_i \quad (85)$$

where
$D_{r,i}$ root zone depletion at the end of day i [mm],
$D_{r,i-1}$ water content in the root zone at the end of the previous day, i-1 [mm],
P_i precipitation on day i [mm],
RO_i runoff from the soil surface on day i [mm],
I_i net irrigation depth on day i that infiltrates the soil [mm],
CR_i capillary rise from the groundwater table on day i [mm],
$ET_{c,i}$ crop evapotranspiration on day i [mm],
DP_i water loss out of the root zone by deep percolation on day i [mm].

Limits on $D_{r,i}$

In Figure 43 it is assumed that water can be stored in the root zone until field capacity is reached. Although following heavy rain or irrigation the water content might temporally exceed field capacity, the total amount of water above field capacity is assumed to be lost the same day by deep percolation, following any ET for that day. By assuming that the root zone is at field capacity following heavy rain or irrigation, the minimum value for the depletion $D_{r,i}$ is zero. As a result of percolation and evapotranspiration, the water content in the root zone will gradually decrease and the root zone depletion will increase. In the absence of any wetting event, the water content will steadily reach its minimum value θ_{WP}. At that moment no water is left for evapotranspiration in the root zone, K_S becomes zero, and the root zone depletion has reached its maximum value TAW. The limits imposed on $D_{r,i}$ are consequently:

$$0 \leq D_{r,i} \leq TAW \quad (86)$$

Initial depletion

To initiate the water balance for the root zone, the initial depletion $D_{r,i-1}$ should be estimated. The initial depletion can be derived from measured soil water content by:

$$D_{r,i-1} = 1000\,(\theta_{FC} - \theta_{i-1})\,Z_r \quad (87)$$

where θ_{i-1} is the average soil water content for the effective root zone. Following heavy rain or irrigation, the user can assume that the root zone is near field capacity, i.e., $D_{r,i-1} \approx 0$.

Precipitation (P), runoff (RO) and irrigation (I)

P_i is equivalent to daily precipitation. Daily precipitation in amounts less than about 0.2 ET_o is normally entirely evaporated and can usually be ignored in the water balance calculations especially when the single crop coefficient approach is being used. I_i is equivalent to the mean

infiltrated irrigation depth expressed for the entire field surface. Runoff from the surface during precipitation can be predicted using standard procedures from hydrological texts.

Capillary rise (CR)

The amount of water transported upwards by capillary rise from the water table to the root zone depends on the soil type, the depth of the water table and the wetness of the root zone. CR can normally be assumed to be zero when the water table is more than about 1 m below the bottom of the root zone. Some information on CR was presented in FAO Irrigation and Drainage Paper No. 24. CR will be a topic in a future FAO publication.

Evapotranspiration (ET_c)

Where the soil water depletion is smaller than RAW, the crop evapotranspiration equals $ET_c = K_c\ ET_o$. As soon as $D_{r,i}$ exceeds RAW, the crop evapotranspiration is reduced and ET_c can be computed from Equation 80 or 81.

Deep percolation (DP)

Following heavy rain or irrigation, the soil water content in the root zone might exceed field capacity. In this simple procedure it is assumed that the soil water content is at θ_{FC} within the same day of the wetting event, so that the depletion $D_{r,\ i}$ in Equation 85 becomes zero. Therefore, following heavy rain or irrigation

$$DP_i = (P_i - RO_i) + I_i - ET_{c,i} - D_{r,\ i-1} \geq 0 \qquad (88)$$

As long as the soil water content in the root zone is below field capacity (i.e., $D_{r,\ i} > 0$), the soil will not drain and $DP_i = 0$.

The DP_i term in Equations 85 and 88 is not to be confused with the $DP_{e,i}$ term used in Equations 77 and 79 for the evaporation layer. Both terms can be calculated at the same time, but are independent of one another.

FORECASTING OR ALLOCATING IRRIGATIONS

Irrigation is required when rainfall is insufficient to compensate for the water lost by evapotranspiration. The primary objective of irrigation is to apply water at the right period and in the right amount. By calculating the soil water balance of the root zone on a daily basis (Equation 85), the timing and the depth of future irrigations can be planned. To avoid crop water stress, irrigations should be applied before or at the moment when the readily available soil water is depleted ($D_{r,i} \leq$ RAW). To avoid deep percolation losses that may leach relevant nutrients out of the root zone, the net irrigation depth should be smaller than or equal to the root zone depletion ($I_i \leq D_{r,i}$).

Example 38 illustrates the application of a water balance of the root zone to predict irrigation dates to avoid water stress. The example utilizes various calculations for K_e from Example 35. A complete "spreadsheet" that includes all necessary calculations for predicting both irrigation schedules and to predict $K_c = K_{cb} + K_e$ for daily timesteps is presented in Annex 8.

EXAMPLE 38
Irrigation scheduling to avoid crop water stress

Plan the irrigation applications for Example 35. It is assumed that:

- irrigations are to be applied when RAW is depleted,
- the depletion factor (p) is 0.6,
- all irrigations and precipitations occur early in the day,
- the depth of the root zone (Z_r) on day 1 is 0.3 m and increases to 0.35 m by day 10,
- the root zone depletion at the beginning of day 1 ($D_{r,i-1}$) is RAW.

From Eq. 82 TAW = 1 000 (0.23 - 0.10) $Z_{r,i}$ = 130 $Z_{r,i}$ [mm]

From Eq. 83 RAW = 0.6 TAW = 78 $Z_{r,i}$ [mm]

On day 1, when Z_r = 0.3 m: $D_{r,i-1}$ = RAW = 78 (0.3) = 23 mm

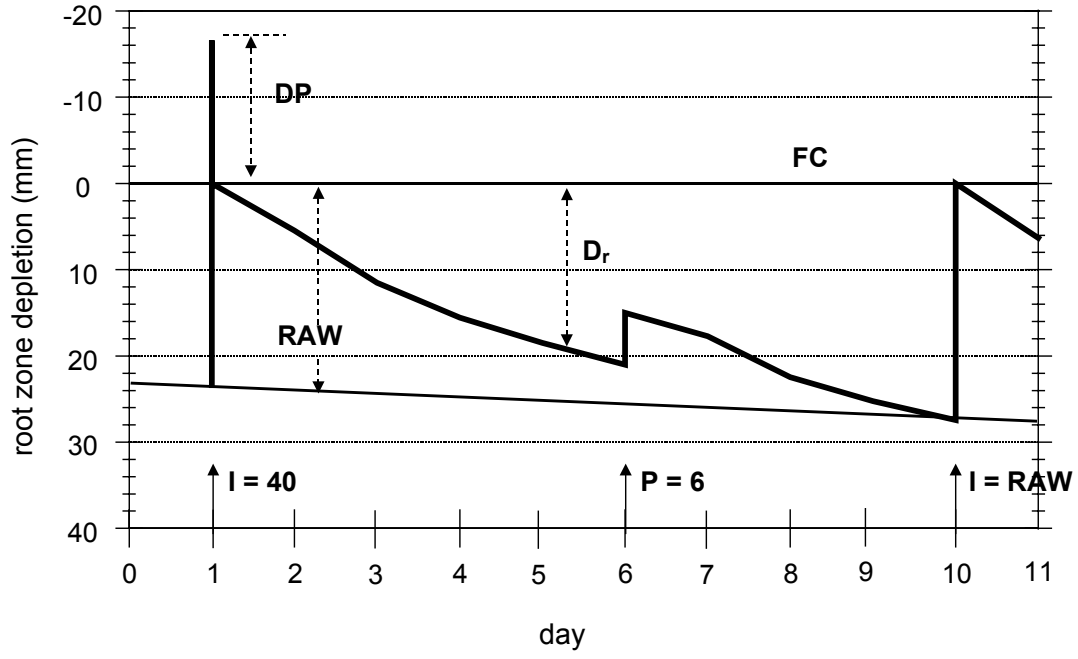

(1) Day	(2) ET_o	(3) Z_r	(4) RAW	(5) $D_{r,i}$ start	(6) P-RO	(7) I	(8) K_s	(9) K_{cb}	(10) K_e	(11) K_c	(12) ET_c	(13) DP	(14) $D_{r,i}$ end
	mm/d	m	mm	mm	mm	mm					mm	mm	mm
start	-	-	-	-	-	-	-	-	-	-	-	-	23
1	4.5	0.30	23	0	0	40	1	0.30	0.91	1.21	5.5	17	5
2	5.0	0.31	24	5	0	0	1	0.31	0.90	1.21	6.1	0	12
3	3.9	0.31	24	12	0	0	1	0.32	0.72	1.04	4.0	0	16
4	4.2	0.32	25	16	0	0	1	0.33	0.37	0.70	2.9	0	18
5	4.8	0.32	25	18	0	0	1	0.34	0.18	0.52	2.5	0	21
6	2.7	0.33	26	15	6	0	1	0.36	0.64	1.00	2.7	0	18
7	5.8	0.33	26	18	0	0	1	0.37	0.45	0.82	4.7	0	22
8	5.1	0.34	26	22	0	0	1	0.38	0.17	0.55	2.8	0	25
9	4.7	0.34	27	25	0	0	1	0.39	0.08	0.47	2.2	0	27
10	5.2	0.35	27	0	0	27	1	0.40	0.81	1.21	6.3	0	6

(1) Day number.
(2) From Example 35.
(3) Z_r is given (interpolated between 0.3 m on day 1 and 0.35 m on day 10).
(4) Eq. 83.
(5) $D_{r,i\ start}$ (root zone depletion at the beginning of the day)

If precipitation and irrigation occur early in the day then

$$D_{r,i\ start} = \text{Max}(D_{r,i-1\ end} - I - (P-RO), \text{or } 0)$$

If precipitation and irrigation occur late in the day, then

$$D_{r,i\ start} = D_{r,i-1end}$$

where $D_{r,i-1end}$ is taken from column 14 of previous day

Since the depth of the root zone increases each day, the water content of the subsoil (θ_{sub}) has to be considered to update $D_{r,i}$

$$D_{r,i} = D_{r,i-1} + 1\,000\ (\theta_{FC} - \theta_{sub,i-1})\ \Delta Z_{r,I}$$

In the example it is assumed that θ_{sub} is at field capacity (due to prior overirrigation and excessive rainfall on previous days). Therefore, a combination of the equations for $D_{r,i}$ can be utilized.

(6) From Example 35.
(7) Irrigation is required when $D_{r,i} \geq$ RAW.
On day 1, the irrigation depth (infiltrating the soil) is given (from Example 35: I = 40 mm)
On day 10, another irrigation is required. An irrigation with a net depth of 27 mm refills the root zone and avoids water loss by deep percolation (DP = 0 mm).
(8) Eq. 84, where $K_s = 1$ for $D_{r,i} \leq$ RAW.
(9) From Example 35.
(10) Day 1 to 9: From Example 35.
Day 10: Following the extra irrigation early in the day, the topsoil will be wet and K_r is 1 or from Eq. 71: $K_e = (1.21 - 0.40) = 0.81$.
(11) $K_c = K_s\ K_{cb} + K_e$.
(12) Eq. 80.
(13) Eq. 88, where $D_{r,i-1}$ is taken from column 14 of previous day.
(14) $D_{r,i}$ (root zone depletion at end of one day) = the starting $D_{r,i}$ at the beginning of the next day (see footnote 5). From Eq. 85, where $D_{r,i-1}$ is taken from column 14 of previous day.

EFFECTS OF SOIL SALINITY

Salts in the soil water solution can reduce evapotranspiration by making soil water less "available" for plant root extraction. Salts have an affinity for water and hence additional force is required for the crop to extract water from a saline soil. The presence of salts in the soil water solution reduces the total potential energy of the soil water solution. In addition, some salts cause toxic effects in plants and can reduce plant metabolism and growth. A function is presented here that predicts the reduction in evapotranspiration caused by salinity of soil water. The function is derived by combining yield-salinity equations from the FAO Irrigation and Drainage Paper N°29 with yield-ET equations from FAO Irrigation and Drainage Paper N°33. The resulting equation provides a first approximation of the reduction in evapotranspiration expected under various salinity conditions.

There is evidence that crop yield and transpiration are not as sensitive to low osmotic potential as they are to low matric potential. Under saline conditions, many plants are able to partially compensate for low osmotic potential of the soil water by building up higher internal solute contents. This is done by absorbing ions from the soil solution and by synthesizing organic osmolytes. Both of these reactions reduce the impact of osmotic potential on water availability. However, synthesis of organic osmolytes does require expenditure of metabolic energy. Therefore plant growth is often reduced under saline conditions. The reduced plant growth impacts transpiration by reducing ground cover and is sometimes additionally due to partial stomatal closure.

Other impacts of salts in the soil include direct sodium and chloride toxicities and induced nutrient deficiencies. These deficiencies reduce plant growth by reducing the rate of leaf elongation, the enlargement, and the division of cells in leaves. The modality depends on the method of irrigation. With sprinkler irrigation, adsorption of sodium and chloride through the leaf can result in toxic conditions for all crop species. With surface or trickle irrigaiton, direct toxic conditions generally occur only in vine and tree crops; however, high levels of sodium can induce calcium deficieincies for all crop species.

Since salt concentration changes as the soil water content changes, soil salinity is normally measured and expressed on the basis of the electrical conductivity of the saturation extract of the soil (EC_e). The EC_e is defined as the electrical conductivity of the soil water solution after the addition of a sufficient quantity of distilled water to bring the soil water content to saturation. EC_e is typically expressed in deciSiemens per meter (dS m^{-1}). Under optimum management conditions, crop yields remain at potential levels until a specific, threshold electrical conductivity of the saturation soil water extract ($EC_{e\ threshold}$) is reached. If the average EC_e of the root zone increases above this critical threshold value, the yield is presumed to begin to decrease linearly in proportion to the increase in salinity. The rate of decrease in yield with increase in salinity is usually expressed as a slope, b, having units of % reduction in yield per dS/m increase in EC_e.

All plants do not respond to salinity in a similar manner; some crops can produce acceptable yields at much higher soil salinity levels than others. This is because some crops are better able to make the needed osmotic adjustments that enable them to extract more water from a saline soil, or they may be more tolerant of some of the toxic effects of salinity. Salt tolerance for many agricultural crops are provided in the FAO Irrigation and Drainage Papers No. 33 and 48. The $EC_{e,threshold}$ and slope b from these sources are listed in Table 23.

As can be observed from the data in Table 23, there is an 8 to 10-fold range in salt tolerance of agricultural crops. The effect of soil salinity on yield and crop evapotranspiration is hence crop specific.

The $EC_{e,\ threshold}$ and b parameters in Table 23 were determined primarily in research experiments using nearly steady-state irrigation where soil water contents were maintained at levels close to field capacity. However, under most types of irrigation scheduling for sprinkler and surface irrigation, the soil water content is typically depleted to well below field capacity, so that the EC of the soil water solution, EC_{sw}, increases prior to irrigation, even though the EC of the saturation extract does not change. The increased salt concentration in the soil water solution reduces the osmotic potential of the soil water solution (it becomes more negative), so that the plant must expend more metabolic energy and may exert more mechanical force to absorb water. In addition, metabolic and toxic effects of salts on plants may become more pronounced as the soil dries and concentrations increase. However, the variation in soil water content during an irrigation interval has not been found to strongly influence crop evapotranspiration. This is because of the rise of soil water content to levels that are above that experienced under steady state irrigation early in a long irrigation interval. There is a similar, counteractive decrease in soil water content later in a long irrigation interval. In addition, the distribution of salts in the root zone under low frequency irrigation can reduce salinity impacts during the first portion of the irrigation interval. Also, under high frequency irrigation of the soil surface, soil evaporation losses are higher. Consequently, given the same application depth, the leaching fraction is reduced. For these reasons, the length of irrigation interval and the change in EC of soil water during the interval have usually not been found to be factors in the reduction of ET, given that the same depths of water are infiltrated into the root zone over time.

In some cases, increased evaporation under high frequency irrigation of the soil surface can counteract reductions in K_c caused by high EC_e of the root zone. Under these conditions, the total K_c and ET_c are not very different from the non-saline, standard conditions under less frequent irrigation, even though crop yields and crop transpiration are reduced. Because of this, under saline conditions, the K_s reducing factor should only be applied with the dual K_c approach.

In review articles on impacts of salinity on crop production, Letey *et al*. (1985) and Shalhevet (1994) concluded that effects of soil salinity and water stress are generally additive in their impacts on crop evapotranspiration. Therefore, the same yield-ET functions may hold for both water shortage induced stress and for salinity induced stress.

YIELD-SALINITY RELATIONSHIP

A widely practiced approach for predicting the reduction in crop yield due to salinity has been described in the FAO Irrigation and Drainage Paper N°29. The approach presumes that, under optimum management conditions, crop yields remain at potential levels until a specific, threshold electrical conductivity of the soil water solution is reached. When salinity increases beyond this threshold, crop yields are presumed to decrease linearly in proportion to the increase in salinity. The soil water salinity is expressed as the electrical conductivity of the saturation extract, EC_e. In equation form, the procedure followed in FAO Irrigation and Drainage Paper N°29 is:

$$\frac{Y_a}{Y_m} = 1 - \left(EC_e - EC_{e\ threshold}\right)\frac{b}{100} \quad (89)$$

for conditions where $EC_e > EC_{e\ threshold}$ where:

Y_a	actual crop yield
Y_m	maximum expected crop yield when $EC_e < EC_{e\ threshold}$
EC_e	mean electrical conductivity of the saturation extract for the root zone [dS m^{-1}]
$EC_{e\ threshold}$	electrical conductivity of the saturation extract at the threshold of EC_e when crop yield first reduces below Y_m [dS m^{-1}]
b	reduction in yield per increase in EC_e [%/(dS m^{-1})]

Values for $EC_{e\ threshold}$ and b have been provided in the FAO Irrigation and Drainage Paper N°29 and 48 and are listed in Table 23 for many agricultural crops.

Salinity-yield data from the FAO Irrigation and Drainage papers Nos. 29 and 48 were mostly from studies where soil water content was held at about –3 m potential (-30 kPa) or higher at the 0.3 to 0.6 m depth, depending on the crop. However, these papers indicate that for most crops, the data are transferable to typical field situations where the readily available soil water (RAW) is depleted between irrigations.

YIELD-MOISTURE STRESS RELATIONSHIP

A simple, linear crop-water production function was introduced in the FAO Irrigation and Drainage Paper N°33 to predict the reduction in crop yield when crop stress was caused by a shortage of soil water:

$$\left(1 - \frac{Ya}{Y_m}\right) = K_y\left(1 - \frac{ET_{c\ adj}}{ET_c}\right) \quad (90)$$

where:
K_y a yield response factor [-]
$ET_{c\ adj}$ adjusted (actual) crop evapotranspiration [mm d^{-1}]
ET_c crop evapotranspiration for standard conditions (no water stress) [mm d^{-1}]

K_y is a factor that describes the reduction in relative yield according to the reduction in ET_c caused by soil water shortage. In FAO N°33, K_y values are crop specific and may vary over the growing season. In general, the decrease in yield due to water deficit during the vegetative and ripening period is relatively small, while during the flowering and yield formation periods it will be large. Values for K_y for individual growth periods and for the complete growing season have been included in the FAO Irrigation and Drainage Paper N°33. Seasonal values for K_y are summarized in Table 24.

COMBINED SALINITY-ET REDUCTION RELATIONSHIP

No water stress (D_r < RAW)

When salinity stress occurs without water stress, Equations 89 and 90 can be combined and solved for an equivalent K_s, where $K_s = ET_{c\ adj}/ET_c$:

$$K_s = 1 - \frac{b}{K_y\ 100}\left(EC_e - EC_{e\,threshold}\right) \qquad (91)$$

for conditions when $EC_e > EC_{e\ threshold}$ and soil water depletion is less than the readily available soil water depth ($D_r < RAW$). D_r and RAW are defined in the previous section.

With water stress ($D_r > RAW$)

When soil water stress occurs in addition to salinity stress, Equation 84 in Chapter 8 and Equations 89 and 90 are combined to yield:

$$K_s = \left(1 - \frac{b}{K_y\ 100}\left(EC_e - EC_{e\,threshold}\right)\right)\left(\frac{TAW - D_r}{TAW - RAW}\right) \qquad (92)$$

for conditions when $EC_e > EC_{e\ threshold}$ and $D_r > RAW$. Figure 44 shows the impact of salinity reduction on K_s as salinity increases. Note that the approach presumes that RAW (and p) do not change with increasing salinity. This may or may not be a good assumption for some crops.

Limitations

Because the impact of salinity on plant growth and yield and on crop evapotranspiration is a time-integrated process, generally only the seasonal value for K_y is used to predict the reduction in evapotranspiration. There are K_y values in FAO Irrigation and Drainage paper N°33 for only about 23 crops. The seasonal values for K_y from paper N°33 are summarized in Table 24. For many crops, the seasonal K_y is nearly 1. For crops where K_y is unknown, the user may use $K_y = 1$ in Equations 91 and 92 or may select the K_y for a crop type that has similar behaviour.

Equations 91 and 92 are suggested as only approximate estimates of salinity impacts on ET, and represent general effects of salinity on evapotranspiration as occurring over an extended period of time (as measured in weeks or months). These equations are not expected to be accurate for predicting ET_c for specific days. Nor do they include other complicating effects such as specific ion toxicity. Application of equations 91 and 92 presumes that the EC_e represents the average EC_e for the root zone.

The equations presented may not be valid at high salinitiy, where the linear relationships between EC_e, crop yield and K_s may not hold. The use of Equations 91 and 92 should usually be restricted to $EC_e < EC_{threshold} + 50/b$. In addition, the equations predict $Y_a = 0$ before $K_s = 0$ when $K_y > 1$ and vice versa.

As indicated earlier, reduction in ET_c in the presence of soil salinity is often partially caused by reduced plant size and fraction of ground cover. These effects are largely included in the coefficient values in Table 23. Therefore, where plant growth is affected by salinity and Equations 91 and 92 are applied, no other reductions in K_c are required, for example using LAI or fraction of ground cover, as described in Chapter 9.

TABLE 23
Salt tolerance of common agricultural crops expressed as electrical conductivity of the soil saturation extract at the threshold when crop yield first reduces below the full yield potential ($EC_{e,\ threshold}$) and as the slope (b) of reduction in crop yield with increasing salinity beyond $EC_{e,\ threshold}$

Crop[1]	$EC_{e,\ threshold}$[2] (dS m^{-1})[3]	b[4] (% / dS m^{-1})	Rating[5]
a. Small vegetables			
Broccoli	2.8	9.2	MS
Brussels sprouts	1.8	9.7	MS
Cabbage	1.0–1.8	9.8-14.0	MS
Carrots	1.0	14.0	S
Cauliflower	1.8	6.2	MS
Celery	1.8-2.5	6.2-13.0	MS
Lettuce	1.3-1.7	12.0	MS
Onions	1.2	16.0	S
Spinach	2.0-3.2	7.7-16.0	MS
Radishes	1.2-2.0	7.6-13.0	MS
b. Vegetables - Solanum Family (*Solanaceae*)			
Egg Plant	-	-	MS
Peppers	1.5-1.7	12.0-14.0	MS
Tomato	0.9-2.5	9.0	MS
c. Vegetables Cucumber Family (*Cucurbitaceae*)			
Cucumber	1.1-2.5	7.0-13.0	MS
Melons	-	-	MS
Pumpkin, winter squash	1.2	13.0	MS
Squash, Zucchini	4.7	10.0	MT
Squash (scallop)	3.2	16.0	MS
Watermelon	-	-	MS
d. Roots and Tubers			
Beets, red	4.0	9.0	MT
Parsnip	-	-	S
Potato	1.7	12.0	MS
Sweet potato	1.5-2.5	10.0	MS
Turnip	0.9	9.0	MS
Sugar beet	7.0	5.9	T
e. Legumes (*Leguminosae*)			
Beans	1.0	19.0	S
Broadbean (faba bean)	1.5-1.6	9.6	MS
Cowpea	4.9	12.0	MT
Groundnut (Peanut)	3.2	29.0	MS
Peas	1.5	14.0	S
Soybeans	5.0	20.0	MT

[1] The data serve only as a guideline - Tolerance vary depending upon climate, soil conditions and cultural practices. Crops are often less tolerant during germination and seedling stage.

[2] $EC_{e,\ threshold}$ means average root zone salinity at which yield starts to decline

[3] Root zone salinity is measured by electrical conductivity of the saturation extract of the soil, reported in deciSiemens per metre (dS m^{-1}) at 25°C

[4] b is the percentage reduction in crop yield per 1 dS/m increase in EC_e beyond EC_e threshold

[5] Ratings are: T = Tolerant, MT = Moderately Tolerant, MS = Moderately Sensitive and S = Sensitive

Table 23 Continued

Crop	$EC_{e,\ threshold}$ (dS m^{-1})	b (% / dS m^{-1})	Rating
f. Perennial Vegetables (with winter dormancy and initially bare or mulched soil)			
Artichokes	-	-	MT
Asparagus	4.1	2.0	T
Mint	-	-	-
Strawberries	1.0-1.5	11.0-33.0	S
g. Fibre crops			
Cotton	7.7	5.2	T
Flax	1.7	12.0	MS
h. Oil crops			
Casterbean	-	-	MS
Safflower	-	-	MT
Sunflower	-	-	MS
i. Cereals			
Barley	8.0	5.0	T
Oats	-	-	MT
Maize	1.7	12.0	MS
Maize, sweet (sweet corn)	1.7	12.0	MS
Millet	-	-	MS
Sorghum	6.8	16.0	MT
Rice[6]	3.0	12.0	S
Wheat (*Triticum aestivum*)	6.0	7.1	MT
Wheat, semidwarf (*T. aestivum*)	8.6	3.0	T
Wheat, durum (*Triticum turgidum*)	5.7-5.9	3.8-5.5	T
j. Forages			
Alfalfa	2.0	7.3	MS
Barley (forage)	6.0	7.1	MT
Bermuda	6.9	6.4	T
Clover, Berseem	1.5	5.7	MS
Clover (alsike, ladino, red, strawberry)	1.5	12.0	MS
Cowpea (forage)	2.5	11.0	MS
Fescue	3.9	5.3-6.2	MT
Foxtail	1.5	9.6	MS
Hardinggrass	4.6	7.6	MT
Lovegrass	2.0	8.4	MS
Maize (forage)	1.8	7.4	MS
Orchardgrass	1.5	6.2	MS
Rye-grass (perennial)	5.6	7.6	MT
Sesbania	2.3	7.0	MS
Sphaerophysa	2.2	7.0	MS
Sudangrass	2.8	4.3	MT
Trefoil, narrowleaf birdsfoot	5.0	10.0	MT
Trefoil, big	2.3	19.0	MS
Vetch, common	3.0	11.0	MS
Wheatgrass, tall	7.5	4.2	T
Wheatgrass, fairway crested	7.5	6.9	T
Wheatgrass, standard crested	3.5	4.0	MT
Wildrye, beardless	2.7	6.0	MT
k. Sugar cane	1.7	5.9	MS

[6] Because paddy rice is grown under flooded conditions, values refer to the electrical conductivity of the soil water while the plants are submerged

Table 23 Continued

Crop	$EC_{e,\ threshold}$ (dS m^{-1})	b (% / dS m^{-1})	Rating
l. Tropical Fruits and Trees			
Banana	-	-	MS
Coffee	-	-	-
Date Palms	4.0	3.6	T
Palm trees	-	-	T
Pineapple (multi-year crop)	-	-	MT
Tea	-	-	-
m. Grapes and berries			
Blackberry	1.5	22.0	S
Boysenberry	1.5	22.0	S
Grapes	1.5	9.6	MS
Hops	-	-	-
n. Fruit trees			
Almonds	1.5	19.0	S
Avocado	-	-	S
Citrus (Grapefruit)	1.8	16.0	S
Citrus (Orange)	1.7	16.0	S
Citrus (Lemon)	-	-	S
Citrus (Lime)	-	-	S
Citrus (Pummelo)	-	-	S
Citrus (Tangerine)	-	-	S
Conifer trees	-	-	MS/MT
Deciduous orchard			
- Apples	-	-	S
- Peaches	1.7	21.0	S
- Cherries	-	-	S
- Pear	-	-	S
- Apricot	1.6	24.0	S
- Plum, prune	1.5	18.0	S
- Pomegranate	-	-	MT
Olives	-	-	MT

Primary sources :
Ayers and Westcot, 1985. FAO Irrigation and Drainage Paper N° 29. Water quality for agriculture ; Rhoades, Kandiah and Mashali, 1992. FAO Irrigation and Drainage Paper N° 48. The use of saline waters for crop productions.

Application

Under steady state conditions, the value for EC_e can be predicted as a function of EC of the irrigation water (EC_{iw}) and the leaching fraction, using a standard leaching formula. For example, the FAO-29 leaching formula $LR = EC_{iw} / (5\ EC_e - EC_{iw})$ predicts the leaching requirement when approximately a 40-30-20-10 percent water extraction pattern occurs from the upper to lower quarters of the root zone prior to irrigation. EC_{iw} is the electrical conductivity of the irrigation water. From this equation, EC_e is estimated as:

$$EC_e = \frac{1 + LF}{LF} \frac{EC_{iw}}{5} \tag{93}$$

TABLE 24
Seasonal yield response functions from FAO Irrigation and Drainage Paper No. 33.

Crop	K_y	Crop	K_y
Alfalfa	1.1	Potato	1.1
Banana	1.2-1.35	Safflower	0.8
Beans	1.15	Sorghum	0.9
Cabbage	0.95	Soybean	0.85
Citrus	1.1-1.3	Spring Wheat	1.15
Cotton	0.85	Sugarbeet	1.0
Grape	0.85	Sugarcane	1.2
Groundnet	0.70	Sunflower	0.95
Maize	1.25	Tomato	1.05
Onion	1.1	Watermelon	1.1
Peas	1,15	Winter wheat	1.05
Pepper	1.1		

where LF, the actual leaching fraction, is used in place of LR, the leaching requirement. Equation 93 predicts $EC_e = 1.5\ EC_{iw}$ under conditions where a 15-20 percent leaching fraction is employed. Other leaching fraction equations can be used in place of the FAO-29 equation to fit local characteristics. Equation 93 is only true if the irrigation water quality and the leaching fraction are constant over the growing season. Time is required to attain a salt equilibrium in the soil. If there are important winter rains of high quality water and often excellent leaching, the salt balance in the soil will be quite different at the beginning of the season and with a lower average EC_e of the root zone than would be predicted from Equation 93. An appropriate local calibration of Equation 93 is desirable under these particular conditions.

FIGURE 44
The effect of soil salinity on the water stress coefficient K_s

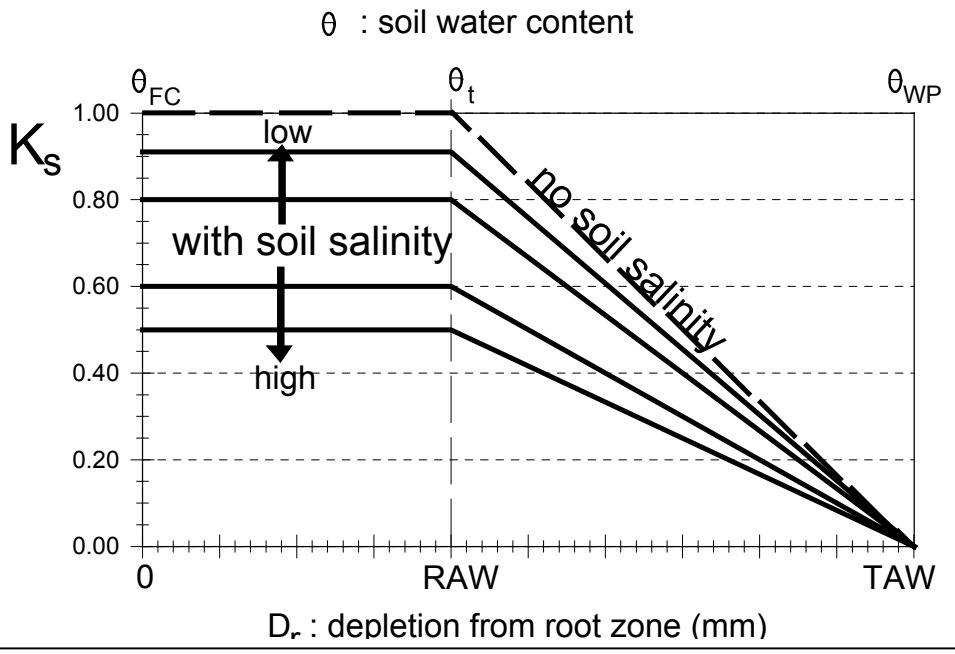

EXAMPLE 39
Effect of soil salinity on crop evapotranspiration

A field of beans is cultivated on a silt loam soil and is irrigated during the midseason period using water having salinity EC_{iw} = 1 dS m^{-1}. A 15 percent leaching fraction is employed. The $EC_{e,threshold}$ and slope from Table 23 are 1.0 dS m^{-1} and 19 %/(dS m^{-1}) respectively. The seasonal K_y from FAO Irrigation and Drainage Paper No 33 and Table 24 for beans is K_y = 1.15. Compare the effect on crop evapotranspiration for various levels of soil water depletion in the root zone under saline and nonsaline conditions. The TAW and RAW for the bean crop are 110 and 44 mm (for p = 0.4).

Since the leaching fraction is 0.15, EC_e is estimated from Equation 93 as $EC_e = 1.5\ EC_w = 1.5\ (1) = 1.5$ dS m^{-1}. The K_s in the presence of salinity stress and absence of moisture stress is:

$$K_s = \left(1 - \frac{b}{K_y\ 100}\left(EC_e - EC_{e\,threshold}\right)\right) = \left(1 - \frac{19}{1.15(100)}(1.5 - 1.0)\right) = 0.92$$

The K_s in the presence of moisture stress, but in the absence of salinity stress is:

$$K_s = \left(\frac{TAW - D_r}{TAW - RAW}\right) = \left(\frac{110 - D_r}{100 - 44}\right) = \left(\frac{110 - D_r}{66}\right)$$

The K_s in the presence of both moisture stress and salinity stress is:

$$K_s = \left(1 - \frac{b}{K_y\ 100}\left(EC_e - EC_{e\,threshold}\right)\right)\left(\frac{TAW - D_r}{TAW - RAW}\right) = 0.92\left(\frac{110 - D_r}{66}\right)$$

The effect on crop evapotranspiration for various soil water depletions in the root zone (D_r) are:

D_r (mm)	K_s no soil salinity		K_s with soil salinity (EC_e = 1.5 dS m^{-1}) (Eq. 92)		Additional reduction in potential ET_c due to salinity
0	1.00	no reduction in ET_c	0.92	8% reduction in ET_c	8%
35	1.00	no reduction in ET_c	0.92	8% reduction in ET_c	8%
40	1.00	no reduction in ET_c	0.92	8% reduction	8%
44	1.00	no reduction in ET_c	0.92	8% reduction	8%
50	0.91	9% reduction	0.83	17% reduction	8%
60	0.76	24% reduction	0.69	31% reduction	7%
70	0.61	39% reduction	0.56	44% reduction	5%
80	0.45	55% reduction	0.42	58% reduction	3%
90	0.30	70% reduction	0.28	72% reduction	2%
100	0.15	85% reduction	0.14	86% reduction	1%
110	0.00	ET_c = 0	0.00	ET_c = 0	--

Chapter 9

ET_c for natural, non-typical and non-pristine vegetation

Non-typical refers to types or arrangements of agricultural crops that are not listed or described in Tables 12 and 17. Non-pristine vegetation is defined, in the usage here, as vegetation having less than perfect growing conditions or stand characteristics (i.e., relatively poorer conditions of density, height, leaf area, fertility, or vitality) as compared to 'pristine' conditions.

The approach whereby a crop is characterized by a crop coefficient, K_c, and the crop evapotranspiration is given by the product of K_c and the reference evapotranspiration ET_o, provides a simple and convenient way of also characterizing the evapotranspiration from natural vegetation and for non-typical cultivation practices. This chapter presents procedures for estimating K_c values for natural vegetation and for agricultural vegetation for which K_c values are not available.

CALCULATION APPROACH

As described in Figure 27, the first step in the K_cET_o approach is the estimation of lengths of growth stages. This also applies to natural and other vegetation. The next step is the development of crop coefficient curves that represent the ratios of ET_c to ET_o during the various growth stages of the vegetation.

Initial growth stage

The procedure to estimate crop coefficients for the initial growth stage for natural, non-typical and non-pristine vegetation is identical to that described in Chapter 6 (single crop coefficient $K_{c\ ini}$) or Chapter 7 (dual crop coefficient, $K_{cb\ ini} + K_e$). The crop coefficient in this stage is primarily determined by the frequency with which the soil is wetted.

Mid and late season stages

The K_c during the mid-season period ($K_{c\ mid}$ and $K_{cb\ mid}$) and to a lesser extent the K_c during the late season period differ from that described in previous chapters. As the ground cover for natural and non-pristine vegetation is often reduced, the K_c is affected to a large extent by the frequency of precipitation and/or irrigation and by the amount of leaf area and ground cover.

Dual crop coefficient approach

The determination of K_c for natural, non-typical or non-pristine vegetation should ordinarily follow the approach described in Chapter 7 whereby separate transpiration (K_{cb}) and evaporation (K_e) coefficients are used. The effects of evaporation from the soil surface can be directly estimated as such.

Two procedures that can be used to adjust the basal crop coefficient ($K_{cb\ mid\ adj}$) for sparse vegetation are presented in this section. In these approaches, $K_{cb\ mid\ adj}$ is estimated either from LAI (Equation 97) or from effective ground cover (Equation 98). After the determination of $K_{cb\ mid\ adj}$, the soil evaporation coefficient, K_e, should be determined to obtain the crop coefficient for the mid-season stage: $K_{c\ mid\ adj} = K_{cb\ mid\ adj} + K_e$. Procedures for calculating K_e are presented in Chapter 7.

Even where the estimated $K_{cb\ mid\ adj}$ is small, the total $K_{c\ adj}$ (= $K_{cb\ adj} + K_e$) following precipitation may sometimes be as high or higher than the K_c for pristine vegetation due to surface evaporation from among sparse vegetation.

Single crop coefficient approach

When the single crop coefficient K_c of Chapter 6 is used, the average effects of soil wetting are incorporated into a general mean K_c. Some guidelines for the estimation of $K_{c\ adj}$ are given in the following sections. The single crop coefficient can also be derived from the adjusted K_{cb} by considering the frequency of soil wetting, i.e., during the midseason period, $K_{c\ adj} = K_{cb\ adj} + 0.05$ for infrequent wetting and $K_{cb\ adj} + 0.10$ for wettings of up to once a week. For more frequent wettings, the dual crop coefficient approach should be used.

Alternatively, Equations 97 and 98 can be used to determine K_c instead of K_{cb}. Then, $K_{c\ min}$ in Equations 97 and 98 can be set equal to $K_{c\ ini}$, where $K_{c\ ini}$ is estimated from Figure 29 or 30. The use of $K_{c\ ini}$ incorporates effects of soil evaporation and therefore serves as a lower limit on the estimate for $K_{c\ mid}$.

Water stress conditions

Where rainfall or irrigation is low, water stress might be induced and the evapotranspiration will drop below the standard crop evapotranspiration, ET_c. The reduction in the value for K_c under conditions of low soil water availability is determined using the stress coefficient K_s as described in Chapter 8.

MID-SEASON STAGE - ADJUSTMENT FOR SPARSE VEGETATION

Adjustment from simple field observations

As a rough approximation for K_c during the mid-season stage for crops that usually nearly completely shade the soil under pristine conditions, but where cover is reduced due to disease, stress, pests, or planting density, the values for $K_{c\ mid}$ and $K_{cb\ mid}$ can be reduced by a factor depending on the actual vegetation development:

$$K_{c\ adj} = K_c - A_{cm} \qquad (94)$$

where K_c the K_c from Table 12 ($K_{c\ mid}$) or 17 ($K_{cb\ mid}$) after adjusting it for climate (Equation 62 or 70),

$K_{c\ adj}$ the adjusted K_c ($K_{c\ mid\ adj}$ or $K_{cb\ mid\ adj}$).

The K_c adjustment using Equation 94 does not apply when crops are frequently wetted and increased soil evaporation compensates for the reduced ground cover. Under these conditions Equation 94 should be applied only to K_{cb}.

The adjustment coefficient, A_{cm}, is estimated from:

$$A_{cm} = 1 - \left[\frac{LAI}{LAI_{dense}}\right]^{0.5} \quad (95)$$

where LAI is the actual leaf area index (Box 17) and LAI_{dense} is the leaf area index expected for the same crop under normal, standard crop management practices. The values for LAI in the above equation can be replaced by values for the ground cover fraction (f_c):

$$A_{cm} = 1 - \left[\frac{f_c}{f_{c\ dense}}\right]^{0.5} \quad (96)$$

EXAMPLE 40
First approximation of the crop coefficient for the mid-season stage for sparse vegetation

A tomato crop was grown at Davis, California, United States in 1980 and only developed 50% ground cover during the midseason period (Pruitt et al., 1984). The height of the tomato crop was 0.75 m. The typical percentage of ground cover for tomatoes at effective full cover at Davis is 85 to 90% and corresponds to the $K_{cb\ mid}$ listed in Table 17 for tomatoes. The mean values for wind speed and minimum relative humidity during the midseason period were u_2 = 1.1 m/s and RH_{min} = 30%. The latitude at Davis is 38.5° N and the midpoint of the midseason occurs on July 20. What is an adjusted $K_{cb\ mid}$ for tomatoes that reflects the 50% ground cover condition?

From Tables 12 and 17, $K_{c\ mid}$ = 1.2 and $K_{cb\ mid}$ = 1.15.

Following adjustments for climate (Eq. 62 and Eq. 70) where u_2 = 1.1 m/s, RH_{min} = 30% and mean crop height = 0.75 m,

$$K_c = K_{c,Table} + [0.04(1.1\text{-}2)\text{-}0.004(30\text{-}45)](0.75/3)^{0.30} = K_{c,Table} + 0.02$$

yields, $K_{c\ mid}$ = 1.22 and $K_{cb\ mid}$ = 1.17.

The ground cover fraction implied in the tabulated values for tomatoes grown under pristine conditions is about 85% ($f_{c\ dense}$ = 0.85). For a sparse tomato crop where f_c = 0.50,

From Eq. 96 $A_{cm} = 1 - (0.50/0.85)^{0.5} = 0.23$

The $K_{cb\ mid\ adj}$ and $K_{c\ mid\ adj}$ for 50% ground cover is

(from Eq. 94) $K_{cb\ mid\ adj} = 1.17 - 0.23 = 0.94$

$K_{c\ mid\ adj} = 1.22 - 0.23 = 0.99$

Compare the results with Example 42 where a more precise derivation of $K_{cb\ mid\ adj}$ is made.

As a first estimate, the crop coefficient is expected to be 20% lower than the value under pristine conditions.

Estimation of $K_{cb\ mid}$ from Leaf Area Index (LAI)

Natural vegetation typically has less leaf area or fraction of ground cover than does agricultural vegetation that has been developed for full ground cover and for soil water conditions favouring vigorous growth. This is especially true in semi-arid and arid climates. The value for $K_{cb\ mid}$ for natural or non-pristine vegetation should be reduced when plant density and/or leaf area are lower than for full cover conditions (generally defined as when LAI ≥ 3). Where LAI can be

measured or approximated, a peak $K_{cb\ mid}$ for natural, non-typical or non-pristine agricultural vegetation can be approximated similar to a procedure used by Ritchie as:

$$K_{cb\ mid} = K_{c\ min} + (K_{cb\ full} - K_{c\ min})(1 - \exp[-0.7\,LAI]) \qquad (97)$$

where
- $K_{cb\ mid}$ estimated basal K_{cb} during the mid-season when plant density and/or leaf area are lower than for full cover conditions,
- $K_{cb\ full}$ estimated basal K_{cb} during the mid-season (at peak plant size or height) for vegetation having full ground cover or LAI > 3 (Equations 99 and 100),
- $K_{c\ min}$ the minimum K_c for bare soil ($K_{c\ min} \approx 0.15$ - 0.20),
- LAI actual leaf area index, defined as the area of leaves per area of underlying ground surface averaged over a large area. Only one side of leaves is counted [$m^2\ m^{-2}$].

Equation 97 is recommended for annual types of vegetation that are either natural or are in a non-pristine state due to sparse density or effects of some type of environmental stress on growth.

The relationship expressed in Equation 97 produces results similar to those suggested by Ritchie (1974). For LAI > 3, $K_{cb\ mid} \approx K_{cb\ full}$. The LAI used in Equation 97 should be the 'green' LAI representing only healthy leaves that are active in vapour transfer.

BOX 17
Measuring and estimating LAI

LAI can be measured directly by harvesting all green healthy leaves from vegetation over a measured or prescribed area, for example, 1 m^2 or 10 m^2, and then measuring and summing the areas of individual leaves using photometric methods or by measuring areas of several representative leaves, averaging, and then multiplying by the total number of leaves counted.

In the absence of measurements for LAI, LAI can be estimated for sparse, annual vegetation as:

$$LAI = LAI_{dense}\left[\frac{Population}{Population_{dense}}\right]^a$$

where
- LAI_{dense} LAI for the particular plant species under normal, 'dense' or pristine growing conditions. LAI_{dense} can be obtained from various physiological sources and textbooks on crops and vegetation.
- Population number of plants per unit area of soil surface under the actual growing conditions [No. m^{-2}].
- $Population_{dense}$ number of plants per unit area of soil surface under the 'dense' or pristine growing conditions [No. m^{-2}].
- a a = 0.5 when population is formed from vigorous growing plants; a = 1 when plants are less vigorous.

The 0.5 exponent in the equation simulates the tendency for vegetation to compensate for reduced stand density by increasing the size and total leaf areas for individual plants. Therefore, LAI does not fall in direct proportion to plant population. Under conditions where the plant size does not increase with reduced stand density, the 'a' exponent in the equation should be set to 1 (a = 1). These latter conditions may occur where soil fertility is poor or where soil salinity, soil water stress, or waterlogging inhibit both growth and stand density, so that the growth of individual plants is retarded.

Estimation of $K_{cb\ mid}$ from effective ground cover ($f_{c\ eff}$)

Where only estimates of the fraction of soil surface effectively covered by vegetation are available, the following approximation for $K_{cb\ mid\ adj}$ can be used:

$$K_{cb\ mid} = K_{c\ min} + \left(K_{cb\ full} - K_{c\ min}\right)\left(\min\left(1,\ 2\,f_c,\ \left(f_{c\ eff}\right)^{\left(\frac{1}{1+h}\right)} \right)\right) \qquad (98)$$

where
- $K_{cb\ mid}$ estimated basal K_{cb} during the mid-season when plant density and/or leaf area are lower than for full cover conditions,
- $K_{cb\ full}$ estimated basal K_{cb} during the mid-season (at peak plant size or height) for vegetation having full ground cover or LAI > 3 (see Equations 99 and 100),
- $K_{c\ min}$ the minimum K_c for bare soil (in the presence of vegetation) ($K_{c\ min} \approx$ 0.15 - 0.20),
- f_c observed fraction of soil surface that is covered by vegetation as observed from nadir (overhead) [0.01 - 1],
- $f_{c\ eff}$ the effective fraction of soil surface covered or shaded by vegetation [0.01-1] (see Box 18),
- h the plant height [m].

Stomatal conductance and water transport within plants may limit ET under conditions of sparse, tall vegetation. Under these conditions, $K_{cb\ mid}$ is limited by the "$2f_c$" term in Equation 98. Equation 98 applies well to trees and shrubs.

BOX 18
Measuring and estimating $f_{c\ eff}$

$f_{c\ eff}$ should normally represent the fraction of the soil surface that is shaded by vegetation. This value is generally larger than f_c, the actual fraction of the soil surface that is covered by vegetation as observed from directly overhead. The amount of shading represents the amount of solar radiation intercepted by plants for potential conversion into evapotranspiration. The total fraction of shading is a function of the sun angle and the horizontal size and shape of individual plants (or rows) relative to their height.

$f_{c\ eff}$ for 'rectangular' shaped canopies such as most agricultural plant rows can be approximated as:

$$f_{c\ eff} = f_c\left[1+\frac{HWR}{\tan(\eta)}\right] \qquad \leq 1$$

where
- f_c observed fraction of soil surface that is covered by vegetation as observed from nadir (overhead) [0.01 - 1],
- HWR height to width ratio of individual plants or groups of plants when viewed from the east or from the west [ ],
- $\tan(\eta)$ tangent of the mean angle of the sun, η, above the horizon during the period of maximum evapotranspiration (generally between 11.00 and 15.00 hours) [ ]. For most applications, η can be computed at solar noon (12.00 hours).

HWR is computed as:

$$HWR = \frac{h_{canopy}\,(\cos(\Gamma))}{Width}$$

where h_{canopy} mean vertical height of the canopy area of the plant [m],
$Width$ mean width of the canopy of a plant or group of plants (e.g., row) [m]
Γ angle of plant row from east-west direction [rad] (for east-west rows, $\Gamma = 0$; for north-south rows, $\Gamma = \pi/2$)

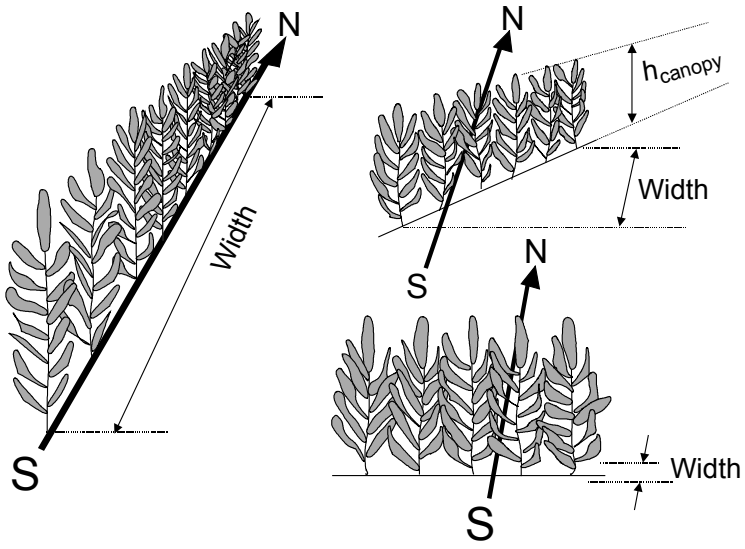

For north-south rows, the HWR would be zero, as $\cos(\pi/2) = 0$. This implies that rows of plants that run from north to south would have $f_{c\ eff} \approx f_c$ as all soil is exposed to the sun at various times of the day and as the shaded area is the same as the fraction of vegetation cover at midday.

For trees or vegetation that do not have canopies that extend to the ground, h_{canopy} does not include the lower trunk length, but only the active canopy. Therefore, in these situations, $h_{canopy} < h$ where h is mean plant height.

For round or spherical shaped canopies such as trees, $f_{c\ eff}$ can be estimated as:

$$f_{c\ eff} = \frac{f_c}{\sin(\eta)} \qquad \leq 1$$

where $\sin(\eta)$ is the sine of the mean angle of the sun, η, above the horizon during the period of maximum evapotranspiration (generally between 11.00 and 15.00) [ ]

Mean angle of the sun above the horizon during the period of maximum evapotranspiration (η)

The sine of η can be calculated for any specific time of day as:

$$\sin(\eta) = \sin(\varphi)\sin(\delta) + \cos(\varphi)\cos(\delta)\cos(\omega)$$

where φ latitude [rad] (negative for southern latitudes)
δ solar declination [rad] (Eq. 24)
ω solar time angle [rad] (Eq. 31)

Generally, $f_{c\ eff}$ can be calculated at solar noon (12.00), so that $\omega = 0$ and the above equation reduces to:

$$\sin(\eta) = \sin(\varphi)\sin(\delta) + \cos(\varphi)\cos(\delta)$$

The value for η can be obtained by taking the arcsine of the above equation.

Estimation of $K_{cb\ full}$

Agricultural crops:

Non-pristine agricultural crops represent crops that have not developed to their potential due to environmental stresses caused by soil water shortage, fertility, disease, grazing or insect damage or due to low plant density. The value for $K_{cb\ full}$ in Equations 97 and 98 can be taken as the $K_{cb\ mid}$ value listed for any "full-cover" crop ($f_{c\ eff} \sim 1$) in Table 17, after adjusting it for climate (Equation 70):

$$K_{cb\ full} = K_{cb\ mid,Table} + [0.04\,(u_2 - 2) - 0.004\,(RH_{min} - 45)]\left(\frac{h}{3}\right)^{0.3} \qquad (99)$$

where u_2 mean value for wind speed at 2 m height during the mid-season [m s^{-1}],
RH_{min} mean value for minimum daily relative humidity during the mid-season [%],
h mean maximum plant height [m].

Natural vegetation and crops not listed in Table 17:

For natural vegetation, nonfull-cover crops, or for crops not listed in Table 17, $K_{cb\ full}$ can be approximated as a function of climate and mean plant height for areas of vegetation that are greater than a few hectares:

$$K_{cb\ full} = K_{cb,h} + [0.04\,(u_2 - 2) - 0.004\,(RH_{min} - 45)]\left(\frac{h}{3}\right)^{0.3} \qquad (100)$$

where $K_{cb,h}$ $K_{cb\ mid}$ for full cover vegetation (LAI > 3) under sub-humid and calm wind conditions (RH_{min} = 45% and u_2 = 2 m s^{-1}), (Equation 101),
u_2 mean value for wind speed at 2 m height during the mid-season [m s^{-1}],
RH_{min} mean value for minimum daily relative humidity during the mid-season [%],
h mean maximum plant height [m].

The value for $K_{cb,h}$ is estimated as:

$$K_{cb,h} = 1.0 + 0.1\,h \qquad \text{for } h \le 2 \text{ m} \qquad (101)$$

where $K_{cb,h}$ is limited to ≤ 1.20 when h > 2 m. The value of 1.2 represents a general upper limit on $K_{cb\ mid}$ for tall vegetation having full ground cover and LAI > 3 under the sub-humid and calm wind conditions. This limit of 1.2 is adjusted for other climatic conditions in Equation 100. Equations 100 and 101 produce a general approximation for the increase in $K_{cb\ full}$ with plant height and climate. The form of these equations adheres to trends represented in Equation 70.

For small, isolated stand sizes, $K_{cb\ full}$ may need to be increased beyond the value given by Equation 99 or 100, as discussed in Chapter 10.

Conclusion

Equations 97 and 98 can be used to estimate or to reduce K_{cb} for non-pristine agricultural vegetation. The exponents in Equations 97 and 98 reflect the effects of microscale advection (transfer) of sensible heat from dry soil surfaces between plants toward plant leaves, thereby increasing ET per unit leaf area, and the effects of increased aerodynamic roughness as the value for LAI decreases. Equation 98 suggests that as h increases, total leaf area and effective roughness of vegetation increase, thereby increasing the crop coefficient. In addition, as h increases, more opportunity for microadvection of heat from soil to canopy occurs and turbulent exchange within the canopy increases for the same amount of ground coverage. All of these factors affect the relative magnitude of $K_{cb\ mid}$.

Equations 97 and 98 should be used with caution as they provide only an estimate of the maximum K_{cb} expected during peak plant growth for vegetation with healthy transpiring leaves and a dry soil surface. Where stomatal control is greater than for typical agricultural vegetation, then the K_{cb} should be further reduced using the recommendations set out in the next section (Equation 102).

EXAMPLE 41
Estimation of mid-season crop coefficient

Estimate $K_{cb\ mid}$ and $K_{c\ mid}$ for rectangular shaped 2 m tall vegetation that is as tall as it is wide, where 30% of the ground is covered by vegetation (f_c = 0.3) on 19 July (day 200 of the year) and at latitude 40°N. RH_{min} = 55% and u_2 = 1.5 m/s during the mid-season period.

On day J = 200 at latitude φ = 40 (π/180) = 0.70 radians (40°N), from Eq. 24, the solar declination δ = 0.36 radians.

At solar noon (ω = 0):

$$\sin(\eta) = \sin(\varphi)\sin(\delta) + \cos(\varphi)\cos(\delta) = 0.94$$

The value for η by taking the arcsine of above value is 1.24 radians and $\tan(\eta)$ = 2.8. If f_c = 0.3 and the HWR for the vegetation is 1, then $f_{c\ eff}$ from Box 18 is: 0.3(1+1/2.8) = 0.41.

From Eq. 101 $K_{cb,h} = 1.0 + 0.1(2) = 1.20$ ($\leq$ 1.20, so OK)

From Eq. 100 $K_{cb\ full} = 1.20 + (0.04(1.5\text{-}2) - 0.004(55\text{-}45))\ (2/3)^{0.3} = 1.15$

Therefore, $K_{cb\ mid}$ estimated by Eq. 98 for $K_{c\ min}$ = 0.15 is

$$K_{cb\ mid} = K_{c\ min} + (K_{cb\ full} - K_{c\ min})\ \min[1, 2f_c, (f_{c\ eff})^{(1/(1+h))}]$$
$$= 0.15+(1.15\text{-}0.15)\ \min[1, 2(0.3), (0.4)^{(1/(1+2))}] = 0.75$$

This value does not need any further adjustment for climate.

$K_{c\ mid}$ (where $K_{c\ mid}$ includes average wetting effects) can be derived from $K_{cb\ mid}$ using the guidelines presented in the calculation procedures at the beginning of this chapter

$$K_{c\ mid} = K_{cb\ mid} + (0.05 \ldots 0.10) = 0.80 \ldots 0.85$$

depending on the frequency of soil wetting.

The estimated crop coefficients for the mid-season stage are $K_{cb\ mid}$ = 0.75 and $K_{c\ mid}$ = 0.80 to 0.85.

EXAMPLE 42
Estimation of mid-season crop coefficient for reduced ground cover

A more precise estimate of $K_{cb\ mid}$ for the tomato crop of Example 40 that only developed 50% ground cover at Davis, California, the United States can be calculated if one knows that the tomato crop was planted in 1.52 m rows running east-west, that the crop reached a plant height of 0.75 m and that the height to width ratio of the tomato crop can be estimated as about 1.0 for the east-west rows. The latitude is 38.5°N and the midpoint of the mid-season occurs on July 20.
What is the adjusted $K_{cb\ mid}$ for tomatoes that reflects the 50% ground cover condition?

On day J = 201 (20 July) at latitude φ = 38.5 (π/180) = 0.67 radians (38.5°N), from Eq. 24 the solar declination δ = 0.36 radians. At solar noon (ω = 0):

$$\sin(\eta) = \sin(\varphi)\sin(\delta) + \cos(\varphi)\cos(\delta) = 0.95$$

The value for η by taking the arcsine of the above value is 1.26 radians. Therefore, for the observed HWR = 1 and f_c = 0.5, the effective soil cover for the east-west rows can be calculated as (Box 18):

$$f_{c\ eff} = 0.5\ [1 + 1/\tan(1.26)] = 0.66$$

The $K_{cb\ mid}$ in Table 17 representing a full cover tomato crop is 1.15 and the average h for fully developed tomatoes (this variety) is about 0.75 also. Following adjustment for climate (using Eq. 99)

$$K_{cb\ full} = 1.15 + [0.04(1.1\text{-}2) - 0.004(30\text{-}45)]\ (0.75/3)^{0.30} = 1.17$$

From Eq. 98 and using $K_{c\ min}$ = 0.15, the adjusted $K_{cb\ mid}$ for 50% ground cover would be:

$$K_{cb\ mid\ adj} = 0.15 + (1.17 - 0.15)\ \min(1,\ 2(0.5),\ 0.66^{1/(1+0.76)}) = 0.95$$

The results $K_{cb\ mid\ adj}$ = 0.95 for 50% ground cover are similar to the first estimate calculated in Example 40 and compare with the measured $K_{cb\ mid}$ ~ 0.90 to1.00 as determined by precision lysimeter by Pruitt *et al*. (1984).

MID-SEASON STAGE - ADJUSTMENT FOR STOMATAL CONTROL

The value for $K_{cb\ full}$ in Equations 97 and 98 may need to be reduced for vegetation that has a high degree of stomatal control. For vegetation such as some types of desert vegetation or trees with leaf resistance significantly greater than that of most agricultural crops where r_l is commonly about 100 s m^{-1}, the $K_{cb\ mid}$ estimated using Equations 97 and 98 can be modified by multiplying by a resistance correction factor, F_r. The resistance correction factor is developed based on the FAO Penman-Monteith equation:

$$F_r \approx \frac{\Delta + \gamma(1 + 0.34 u_2)}{\Delta + \gamma\left(1 + 0.34 u_2 \frac{r_l}{100}\right)} \qquad (102)$$

where r_l mean leaf resistance for the vegetation in question [s m^{-1}].

The mean leaf resistance r_l is 100 s m^{-1} for the grass ET_o reference and for many agricultural crops. Values for r_l for many agricultural and non-agricultural plants can be found in Körner *et al*. (1978) and Allen *et al*. (1996). Equation 102 reflects the fixed aerodynamic roughness of grass rather than the roughness of the specific vegetation, since the adjusted K_c is multiplied by the grass ET_o and the K_c already reflects the effects of the aerodynamic roughness for the specific vegetation.

EXAMPLE 43
Estimation of $K_{cb\ mid}$ from ground cover with reduction for stomatal control

A grove of olive trees has a tree spacing of 10 m. The horizontal diameter of the trees as viewed from overhead is 5 m. The tree height is 5 m. The lower 1.5 m of the trees have no foliage. The ground cover between the trees is bare. The mean u_2 during the mid-season growth stage is 2 m/s and the mean RH_{min} = 25%. The midpoint of the mid-season growth stage is on 29 June (i.e., day 180 of the year). The latitude of the location is 30°N.

Estimate $K_{cb\ mid}$ using Eq. 98 for the 10x10 m and for a 5x10 m spacing.

On day J = 180 (29 June) at latitude $\varphi = 30\ (\pi/180) = 0.52$ radians (30°N) and from Eq. 24 the solar declination $\delta = 0.405$ radians. At solar noon ($\omega = 0$):

$$\sin(\eta) = \sin(\varphi)\sin(\delta) + \cos(\varphi)\cos(\delta) = 0.99$$

As olive trees have somewhat round shapes, the effective fraction of ground cover (Box 18) can be estimated as $f_{c\ eff} = f_c/(\sin(\eta))$.

f_c = area of canopy/area tree spacing = $(\pi(5)^2/4)/(10)(10) = 0.196$
$f_{c\ eff} = 0.196/0.99 = 0.20$

From Eq. 101: $K_{cb,h} = 1.0 + 0.1(5) > 1.2$ or $K_{cb,h} = 1.2$
From Eq. 100: $K_{cb\ full} = 1.2 + [0-0.004(25-45)]\ (5/3)^{0.3} = 1.29$
From Eq. 98 and using $K_{c\ min} = 0.15$:

$$K_{cb\ mid} = 0.15 + (1.29 - 0.15)\ \min(1, 2(0.196), (0.20)^{1/(1+5)}) = 0.60$$

Körner *et al*. (1979) indicate that olives (*Olea europaea*) have r_l of about 420 s/m. Therefore, assuming that average T_{mean} = 25°C and that the elevation of the grove is 0 m (sea level), so that $\Delta = 0.189$ kPa (Eq. 13) and $\gamma = 0.0676$ kPa (Eq. 8), F_r is estimated from Eq. 102 as:

$$F_r \approx \frac{0.189 + 0.0676\ (1 + 0.34\ (2))}{0.189 + 0.0676\left(1 + 0.34\ (2)\left(\frac{420}{100}\right)\right)} = 0.67$$

The $K_{cb\ mid}$ adjusted for increased stomatal control using F_r is then

$$K_{cb\ mid\ adj} = F_r\ K_{cb\ mid} = 0.67\ (0.60) = 0.40$$

The value $K_{cb\ mid\ adj} = 0.40$ estimated for $f_c = 0.20$ is less than the value for $K_{cb\ mid}$ in Table 17 for olives for f_c = 0.40 to 0.67, due to the differences in f_c. The value from Table 17 is 0.70, which after adjustment for climate using Eq. 70 equals 0.79.

If the olives had been planted on a 5x10 m spacing, as is common in California, the United States, and which is reflected in the K_{cb} values for olives in Table 17, then $f_c = 0.39$, $f_{c\ eff} = 0.40$, and $K_{cb\ mid}$ from Eq. 98 is $K_{cb\ mid} = 1.04$, so that the estimated $K_{cb\ mid}$ adjusted for stomatal control using F_r = 0.67 is $K_{cb\ mid\ adj} = 0.67(1.04) = 0.70$. This value compares with the value of 0.79 obtained from Table 17 for mature trees, after adjustment for climate.

The basal crop coefficient, $K_{cb\ mid}$, taking the low density, climatic condition and stomatal control into account is 0.40. It increases to 0.70 for the 5x10 m spacing.

The equation would underestimate F_r (overestimate the reduction in K_{cb}) if used with the actual roughness of the vegetation when $r_l > 100$ s m^{-1} because of the lack in Equation 102 of feedback effects that reduced ET_c has on temperature and vapour pressure deficit profiles over the crop. These parameters generally increase with decreasing ET_c and therefore dampen the reduction in ET_c.

LATE SEASON STAGE

During the late season stage, the K_{cb} begins to decrease until it reaches $K_{cb\ end}$ at the end of the growing period. Values for $K_{cb\ end}$ can be scaled from $K_{cb\ mid}$ in proportion to the health and leaf condition of the vegetation at termination of the growing season and according to the length of the late season period (i.e., whether leaves senesce slowly or are killed by frost). Values for $K_{c\ end}$ can be similarly scaled from $K_{c\ mid}$; however, the reduction in $K_{c\ end}$ will be affected by the frequency of wetting by irrigation or precipitation and $K_{c\ end}$ may be proportionally less.

If estimated from Equations 97 and 98, $K_{cb\ end}$ should be reduced if it is to represent K_c values for plants with stomatal control that is greater than that for agricultural vegetation (where $r_l \approx 100$ s m^{-1}) or to reflect effects of ageing and senescence on stomatal control. In these situations, the estimated $K_{cb\ end}$ values should be multiplied by the F_r from Equation 102. Alternatively, they can be reduced by about 10% for each doubling of r_l above 100 s m^{-1} when mean daily air temperature (T_{mean}) is about 30° C and by about 20% for each doubling of r_l above 100 s m^{-1} when T_{mean} is about 15° C.

Alternatively, the value for $K_{cb\ end}$ can be reduced relative to the calculated value for $K_{cb\ mid}$ in proportion to the fraction of green healthy leaves remaining at the end of the late season stage relative to that during the mid-season. This can often be based on a visual survey of the field and may therefore be a subjective observation.

The f_c parameter and h are probably the simplest indices to estimate in the field. Again, Equations 97 and 98 should be used only as general or preliminary estimates of $K_{cb\ end}$.

ESTIMATING $ET_{c\ adj}$ USING CROP YIELDS

A simple, linear crop-water production function was introduced in the FAO Irrigation and Drainage Paper No. 33 to predict the reduction in crop yield when crop stress is caused by a shortage of soil water. This function was presented earlier as Equation 90:

$$\left(1-\frac{Y_a}{Y_m}\right) = K_y\left(1-\frac{ET_{c\,adj}}{ET_c}\right) \qquad (90)$$

where
- Y_a = actual yield of the crop [kg ha^{-1}]
- Y_m = maximum (expected) yield in absence of environmental or water stresses
- K_y = yield response factor [ ]
- ET_c = potential (expected) crop evapotranspiration in the absence of environmental or water stresses ($K_c\ ET_o$)
- $ET_{c\ adj}$ = actual (adjusted) crop evapotranspiration as a result of environmental or water stresses

Values for K_y have been reported in Paper No. 33 for a wide range of crops for predicting the effect of water stress and associated reduction in $ET_{c\ adj}$ on crop yield. Factors are presented there for predicting yield reductions for when stress occurs in only one crop growth stage, or when stress is distributed throughout the growing period. Seasonal yield response functions are summarized in Table 24.

Many environmental stresses such as water shortage, salinity, low fertility and disease impact yield by reducing the amount of $ET_{c\ adj}$ relative to the potential amount ET_c. The same can be true for when yields are reduced due to the use of low densities for plant populations. Therefore, for very general estimates of $ET_{c\ adj}$, one can invert Equation 90 and solve for the stress factor, K_S:

$$K_s = 1 - \frac{1}{K_y}\left(1 - \frac{Y_a}{Y_m}\right) \qquad (103)$$

where K_S is multiplied by K_{cb} or by K_c in equations 80 or 81 to predict the $ET_{c\ adj}$ in the presense of the water or other environmental stresses or for low plant populations or virility. The $ET_{c\ adj}$ predicted using K_S from equation 103 provides only a very general and approximate estimate of monthly or even seasonal evapotranspiration. Equation 103 works best for forage or other indiscriminate crops where the value for K_y is relatively constant during the season.

Equation 103 is generally only valid for use in predicting actual crop evapotranspiration for use in regional water balance studies, for studies of ground-water depletion and recharge, or for estimating historical water use. The procedure is not valid for predicting ET_c for daily or weekly time periods due to the very general nature of the K_y coefficient and the seasonal time scale of the crop yield. The procedures presented previously for adjusting ET_c using a daily soil water balance, salinity functions, or reductions in K_c based on leaf area or fraction of ground cover are recommended over the use of equation 103.

EXAMPLE 44
Approximate estimation of K_S from crop yield data

An irrigation scheme (project) cultivates dry, edible beans. There is known to be a shortage of irrigation water and a corresponding reduction in crop yield. The reported yield for the scheme averages 1100 kg/ha. The potential yield for the region and variety of beans, in the absence of water or environmental stresses and with good soil fertility is 1800 kg/ha.

From FAO Irrigation and Drainage Paper No. 33 or Table 24, the K_y for dry beans, assuming that stresses are distributed uniformly through the growing season, is 1.15. Therefore, from Equation 103, the estimated K_S to apply with Equation 80 for the growing season is:

$$K_s = 1 - \frac{1}{1.15}\left(1 - \frac{1100}{1800}\right) = 0.66$$

Therefore, the $ET_{c\ adj}$ for the season is predicted to be only 0.66 of maximum ET_c under pristine growing conditions.

The estimated seasonal $ET_{c\ adj}$ is predicted to be $ET_{c\ adj}$ = 0.66 ET_c where ET_c is predicted as $ET_c = K_c\ ET_o$.

Chapter 10

ET_C under various management practices

This chapter discusses various types of factors that may cause the values for K_c and ET_c to deviate from the standard values described in the Chapters 6 and 7. These factors refer to the effects of surface mulches, intercropping, small areas of vegetation and specific cultivation practices.

This chapter is intended to serve as a resource for situations where cultivation practices are known to deviate from those assumed in Tables 12 and 17, but where estimates of K_c and ET_c are still necessary. This chapter is by no means exhaustive. The intent is to demonstrate some of the procedures that can be used to make adjustments to K_c to account for deviations from standard conditions.

EFFECTS OF SURFACE MULCHES

Mulches are frequently used in vegetable production to reduce evaporation losses from the soil surface, to accelerate crop development in cool climates by increasing soil temperature, to reduce erosion, or to assist in weed control. Mulches may be composed of organic plant materials or they may be synthetic mulches consisting of plastic sheets.

Plastic mulches

Plastic mulches generally consist of thin sheets of polyethylene or a similar material placed over the ground surface, especially along the plant rows. Holes are cut into the plastic film at plant spacings to allow the plant vegetation to emerge. Plastic mulches can be transparent, white or black. Colour influences albedo mainly during the early stages of the crop. However, as the intention is to use a simple procedure for adjusting K_c for mulched crops, no distinction is made between the different types of plastic mulches.

Plastic mulches substantially reduce the evaporation of water from the soil surface, especially under trickle irrigation systems. Associated with the reduction in evaporation is a general increase in transpiration from vegetation caused by the transfer of both sensible and radiative heat from the surface of the plastic cover to adjacent vegetation. Even though the transpiration rates under mulch may increase by an average of 10-30% over the season as compared to using no mulch, the K_c values decrease by an average of 10-30% due to the 50-80% reduction in soil evaporation. A summary of observed reductions in K_c, in evaporation, and increases in transpiration over growing seasons is given in Table 25 for five horticultural crops. Generally, crop growth rates and vegetable yields are increased by the use of plastic mulches.

TABLE 25
Approximate reductions in K_c and surface evaporation and increases in transpiration for various horticultural crops under complete plastic mulch as compared with no mulch using trickle irrigation

Crop	Reduction[1] in K_c (%)	Reduction[1] in evaporation (%)	Increase[1] in transpiration (%)	Source
Squash	5-15	40-70	10-30	Safadi (1991)
Cucumber	15-20	40-60	15-30	Safadi (1991)
Cantaloupe	5-10	80	35	Battikhi and Hill (1988)
Watermelon	25-30	90	-10	Battikhi and Hill (1986), Ghawi and Battikhi (1986)
Tomato	35	not reported	not reported	Haddadin and Ghawi (1983)
Average	10-30	50-80	10-30	

[1] Relative to using no mulch

Single crop coefficient, K_c

To consider the effects of plastic mulch on ET_c, the values for $K_{c\ mid}$ and $K_{c\ end}$ for the horticultural crops listed in Table 12 can be reduced by 10-30%, depending on the frequency of irrigation (use the higher value for frequent trickle irrigation). The value for $K_{c\ ini}$ under mulch is often as low as 0.10. When the plastic mulch does not entirely cover the soil wetted by the drip emitters, or where substantial rainfall occurs, then the reduction in $K_{c\ mid}$ or $K_{c\ end}$ will be less, in proportion to the fraction of wet surface covered by the mulch.

Dual crop coefficient, $K_{cb} + K_e$

When estimating basal K_{cb} for mulched crops, less adjustment is normally needed to the K_{cb} curve, being of the order of a 5-15% reduction in K_{cb}, as it is generally understood that the 'basal' evaporation of water from the soil surface is less with a plastic mulch, though the transpiration is increased. The effect on K_{cb} could be greater in some situations and with some types of low density crops. Local calibration of K_{cb} (and K_c) for use with mulch culture is encouraged.

When calculating the soil evaporation coefficient K_e with plastic mulch, the f_w should represent the relative equivalent fraction of the ground surface that can contribute to evaporation through the vent holes in the plastic cover and to the fraction of surface that is wetted, but is not covered by the mulch. The effective area of vent holes is normally two to four times the physical area of the vents (or even higher) to account for vapour transfer from under the sheet.

Organic mulches

Organic mulches are often used with orchard production and with row crops under reduced tillage operations. Organic mulches may consist of unincorporated plant residues or foreign material imported to the field such as straw. The depth of the organic mulch and the fraction of the soil surface covered can vary widely. These two parameters will affect the amount of reduction in evaporation from the soil surface.

EXAMPLE 45
Effects of surface mulch

A plastic mulch is placed over cucumbers under drip irrigation. The mulch is clear plastic covering the entire field surface, with small openings at each plant. Adjust both the mean and basal K_c values for this crop to reflect the presence of the mulch.

From Table 12, $K_{c\ ini}$, $K_{c\ mid}$ and $K_{c\ end}$ for fresh market cucumbers have values equal to 0.4, 1.0 and 0.75.

As the plastic mulch is continuous with only small vents at each plant, the $K_{c\ ini}$ is assumed to be only 0.10 (this value should be adjusted upward if precipitation occurs).

The $K_{c\ mid}$ and $K_{c\ end}$ values are estimated as:

$$K_{c\ mid} = 0.85\ (1.0) = 0.85$$
$$K_{c\ end} = 0.85\ (0.75) = 0.64$$

where the 0.85 multipliers are derived from Table 25 and reflect an assumed 15% reduction in ET_c due to the mulch, assuming an approximately weekly irrigation frequency.

From Table 17, the values for $K_{cb\ ini}$, $K_{cb\ mid}$, and $K_{cb\ end}$ are 0.15, 0.95 and 0.7 for this same cucumber crop. The $K_{cb\ ini}$ is assumed to be similar to the $K_{c\ ini}$ for mulched cover and is therefore set equal to 0.10. The $K_{cb\ mid}$ and $K_{cb\ end}$ values are estimated to be reduced by 10% so that:

$$K_{cb\ mid} = 0.9\ (0.95) = 0.86$$
$$K_{cb\ end} = 0.9\ (0.7) = 0.63$$

These basal values are similar to the adjusted values for K_c. This is expected as evaporation from the mulch covered surface can be ignored. Additional adjustment to these K_c values to account for climate is necessary using Eq. 62 and 70.

The values for mean K_c and K_{cb} are similar with values of 0.10 for the initial stage, 0.85 for the mid-season stage and 0.64 at the end of the late season stage.

Single crop coefficient, K_c

A general rule when applying K_c from Table 12 is to reduce the amount of soil water evaporation by about 5% for each 10% of soil surface that is effectively covered by an organic mulch.

For example, if 50% of the soil surface were covered by an organic crop residue mulch, then the soil evaporation would be reduced by about 25%.

- In the case of $K_{c\ ini}$, which represents mostly evaporation from soil, one would reduce $K_{c\ ini}$ by about 25% in this situation.
- In the cases of $K_{c\ mid}$ and $K_{c\ end}$, one would reduce these values by 25% of the difference between ($K_{c\ mid}$ - $K_{cb\ mid}$) and ($K_{c\ end}$ - $K_{cb\ end}$) from Tables 12 and 17. Generally, the differences between values in Tables 12 and 17 are only 5-10% so that the adjustment to $K_{c\ mid}$ and $K_{c\ end}$ to account for an organic mulch may not be very large.

FIGURE 45
Different situations of intercropping

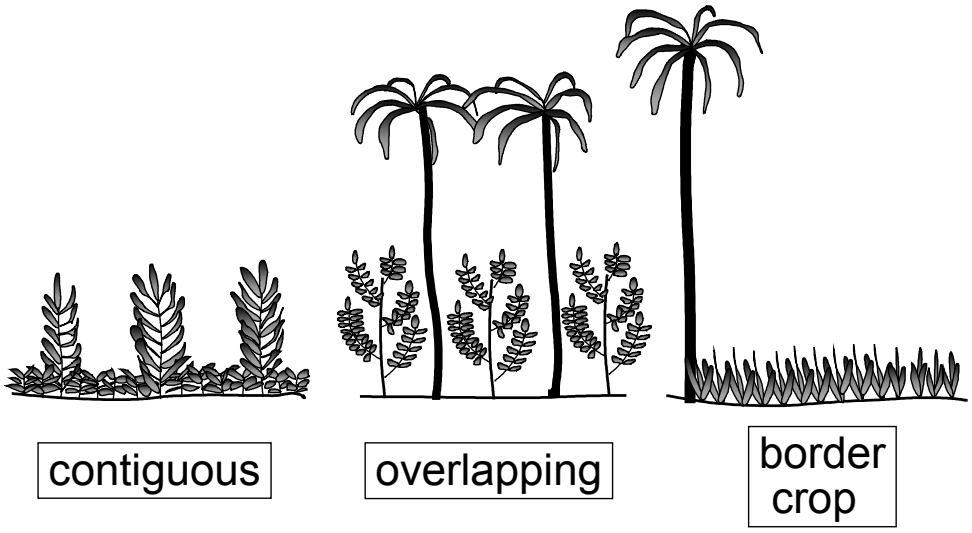

Dual crop coefficient, $K_{cb} + K_e$

When applying the approach with a separate water balance of the surface soil layer, the magnitude of the evaporation component (K_e ET_o) should be reduced by about 5% for each 10% of soil surface covered by the organic mulch. K_{cb} is not changed.

These recommendations are only approximate and attempt to account for the effects of partial reflection of solar radiation from residue, microadvection of heat from residue into the soil, lateral movement of soil water from below residue to exposed soil, and the insulating effect of the organic cover. As these parameters can vary widely, local observations and measurements are required if precise estimates are required.

INTERCROPPING

Intercropping refers to the situation where two different crops are grown together within one field. For the estimation of the crop coefficient, a distinction is made between (Figure 45):

- Contiguous vegetation, where the canopies of the two crops intermingle at some height (e.g., corn and beans intercropping);
- Overlapping crops, where the canopy of one crop is well above that of the other so that the canopies cannot be considered to be contiguous (e.g., date trees overlapping pomegranate trees at an oasis); and
- Border crops, where tall crops such as windbreaks border fields of shorter crops, or high trees border a field crop.

There is an upper limit to the energy available to evaporate water. This is represented by $K_{c\ max}$ (Equation 72 of Chapter 7) for all crops in cultivated fields larger than 3-5 ha:

$$K_{c\,max} = \max\left(\left\{1.2 + [0.04(u_2 - 2) - 0.004\,(RH_{min} - 45)]\left(\frac{h}{3}\right)^{0.3}\right\}, \{K_{cb} + 0.05\}\right) \quad (72)$$

where h is the height for the taller crop. Under all conditions when combining crop coefficients for multiple crops, K_c should be constrained by this upper bound ($K_c \leq K_{c\,max}$).

Contiguous vegetation

Where the taller crop has canopy foliage that extends down to the same elevation as that of the top of the shorter crop, the vegetation canopy can be considered to be contiguous. For example, in Africa and South America, maize and beans are frequently intercropped as contiguous vegetation, with one row of maize planted per one or more rows of beans. Another example is the cultivation of five to seven rows of wheat intercropped with three rows of maize in many areas of China.

Similar ground cover

Where the leaf area or fraction of ground covered by the vegetation (f_c) is similar for each crop, the K_c in Tables 12 and 17 for the taller crop (if this K_c is higher) can be taken to represent the entire field. The taller crop will act in some sense as a clothesline so that K_c (and ET_c) for the taller crop per unit of ground area is increased over that given in Table 12 or 17. However, the K_c (and ET_c) for the shorter crop will be reduced due to the windbreak effect by the taller crop. As a result, the K_c for the field as a whole may be similar to the weighted average of the K_c values for the two crops from Tables 12 and 17, or, the total K_c may more closely follow the K_c predicted for a field sown entirely to the taller crop ($K_{c\,field} \approx K_{c\,taller\,crop}$). Yields for the shorter crop may be reduced relative to those for single cultivar production due to the effects of shading by the taller crop and the competition for soil water.

Different ground cover

Where the fractions of ground covered by each crop are different, the K_c for an intercropped field can be estimated by weighting the K_c values for the individual crops according to the fraction of area covered by each crop and by the height of the crop:

$$K_{c\,field} = \frac{f_1 h_1 K_{c1} + f_2 h_2 K_{c2}}{f_1 h_1 + f_2 h_2} \quad (104)$$

where f_1 and f_2 are the fractions of the field surface planted to crops 1 and 2, h_1 and h_2 are the heights of crops 1 and 2, and K_{c1} and K_{c2} are the K_c values for crops 1 and 2.

Overlapping vegetation

Where intercropping entails overlapping of spacings, the canopy of one crop is well above the other. This is the case, for example in southern California, where citrus trees are planted in date palm groves. Where a normal dense spacing is used for both the dates and for the citrus trees, the K_c may increase as the density of the combined vegetation increases, proportional to the increase in LAI (Example 47), with maximum K_c constrained by either $K_{c\,max}$ (Equation 72) or by $K_{cb\,full}$ (Equations 99 and 100) unless the total field area is small so that there is an additional clothesline or oasis effect as discussed in the next section.

EXAMPLE 46
Intercropped maize and beans

Determine the representative $K_{c\ mid}$ for a situation where a single 1 m wide row of maize is grown for each 2 m of squash, where $RH_{min} \approx 45\%$ and $u_2 \approx 2$ m/s.

From Table 12, the $K_{c\ mid}$ and h for maize is 1.20 and 2 m and the $K_{c\ mid}$ and h for squash is 0.95 and 0.3 m. No correction is needed for climate. The representative $K_{c\ mid}$ can be obtained by weighting the individual $K_{c\ mid}$ values according to the fraction of the field surface allocated to each crop ($f_1 \approx 0.3$ for maize and $f_2 \approx 0.7$ for squash) and according to the heights of the crops as (Eq. 104):

$$K_{c\ mid} = \frac{0.30\,(2)(1.20) + 0.70\,(0.3)(0.95)}{0.30\,(2) + 0.70\,(0.3)} = 1.14$$

Values can be obtained for daily K_c in a similar manner by constructing individual K_c curves and then weighting interpolated values from the individual K_c curves for any specific day using Eq. 104.

The crop coefficient for the mid-season and entire field is 1.14.

Border crops

Where tall crops such as windbreaks or date palms border fields of shorter crops, the upper storey of the taller crop can intercept extra sensible heat energy from the air stream. Under these conditions, the K_c is weighted according to the areas for each crop. However, prior to the weighting, the K_c for the border crop, if taller than the field (interior) crop, should be adjusted for potential clothesline impact (next section).

SMALL AREAS OF VEGETATION

Natural vegetation and some subsistence agriculture frequently occurs in small groups or stands of plants. The value for K_c for these small stands depends on the type and condition of other vegetation surrounding the small stand.

Areas surrounded by vegetation having similar roughness and moisture conditions

In the majority of cases for natural vegetation or for non-pristine agricultural vegetation, the value for K_c must adhere to upper limits for K_c of approximately 1.20-1.40, when the areal expanse of the vegetation is larger than about 2 000 m^2. This is required as ET from large areas of vegetation is governed by one-dimensional energy exchange principles and by the principle of conservation of energy. ET from small stands (< 2 000 m^2) will adhere to these same principles and limits only where the vegetation height, leaf area, and soil water availability are similar to that of the surrounding vegetation.

EXAMPLE 47
Overlapping vegetation

A 20 ha date palm grove in Palm Desert, California, the United States has a tree spacing of 6 m. Interplanted among the rows of palms are small orange trees (50% canopy) on a 6 m spacing. The palm and citrus trees are 3 m from one another in the rows. Height of the palms is 10 m and height of the citrus is 3 m. The canopy foliage of the palms is well above that of the citrus so that the canopies cannot be considered contiguous. Mean average RH_{min} during the mid-season is 20% and u_2 = 2 m/s. The $K_{c\ mid}$ from Table 12 for dates is 0.95 and when adjusted for humidity and wind using Eq. 62 is $K_{c\ mid}$ = 1.09. The $K_{c\ mid}$ from Table 12 for citrus having 50% canopy with no ground cover is 0.60 and when adjusted for humidity and wind using Eq. 62 is $K_{c\ mid}$ = 0.70.

The interplanting of citrus among the date palms has increased the total leaf area of the orchard so that ET_c for the combined planting (palms and citrus together) will be greater than for either planting alone. The estimated combined $K_{c\ mid}$ will be estimated as a function of the increase in total LAI. First the LAI values of the individual plantings are estimated by inverting Eq. 97 to solve for LAI:

$$LAI = -1.4 \ln\left[1 - \frac{K_{cb} - K_{c\ min}}{K_{cb\ full} - K_{c\ min}}\right]$$

where $K_{c\ min}$ is the minimum basal K_c for bare soil (≈ 0.15 to 0.20) and $K_{cb\ full}$ is the maximum mid-season K_c expected for the crop if there were complete ground cover, calculated using Eq. 99. Based on Eq. 99, with h = 10 m for the date palms and h = 3 m for the citrus, the $K_{cb\ full}$ values for the two crops, assuming complete ground cover for each, are $K_{cb\ full}$ = 1.34 for palms and $K_{cb\ full}$ = 1.30 for citrus (using RH_{min} = 20% and u_2 = 2 m/s). These estimates ignore effects of any unique stomatal control. Therefore, using the above equation, the effective LAI values of the date palms and citrus are estimated to be approximately:

LAI_{palms} = - 1.4 ln[1-(1.09-0.15)/(1.34-0.15)] = 2.2
LAI_{citrus} = - 1.4 ln[1-(0.70-0.15)/(1.30-0.15)] = 0.9

Therefore, the effective LAI for the date palm-citrus combination is estimated to be approximately
$LAI_{combined} = LAI_{palms} + LAI_{citrus}$ = 2.2 + 0.9 = 3.1.

The increase in $K_{c\ mid}$ for the date palm orchard resulting from the increase in LAI from the interplanting of citrus is estimated using a ratio of the LAI-based function introduced in Eq. 97. This results in the relationship:

$$K_{c\ mid} = K_{c\ mid,\ single\ crop}\left[\frac{1 - \exp\left(-0.7 LAI_{combined}\right)}{1 - \exp\left(-0.7 LAI_{single\ crop}\right)}\right]$$

where $LAI_{combined}$ is the LAI for the two intercropped plantings combined and $LAI_{single\ crop}$ is the LAI for the taller, single crop. $K_{c\ mid\ single\ crop}$ is the mid-season K_c for the taller, single crop (in this case the date palms). In this application, the above equation is solved as:

$$K_{c\ mid} = 1.09\left[\frac{1 - \exp\left(-0.7(3.1)\right)}{1 - \exp\left(-0.7(2.2)\right)}\right] = 1.23$$

Therefore, the $K_{c\ mid}$ estimated for the complex of date palms and citrus together is 1.23. This value is compared with the maximum expected K_c based on energy limitations, represented by $K_{c\ max}$ of Eq. 72 which in this case for h=10 m is $K_{c\ max}$ = 1.34. Because $K_{c\ mid} < K_{c\ max}$ (i.e., 1.23 < 1.34), the $K_{c\ mid}$ = 1.23 is accepted as the approximate estimate of the $K_{c\ mid}$ for the intercropped field.

Clothesline and oasis effects

Under the clothesline effect, where vegetation height is greater than that of the surroundings (different roughness conditions), or under the oasis effect, where vegetation has higher soil water availability than the surroundings (different moisture conditions), the peak K_c values may exceed the 1.20-1.40 limit. The user should exercise caution when extrapolating ET measurements taken from these sorts of vegetation stands or plots to larger stands or regions as an overestimation of regional ET may occur.

Small expanses of tall vegetation that are surrounded by shorter cover can exhibit a clothesline effect. This occurs where turbulent transport of sensible heat into the canopy and transport of vapour away from the canopy is increased by the 'broadsiding' of wind horizontally into the taller vegetation. In addition, the internal boundary layer above the vegetation may not be in equilibrium with the new surface. Therefore, ET from the isolated expanses, on a per unit area basis, may be significantly greater than the corresponding ET_o computed for the grass reference. Examples of the clothesline or oasis effects would be ET from a single row of trees surrounded by short vegetation or surrounded by a dry non-cropped field, or ET from a narrow strip of cattails (a hydrophytic vegetation) along a stream channel. K_c values up to and exceeding two have been recorded for such situations.

Where ET estimates are needed for such small, isolated expanses of vegetation surrounded by shorter cover (clothesline effect) or dry land (oasis effect), then the K_c may exceed the grass reference by 100% or more. Estimates of K_c for the expanses of vegetation should contain u_2, RH_{min} and h parameters to adjust K_c values, and parameters expressing the aridity of the surrounding area, the general width of the vegetation stand and the ability of the wind to penetrate into the vegetation. The equation should also consider the LAI of the vegetation to account for the ability of the vegetation to conduct and transpire the amount of water demanded by the clothesline/climatic condition. An upper limit of 2.5 is usually placed on K_c to represent an upper limit on the stomatal capacity of the vegetation to supply water vapour to the air stream under the clothesline or oasis conditions. For vegetation with a great leaf resistance, such as for some types of desert vegetation or trees, the upper limit should be multiplied by a resistance correction factor, F_r, calculated in Chapter 9 using Equation 102.

Figure 46 presents example curves of K_c for small areas of vegetation versus vegetation stand width, for conditions where u_2 = 2 m/s, RH_{min} = 30%, vegetation height = 2 m, and LAI = 3. The upper curve represents conditions where the specific vegetation is surrounded by dead vegetation, dry bare soil, or even gravel or asphalt. In this situation, large amounts of sensible heat are generated from the surrounding area due to the lack of ET. Some of this sensible heat is advected into the vegetation downwind. The lower curve represents conditions where the vegetation is surrounded by well-watered grass. In this situation, there is much less sensible heat available from the surrounding area to increase ET (and K_c) of vegetation downwind. The influence of the aridity of the surroundings on the K_c for a small expanse is apparent. The two curves shown will change with changes in u_2, RH_{min}, h, and LAI. The user is cautioned that Figure 46 provides only general estimates of K_c under clothesline and oasis conditions. These estimates should be verified where possible using valid local measurements.

ET estimates from large expanses of vegetation or from small expanses of vegetation that are surrounded by mixtures of other vegetation having similar roughness and moisture conditions should almost always be less than or equal to 1.4 ET_o, even under arid conditions.

FIGURE 46
K_c curves for small areas of vegetation under the oasis effect as a function of the width of the expanse of vegetation for conditions where RH_{min} = 30%, u_2 = 2 m/s, vegetation height (h) = 2 m and LAI = 3

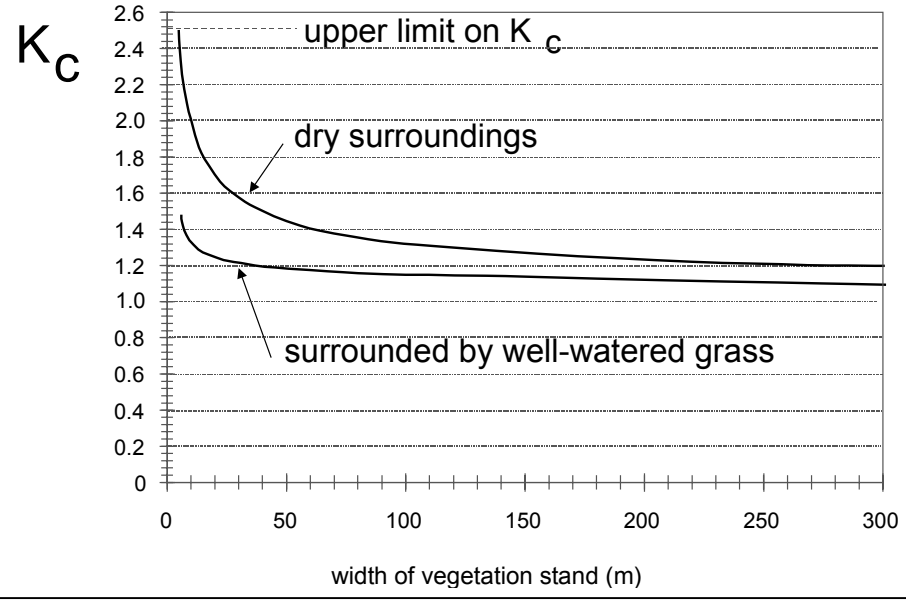

For tall wind breaks, such as single rows of trees, an approximate estimate for K_c is:

$$K_c = \min\left(1.2 + \frac{F_r \; h_{canopy}}{\text{Width}},\; 2.5\right) \qquad (105)$$

where F_r stomatal resistance correction factor (Equation 102)
h_{canopy} mean vertical height of canopy area [m]
Width width (horizontal thickness) of the windbreak [m]

The K_c = 2.5 limit imposed in Equation 105 represents an approximate upper limit on ET_c of trees per unit ground area. However, this value has large uncertainty. Because availability of soil water may limit evapotranspiration from wind breaks, a soil water balance and calculation of the K_s stress factor should be conducted.

MANAGEMENT INDUCED ENVIRONMENTAL STRESS

Many agricultural crops are intentionally water stressed during specific crop growth periods to encourage particular crop characteristics. The water stress is initiated by withholding or by reducing irrigations. In situations where this type of cultural management is practised, the K_c should be reduced to account for the reduction in evapotranspiration.

Environmental stress from soil water shortage, low soil fertility, or soil salinity can cause some types of plants to accelerate their reproductive cycle. In these situations, the length of the growing season may be shortened, particularly the mid-season period. Stress during the

development period may increase the length of that period. Therefore, the length of the mid-season, L_{mid}, and perhaps the lengths of the development and late seasons may need to be adjusted for environmentally stressed or damaged vegetation. Local research and observation is critical to identify the magnitudes and extent of these adjustments. Some examples of modifications to K_c and to lengths of growing periods are described below.

Alfalfa seed

Some forage crops such as alfalfa that are grown for seed production are intentionally water stressed to reduce the amount of vegetation and to encourage increased production of flowers and seed. In areas subject to freezing winters, the reduction in K_c for deep rooted crops such as alfalfa depends upon the amount of water made available from precipitation during the dormant (winter) season and upon the amount of rainfall and limited irrigation during the growing season. Therefore, the effects of the intentional stress on the values for K_c should be modelled using the basal crop procedure presented in Chapter 7 and the K_s coefficient and water balance procedure presented in Chapter 8.

Cotton

In cotton production, soil water stress may be initiated during the development period to delay flower development and to encourage boll development. This practice retards the growth rate of the cotton plant and delays the date of full cover. For cotton, the attainment of full cover and the beginning of the mid-season generally occurs when the LAI reaches approximately three. When soil water stress and growth retardation is practised, full cover may occur after the beginning of flowering. The effect of stress during the development period on ET_c can be incorporated into the K_c curve by extending the length of the development period into the mid-season period. The length of the total season generally remains the same.

Sugar beets

Sugar beets are frequently managed to initiate mild soil water stress during the late season period to dehydrate roots and concentrate sugars. A terminal irrigation may be needed just prior to harvest to assist in root extraction. When this type of water stress is practised, the value for $K_{c\ end}$ is reduced from 1.0 to 0.6 (Table 12, Footnote 5).

Coffee

Coffee plants are often intentionally water stressed to reduce vegetation growth and to encourage development of berries. Under these conditions, K_c values from Table 12 should be reduced. In addition, coffee fields may be bordered by trees that serve as windbreaks. The effect of windbreaks is to reduce the K_c of the coffee plants due to a reduction in wind and solar radiation over the plants. The reduction in K_c could be significant where windbreaks are tall and frequent. However, the K_c for the entire field area, including the windbreaks, may be increased by the presence of the trees, relative to the values for K_c for coffee shown in Table 12, due to increased total leaf area of the coffee-tree combination and the increased aerodynamic roughness.

Tea

Initiation and development of new leaves on tea plants often occurs following the start of the rainy season. During the dry season, initiation of new leaves is slow or non-existent. The transpiration from older leaves is lower than for new leaves due to effects of leaf age on

stomatal conductance. Therefore, the K_c, when leaves have aged (more than 2-3 months old), will be perhaps 10-20% lower than shown in Tables 12 and 17. Similar to coffee, tea fields may be bordered by trees that serve as windbreaks. The effect of windbreaks is to reduce the K_c of the tea plants, but to potentially increase the K_c for the entire plantation, as described for coffee.

Olives

Growers may increase spacings of olive trees under rainfed conditions in areas with less rainfall. This is done to increase the ground area per tree that contributes infiltrated rain to transpiration of the tree. For example, in Tunisia, the spacing of olive trees changes from the north to the south, in proportion to annual rainfall. The tree spacing influences the K_c for the crop (Example 43).

Chapter 11

ET_c during non-growing periods

This chapter describes procedures for predicting ET_c during non-growing periods. Non-growing periods are defined as periods during which no agricultural crop has been planted. In temperate climates, non-growing periods may include periods of frost and continuously frozen conditions.

TYPES OF SURFACE CONDITIONS

The type and condition of the ground surface during non-growing periods dictates the range for ET_c. Where the surface is bare soil, then the K_c will be quite similar to the $K_{c\ ini}$ predicted in Chapter 6. Where the surface is covered by nearly dead vegetation or some type of organic mulch or crop residue, then the K_c will be similar to that for agriculture that uses a surface mulch. Where the surface is covered by weed growth or growth of 'volunteer' plants, then the K_c will vary according to the leaf area or fraction of ground covered by the vegetation and by the availability of soil water. Where the surface is snow covered or frozen, then the K_c is difficult to predict and a constant value for ET_c may have to be assumed.

Bare soil

Single crop coefficient

Where the ground is left mostly bare following harvest, then the K_c following harvest will be strongly influenced by the frequency and amount of precipitation. K_c for bare soil can be calculated as $K_c = K_{c\ ini}$ where $K_{c\ ini}$ is calculated using the procedure of Chapter 6.

Dual crop coefficient

Where a daily soil water balance can be applied, the user may elect to apply the dual K_c approach of Chapter 7. In this situation, the topsoil layer may dry to very low water contents during periods having no precipitation. Therefore, the values for K_{cb} and for $K_{c\ min}$ in Equations 71 and 76 should be set equal to zero. This provides for the opportunity to predict $ET_c = 0$ during long periods having no rainfall. This is necessary to preserve the water balance of the evaporation layer and of the root zone in total. The daily water balance calculation, given $K_{cb} = 0$, will provide the most accurate estimates of ET_c during the non-growing periods.

Surface covered with dead vegetation

Single crop coefficient

Where the ground surface has a plant residue or other dead organic mulch cover, or where part of the unharvested crop remains suspended above the surface in a dead or senesced condition, then the surface will respond similarly to a surface covered by mulch. In this case, K_c can be

set equal to $K_{c\ ini}$ as predicted from figures 29 and 30, but the value for $K_{c\ ini}$ can be reduced by about 5% for each 10% of soil surface that is effectively covered by an organic mulch.

Dual crop coefficient

Evaporation from dead, wet vegetation can be substantial for a few days following a precipitation event. Therefore, in the dual K_c approach, the value for f_c should be set equal to zero to reflect the lack of green cover and f_w should be set equal to 1.0 to reflect the wetting of both soil and mulch cover by precipitation.

The dead mulch or vegetation will dry more quickly than would the underlying soil if it were exposed. In addition, the soil will be protected somewhat from evaporation by the dead mulch or vegetation cover. Therefore, total evaporation losses will be less than the TEW predicted from Equation 73. This can be accounted for by reducing the value for TEW by 5% for each 10% of soil surface that is effectively covered by an organic mulch. The value for REW should be limited to less than or equal to that for TEW.

Surface covered with live vegetation

During frost-free periods following harvest, weeds may begin to germinate and grow. This vegetation is supplied with water from storage in the soil profile and from any rainfall. In addition, crop seed lost during harvest may germinate following rainfall events and add to the ground cover. The amount of ground surface covered by vegetation will depend on the severity of weed infestation; the density of the volunteer crop; the frequency and extent of soil tillage; the availability of soil water or rain, and any damage by frost.

The value for K_{cb} during the non-growing period can be predicted over time according to the amount of vegetation covering the surface. This can be done through estimates of LAI using Equation 97 or estimates of the fraction of ground cover, f_c, using Equation 98.

Single crop coefficient

In the single crop coefficient approach, the value for K_{cb} determined using procedures in Chapter 9 can be converted into an equivalent K_c by adding 0.05 to 0.15 according to the frequency of rainfall and surface wetting.

It is important that the K_c for vegetation during the non-growing period be limited according to the amount of soil water available to supply evapotranspiration. Otherwise, the law of conservation of mass will be violated. Under all conditions, the integration of $K_c\ ET_o$ over the course of the non-growing period cannot exceed the sum of the precipitation occurring during the period plus any residual soil water in the root zone following harvest that can be depleted by the subsequent vegetation. The root zone in this case is the root zone for the weed or volunteer crops. A daily soil water balance may provide for the best estimate of soil water induced stress and associated reduction in K_c and ET_c.

Dual crop coefficient

Under the dual crop coefficient approach, K_{cb} can be predicted according to the amount of surface that is covered by vegetation using Equation 97 or 98. Then, a full daily soil water

balance of the topsoil together with a full daily soil water balance of the root zone can be employed as described in Chapter 7. The soil water balances will automatically adhere to the law of conservation of mass, so that total ET_c from the weed or volunteer vegetation will not be overestimated. Again, because the topsoil layer may dry to below wilting point under conditions of sparse rainfall, the values for K_{cb} and $K_{c\ min}$ used in Equations 71 and 76 should be set equal to zero. In this manner, the daily soil water balance with dual K_c calculations can progress throughout the non-growing period with good results.

Frozen or snow covered surfaces

Where the ground surface is snow covered or frozen, any vegetation will be largely non-responsive and non-contributing to ET_c, and the amount of ET_c will be closely related to the availability of free water at the surface and to the albedo of the surface.

The albedo of snow covered surfaces can range from 0.40 for old, dirty snow cover to 0.90 for fresh, dry snow. Therefore, the ET_c for snow cover will be less than ET_o for grass, as 25-85% less shortwave energy is available. In addition, some energy must be used to melt the snow before evaporation.

The use of ET_o under such conditions is of limited value, as the assumption of conditions sustaining a green grass cover is violated. It is even possible to obtain negative values for ET_o on some winter days where the longwave radiation from the surface is large and the vapour pressure deficit is small. It is under these conditions that net condensation of water from the atmosphere is possible. This would be similar to negative evaporation.

Given the limited value of ET_o (or even ET_p) under snow covered or frozen conditions, a single, average value may be best used to predict ET_c. Wright (1993) found that ET_c averaged 1 mm/day over winter periods at Kimberly, Idaho, the United States, that were six months long (1 October to 30 March). The latitude of Kimberly is 42°N and the elevation is about 1 200 m. Over the six-year study period, the ground was 50% covered by snow for 25% of the time from 1 October to 30 March. The ground, when exposed, was frozen about 50% of the time. The K_c averaged 0.25 during periods when the soil was not frozen but where frosts were occurring (October and early November). When the ground had 50% snow cover or greater, the ET_c averaged only 0.4 mm/day. Wright found that over the six-month non-growing period, total cumulative ET_c exceeded precipitation by about 50 mm.

Figure 47 shows the mean measurements of ET_c during the 1985-1991 study period. The measurements have high correspondence to the total shortwave radiation energy available on a clear day, R_{so}, estimated as 0.75 R_a. There is some lag between ET_c and R_{so} and R_s caused by cooler temperatures in January – March as compared to the October – December period. The ET_c/R_{so} ratio averaged only 0.17 over the six-month period, and averaged 0.11 from 1 Dec. – 10 Mar. The ET_c/R_s ratio averaged 0.23 over the six-month period, and averaged 0.15 from 1 Dec. – 10 Mar.

A similar study conducted in Logan, Utah, the United States (latitude 41.6°N, elevation 1 350 m) over an eight-year period showed that ET_c varied widely with soil surface wetness and air temperature during the winter months. The 'average' K_c from November to March was 0.5 for days having no snow cover. For days with snow cover, 'ET_c' ranged from 0 to 1.5 mm/day. Similarly, K_c is about 0.4 for winter wheat during frozen periods in the region of northern China (latitude near 39°N.

FIGURE 47
Mean evapotranspiration measured during non-growing, winter periods at Kimberly, Idaho, United States by Wright (1993)

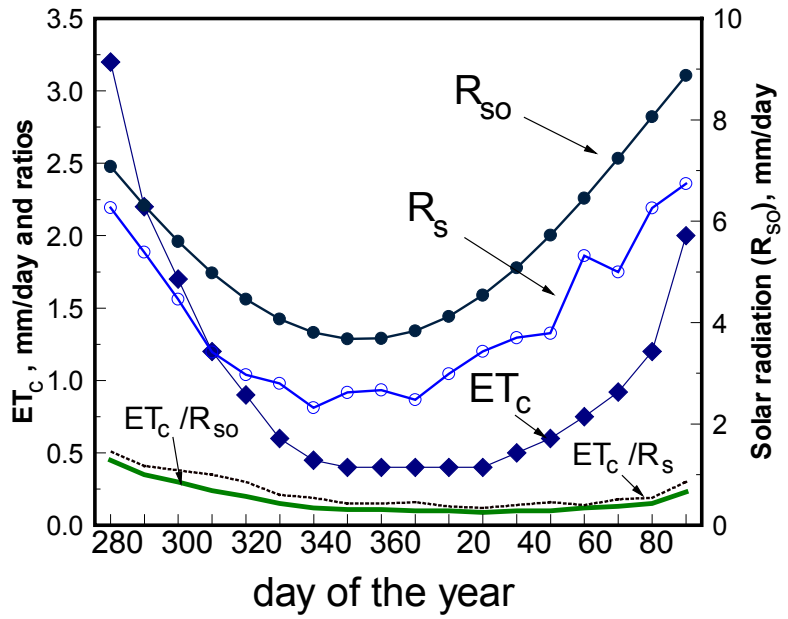

Single Crop Coefficient

The above procedure can provide estimates for the single K_c during non-growing season periods having snow cover or freezing conditions. However, the actual value for K_c is known to vary widely and will be less when water is less available at the soil surface.

Dual Crop Coefficient

A daily soil water balance using the dual crop coefficient approach is necessary to accurately predict ET_c under freezing and snow cover conditions. In the dual crop coefficient method, a daily water balance is conducted for the topsoil and the estimate for K_c can be reduced according to available water. However, in addition to the limited validity of the concept of ET_o under frozen or snow covered conditions, the evaporation coefficient, K_e, may be reduced when the ground surface is frozen, as the water in a frozen state is less available.

Other, more complex models for predicting ET_c under non-growing season conditions, snow cover, and freezing, are available in the literature and should be consulted and perhaps applied when precise estimates for ET_c are needed. Some of these are listed in section K of the References.

Annex 1

Units and symbols

PREFIXES

Units can be used as such or in multiples:

Tera	(T) and which is	10^{12}	Centi	(c)	10^{-2}
Giga	(G)	10^{9}	Milli	(m)	10^{-3}
Mega	(M)	10^{6}	Micro	(μ)	10^{-6}
Kilo	(k)	10^{3}	Nano	(n)	10^{-9}
Hecto	(h)	10^{2}	Pico	(p)	10^{-12}
Deca	(da)	10^{1}	Femto	(f)	10^{-15}
Deci	(d)	10^{-1}	Atto	(a)	10^{-18}

TEMPERATURE

Standard unit: degree Celsius (°C)

degree Fahrenheit (°F)	(°C) = (°F-32) 5/9
Kelvin (K)	1 K = (°C) + 273.16

PRESSURE
(air pressure, vapour pressure)

Standard unit: kilopascal (kPa)

millibar (mbar)	1 mbar = 0.1 kPa
bar	1 bar = 100 kPa
centimetre of water (cm)	1 cm of water = 0.09807 kPa
millimetre of mercury (mmHg)	1 mmHg = 0.1333 kPa
atmospheres (atm)	1 atm = 101.325 kPa
pound per square inch (psi)	1 psi = 6.896 kPa

WIND SPEED

Standard unit: metre per second (m s^{-1})

kilometre per day (km day^{-1})	1 km day^{-1} = 0.01157 m s^{-1}
nautical mile/hour (knot)	1 knot = 0.5144 m s^{-1}
foot per second (ft s^{-1})	1 ft/s = 0.3048 m s^{-1}

RADIATION

Standard unit: megajoule per square metre and per day (MJ m^{-2} day^{-1}) or as equivalent evaporation in mm per day (mm day^{-1})

equivalent evaporation (mm/day)	1 mm day^{-1} = 2.45 MJ m^{-2} day^{-1}
joule per cm^2 per day (J cm^{-2} day^{-1})	1 J cm^{-2} day^{-1} = 0.01 MJ m^{-2} day^{-1}
calorie per cm^2 per day (cal cm^{-2} day^{-1})	1 cal = 4.1868 J = 4.1868 10^{-6} MJ
	1 cal cm^{-2} day^{-1} = 4.1868 10^{-2} MJ m^{-2} day^{-1}
watt per m^2 (W m^{-2})	1 W = 1 J s^{-1}
	1 W m^{-2} = 0.0864 MJ m^{-2} day^{-1}

EVAPOTRANSPIRATION

Standard unit: millimetre per day (mm day^{-1})

m^3 per hectare per day (m^3 ha^{-1} day^{-1})	1 m^3 ha^{-1} day^{-1} = 0.1 mm day^{-1}
litre per second per hectare (l s^{-1} ha^{-1})	1 l s^{-1} ha^{-1} = 8.640 mm day^{-1}
equivalent radiation in megajoules per square metre per day (MJ m^{-2} day^{-1})	1 MJ m^{-2} day^{-1} = 0.408 mm day^{-1}

Annex 2

Meteorological tables

2.1 Atmospheric pressure (P) for different elevations above sea level (z)
2.2 Psychrometric constant (γ) for different elevations above sea level (z)
2.3 Saturation vapour pressure ($e^o(T)$) for different temperatures (T)
2.4 Slope of vapour pressure curve (Δ) for different temperatures (T)
2.5 Number of the day in the year (J)
2.6 Daily extraterrestrial radiation (R_a) for different latitudes
2.7 Mean daylight hours (N) for different latitudes
2.8 σT_K^4 (Stefan-Boltzmann law) at different temperatures (T)
2.9 Conversion factors to convert wind speed measured at given height to wind speed measured at standard height of 2 m above ground surface

TABLE 2.1
Atmospheric pressure (P) for different altitudes (z)

$$P = 101.3\left(\frac{293 - 0.0065\ z}{293}\right)^{5.26} \qquad \textbf{(Eq. 7)}$$

Z (m)	P (kPa)	z (m)	P (kPa)	z (m)	P (kPa)	z (m)	P (kPa)
0	101.3	1000	90.0	2000	79.8	3000	70.5
50	100.7	1050	89.5	2050	79.3	3050	70.1
100	100.1	1100	89.0	2100	78.8	3100	69.6
150	99.5	1150	88.4	2150	78.3	3150	69.2
200	99.0	1200	87.9	2200	77.9	3200	68.8
250	98.4	1250	87.4	2250	77.4	3250	68.3
300	97.8	1300	86.8	2300	76.9	3300	67.9
350	97.2	1350	86.3	2350	76.4	3350	67.5
400	96.7	1400	85.8	2400	76.0	3400	67.1
450	96.1	1450	85.3	2450	75.5	3450	66.6
500	95.5	1500	84.8	2500	75.0	3500	66.2
550	95.0	1550	84.3	2550	74.6	3550	65.8
600	94.4	1600	83.8	2600	74.1	3600	65.4
650	93.8	1650	83.3	2650	73.7	3650	65.0
700	93.3	1700	82.8	2700	73.2	3700	64.6
750	92.7	1750	82.3	2750	72.7	3750	64.1
800	92.2	1800	81.8	2800	72.3	3800	63.7
850	91.6	1850	81.3	2850	71.8	3850	63.3
900	91.1	1900	80.8	2900	71.4	3900	62.9
950	90.6	1950	80.3	2950	71.0	3950	62.5
1000	90.0	2000	79.8	3000	70.5	4000	62.1

TABLE 2.2
Psychrometric constant (γ) for different altitudes (z)

$$\gamma = \frac{c_p\, P}{\varepsilon\, \lambda} = 0.665 \times 10^{-3}\, P \qquad \textbf{(Eq. 8)}$$

Z (m)	γ kPa/°C	z (m)	γ kPa/°C	z (m)	γ kPa/°C	z (m)	γ kPa/°C
0	0.067	1000	0.060	2000	0.053	3000	0.047
100	0.067	1100	0.059	2100	0.052	3100	0.046
200	0.066	1200	0.058	2200	0.052	3200	0.046
300	0.065	1300	0.058	2300	0.051	3300	0.045
400	0.064	1400	0.057	2400	0.051	3400	0.045
500	0.064	1500	0.056	2500	0.050	3500	0.044
600	0.063	1600	0.056	2600	0.049	3600	0.043
700	0.062	1700	0.055	2700	0.049	3700	0.043
800	0.061	1800	0.054	2800	0.048	3800	0.042
900	0.061	1900	0.054	2900	0.047	3900	0.042
1000	0.060	2000	0.053	3000	0.047	4000	0.041

Based on λ= 2.45 MJ kg^{-1} at 20°C.

TABLE 2.3
Saturation vapour pressure ($e^o(T)$) for different temperatures (T)

$$e^{o}(T) = 0.6108 \exp\left[\frac{17.27\,T}{T + 237.3}\right] \qquad \textbf{(Eq. 11)}$$

T °C	e_s kPa	T °C	e°(T) kPa	T °C	e°(T) kPa	T °C	e_s kPa
1.0	0.657	13.0	1.498	25.0	3.168	37.0	6.275
1.5	0.681	13.5	1.547	25.5	3.263	37.5	6.448
2.0	0.706	14.0	1.599	26.0	3.361	38.0	6.625
2.5	0.731	14.5	1.651	26.5	3.462	38.5	6.806
3.0	0.758	15.0	1.705	27.0	3.565	39.0	6.991
3.5	0.785	15.5	1.761	27.5	3.671	39.5	7.181
4.0	0.813	16.0	1.818	28.0	3.780	40.0	7.376
4.5	0.842	16.5	1.877	28.5	3.891	40.5	7.574
5.0	0.872	17.0	1.938	29.0	4.006	41.0	7.778
5.5	0.903	17.5	2.000	29.5	4.123	41.5	7.986
6.0	0.935	18.0	2.064	30.0	4.243	42.0	8.199
6.5	0.968	18.5	2.130	30.5	4.366	42.5	8.417
7.0	1.002	19.0	2.197	31.0	4.493	43.0	8.640
7.5	1.037	19.5	2.267	31.5	4.622	43.5	8.867
8.0	1.073	20.0	2.338	32.0	4.755	44.0	9.101
8.5	1.110	20.5	2.412	32.5	4.891	44.5	9.339
9.0	1.148	21.0	2.487	33.0	5.030	45.0	9.582
9.5	1.187	21.5	2.564	33.5	5.173	45.5	9.832
10.0	1.228	22.0	2.644	34.0	5.319	46.0	10.086
10.5	1.270	22.5	2.726	34.5	5.469	46.5	10.347
11.0	1.313	23.0	2.809	35.0	5.623	47.0	10.613
11.5	1.357	23.5	2.896	35.5	5.780	47.5	10.885
12.0	1.403	24.0	2.984	36.0	5.941	48.0	11.163
12.5	1.449	24.5	3.075	36.5	6.106	48.5	11.447

TABLE 2.4
Slope of vapour pressure curve (Δ) for different temperatures (T)

$$\Delta = \frac{4098\left[0.6108\exp\left(\frac{17.27\,T}{T+237.3}\right)\right]}{(T+237.3)^2} \qquad \textbf{(Eq. 13)}$$

T °C	Δ kPa/°C	T °C	Δ kPa/°C	T °C	Δ kPa/°C	T °C	Δ kPa/°C
1.0	0.047	13.0	0.098	25.0	0.189	37.0	0.342
1.5	0.049	13.5	0.101	25.5	0.194	37.5	0.350
2.0	0.050	14.0	0.104	26.0	0.199	38.0	0.358
2.5	0.052	14.5	0.107	26.5	0.204	38.5	0.367
3.0	0.054	15.0	0.110	27.0	0.209	39.0	0.375
3.5	0.055	15.5	0.113	27.5	0.215	39.5	0.384
4.0	0.057	16.0	0.116	28.0	0.220	40.0	0.393
4.5	0.059	16.5	0.119	28.5	0.226	40.5	0.402
5.0	0.061	17.0	0.123	29.0	0.231	41.0	0.412
5.5	0.063	17.5	0.126	29.5	0.237	41.5	0.421
6.0	0.065	18.0	0.130	30.0	0.243	42.0	0.431
6.5	0.067	18.5	0.133	30.5	0.249	42.5	0.441
7.0	0.069	19.0	0.137	31.0	0.256	43.0	0.451
7.5	0.071	19.5	0.141	31.5	0.262	43.5	0.461
8.0	0.073	20.0	0.145	32.0	0.269	44.0	0.471
8.5	0.075	20.5	0.149	32.5	0.275	44.5	0.482
9.0	0.078	21.0	0.153	33.0	0.282	45.0	0.493
9.5	0.080	21.5	0.157	33.5	0.289	45.5	0.504
10.0	0.082	22.0	0.161	34.0	0.296	46.0	0.515
10.5	0.085	22.5	0.165	34.5	0.303	46.5	0.526
11.0	0.087	23.0	0.170	35.0	0.311	47.0	0.538
11.5	0.090	23.5	0.174	35.5	0.318	47.5	0.550
12.0	0.092	24.0	0.179	36.0	0.326	48.0	0.562
12.5	0.095	24.5	0.184	36.5	0.334	48.5	0.574

TABLE 2.5
Number of the day in the year (J)

Day	January	February	March*	April*	May*	June*
1	1	32	60	91	121	152
2	2	33	61	92	122	153
3	3	34	62	93	123	154
4	4	35	63	94	124	155
5	5	36	64	95	125	156
6	6	37	65	96	126	157
7	7	38	66	97	127	158
8	8	39	67	98	128	159
9	9	40	68	99	129	160
10	10	41	69	100	130	161
11	11	42	70	101	131	162
12	12	43	71	102	132	163
13	13	44	72	103	133	164
14	14	45	73	104	134	165
15	15	46	74	105	135	166
16	16	47	75	106	136	167
17	17	48	76	107	137	168
18	18	49	77	108	138	169
19	19	50	78	109	139	170
20	20	51	79	110	140	171
21	21	52	80	111	141	172
22	22	53	81	112	142	173
23	23	54	82	113	143	174
24	24	55	83	114	144	175
25	25	56	84	115	145	176
26	26	57	85	116	146	177
27	27	58	86	117	147	178
28	28	59	87	118	148	179
29	29	(60)	88	119	149	180
30	30	-	89	120	150	181
31	31	-	90	-	151	-

TABΛE 2.□ add 1 if leap year

J can be determined for each day (D) of month (M) by
J = **INTEGER**(275 M/9 – 30 + D) – 2
IF (M < 3) **THEN** J = J + 2
also, **IF** (leap year and (M > 2)) **THEN** J = J + 1
For ten-day calculations, compute J for day D = 5, 15 and 25
For monthly calculations, J at the middle of the month is approximately given by
J = **INTEGER**(30.4 M – 15)

TABLE 2.5 (continued)
Number of the day in the year (J)

Day	July*	August*	September*	October*	November*	December*
1	182	213	244	274	305	335
2	183	214	245	275	306	336
3	184	215	246	276	307	337
4	185	216	247	277	308	338
5	186	217	248	278	309	339
6	187	218	249	279	310	340
7	188	219	250	280	311	341
8	189	220	251	281	312	342
9	190	221	252	282	313	343
10	191	222	253	283	314	344
11	192	223	254	284	315	345
12	193	224	255	285	316	346
13	194	225	256	286	317	347
14	195	226	257	287	318	348
15	196	227	258	288	319	349
16	197	228	259	289	320	350
17	198	229	260	290	321	351
18	199	230	261	291	322	352
19	200	231	262	292	323	353
20	201	232	263	293	324	354
21	202	233	264	294	325	355
22	203	234	265	295	326	356
23	204	235	266	296	327	357
24	205	236	267	297	328	358
25	206	237	268	298	329	359
26	207	238	269	299	330	360
27	208	239	270	300	331	361
28	209	240	271	301	332	362
29	210	241	272	302	333	363
30	211	242	273	303	334	364
31	212	243	-	304	-	365

* add 1 if leap year

TABLE 2.8
σT_K^4 (Stefan-Boltzmann law) at different temperatures (T)

With $\sigma = 4.903\ 10^{-9}$ MJ K^{-4} m^{-2} day^{-1}
and $T_K = T[°C] + 273.16$

T (°C)	σT_K^4 (MJ m^{-2} d^{-1})	T (°C)	σT_K^4 (MJ m^{-2} d^{-1})	T (°C)	σT_K^4 (MJ m^{-2} d^{-1})
1.0	27.70	17.0	34.75	33.0	43.08
1.5	27.90	17.5	34.99	33.5	43.36
2.0	28.11	18.0	35.24	34.0	43.64
2.5	28.31	18.5	35.48	34.5	43.93
3.0	28.52	19.0	35.72	35.0	44.21
3.5	28.72	19.5	35.97	35.5	44.50
4.0	28.93	20.0	36.21	36.0	44.79
4.5	29.14	20.5	36.46	36.5	45.08
5.0	29.35	21.0	36.71	37.0	45.37
5.5	29.56	21.5	36.96	37.5	45.67
6.0	29.78	22.0	37.21	38.0	45.96
6.5	29.99	22.5	37.47	38.5	46.26
7.0	30.21	23.0	37.72	39.0	46.56
7.5	30.42	23.5	37.98	39.5	46.85
8.0	30.64	24.0	38.23	40.0	47.15
8.5	30.86	24.5	38.49	40.5	47.46
9.0	31.08	25.0	38.75	41.0	47.76
9.5	31.30	25.5	39.01	41.5	48.06
10.0	31.52	26.0	39.27	42.0	48.37
10.5	31.74	26.5	39.53	42.5	48.68
11.0	31.97	27.0	39.80	43.0	48.99
11.5	32.19	27.5	40.06	43.5	49.30
12.0	32.42	28.0	40.33	44.0	49.61
12.5	32.65	28.5	40.60	44.5	49.92
13.0	32.88	29.0	40.87	45.0	50.24
13.5	33.11	29.5	41.14	45.5	50.56
14.0	33.34	30.0	41.41	46.0	50.87
14.5	33.57	30.5	41.69	46.5	51.19
15.0	33.81	31.0	41.96	47.0	51.51
15.5	34.04	31.5	42.24	47.5	51.84
16.0	34.28	32.0	42.52	48.0	52.16
16.5	34.52	32.5	42.80	48.5	52.49

TABLE 2.9
Conversion factors to convert wind speed measured at given height (over grass) to wind speed measured at standard height of 2 m above ground surface

$$\text{conversion factor} = \frac{4.87}{\ln(67.8\ z - 5.42)} \qquad \textbf{(Eq. 47)}$$

z height (m)	conversion factor	z height (m)	conversion factor	z height (m)	conversion factor	z height (m)	conversion factor
-	-	2.2	0.980	4.2	0.865	6.0	0.812
-	-	2.4	0.963	4.4	0.857	6.5	0.802
-	-	2.6	0.947	4.6	0.851	7.0	0.792
-	-	2.8	0.933	4.8	0.844	7.5	0.783
1.0	1.178	3.0	0.921	5.0	0.838	8.0	0.775
1.2	1.125	3.2	0.910	5.2	0.833	8.5	0.767
1.4	1.084	3.4	0.899	5.4	0.827	9.0	0.760
1.6	1.051	3.6	0.889	5.6	0.822	9.5	0.754
1.8	1.023	3.8	0.881	5.8	0.817	10.0	0.748
2.0	1.000	4.0	0.872	6.0	0.812	10.5	0.742

Annex 3

Background on physical parameters used in evapotranspiration computations

Latent Heat of Vaporization (λ)[1]

$$\lambda = 2.501 - (2.361 \times 10^{-3}) T \qquad (3\text{-}1)$$

where: λ latent heat of vaporization [MJ kg^{-1}]
T air temperature [$^{\circ}C$]

The value of the latent heat varies only slightly over normal temperature ranges. A single value may be taken (for $T = 20\ ^{\circ}C$): $\lambda = 2.45$ MJ kg^{-1}.

Atmospheric Pressure (P)[2]

$$P = P_o \left(\frac{T_{Ko} - \alpha_l (z - z_o)}{T_{Ko}} \right)^{\frac{g}{\alpha_l R}} \qquad (3\text{-}2)$$

where: P atmospheric pressure at elevation z [kPa]
P_o atmospheric pressure at sea level = 101.3 [kPa]
z elevation [m]
z_o elevation at reference level [m]
g gravitational acceleration = 9.807 [m s^{-2}]
R specific gas constant = 287 [J kg^{-1} K^{-1}]
a_l constant lapse rate moist air = 0.0065 [K m^{-1}]
T_{Ko} reference temperature [K] at elevation z_o given by

$$T_{Ko} = 273.16 + T \qquad (3\text{-}3)$$

where: T mean air temperature for the time period of calculation [^{o}C]

---

[1] Reference: Harrison (1963)

[2] Reference: Burman *et al.* (1987)

When assuming P_o = 101.3 [kPa] at z_o = 0, and T_{Ko} = 293 [K] for T = 20 [°C], equation (3-3) becomes:

$$P = 101.3\left(\frac{293 - 0.0065z}{293}\right)^{5.26} \tag{3-4}$$

Atmospheric Density (ρ)[3]

$$\rho = \frac{1000\,P}{T_{Kv}\,R} = 3.486\frac{P}{T_{Kv}} \tag{3-5}$$

where: ρ atmospheric density [kg m^{-3}]
R specific gas constant = 287 [J kg^{-1} K^{-1}]
T_{Kv} virtual temperature [K]

$$T_{Kv} = T_K\left(1 - 0.378\frac{e_a}{P}\right)^{-1} \tag{3-6}$$

where: T_K absolute temperature [K] : T_K = 273.16 + T [°C]
e_a actual vapour pressure [kPa]

For average conditions (e_a in the range 1 - 5[kPa] and P between 80 - 100 [kPa]), equation (3-6) may be substituted by:

$$T_{Kv} \approx 1.01(T + 273) \tag{3-7}$$

T is set equal to mean daily temperature for 24-hour calculation time steps.

Saturation Vapour Pressure (e_S)[4]

$$e^o(T) = 0.611\exp\left(\frac{17.27\,T}{T + 237.3}\right) \tag{3-8}$$

where: $e^o(T)$ saturation vapour pressure function [kPa]
T air temperature [°C]

[3] Reference: Smith *et al.* (1991)

[4] Reference: Tetens (1930)

Slope Vapour Pressure Curve (Δ)[5]

$$\Delta = \frac{4098\, e°(T)}{(\mathrm{T}+237.3)^2} = \frac{2504 \exp\left(\frac{17.27\,\mathrm{T}}{\mathrm{T}+237.2}\right)}{(\mathrm{T}+237.3)^2} \qquad (3\text{-}9)$$

where: Δ slope vapour pressure curve [kPa °C^{-1}]
T air temperature [°C]
e°(T) saturation vapour pressure at temperature T [kPa]

In 24-hour calculations, Δ is calculated using mean daily air temperature. In hourly calculations T refers to the hourly mean, T_{hr}.

Psychrometric Constant (γ)[6]

$$\gamma = \frac{cp\,P}{\varepsilon\,\lambda} \times 10^{-3} = 0.00163\,\frac{P}{\lambda} \qquad (3\text{-}10)$$

where: γ psychrometric constant [kPa °C^{-1}]
c_p specific heat of moist air = 1.013 [kJ kg^{-1} °C^{-1}]
P atmospheric pressure [kPa]: equations 2 or 4
ε ratio molecular weight of water vapour/dry air = 0.622
λ latent heat of vaporization [MJ kg^{-1}]

Dew Point Temperature (T_{dew})[7]

When it is not observed, T_{dew} can be computed from e_a by:

$$\mathrm{T_{dew}} = \frac{116.91 + 237.3\,\ln(\mathrm{e_a})}{16.78 - \ln(\mathrm{e_a})} \qquad (3\text{-}11)$$

where: T_{dew} dew point temperature [°C]
e_a actual vapour pressure [kPa]

For the case of measurements with the Assmann psychrometer, T_{dew} can be calculated from

$$\mathrm{T_{dew}} = (112 + 0.9\,\mathrm{T_{wet}})\left(\frac{\mathrm{e_a}}{\mathrm{e^o(T_{wet})}}\right)^{1/8} - 112 + 0.1\,\mathrm{T_{wet}} \qquad (3\text{-}12)$$

---

[5] References: Tetens (1930), Murray (1967)

[6] Reference: Brunt (1952)

[7] Reference: Bosen (1958); Jensen *et al.* (1990)

Short Wave Radiation on a Clear-Sky Day (R_{so})[8]

The calculation of R_{so} is required for computing net long wave radiation and for checking calibration of pyranometers and integrity of R_{so} data. Q good approximatino for R_{so} for daily and hourly periods is:

$$R_{so} = \left(0.75 + 2 \text{x} 10^{-5}\ z\right) R_a \qquad (3\text{-}13)$$

where: z station elevation [m]
R_a extraterrestrial radiation [MJ m^{-2} d^{-1}]

Equation (3-13) is valid for station elevations less than 6000 m having low air turbidity. The equation was developed by linearizing Beer's radiation extinction law as a function of station elevation and assuming that the average angle of the sun above the horizon is about 50^o.

For areas of high turbidity caused by pollution or airborne dust or for regions where the sun angle is significantly less than 50^o so that the path length of radiation through the atmosphere is increased, an adaption of Beer's law can be employed where P is used to represent atmospheric mass:

$$R_{so} = R_a \exp\left(\frac{-0.0018\ P}{K_t\ \sin\phi}\right) \qquad (3\text{-}14)$$

where: K_t turbidity coefficient [], $0 < K_t \leq 1.0$ where $K_t = 1.0$ for clean air and $K_t = 1.0$ for extremely trubid, dusty or polluted air.
P atmospheric pressure [kPa]
ϕ angle of the sun above the horizon [rad]
R_a extraterrestrial radiation [MJ m^{-2} d^{-1}]

For hourly or shorter periods ϕ is calculated as:

$$\sin\phi = \sin\varphi\ \sin\delta + \cos\varphi\ \cos\delta\ \cos\omega \qquad (3\text{-}15)$$

where: φ latitude [rad]
δ solar declination [rad] (Equation 24 in Chapter 3)
ω solar time angle at midpoint of hourly or shorter period [rad] (Equation (31) in chapter 3)

For 24-hour periods, the mean daily sun angle, weighted according to R_a, can be approximated as:

[8] Reference: Allen (1996)

$$\sin\phi_{24} = \sin\left[0.85 + 0.3\varphi\sin\left(\frac{2\pi}{365}J - 1.39\right) - 0.42\varphi^2\right] \quad (3\text{-}16)$$

where: ϕ_{24} average ϕ during the daylight period, weighted according to R_a [rad]
φ latitude [rad]
J day in the year []

The ϕ_{24} variable is used in Equation (3-14) or (3-18) to represent the average sun angle during daylight hours and has been weighted to represent integrated 24-hour transmission effects on 24-hour R_{so} by the atmosphere. ϕ_{24} in Equation (3-16) should be limited to ≥ 0.

In some situations, the estimation for R_{so} can be improved by modifying Equation (3-14) to consider the effects of water vapour on short wave absorption, so that:

$$R_{so} = (K_B + K_D) R_a \quad (3\text{-}17)$$

where: K_B the clearness index for direct beam radiation []
K_D the corresponding index for diffuse beam radiation []
R_a extraterrestrial radiation [MJ m^{-2} d^{-1}]

$$K_B = 0.98\exp\left[\frac{-0.00146\ P}{K_t \sin\phi} - 0.091\left(\frac{W}{\sin\phi}\right)^{0.25}\right] \quad (3\text{-}18)$$

where: K_t turbidity coefficient [], $0 < K_t \leq 1.0$ where $K_t = 1.0$ for clean air and $K_t = 1.0$ for extremely trubid, dusty or polluted air.
P atmospheric pressure [kPa]
ϕ angle of the sun above the horizon [rad]
W precipitable water in the atmosphere [mm]

$$W = 0.14 e_a P + 2.1 \quad (3\text{-}19)$$

where: W precipitable water in the atmosphere [mm]
e_a actual vapour pressure [kPa]
P atmospheric pressure [kPa]

The diffuse radiation index is estimated from K_B:

$$\begin{aligned} K_D &= 0.35 - 0.33 K_B \quad \text{for } K_B \geq 0.15 \\ K_D &= 0.18 + 0.82 K_B \quad \text{for } K_B < 0.15 \end{aligned} \quad (3\text{-}20)$$

As with Equation (3-14), the ϕ_{24} variable from Equation (16) is used for ϕ in Equation (3-18) for 24-hour estimates of R_{so}.

Ordinarily, R_{SO} computed using Equations (3-13), (3-14) or (3-16) should plot as an upper envelope of measured R_S and is useful for checking calibration of instruments. This is illustrated in Annex 5.

Annex 4

Statistical analysis of weather data sets[1]

COMPLETING A DATA SET

Quite often data sets containing a weather variable Y_i observed at a given station are incomplete due to short interruptions in observations. Interruptions can be due to a large number of causes, the most frequent being the breakage or malfunction of instruments during a certain time period. When data are missing, it may be appropriate to complete these data sets from observations X_i from another nearby and reliable station. However, to use portions of data set X_i to replace data set Y_i, both data sets X_i and Y_i must be homogeneous. In other words, they need to represent the same conditions. The procedure for completing data sets is applied after the test for homogeneity and any needed correction for nonhomogeneity has been performed. The substitution procedure proposed herein consists of using an appropriate regression analysis.

The procedure for substituting nearby data into an incomplete data set can be summarized as follows:

1. Select a nearby weather station for which the data set length covers all periods for which data are missing.

2. Characterize the data sets from the nearby station, X_i, and of the station having missing data, Y_i, by computing the mean $\overline{x}$ and the standard deviation s_x for the data set X_i:

$$\overline{x} = \sum_{i=1}^{n} x_i \; / \; n \tag{4-1}$$

$$s_x = \left(\sum_{i=1}^{n} \left(x_i - \overline{x} \right)^2 / \left(n - 1 \right) \right)^{1/2} \tag{4-2}$$

and the mean $\overline{y}$ and standard deviation s_y for data set Y_i:

$$\overline{y} = \sum_{i=1}^{n} y_i \; / \; n \tag{4-3}$$

[1] With contributions from J.L. Teixeira, Instituto Superior de Agronomia, Lisbon, Portugal.

$$s_y = \left(\sum_{i=1}^{n} (y_i - \bar{y})^2 / (n - 1) \right)^{1/2} \quad (4\text{-}4)$$

for the periods when the data in both data sets are present, where x_i and y_i are individual observations from data sets X_i and Y_i, and n is the number of observations in each set.

3. Perform a regression of y on x for the periods when the data in both data sets are present:

$$\hat{y}_i = a + b\, x_i \quad (4\text{-}5)$$

with

$$b = \frac{cov_{xy}}{s_x^2} = \frac{\sum_{i=1}^{n} (x_i - \bar{x})(y_i - \bar{y})}{\sum_{i=1}^{n} (x_i - \bar{x})^2} \quad (4\text{-}6)$$

$$a = \bar{y} - b\,\bar{x} \quad (4\text{-}7)$$

where a and b are emprical regression constants, and cov_{xy} is the covariance between X_i and Y_i. Plot all points x_i and y_i and the regression line for the range of observed values. If deviations from the regression line increase as y increases then substitution is not recommended because this indicates that the two sites have a different behaviour relative to the particular weather variable, and they may not be homogeneous. Another nearby station should be selected.

4. Compute the correlation coefficient r:

$$r = \frac{cov_{xy}}{s_x\, s_y} = \frac{\sum_{i=1}^{n} (x_i - \bar{x})(y_i - \bar{y})}{\left(\sum_{i=1}^{n} (x_i - \bar{x})^2 \sum_{i=1}^{n} (y_i - \bar{y})^2 \right)^{1/2}} \quad (4\text{-}8)$$

Both a high r^2 ($r^2 \geq 0.7$) and a value for b that is within the range ($0.7 \leq b \leq 1.3$) indicate good conditions and perhaps sufficient homogeneity for replacing missing data in the incomplete data series. These parameters r^2 and b can be used as criteria for selecting the best nearby station.

5. Compute the data for the missing periods k = n + 1, n + 2…, m using the regression equation caracterized by the parameters a and b (equations 4-6 and 4-7), thus

$$\hat{y}_k = a + b\, x_k \quad (4\text{-}9)$$

6. The complete data set with dimension m will now be

$$\begin{aligned} Y_j &= y_i && (j = i = 1,\ldots,n) \\ Y_j &= \bar{y}_k && (j = k = n+1,\ n+2,\ldots,m) \end{aligned} \qquad (4\text{-}10)$$

Note that estimates $Y_j = \bar{y}_k$ taken from the regression equations are useful for predicting evapotranspiration. However, they cannot be treated as random variables[2].

ANALYSIS OF THE HOMOGENEITY OF DATA SERIES

Weather data collected at a given weather station during a period of several years may be not homogeneous, i.e., the data set representing a particular weather variable may present a sudden change in its mean and variance in relation to the original values. This phenomenon may occur due to several causes, some of which are related to changes in instrumentation and observation practices, and others which relate to modification of the environmental conditions of the site, such as rapid urbanization or, on the contrary, perhaps development of irrigation in the area.

Changes relative to data collection may be caused by:

- change in type of sensor or instrument;
- change in the observer and or change in the timing of observations;
- "sleeping" data collector;
- deterioration of sensors, such as with some types of pyranometers and RH sensors, or malfunctionning of mechanical parts, such as with a tipping bucket rain gauge, or by an intermittently broken or shorted wire;
- aging of bearings on anemometers;
- use of incorrect calibration coefficients;
- variation in power supply or electronic behaviour of instruments;
- growth of trees or planting of tall crops or construction of buildings or fences near a raingauge, anemometer, or evaporation pan;
- change in the location of the weather station, or in the types of shelters for housing temperature and humidity sensors;
- change in the watering, type or maintenance of vegetation in the vicinity of the weather station;
- significant change in the watering or type of vegetation of the region surrounding the weather station.

These changes cause observations made prior to the change to belong to a statistically different population than data collected after the change. It is therefore necessary to apply appropriate techniques to evaluate whether a given data set can be considered to be

---

2 To create random values,, one can add to $\bar{y}_k$ (equation 4-9) the residuals ε_k synthetically generated from a population $\mathcal{N}(0, s_{y,x})$. The residuals are created using tables of random numbers. In that case the estimates Y_j can be treated as random variables.

homogeneous and, if not, to introduce the appropriate corrections. To do so requires the identification of which sub-data series is to be corrected. To do this requires local information.

Procedures indicated herein are simple but are well proven in practice. They rely upon the statistical comparison of two data sets, one considered homogeneous and constituted by the observations X_i, the other being the one under analysis and consitutued by the observations Y_i of the same weather variable (T_{max}, T_{min}, u_2, RH_{max},..., etc). Both sets X_i and Y_i should be collected at two stations that are in the same climatic region, i. e., X_i and Y_i should present the same trends in time despite the space variability when short time scales (daily, weekly or decadaily) are utilized.

The reference observations X_i are selected from a weather station for which the data set can be considered to be homogeneous.(3) The X_i data set should have the same time length of observations as the set of observations Y_i.

Method of Cumulative Residuals

When relating two weather data sets from two weather stations, where the first is considered to be homogeneous, the data set of the second station can be considered to be homogeneous if the cumulative residuals of the second data set from a regression line based on the first data set are not biased. The bias hypothesis can be tested for a given probability p. This is done by verifying whether the residuals can be contained within an elipsis that has axis α and axis β. The magnitudes of α and β depend on the size of the data set, on the standard deviation of the sample being tested and on the probability p used to test the hypothesis(4).

The procedure for analysing the homogeneity of a weather data set Y_i collected in a given weather station environment can be summarized as follows:

1. Select a reference weather station inside the same climatic region that is known to have an homogeneous data set X_i of the same weather variable. As an alternative, construct a "regional" homogeneous data set by averaging the observations at several weather stations in the same region.

2. Organize both data sets x_i and y_i in chronological order i = 1, 2,..., n, where the starting time and time increment are identical for both data sets.

3. For both data sets, compute the mean and standard deviation (equations 1 to 4) for the homogeneous variable (x_i) and for the variable to be tested (y_i).

---

3 When, for a given climatic region, there is no information concerning the homogeneity of data, then the average of observations of the same variable from all stations (excluding the one in the analysis), $X_i = \sum X_{j,\,i} / m$, can be used to constitute the homogeneous data set.

4 This test utilizes results from residuals from the linear regression of Y on X. The residuals should follow a normal distribution with mean zero and standard deviation $s_{y,x}$, i.e. the error $\varepsilon_i \in \mathcal{N}(0,s_{y,x})$. The residuals from the regression should be considered to be independent random variables (i.e., they should exhibit homoscedaticity).

FIGURE 4.1
Regression between two sets of weather data, with the X data set being homogeneous. The example shows that the homoscedaticity condition was satisfied.

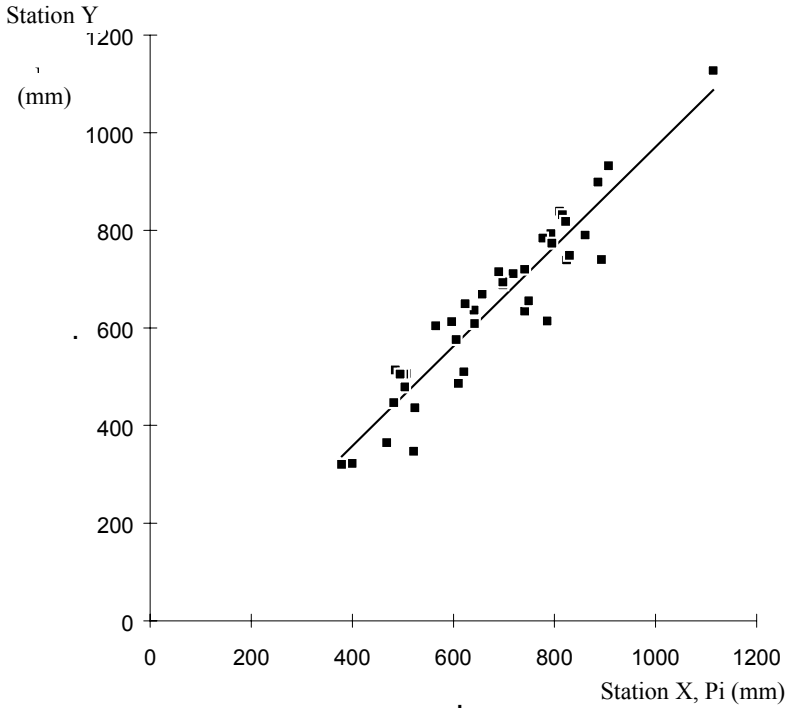

4. Calculate the regression line between the two variables y_i and x_i and the associated correlation coefficient (equations 4-5 to 4-8). The regression equation among the full sets is expressed as

$$\hat{y}_i = a_f + b_f x_i \qquad (i = 1, 2, \ldots, n) \qquad (4\text{-}11)$$

where the subscript f refers to the full set. Whenever possible, plot x_i, y_i and the regression line to visually verify whether the homoscedaticity hypothesis[5] can be accepted (see Figure 4.1)[6]

5. Compute the residuals of the observed y_i values to the regression line (equation 4-5), the standard deviation $s_{y,x}$ of the residuals and the corresponding cumulative residual E_i:

---

5 The homoscedaticity hyphotesis is accepted when the residuals ε_i of the dependent variable to the regression line (equation 4-5) can be considered to be independent random variables. This can be visually assessed when the deviations of y_i to the regression estimates $\hat{y}_i$ are within the same range for all x_i, i.e., when these deviations are not increasing (or decreasing) with increasing values of x_i.

6 Data in this example were provided by J.L. Teixeira (personal communication, 1995).

$$\varepsilon_i = y_i - \bar{y}_i \tag{4-12}$$

$$s_{y,x} = s_y \left(1 - r^2\right)^{1/2} \tag{4-13}$$

$$E_i = \varepsilon_i + \sum_{j=1}^{i-1} \varepsilon_j \qquad (j = 1,\ldots i-1) \tag{4-14}$$

6. Select a probability p for accepting the hypothesis of homogeneity. The value p = 80% is commonly utilized. Then compute the elipsis equation having axes

$$\alpha = n/2 \tag{4-15}$$

$$\beta = \frac{n}{(n-1)^{1/2}} z_p s_{y,x} \tag{4-16}$$

where:

n	size of the sample under analysis
z_p	standard normal variate for the probability p (usually p = 80% for non excedancy): Table 4.1
$s_{y,x}$	standard deviation of the residuals of y (equation 4-13)

The parametric equation of the elipsisis is then

$$\begin{aligned} X &= \alpha \cos(\theta) \\ Y &= \beta \sin(\theta) \end{aligned} \tag{4-17}$$

with θ [rad] varying from 0 to 2 π.

TABLE 4.1
Value of the standard normal variate z_p for selected probabilities P of non-excedance

p (%)	z_p	p (%)	z_p
50	0.00	80	0.84
60	0.25	85	1.04
70	0.52	90	1.28
75	0.67	95	1.64

Note: given the symmetry of the normal distribution, the values for p < 50% correspond to (100 - p) but with the opposite sign. Ex: p = 20% is associated with z = $-z_{80}$ = -0.84

It can therefore be concluded, at the level of probability p, that there is no bias in the distribution of residuals, i.e., the data set y_i is considered to be homogeneous, when the computed values for E_i fall inside the elipsis (equation 4-17).

7. Plot the cumulative residuals E_i against time using the time scale (interval) of the variable under analysis (Figure 4-2).

8. Draw the elipsis on the same plot and verify whether the E_i all lie inside the elipsis. If they do, then the hypothesis of homogeneity is accepted at the p level of confidence (Figure 4.4).

FIGURE 4.2
Plot of cumulative residuals against time and associated elipsis for the probability p = 80%, with results indicating that data set Y is not homogeneous (relative to data set X).

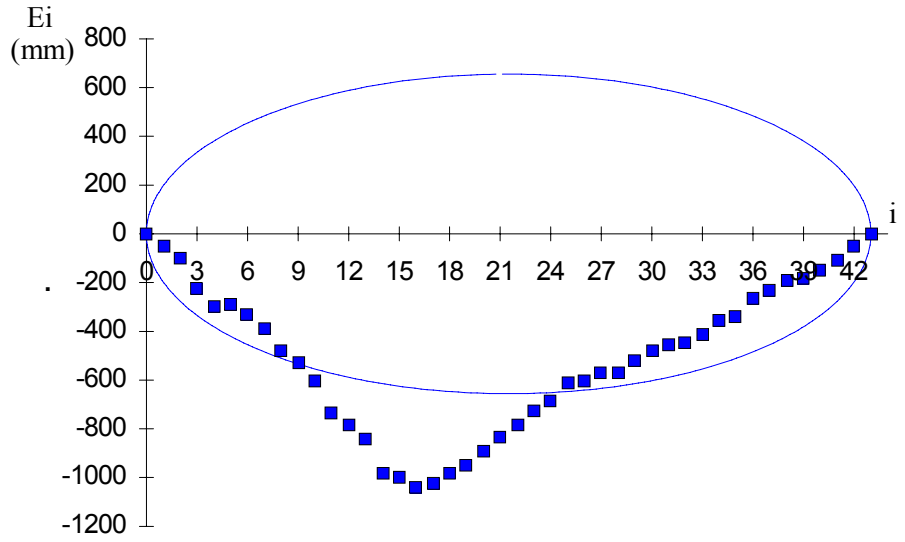

9. If the hypothesis of homogeneity cannot be accepted (this is the case in Figure 4.2), then one can select the break point where it appears that E_i ceases to increase (or to decrease) and begins to decrease (or to increase), for example at I = 16 in Figure 4.2. This break point is termed k = i.

10. The data set is now divided into two subsets, the first from 1 to k, the second from k + 1 to n. Then, new regression equations are computed between Y and X for both subsets. If we presume that the second subset is homogeneous but that the first is not, then we have

$$\bar{y}_i = a_{nh} + b_{nh} x_i \qquad (i = 1, 2, \ldots, k) \qquad (4\text{-}18)$$

and

$$\bar{y}_i = a_h + b_h x_i \qquad (i = k + 1, k + 2, \ldots, n) \qquad (4\text{-}19)$$

where the subscripts h and nh identify the regression coefficients of the homogeneous and the non homogeneous subsets, respectively (see Figure 4-3).

11. Compute the differences between the two regression lines

$$\Delta \bar{y}_i = \left(a_h + b_h x_i\right) - \left(a_{nh} + b_{nh} x_i\right) \qquad (4\text{-}20)$$

for the non homogeneous set (i = 1, 2, …, k)

FIGURE 4.3
The regression lines for the two subsets obtained from the data sets of Figures 4.1 and 4.2. Selection was made after definition of the break point in Figure 4.2.

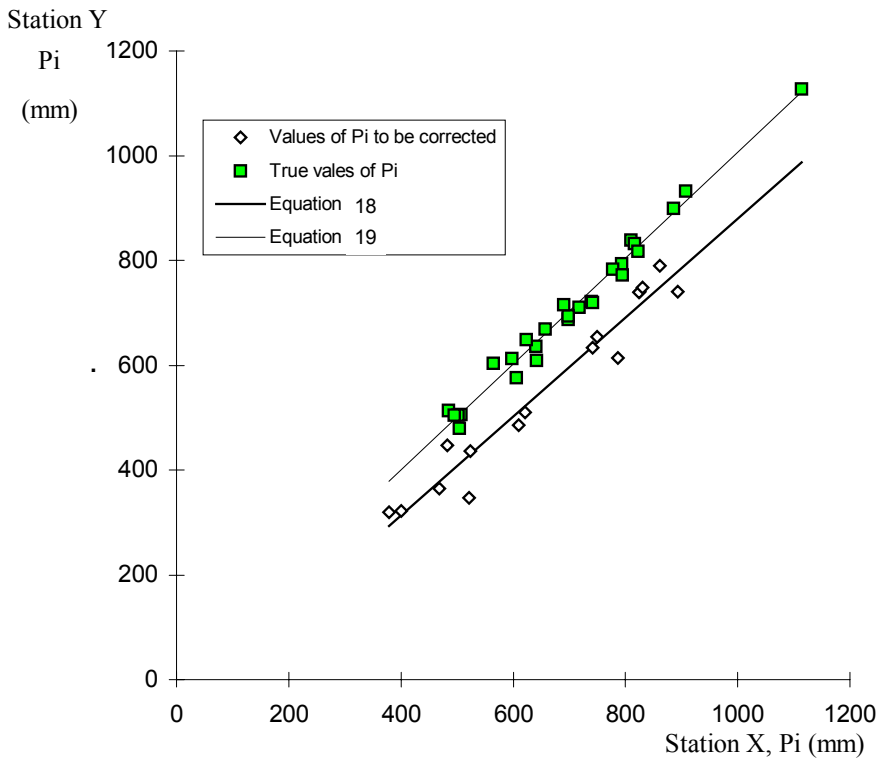

FIGURE 4.4
Plot of cumulative residuals against time and the associated elipsis for p = 80% after correction of variable y.

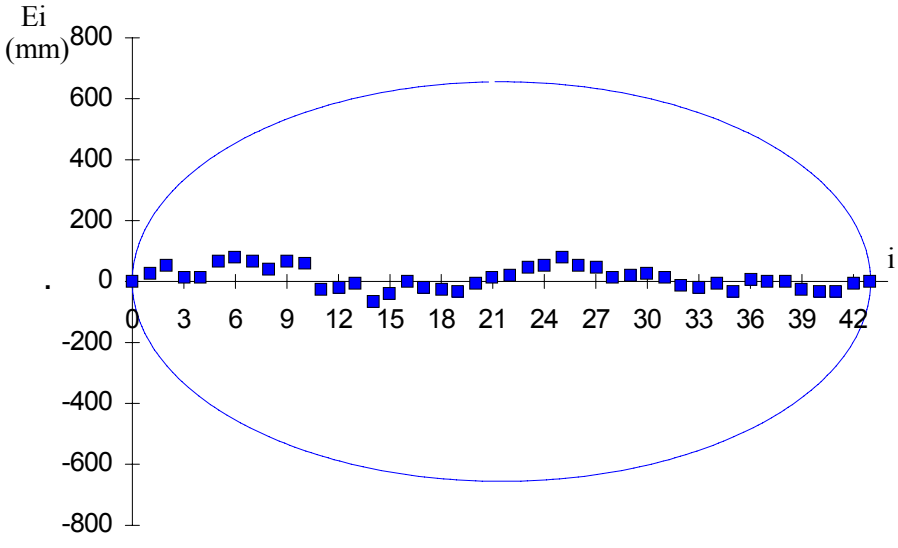

12. Correct the non homogeneous subset portion of data set Y

$$y_{c,i} = y_i + \Delta\bar{y}_i \qquad (i = 1, 2, \ldots, k) \qquad (4\text{-}21)$$

where the subscript c identifies the corrected values. Thus, the corrected, homogeneous full set for weather variable Y is composed by

$$\begin{aligned} Y_i &= y_{c,i} \quad \text{for} \quad i = 1, 2, \ldots, k \\ Y_i &= y_i \quad \text{for} \quad i = k + 1, k + 2, \ldots, n \end{aligned} \qquad (4\text{-}22)$$

A similar procedure would be utilized if it was presumed that the second sub-set requires correction, rather than the first sub-set.

Note that the variables Y_i are still considered to be random variables despite that the mean and the variance have been modified due to the correction introduced. To confirm the results of the correction of data set Y for homogeneity, the homogeneity test methodology can be applied again to the corrected variable Y to provide evidence of homogeneity in the graph of residuals. This has been done in Figure 4.4.

In this example, it was presumed that the latter sub-set (k to I) was the correct (representative) data set, or the data set displaying the desired attributes. It was therefore presumed that prior to time k, the readings were biased by instrument calibration, different location of the station or the instrument within the station, change in type or manufacturer of the instrument, or change in general environment of the station. It appears in Figure 3 that the data prior to i = k were biased downward by approximately 100 mm of annual precipitation.

Double-Mass Technique

The double-mass technique is also useful for assessing homogeneity in a weather parameter. As with the method of cumulative residuals discussed in the last section, the double-mass technique requires data sets from two weather stations, where X_i (i = 1, 2,…,n) is a chronologic data set for a given weather variable observed for a certain time length at a "reference" station, and which is considered to be homogeneous, and where Y_i is a data set of the same variable, with the same time length, observed at another station and for which homogeneity needs to be analysed.

In the double-mass technique, starting with the first observed pair of values X_1 and Y_1, cumulative data sets are created by progressively summing values of X_i and Y_i to verify whether the long term trends in variation of X_i and Y_i are the same. Thus the following cumulative variables are obtained

$$x_i = X_i + \sum_{j=1}^{i-1} X_j \qquad (4\text{-}23)$$

and

FIGURE 4.5
Double mass analysis applied to two series of precipitation when data from station Y are not homogeneous

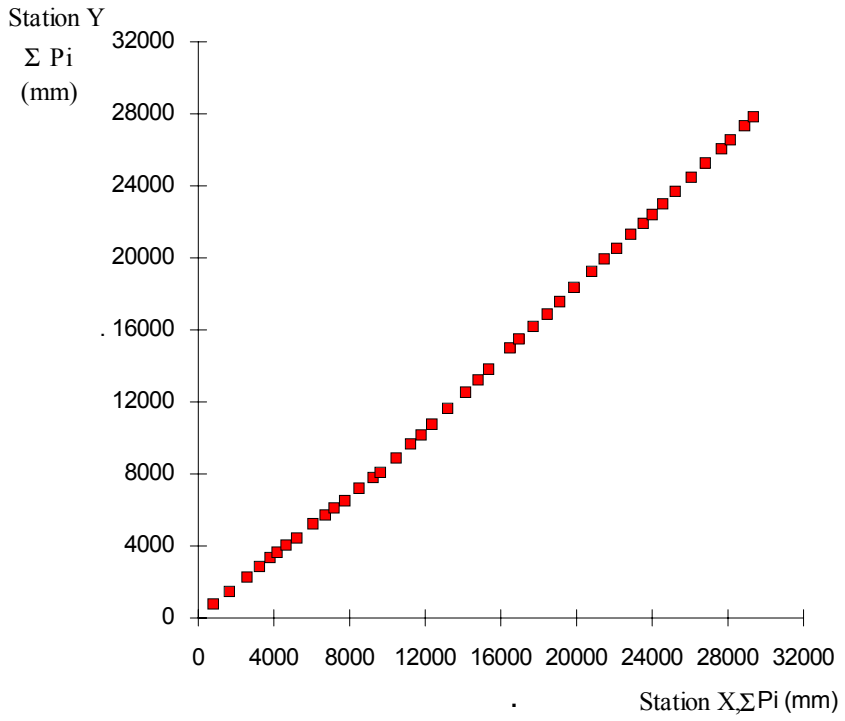

$$y_i = Y_i + \sum_{j=1}^{i-1} Y_j \qquad (4\text{-}24)$$

with $i = 1,\ldots, n$ and $j = 1,\ldots, i - 1$.

These variables x_i and y_i are still considered to be random variables and are characterized by the mean and the standard deviation (equations 4-1 to 4-4). The y_i and x_i variables can be related through linear regression (equations 4-5 to 4-8). However, the double mass technique is typically applied as a graphical procedure.

The graphical application of the double-mass analysis is done by plotting all coordinate points x_i and y_i. The plot is then visually analysed to determine whether successive points of x_i and y_i follow an unique straight line, indicating the homogeneity of the data set Y_i relative to data set X_i. If there appears to be a break (or more than one break) in the the plot of y_i to x_i, then there is a visual indication that the data series Y_i (or perhaps X_i) is not homogeneous (Figure 4.5). The break at coordinates x_k and y_k can be used to separate two subsets ($i = 1, 2, \ldots, k$) and ($k + 1, k + 2,\ldots, n$). One of the subsets is to be corrected. The appropriate one to correct needs to be identified by consulting the records of the weather station, when available.

FIGURE 4.6
Residuals of double mass to the straight line (equation 26) indicating the non homogeneity of the residuals of the series of precipitation of station Y.

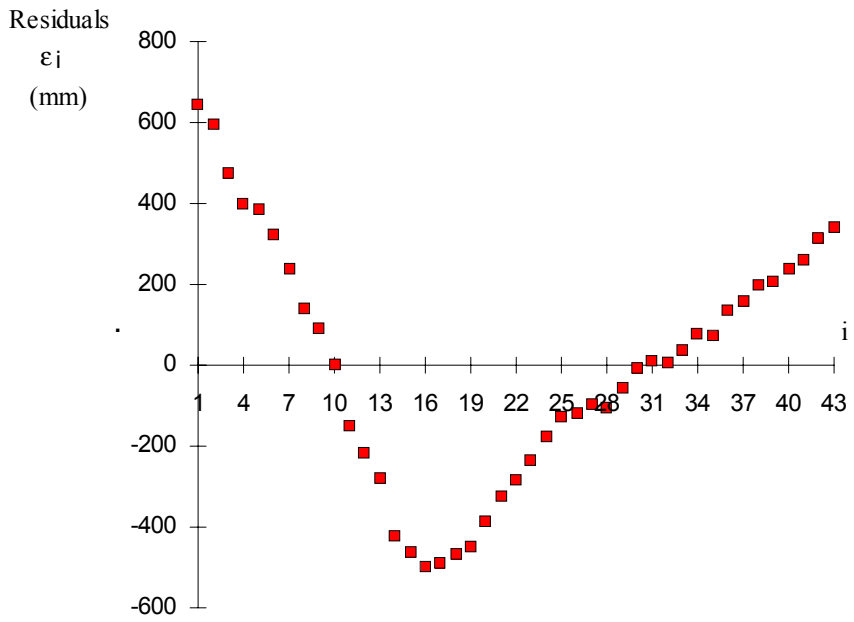

Often, visual interpretation of the double-mass balance is difficult. Thus the following numerical regression procedure is recommended:

1. Compute the regression line through the origin for the full set of data x_i and y_i

$$\bar{y}_i = b\, x_i \qquad (i = 1, 2, \ldots, n) \qquad (4\text{-}25)$$

$$\text{with } b = \sum\left(x_i - \bar{x}\right)\left(y_i - \bar{y}\right) \,/\, \sum\left(x_i - \bar{x}\right)^2$$

2 Compute the residuals to the regression line

$$\varepsilon_i = y_i - b\, x_i \qquad (4\text{-}26)$$

3. Analyse the distribution of residuals. If the residuals plot as independent, random variables, then the set can be considered to be homogeneous. However, if the distribution of residuals is biased over i = k, then the homogeneity hypothesis is rejected. The bias can be visually assessed by plotting (ε_i, i). The example in Figure 4.6 shows that residuals follow a trend of decreasing ε_i until i = k (= 16). Following that, the trend is to increase. This plot demonstrates a bias indicating that the data set Y is not homogeneous.

4. The break point at i = k defines two subsets (i = 1, 2, …, k) and (i = k + 1, k + 2, …, n). Using local information on data collection, the user must decide which subset requires correction.

5. **When the first subset is homogeneous** the following correction procedure can be applied:

a) compute the two regression lines, the first through the origin

$$\hat{y}_i = b_h x_i \qquad (i = 1, 2, \ldots, k) \qquad (4\text{-}27)$$

and

$$\hat{y}_{nh,i} = a_{nh} + b_{nh} x_i \qquad (i = k + 1, k + 2, \ldots, n) \qquad (4\text{-}28)$$

where subscripts h and nh identify respectively the homogenous and non homogeneous subsets.

b) compute the differences between both regression lines for i = k + 1, k + 2, …, n

$$\Delta \hat{y}_i = b_h x_i - \left(a_{nh} + b_{nh} x_i\right) \qquad (4\text{-}29)$$

6. **When the second subset is homogeneous**:

a) compute the regression line for the homogeneous subset (i = k +1, k + 2, …, n) after correcting the coordinates (x_i, y_i) using the coordinates of the break point (x_k, y_k), i.e. moving the origin of coordinates from (0, 0) to (x_k, y_k). This regression is therefore

$$y_i - y_k = b_h \left(x_i - x_k\right) \qquad (4\text{-}30)$$

thus

$$\hat{y}_i = \left(y_k - b_h x_k\right) + b_h x_i \qquad (i = k +1, k + 2, \ldots, n.) \qquad (4\text{-}31)$$

b) compute the regression line for the non homogeneous subset forced to the origin

$$\hat{y}_i = b_{nh} x_i \qquad (i = 1, 2, \ldots, k) \qquad (4\text{-}32)$$

c) compute the differences between the regression lines (4-31) and (4-32)

$$\Delta \hat{y}_i = \left[\left(y_k - b_h x_k\right) + b_h x_i\right] - b_{nh} x_i \qquad (4\text{-}33)$$

7. For both cases, correct the variables y_i corresponding to the non homogeneous subset as

$$y_{c,i} = y_i + \Delta \hat{y}_i \qquad (4\text{-}34)$$

FIGURE 4.7
Double mass after correction of data set Y (case of Figure 4.3)

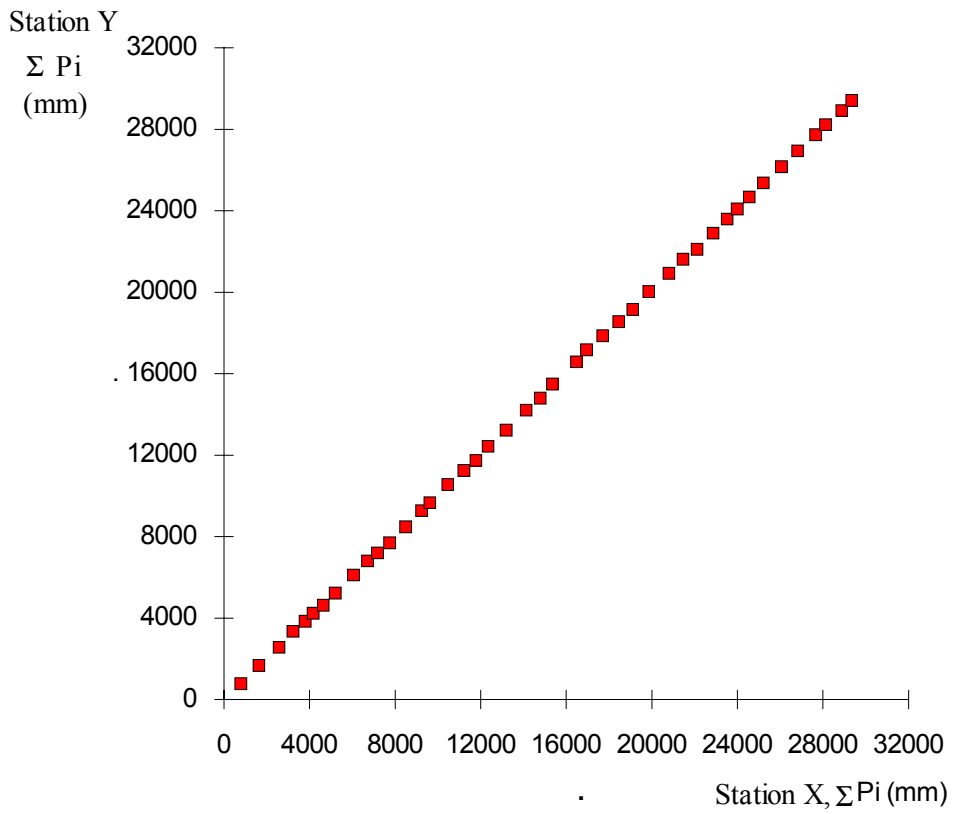

with $\Delta \bar{y}_i$ given by equations (4-29) or (4-33).

8. Compute the corrected estimates of the weather variables Y_i by solving equation (4-24) for Y_i.

Figure 4.7 illustrates the double mass after correction of subset Y in Figure 4.3, where the cumulative sums now follow a straight line.

Figure 4.8 is a plot of the corresponding residuals, which now follow a normal distribution. Similar verification can be easily made by the user. This procedure can be easily applied using a spreadsheet computation and graphical packages that are currently available.

FIGURE 4.8
Residuals of the double mass after correction of data set Y (compare to Figure 4.4)

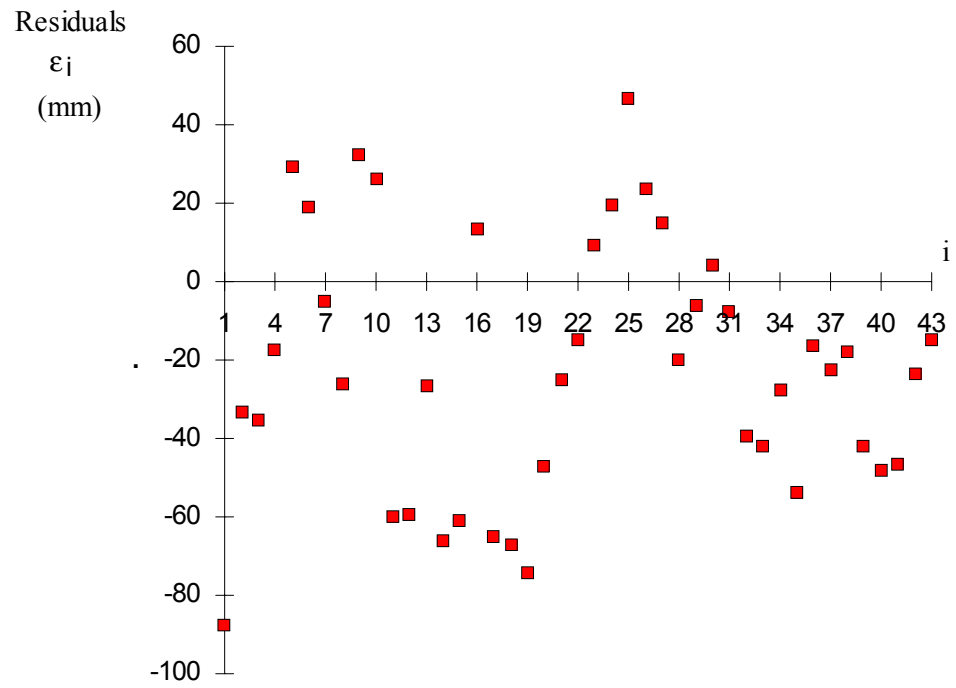

SELECTED BIBLIOGRAPHY ON STATISTICAL ANALYSIS

Dubreuil, P. 1974. *Initiation à l'analyse hydrologique*. Masson & Cie. et ORSTOM, Paris.

Haan, C. T. 1977. *Statistical Methods in Hydrology*. The Iowa State University Press, Ames.

Kite, G. W. 1988. *Frequency and Risk Analyses in Hydrology*. Water Resources Publications, Littleton, CO, 257 pp.

Natural Environment Research Council (NERC) 1975. *Flood Studies Report, Vol I - Hydrology Studies*. Natural Environmental Research Council, London, 550 pp.

NOTATION IN STATISTICAL ANALYSIS

a	regression coefficient
b	regression coefficient
cov_{xy}	covariance of variables x and y
E_i	cumulative residuals
i	number of order of variable x_i in the sample
j, k	number of a variable in a subset
n	size of the sample
p	probability
p (x)	probability distribution density function
r	correlation coefficient
r^2	coefficient of determination
s_x	estimate of the standard deviation of the variable x
s_x^2	estimate of the variance of the variable x
s_y	estimate of the standard deviation of the variable y
s_y^2	estimate of the variance of the variable y
$s_{y,x}$	standard deviation of the residuals of y estimated from the regression
X	random variable
X_i	value of a variable in a data set
x_i	random variable
$\hat{x}_p$	estimated value for the variable x with probability of non excedance p
$\bar{x}$	estimate of the mean, or mean of a sample of the random variable x_i
Y	transformed variable from X
Y_i	value of a variable in a data set
y_i	random variable
$\hat{y}_i$	value of y_i estimated from the regression
$\bar{y}$	estimate of the mean, or mean of a sample of the random variable y_i
Z	standard normal variable
z_p	value of the standard normal variable for the probability p
ε_i	residuals of y estimated from the regression
μ	mean of a population
σ	standard deviation of a population

Annex 5

Measuring and assessing integrity of weather data

Estimates of reference evapotranspiration (ET_o) are no better than weather data upon which they are based. Assessments of weather data integrity and quality need to be conducted before data are utilized in ET_o equations. When necessary and when possible, corrections to the data should be made to account for poor sensor calibration. Some of these corrections are described in section 1 of Annex 4.

A good cautionary statement in data analysis and application is that "no data are better than bad data." This statement applies primarily to measurements of evapotranspiration that are used to develop or to calibrate reference ET equations or to determine crop coefficients. However, it also applies to weather data. When one has no data, one can look to regional weather or ET data summaries for information that might be useful to represent conditions within the local area. In the case of ET data, one might go to a publication such as this one to make reasonably accurate estimates of ET_o and ET_c. However, in the case of "bad" data, meaning biased, or faulty, or nonrepresentative data collected locally, one is "stuck" with weather data and associated predictions of ET_o and ET_c, or with local measurements of ET_c that can be biased, faulty, or nonrepresentative. The result is application of evapotranspiration data or evapotranspiration calculations to irrigation water management, to water resources operations, or to irrigation and water resources systems design that can actually cause more economic and hydrologic problems than if only reasonable estimates or even "textbook" values for ET_c had been used instead. Humanity can be worse off because of faulty data as compared to no data.

Some years ago, when computer modeling was in its infancy, a common cautionary advice was to "do not trust any model until it has been validated using independent data." Today, with some of the more common mathematical models becoming proven and trustworthy, the corollary of this expression is commonly advocated, where "one should not trust any data until they are validated using a model!" Certainly, some place in between these two cautionary advocations is appropriate. Often a valid model can be valuable for evaluating data to identify errors, outliers and biases. And of course, valid data are required for selecting or calibrating a particular model.

This Annex presents guidelines to be used to calculate both extreme ranges for weather data measurements and also means to assess integrity of data that fall between the extremes. A review on instrumentation for agricultural weather stations is given first.

INSTRUMENTATION FOR MEASURING WEATHER VARIABLES[1]

Data Acquisition and Instrumentation

Radiation

Solar radiation is commonly measured with **pyranometers.** Pyranometers measure the shortwave incoming radiation in a solid angle in the shape of a hemisphere oriented upwards. Currently, in the most common "glassed dome" pyranometers, a thermopile is used within the instrument as the sensor, where thermal gradients are measured across hot and cold areas (black and white). The radiation intensity is proportional to the temperature differences between the two sensing areas. Accuracy depends upon the sensitivity of the material used in the sensors, the response time and the distortion characteristics of the material constituting the dome covering the sensors. A second type of pyranometer that is less expensive and that is gaining acceptance is the silicon diode instrument where electric current is generated by a photo sensitive diode in proportion to solar intensity. Ordinarily, silicon diode pyranometers are not fully sensitive to the full spectrum of visible light, so that the calibration of the instrument is only valid for upward solar measurements.

When a pyranometer is oriented downwards it measures the reflected shortwave radiation, and is thus called an **albedometer.** When two pyranometers are associated, one oriented upwards and the other downwards, the net short wave radiation is measured. The instrument is then called a **net pyranometer**. A point of caution is that any instrument used as an albedometer or net pyranameter must have full sensitivity to all spectra of visible light. This is important since the composition of reflected light from vegetation is highly biased toward green. Therefore, most albedometers must be of the glass domed thermopile type and not the photo diode type.

Net radiation is measured by **pyradiometers (or net radiometers)**, which sense both short and long wave radiation. They have two bodies, one oriented upwards and the other downwards, both covering a solid angle in the shape of a hemisphere. The sensors are made from several thermocouples sensing heat generated by radiation from all wavelengths, and are protected by domes made in general of polyethylene treated in a specific manner. The black bodies can loose their sensing capabilities with time, so that these instruments require regular and frequent calibrations. Other **net radiometers** are comprised of ventilated differential thermopiles, but they are very seldom utilized. All radiometers refered to above transform the radiation energy into thermal energy, a portion of which is transformed into an electric voltage gradient that provides appropriate conditions for continuous recording using dataloggers.

Sunshine duration is most commonly recorded with the Campbell-Stokes heliograph. A glass globe focuses the radiation beam to a special recording paper and a trace is burned on the paper as the sun is moving. No records occur when no bright sunshine is sensed. Measurements are reliable when the recording paper is placed in the right position according to the relative position of the sun. Care is required to avoid accumulation of rain water on the paper. The heliograph has to be oriented South in the northern hemisphere and North in the

---

[1] Details on weather station instrumentation can be found in FAO 27 (Doorenbos, 1976), in the WMO Guide to Agrometeorological Practices (WMO, 1981, 1983), or in meteorology handbooks (Seemann *et al.,* 1979; Rosenberg *et al.,* 1983; Kessler *et al.,* 1990).

southern hemisphere. In China, another type of heliograph is used. The solar beam penetrates through an orifice and traces a recording paper treated with a sensible chemical substance. Electronic records of sunshine duration are obtained through the photo-electric or the rotating optical fibre sunshine recorders.

Windspeed

Windspeed is measured using anemometers, always placed at an height not less than 2 m above the ground, and often at 5 m, following recommendations by WMO. Most common are the three-cup anemometers. Also common are propeller anemometers. Measurements by both types are reliable provided that maintenance ensures appropriate functioning of the mechanical parts. Older designs of anemometers utilize mechanical counters as the output device. Modern anemometers may be equipped with generators giving a voltage signal that is proportional to the windspeed. Other anemometers may be equipped with small magnetic reed switches or with opto-electronic couplers that generate electric impulses in proportion to the windspeed. The electronic devices are utilized in automatic weather stations. Accuracy of windspeed measurements depends on the upwind fetch as much as on instrumentation. A large upwind fetch that is free of buildings and trees is definitely required for representative measurements.

Temperature

The most commonly utilized sensor for measuring temperature are still the mercury thermometers. Maximum and minimum thermometers use mercury and alcohol. Bimetallic thermographs are the most common mechanical temperature recorders. They are easy to read and maintain. However, mechanical thermographs do require verification and adjustment of the position of the pen recorder. These instruments are installed in shelters that are naturally ventilated.

Modern temperature sensors have been developed, namely the thermistor and the thermocouple. These provide very accurate analogue measurements and are normally utilized in automatic weather stations. Thermistors provide independent measurements of air or soil temperature, whereas thermocouples require an additional base temperature reading, normally provided by a thermistor. To maintain the accuracy and representativeness of these instruments, they are installed in special radiation shields (shelters) having natural ventilation. Occasionally the shields or shelters are artificially aspirated to reduce biases caused by heat loading from the sun.

Humidity

Dew point temperature is often measured with a mirrorlike metallic surface that is artificially cooled. When dew forms on the surface, its temperature is sensed as T_{dew}. Other dew sensor systems use chemical or electric properties of certain materials that are altered when absorbing water vapour. Instruments for measuring dew point temperature require careful operation and maintenance and are seldom available in weather stations. The accuracy of estimation of the actual vapour pressure from T_{dew} is generally very high.

Relative humidity is measured using hygrometers. Most frequently used in mechanically-based field stations are the hair hygrometers, normally operated as mechanical hygrographs. Measurements loose accuracy with dust and ageing of the hairs. Modern hygrometers use a film from a dielectric polymer that changes its dielectric constant with

changes in surface moisture, thus inducing a variation of the capacity of a condensator using that dielectric. These instruments are normally called dielectric polymer capacitive hygrometers. Accuracy can be higher than for hair hygrometers. These electronic devices are utilized in most modern automatic weather stations.

The **dry and wet bulb temperatures** are measured using psychrometers. Most common are those using two mercury thermometers, one of them having the bulb covered with a wick saturated with distilled water, and which measures a temperature lowered due to the evaporative cooling. When they are naturally ventilated inside a shelter, problems can arise if air flow is not sufficient to maintain an appropriate evaporation rate and associated cooling. The Assmann psychrometer has a forced ventilation of the wet bulb and dry bulb thermometers.

The dry and wet bulb temperature can be measured by thermocouples or by thermistors, the so called thermocouple psychrometers and thermosound psychrometers. These psychrometers are used in automatic weather stations and, when properly maintained and operated, provide very accurate measurements.

ASSESSING INTEGRITY OF WEATHER DATA[2]

Solar Radiation using Clear Sky Comparisons

Pyranometer operation and calibration accuracy can be evaluated for a particular weather location by plotting hourly or daily average readings of solar radiation (R_S) against computed short wave radiation that is expected to occur under clear sky conditions (R_{SO}). R_{SO} can be computed for any day or hour as

$$R_{so} = K_T \, R_a \tag{5-1}$$

where R_a is extraterrestrial radiation[3] and K_T is a "clearness" or transmission index.

R_{SO} computed with equation (5-1) should plot as an upper envelope of measured R_S and is useful to check the calibration of pyranometers. Equations (3-13), (3-14), or (3-17) to (3-20) of Annex 3 should be used for predicting K_T for low air turbidity. Equations (3-14) or (3-17) to (3-20) of Annex 3 are appropriate for areas with high turbidity caused by pollution or airborne dust or for regions where the sun angle is significantly less than 50°.

The example in Figure 5.1 shows one application concerning 24-hour calculations for Logan, Utah, where the highest observed values for R_S correspond to the envelope of calculated R_{SO}, thus showing appropriate calibration of the pyranometer being utilized. In Figure 5.2, the half-hour observations of R_S for Logan are compared with the computed R_{SO} envelopes. This figure shows good agreement between observed and computed values. However, as shown for day 7, R_S may sometimes exceed the predicted R_{SO} when there is reflection of radiation from nearby clouds during periods when no clouds shade the pyranometer.

---

2 These guidelines are based on an article by Allen (1996).

3 For R_a daily computations see Chapter 3, Equations (21) - (24) and for hourly computations see Equations (28) - (33). For K_T see R_{SO} equations (3-13) - (3-20) of Annex 3.

FIGURE 5.1
24-hour average R_s and estimated R_{so} envelopes at Logan, UT during 1992 showing an appropriate calibration of the pyranometer utilized

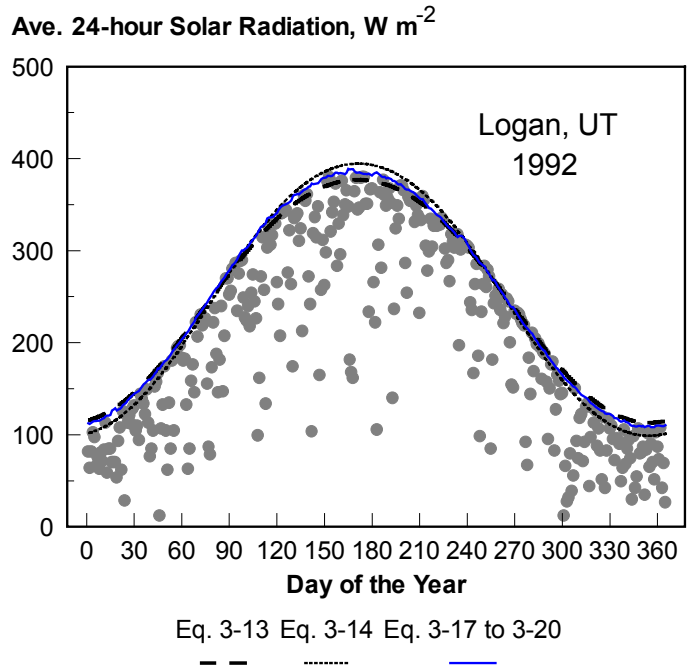

When the R_s observations on obviously clear days fall significantly above or below the computed R_{so} curves, then corrective action may be warranted. The correction may be in the form of applying a correction multiplier to the observed data, so that $(R_s)_{cor} = a\ R_s$, where a is a derived correction factor. Or, an additive correction may be warranted, where $(R_s)_{cor} = R_s + c$. Or, correction may be made by a combination of multiplicative and additive factors. Obviously, the corrections based on the computed R_{so} curves presume that the curve is accurate. The accuracy of the R_{so} envelope may need to be confirmed in a region by using accurate radiation measurements obtained from a calibration-grade pyranometer that has a calibration coefficient that is traceable to the international standard. The calibration pyranometer should be used only for short term periods of 10 – 14 days, and then should be stored in darkness to extend its life and to preserve the calibrated accuracy. Care should be exercised in selection of the turbidity coefficient in Equation (3-14) and (3-18) of Annex 3. Unfortunately, little information is available on this topic.

Net radiation

Equations for estimating hourly and 24-hour average rates of net radiation (R_n) using R_s measurements are generally accurate under most conditions. Therefore, measured R_n data should always be plotted against R_n that has been estimated using equations[4] that are based on

[4] See equations (38) through (40) in Chapter 3.

FIGURE 5.2
30-minute average R_s and estimated R_{so} envelopes at Logan, UT during July 7 and July 25, 1992

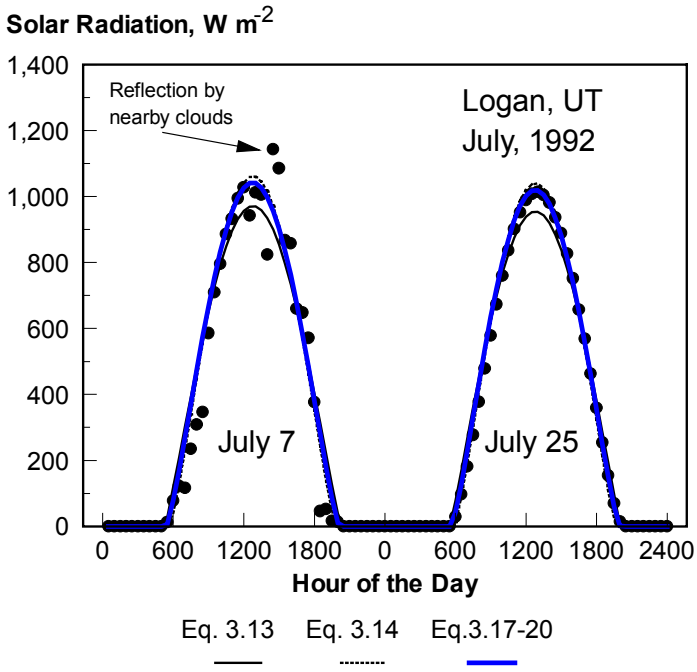

measured R_s, air temperature and vapour pressure. The value for albedo (α) used in the R_n estimating equation should represent conditions of the surface beneath the radiometer.

If measured values for R_n chronically deviate from estimated values by more than 3-5%, then the calibration or operation of the R_n device (radiometer) should be scrutinized. This type of comparison can readily identify days or periods during which the radiometer device has malfunctioned due to effects of dust, bird droppings, moisture condensation inside the plastic domes, a lack of levelness of the intrument, or a lack of green vegetation beneath the sensor. Of course, the R_s measurement used in the R_n equations should also be scrutinized as discussed in the previous section.

The user of net radiometer data must be aware that net radiometers manufactured by different companies may not yield the same measurements of radiation even when placed over the same surface. These differences are due to differences in sensitivities of various radiometers to long wave and short wave radiation and variations among methods for calibrating sensors during manufacturing.

The type, density and height of vegetation beneath the net radiometer and relative soil moisture content should be monitored and reported with the data. Care should be exercised when positioning the radiometer to avoid shading the sensed vegetation with other instruments or structures and to insure that the radiometer is not shaded by other instruments or structures at any time of the day or year.

FIGURE 5.3
Measured and estimated R_n during 20 minute periods over mature cattail vegetation near Logan, UT during August, 1993 (from Allen *et al.*, 1994)

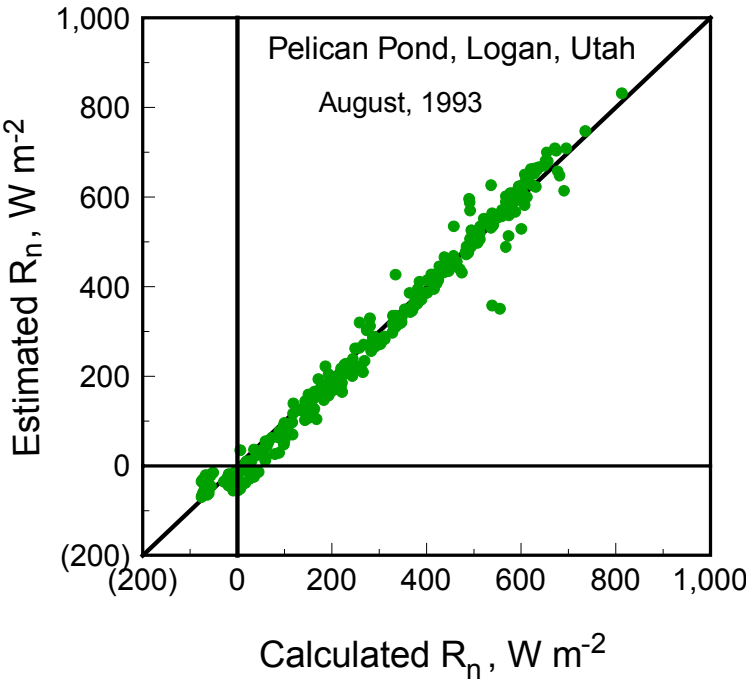

Figure 5.3 shows measured and estimated R_n for cattail vegetation near Logan, UT during 1993. The measurement and calculation time step was 20 minutes. The agreement between measurements and equation estimates was fairly good. Perfect agreement between the R_n measurements and R_n equations should not be expected, due to limitations of assumptions used in the equations (e.g., the value for albedo, means for estimating the net long wave radiation component, etc.).

Soil Heat Flux

A relationship proposed by Choudhury (1989) for predicting soil heat flux density (G) under daylight conditions[5] is:

$$G = 0.4 \exp^{(-0.5\ LAI)} R_n \qquad (5\text{-}2)$$

where LAI is the leaf area index, exp() is the natural number raised to the exponent, and G has the same units as R_n.

---

[5] This equation predicts $G = 0.1\ R_n$ for LAI = 2.8, which is typical for clipped grass (equation (45) in Chapter 3). Soil heat flux under forage grass during nighttime hours was found to be about 0.5 R_n. Pruitt (1995, personal communication) observed $G = 0.3\ R_n$ during nighttime hours under clipped grass at Davis, CA.

Equation (5-2) can be used to check the functioning and relative accuracy of soil heat flux plates after correcting measurements for temperature change of soil above the plates. The relationship of Equation (5-2) does not hold for 24-hour data, as a positive 24-hour soil heat flux estimate would always result. The user must be aware that Eq. (5-2) is only approximate and does not consider effects of plant spacing, sun angle, soil colour, soil moisture, or soil texture, nor the sensible heat balance at the surface on the ratio of G to R_n. Generally, more than one soil heat flux plate is used due to spatial variation in soil, soil water content, and vegetation.

Windspeed

Accuracy of wind measurements is difficult to assess unless duplicate instruments are used. One should always scan wind records for the presence of consistently low wind recordings. For electronic instruments, these recordings may represent a numerical "offset" in the anemometer calibration equation. The presence of these constant and consistent offsets in the data set indicates either the presence of exceptionally calm conditions (wind speeds less than about 0.5 m s^{-1} during the entire sampling period (which is rare)) or a malfunctioning of the wind speed sensor due to electrical shorting or perhaps due to fatigue of bearings. These problems may not be noticed by the station operator.

When possible, a second anemometer[6] of the same design, but with fresh bearings, should be placed at the weather location for a three or four day period at least once each year, and recordings compared with the permanent instrument. Variations between recordings can signal a need to replace bearings, switches, or other parts.

Relative Humidity and Vapour Pressure

Vapour pressure of air is difficult to measure accurately. Some older electronic humidity sensors were commonly plagued by hysteresis, nonlinearity and calibration errors. Some of these errors are inherent in the sensor design and still plague some modern sensors. Other errors result from dust, moisture, insects, pollution, and age.

Replication of RH Instruments

It is strongly recommended that duplicate RH and air temperature sensors be permanently employed in electronic weather stations, at least for some period each year. When duplicate RH and air temperature sensors yield similar measurments, then it is likely that both sensors are functioning properly, provided proper calibration equations have been used. However, even though duplicate sensors are in agreement does not mean that the readings are free from calibration errors and biases due to nonlinearity, etc..

Trends in Computed Dew Point Temperature with Time

When air humidity is measured using RH sensors, the actual vapour pressure of the air (e_a) is calculated as:

---

[6] If a second data logger is used to record the temporary anemometer, one should be careful to synchronize data logger clocks. Also, one should be careful that anemometers do not interfere with one another's wind stream.

$$e_a = \frac{RH}{100} e^o(T) \tag{5-3}$$

where e^o (T) is the saturation vapour pressure at air temperature T and RH is in %. RH and T must be taken for the same time period, preferably for ≤ 1 hour .

Hourly (or shorter) measurements of RH, dew point temperature (T_{dew}) or vapour pressure (e_a) can be preliminarily assessed by plotting hourly measurements of computed T_{dew} or e_a with time. Relative humidity will vary significantly with time of day, and inversely with air temperature as shown in Figure 12 of Chapter 3. However, both T_{dew} and e_a, either measured directly, or computed using RH and T measurements, should remain somewhat constant throughout a 24-hour period when the air mass is stable and advection of dry air from outside the area does not occur. During these stable periods, one should expect some rise in T_{dew} and e_a during daytime periods, when ET fluxes humidify the equilibrium boundary layer. However, this increase is usually less than about 10 to 20%. Variation in T_{dew} increases significantly when a weather front passes overhead. Since e_a is calculated as the product of RH and saturation vapour pressure at air temperature, any error in the RH calibration tends to cause false variation in T_{dew} and e_a with changing air temperature.

Figure 5.4 shows T_{dew} computed from measurements of RH and air temperature at a weather station in the center of a wetland near Logan, UT (20-minute data). T_{dew} generally varied from hour to hour due to air mass instability and increased during most days of this period as evaporation from the local wetland vegetation added humidity to the air. The data sequence shows some periods of relatively constant measurement (calculation) of T_{dew} throughout a 24-hour period (for example day of year 199), even though air temperature varied substantially. This is a good indication that the RH sensor was probably functioning correctly and that the instrument calibrations were probably valid.

Figure 5.4 also shows, for the same weather station, a comparison between RH measured using two different and independent relative humidity sensors. The two sensors, one a "chilled-mirror" device that measures T_{dew} directly, and the other, a device that measures RH directly, agreed very well with each other during the 8 days shown. The value of having "redundancy" in instrumentation is demonstrated in this example, where the two different devices measuring the same parameter (in this case RH) leave no question concerning the validity and accuracy of the RH measurements, due to the close agreement. The use of only a single instrument would leave some question as to accuracy.

One can notice in Figure 5.4 that the RH approached 100% on day 200, which is expected for a well-watered setting. The difference between minimum daily temperature and T_{dew} was generally 1 to 2 ^oC for many of the days. This is expected in dry, advective environments, as discussed in Chapter 3 and Annex 6.

Observations During Periods of Dew and Rainfall

In many climates, especially those where nightime dew occurs, T_d during early morning hours before sunrise should coincide closely with recorded T_{min} and RH should approach 100%. For automatic recording weather stations where recording rain gauges are used, one should expect RH recordings during periods of rain or light drizzle to exceed 95%. Relative humidity recordings that exceed 100% by more than 3-5% during early morning hours or during precipitation events indicate a need for recalibration and numerical adjustment of collected data.

FIGURE 5.4
T_{dew} and RH from measurements near Logan, Utah, the United States during 1995 (20-minute data)

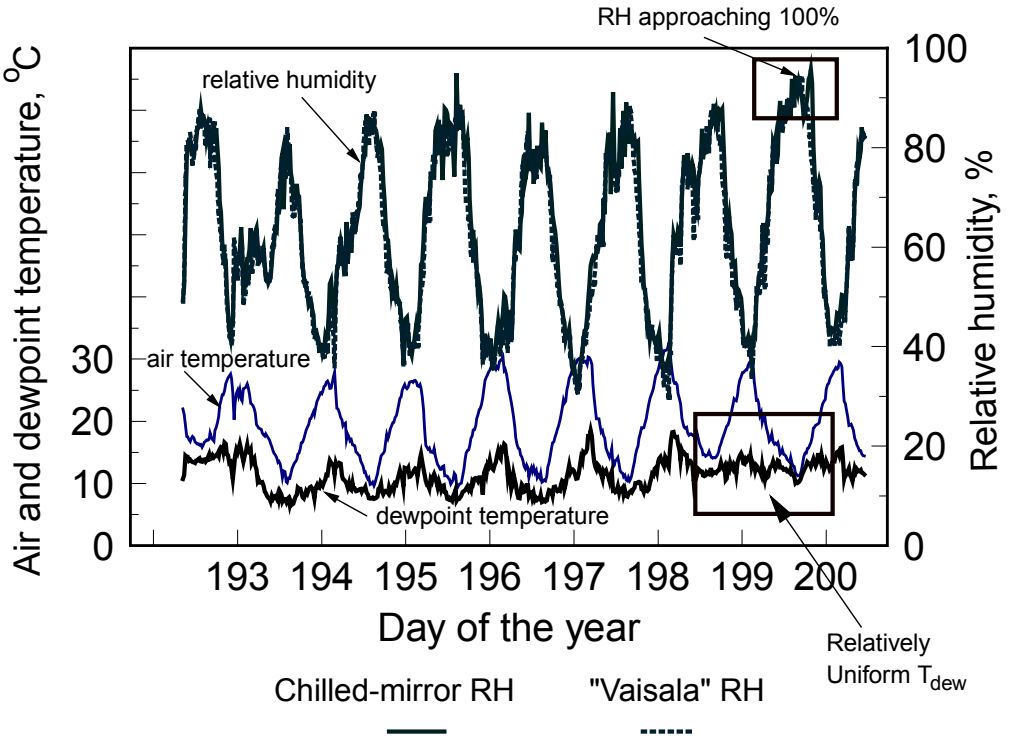

Maximum Daily Relative Humidity

When humidity data are measured in a reference setting, early morning RH will often approach 100%, even in semiarid areas if measurements are taken inside an irrigated region. Values of maximum relative humidity (RH_{max}) that consistently fall below 80% to 90% when in an irrigated or well-watered setting may indicate problems in RH sensor calibration or functioning or may indicate aridity of the measurement site and deviation from reference conditions.

Figure 5.5 shows daily measurements of RH_{max} from an electronic agricultural weather station located near North Baltimore, Ohio over a five year period. One would expect RH_{max} to approach 100% in this subhumid setting. However, one can see clear evidence in Figure 5.5 that the RH sensor was undermeasuring RH_{max} during several years, with decreasing trends in RH_{max} visible during these years. This indicates that the RH sensor was functioning electronically, except during the first half of 1988. However the calibration of the sensor element had seriously decayed and was not valid for 1988, 1990 and 1992. Sensor elements were typically replaced in September of each year. RH data for 1990 and 1992 could potentially be corrected by multiplying the RH measurements by a correction factor or by adding an offset.

FIGURE 5.5
Daily values of measured RH_{max} at North Baltimore, Ohio (1988-92) showing inappropriate calibration of the sensor for 1988, 1990 and 1992

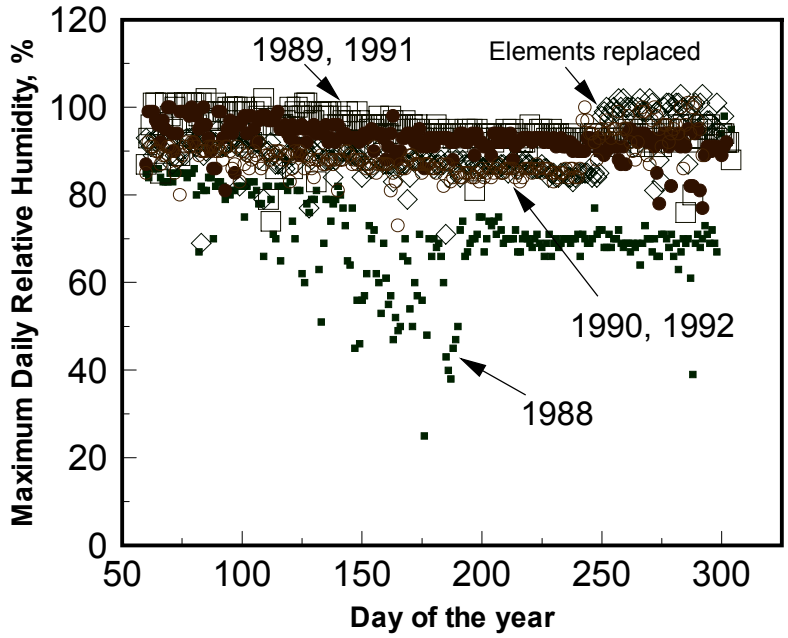

The type of plotting and screening demonstrated in Figures 5.4 and 5.5 shows the simple types of integrity assessments that can be utilized in near-real-time or with historical data. These types of assessments can be applied to all weather data used in evapotranspiration estimation and should be adopted by operators of agricultural weather networks.

Annex 6

Correction of weather data observed in non-reference weather sites to compute ET_o

The concept on which the FAO Penman – Monteith method for computing ET_o is based requires that weather data be measured in environmental conditions that correspond to the definition of reference evapotranspiration. In other words, the weather data are to be measured above an extensive grass crop that is actively evapotranspiring, or in an environment with healthy vegetation not short of water[1]. Under these reference conditions, the energy available at the surface (R_n - G) is partitioned between sensible and latent heat (H and λE, respectively) in such a way that, in general, the ratio $\beta = H/\lambda E_{ref} \leq 0.5$. The subscript *ref* indicates reference conditions.

Environmental conditions of arid lands that surround a non reference (arid) weather site do not allow for the reference rate of evapotranspiration to be attained. This is generally caused by lack of well-watered conditions. Thus, $\lambda E_{n/ref} < \lambda E_{ref}$ (subscript *n/ref* for non reference conditions). If the available energy (R_n - G) is the same, then the partitioning among sensible and latent heat changes, with $H_{n/ref} > H_{ref}$ and, often, $\beta_{n/ref} > 0.5$. Consequently, since air temperature increases with increasing H, the air temperatures measured at non reference sites are higher than those that would have been measured if reference conditions had existed, i.e. $T_{n/ref} > T_{ref}$. On the contrary, humidity measured at a non reference site is lower than that which would have occurred under reference conditions, thus $e_{a\ n/ref} < e_{a\ ref}$ and $VPD_{n/ref} > VPD_{ref}$.

When computing ET_o using standard estimates for R_n - G, r_a and r_s, ET_o will be overestimated when calculated using $T_{n/ref}$ and $VPD_{n/ref}$. A correction is therefore required to bring temperature and humidity data closer to the reference conditions.

In an environment having healthy vegetation and adequate soil moisture (reference conditions), minimum air temperature T_{min} usually approaches dew point temperature, T_{dew}, (see Figure 6.2 for Kimberly, Idaho, the United States)[2]. This especially occurs if the wind dies down by early morning and when soil moisture is high (illustrated through the ratio precipitation/ET_o, in Figure 6.1). Air temperatures decrease during night time due to surface cooling caused by long-wave emission and evaporation when VPD is positive. When near surface air temperature T approaches T_{dew}, T is prevented from decreasing below T_{dew} by condensation of vapour from the air and the correspondent heating effect of released latent heat. Thus, for reference conditions the relationship $(T_{min})_{ref} = (T_{dew})_{ref}$ is generally valid.

---

1 More detailed discussions are given in Allen (1996) and Allen *et al* (1996).

2 However, air temperature may not decrease to the dew point when large amounts of warm and dry air are transported to the surface by wind.

FIGURE 6.1
Comparison of differences between the monthly values of minimum and dew point temperature (T_{min} - T_{dew}) corresponding to monthly ratios of precipitation/ET_o Sudan, Africa and the United States

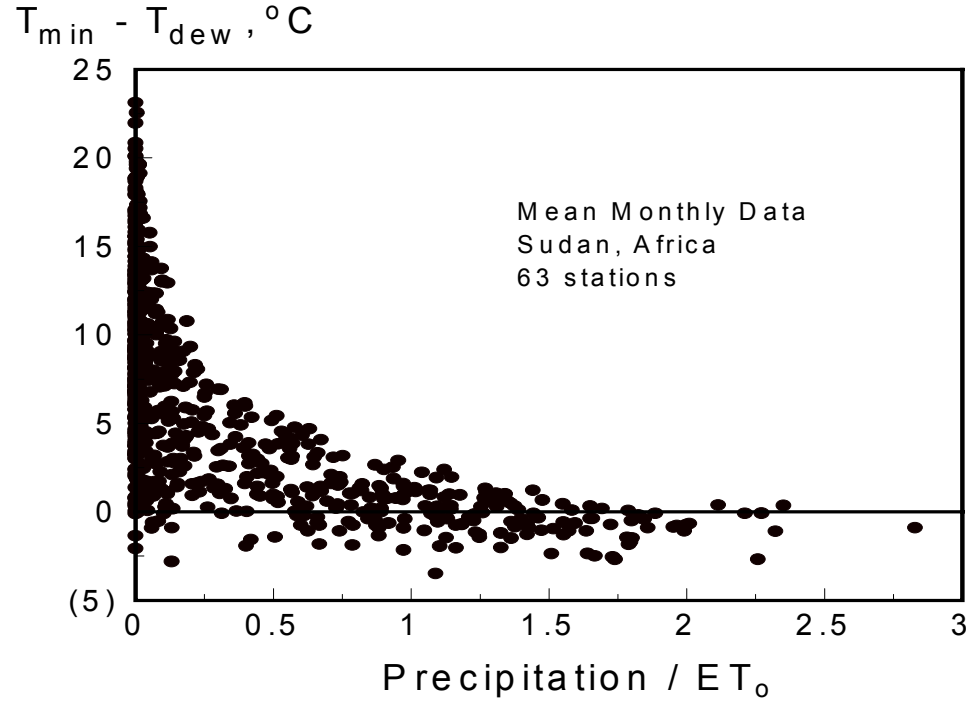

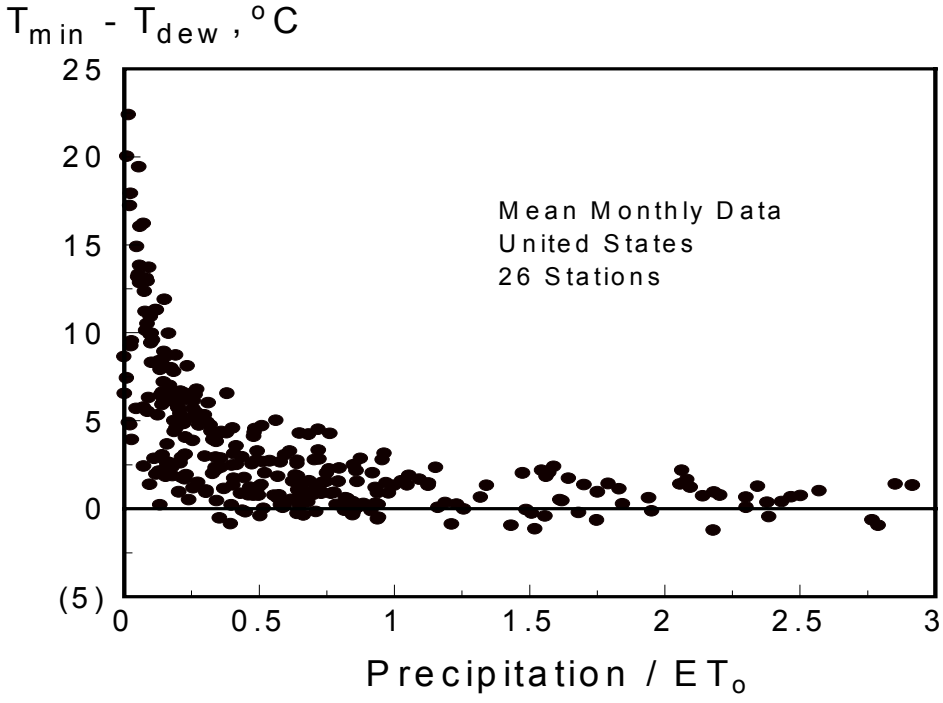

For non reference sites, soil moisture and/or vegetation limitations make $\lambda ET_{n/ref} < \lambda ET_{ref}$ or $ET_{n/ref} < ET_o$. Thus T_{min} may remain above T_{dew}. One cause of this phenomenon is the large "reservoir" of sensible heat created during daytime in the atmosphere ($H_{n/ref} > H_{ref}$, as suggested before), which is transferred towards the surface during the night, reducing the effect of cooling by long wave radiation. Another cause is the lack of soil moisture for evaporative cooling during night time.

This phenomenon can be observed in Figure 6.1, where monthly means for $T_{min} - T_{dew}$ are plotted for weather stations operated by national governments of two countries, Sudan and the United States. The data are plotted against the monthly ratios of precipitation to reference ET_o. The P/ET_o ratios indicate the availability of adequate soil water to support reference (well-watered) conditions in the absense of irrigation. As illustrated by the data, T_{min} approaches T_{dew} for nearly all stations when the ratio P/ET_o approaches and exceeds 1. When $P/ET_o < 1$, then the aridity of the station causes T_{min} to substantially exceed measured T_{dew}. The exception is for those weather stations that have $P/ET_o < 1$, but are irrigated or have adequate soil water reserves from a prior month. The similarity between data of Sudan and the United States indicates that this is a general phenomenon.

An additional comparison is given in Figure 2, where $T_{min} - T_{dew}$ are compared for two semiarid locations in Idaho, the United States that are separated by 200 km. One location, Kimberly, is a reference site in the middle of a large irrigated area. The other, Boise, is a non reference site, located at an airport and surrounded by a mixture of irrigated and non irrigated rangeland. It can be seen that T_{min} approaches T_{dew} frequently for the irrigated site at Kimberly, with only small differences occuring during months where a dry climate occurs (low precipitation/ET_o ratio). On the contrary, T_{min} was as much as 10°C higher than T_{dew} for the nonreference Boise station. From this graphical comparison, one can conclude that data for the nonreference Boise site require appropriate correction before being utilized to compute ET_o using the FAO - PM method. This is necessary to avoid overestimation of ET_o due to overestimation of air temperature and VPD.

Adjustment of T_{max}, T_{min} and T_{dew}

The empirical method described herein intends to correct the observed temperatures, T_{max} and T_{min} in proportion to the difference ($T_{min} - T_{dew}$), which works as an indicator of the overestimation of ($T_{n/ref} - T_{ref}$). Since T_{dew} defines the actual vapour pressure ($e_a = e^o(T_{dew})$), correcting T_{dew} also provides an adjustment for VPD.
The methodology proposed is the following:

1. Compare $T_{min} - T_{dew}$ (T_{dew} measured or computed from e_a using equations (11) or (12) in Annex 3) from a non reference site with those from a reference site using a graphical procedure such as in Figure 6.2 and using monthly ratios of Precipitation/ET_o as the abcissa. Daily or monthly data are utilized to compute $T_{min} - T_{dew}$.

2. When differences $T_{min} - T_{dew}$ for the non reference site are systematically higher than about 2°C relative to the reference site, then compute the average differences

$$\Delta T = T_{min} - T_{dew} \qquad (6\text{-}1)$$

for the months which require correction (in general this will occur when the monthly ratio Precipitation/ET_o does not exceed 0.5).

FIGURE 6.2
Comparison of differences between the monthly values of minimum and dew point temperature (T_{min} - T_{dew}) corresponding to monthly ratios of precipitation/ET_o for a reference site (Kimberly, Idaho, the United States) and for a non reference site (Boise, Idaho, the United States) in the same region

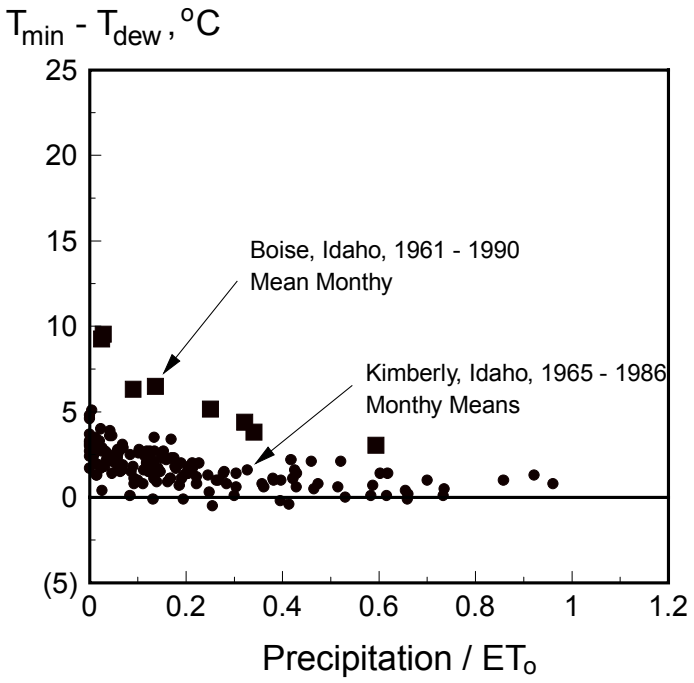

Or, if comparing T_{min} - T_{dew} from the nonreference sets to T_{min} - T_{dew} from the reference site, then calculate ΔT as:

$$\Delta T = \left(T_{min} - T_{dew}\right)_{n/ref} - \left(T_{min} - T_{dew}\right)_{ref} \quad (6\text{-}2)$$

3. Correct temperatures for each month (or day) by:

$$\left(T_{max}\right)_{cor} = \left(T_{max}\right)_{obs} - \left(\frac{\Delta T - K_o}{2}\right) \quad (6\text{-}3)$$

$$\left(T_{min}\right)_{cor} = \left(T_{min}\right)_{obs} - \left(\frac{\Delta T - K_o}{2}\right) \quad (6\text{-}4)$$

for $\Delta T > K_o$, where subscripts *cor* and *obs* refer to corrected and observed values, respectively. K_o is a "conservative" factor equal to 2°C when the nonreference station is not compared to a reference station (ΔT is from Equation (1)). $K_o = 0$ when ΔT is from Equation (6-2).

4. Correct T_{dew} for the same months or days as:

$$(T_{dew})_{cor} = (T_{dew})_{obs} + \left(\frac{\Delta T - K_o}{2} \right) \quad (6\text{-}5)$$

where K_o has the same value as for Equations (6-3) and (6-4), and utilizing either the observed or the calculated values for T_{dew} (equations (3-11) or (3-12) in Annex 3). The user should always insure that $(T_{min})_{cor} \geq (T_{dew})_{cor}$.

5. Compute ET_o with the corrected values for T_{max}, T_{min} and T_{dew}.

Adjustment of T_{dew} only

When RH, e_a, or T_{dew} data are not dependable or where "correction" of T_{max} and T_{min} as is done in the previous section is undesireable, a second means for "correcting" the weather data set for station aridity is possible. This second method is to merely set

$$T_{dew} = T_{min} - K_o \quad (6\text{-}6)$$

in the calculation for ET_o where $K_o = 0°C$ for humid and subhumid climates and $K_o = 2°C$ for arid and semiarid climates. The result of this procedure is to increase T_{dew} to reflect the higher humidity anticipated under reference conditions. It is noted that in a nonreference setting, the measured T_{min} may be too high, as compared to T_{min} expected for a reference setting, so that Equation (6-6) may result in values for T_{dew} that are overestimated, even for a reference condition. However, since the computation of vapor pressure deficit, VPD, in the ET_o equation, where $VPD = 0.5(e^o(T_{max}) + e^o(T_{min})) - e^o(T_{dew})$, utilizes values for air temperature and dew point temperature that may both be too high, the upward bias in all temperature parameters will tend to cancel, thereby presenting a VPD that is representative of a reference condition.

Index for station aridity

For non reference sites, when humidity data are available, one can compute an **aridity bias index** A_{bi} (for monthly time scales)

$$A_{bi} = \frac{(ET_o)_{obs}}{(ET_o)_{T_{dew} = T_{min}}} - 1 \quad (6\text{-}7)$$

between the ET_o computed from the observed (non-corrected) data (subscript obs) and, for the same period, using T_{min} as an estimate of T_{dew}. If there is not a large difference between T_{min} and T_{dew}, then $A_{bi} \sim 0$. When $\Delta T = T_{min} - T_{dew}$ is large (i.e., for a nonreference condition), then the aridity bias index A_{bi} becomes > 0.

The user should compare aridity bias indices for the dry and humid months and decide whether higher values for A_{bi} result from aridity or from other causes. A correction may be required when A_{bi} are consistently greater than 0.05. The correction of temperature and humidity data can be performed as indicated in the previous sections.

It is important for the user to realize that these corrections are to improve the calculations of ET_o only, since ET_o is defined for a well-watered environment. For hydrology studies where actual ET is required, then no adjustment should be made to air temperature and dew point temperature, since the $ET_{o\ n/ref}$ characterises the natural evaporation demands of the climate.

Any corrected T_{max}, T_{min}, T_{dew} data should not be reintroduced into the original historical data series. Also, the user should note that all of the correction procedures presented here are only approximate attempts to bring the ET_o calculations closer to the "real" ET_o that reflects a well-watered environment. Any errors or uncertainties introduced by these adjustments at a specific site will remain largely unknown. Therefore the user is encouraged to use caution.

Annex 7

Background and computations for K_c for the initial stage for annual crops

ET during the initial stage for annual crops is predominately in the form of evaporation. Therefore, accurate estimates for $K_{c\ ini}$ must consider the frequency that the soil surface is wetted during the initial period. The initial period was defined in Chapter 6 for annual crops as the period between the planting date and the date of approximately 10% ground cover.

Chapter 6 presents background and figures for predicting $K_{c\ ini}$ as a function of reference evapotranspiration (ET_o), soil texture, and frequency and depth of wetting. Additional background and equations are given in Chapter 7. This annex provides further background on development of the $K_{c\ ini}$ curves that are presented in Figures 29 and 30 of Chapter 6. Equations are presented here that can be used in place of Figures 29 and 30 when computers are used.

INTRODUCTION

Evaporation from bare soil (E_s) can be characterized as occurring in two distinct stages. The stage 1 is termed the "energy limited" stage. During this stage, moisture is transported to the soil surface at a rate sufficient to supply the potential rate of evaporation (E_{so}), which, in turn, is governed by energy availability at the soil surface. In this procedure, E_{so} is estimated from

$$E_{so} = 1.15\ ET_o \tag{7-1}$$

where E_{so} is the potential rate of evaporation [mm d^{-1}] and ET_o is the the mean ET_o during the initial period [mm d^{-1}]. The value 1.15 represents increased evaporation potential due to low albedo of wet soil and the possibility of heat stored in the surface layer during previous dry periods.

Stage 2 is termed the "soil limited" stage, where hydraulic transport of subsurface water to the soil surface is unable to supply water at the potential evaporation rate. During stage 2, the soil surface appears partially dry and a portion of the evaporation occurs from below the soil surface. The energy required for subsurface evaporation is supplied by transport of heat from the soil surface into the soil profile. The evaporation rate during stage 2 drying decreases as soil water content decreases as shown in Figure 7.1 (see also Figure 38 of Chapter 7). The evaporation rate can therefore be expressed as being proportional to the water remaining in the evaporation layer relative to the maximum depth of water that can be evaporated from the same soil layer during stage 2 drying.

The maximum total depth of water that can be evaporated from the surface soil layer is termed "total evaporable water" or TEW. Equation 73 of Chapter 7 is used to predict TEW. In turn, the maximum total depth of water that can be evaporated during stage 1 is termed "readily evaporable water" or REW. Table 19 of Chapter 7 includes recommended values for REW.

If the evaporation rate during stage 2 drying is assumed to be linearly proportional to the equivalent depth of water remaining in the evaporation layer, as shown in Figure 7.1, then the average soil water evaporation rate during stage 2 can be estimated, similar to Equation 74 of Chapter 7:

$$E_s = E_{so}\left[\frac{TEW - D_e}{TEW - REW}\right] \qquad (7\text{-}2)$$

for when $D_e > REW$, where E_s is the actual evaporation rate [mm d^{-1}] at any particular time when the depletion from the soil surface layer equals D_e. D_e is the depletion from the surface layer [mm] and REW is the readily evaporable water in the surface layer [mm]. The length of time required to complete stage 1 drying (t_1) is equal to $t_1 = REW/E_{so}$.

FIGURE 7.1
Two stage model for soil evaporation during the initial period

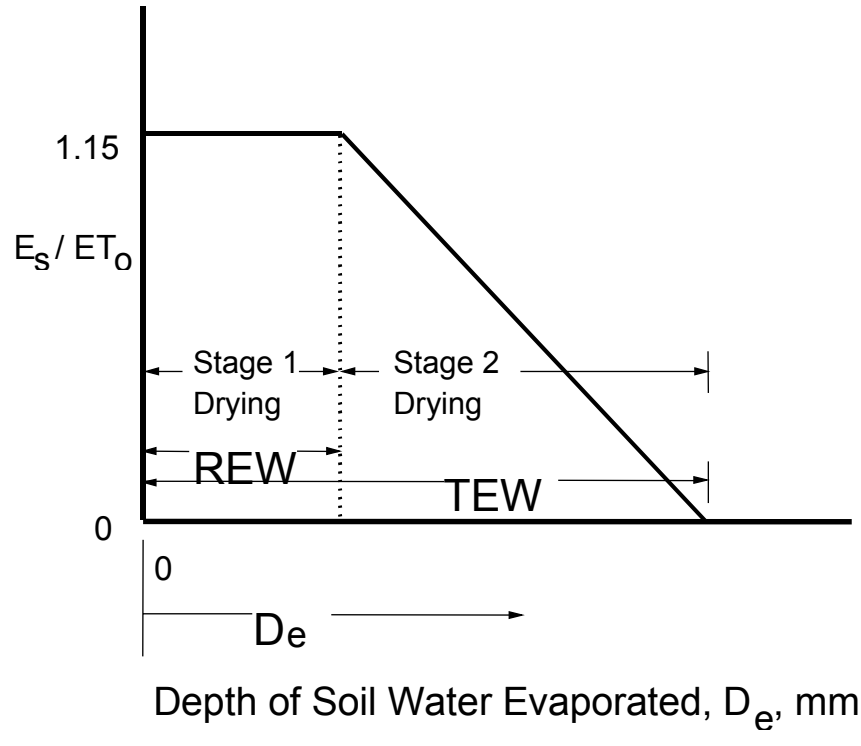

GENERAL EQUATION FOR $K_{c\ ini}$

Equation 7-2 can be integrated over the range REW to TEW, resulting in the basic equation for $K_{c\ ini}$ during stage 2:

$$K_{c\ ini} = \frac{TEW - (TEW - REW)\exp\left(\frac{-(t_w - t_1)\ E_{so}\left(1+\frac{REW}{TEW-REW}\right)}{TEW}\right)}{t_w\ ET_o} \qquad (7\text{-}3)$$

for $t_w > t_1$, where $K_{c\ ini} = E_s/ET_o$, t_w is the mean interval between wetting events [days] and t_1 is the time when stage 1 drying is completed ($t_1 = REW / E_{so}$) [days]. The "exp" parameter represents the exponential of the value contained within the parenthesis following the parameter. The $K_{c\ ini}$ calculated from Equation 7-3 is limited to $K_{c\ ini} \leq 1.15$.

When $t_w < t_1$, i.e. the entire process resides within stage 1, so that:

$$K_{c\ ini} = \frac{E_{so}}{ET_o} = 1.15 \qquad (\text{for } t_w < t_1) \qquad (7\text{-}4)$$

Where furrow or trickle irrigation is practiced, and only a portion of the soil surface is wetted, the value calculated for $K_{c\ ini}$ in Equations 7-3 and 7-4 should be reduced in proportion to the average fraction of surface wetted, f_w [0,1]. Indicative values for f_w are given in Table 20 of Chapter 7. Equation 60 of Chapter 6 is used to make the adjustment:

$$K_{c\ ini} = f_w\ K_{c\ ini(f_w=1)}$$

where f_w is the fraction of surfaced wetted by irrigation or rain [0 - 1], and $K_{c\ ini\ (fw=1)}$ is the value for $K_{c\ ini}$ for $f_w = 1$ from Equation 7-3 or 7-4.

Accordingly, the value for the infiltration depth from irrigation (I_w) should be adjusted using Equation 61 of Chapter 6:

$$I_w = \frac{I}{f_w}$$

where I_w is the depth of irrigation water that is infiltrated over the part of the surface that is wetted [mm] and I is the depth of water infiltrated from irrigation, expressed as one-dimensional depth over the entire surface area [mm].

TOTAL EVAPORABLE WATER

The value for TEW is the maximum depth of water that can be evaporated from the soil following wetting. The value for TEW is governed by the depth of the soil profile contributing to soil water evaporation and by the soil water holding properties within the evaporating layer. In addition, the value for TEW is affected by the unsaturated hydraulic

conductivity, by the presence of a hydraulically limiting layer beneath the evaporating layer, and by the conduction of sensible heat into the soil to supply energy for subsurface evaporation. An approximation for the maximum value of TEW for initial periods having $ET_o \geq 5$ mm $d^{-1}$is:

$$TEW = 1000\left(\theta_{FC} - 0.5\,\theta_{WP}\right)Z_e \tag{7-5}$$

where TEW has units of mm, θ_{FC} is soil water content at field capacity [$m^3\ m^{-3}$], θ_{WP} is soil water content at wilting point [$m^3\ m^{-3}$], and Z_e is the depth of the soil surface soil layer that is subject to drying by way of evaporation [0.10 to 0.15 m]. If unknown, a value of Z_e = 0.15 m is recommended. Typical values for θ_{FC} and θ_{WP} are given in Table 19 of Chapter 7.

During winter and other cool season months, less radiation energy is available to penetrate the soil surface and to evaporate water from within a drying soil, and TEW may be less. Therefore, when $ET_o < 5$ mm d^{-1}, TEW for use in Equation 7-3 is estimated as:

$$TEW = 1000\left(\theta_{FC} - 0.5\,\theta_{WP}\right)Z_e \sqrt{\frac{ET_o}{5}} \tag{7-6}$$

where ET_o is reference ET in mm/day. Equation 7-6 is intended to correct TEW for use during the initial stage with mostly bare soil. It is not intended for use with the dual K_c procedure of Chapter 7. REW is limited so that REW ≤ TEW.

NUMBER OF WETTING EVENTS AND AVERAGE DEPTH

Estimating the number of wetting events and the corresponding time between wetting events during the initial period is described in Chapter 6. The number of wetting events (both from precipitation and irrigation) occurring during the initial period is determined by considering that two wetting events occurring on adjoining days can be counted as one event, and individual wetting events of less than 0.2 ET_o can be ignored.

The average time between wetting events during the initial period (t_w) is approximated as:

$$t_w = \frac{L_{ini}}{n_w + 0.5} \tag{7-7}$$

where t_w is in days, L_{ini} is the length of the initial period [days], and n_w is the number of wetting events during the initial period.

The average depth of water added to the evaporating layer at each wetting event is determined by dividing the sum of the precipitation and irrigation infiltration occurring during all wetting events by the number of events, thus:

$$P_{mean} = \frac{\left(\sum P_n + \sum I_w\right)}{n_w} \tag{7-8}$$

where P_{mean} is the average depth of infiltrated water per wetting event [mm], P_n is the depth of infiltrated precipitation occurring during the initial period, and I_w is the infiltrated irrigation depth for the part of the surface that is wetted [mm] (Equation 61). Each individual value of P_n and I_w must be limited in Equation 7-8 so that $P_n \leq TEW$ and $I_w \leq TEW$ where TEW is from Equation 7-5 or 7-6.

LIMITATIONS ON TEW AND REW

In the case of wetting depths (P_{mean}) that are smaller than the TEW, the evaporation process, including stage 1 drying, may terminate sooner than expected. The actual values for TEW and REW must be corrected according to P_{mean}. Therefore, TEW and REW are calculated according to the average total water available during each drying cycle:

$$TEW_{cor} = \min\left(TEW, \quad P_{mean} + \frac{W_{ini}}{n_w} \right) \tag{7-9}$$

and

$$REW_{cor} = REW\left[\min\left(\frac{P_{mean} + \frac{W_{ini}}{n_w}}{TEW}, \ 1 \right) \right] \tag{7-10}$$

where "min ()" is a function to select the minimum value of those in braces that are separated by the comma, and where TEW is from Equation 7-5 or 7-6. W_{ini} is the equivalent depth of water [mm] in the evaporation layer (of thickness Z_e) at the time of planting (beginning of the initial period). W_{ini} has a maximum value of TEW when the initial soil water content of the evaporation layer is at field capacity. Values for TEW_{cor} and REW_{cor} from Equations 7-9 and 7-10 are used in place of TEW and REW in Equation 7-3.

EQUATIONS FOR FIGURES 29 AND 30 OF CHAPTER 6

Figures 29 and 30 of Chapter 6 can be reproduced numerically by applying Equation 7-3 under the following conditions. For all applications:

$t_1 = REW_{cor} / E_{so}$ and $E_{so} = 1.15\ ET_o$ (Equation 1).

If $t_1 < t_w$ then $K_{c\ ini} = 1.15$ (Equation 4), and Equation 7-3 is <u>not</u> applied.

Otherwise, apply Equation 3 using the following parameters (TEW_{cor} and REW_{cor} are used in place of TEW and REW in Equation 3):

For Figure 29 (all soil textures having light infiltration depths (< 10 mm)):

$TEW_{cor} = 10$ mm

$REW_{cor} = \min(\ \max(2.5,\ 6 / (ET_o)^{0.5}),\ 7\ )$

For Figure 30a (coarse soil textures having large infiltration depths (≥40 mm)):

$$TEW_{cor} = \min(15, 7\ (ET)^{0.5})$$

$$REW_{cor} = \min(6, TEW_{cor} - 0.01)$$

For Figure 30b (medium and fine soil textures having large infiltration depths (≥ 40 mm)):

$$TEW_{cor} = \min(28, 13\ (ET)^{0.5})$$

$$REW_{cor} = \min(9, TEW_{cor} - 0.01)$$

The max() and min() functions indicate the selection of the maximum or minimum value of the parameters that are separated by the comma. Most programming languages and spreadsheet programs include these functions.

The numerical application of Equation 7-3 using the parameters and constraints listed here will fully reproduce Figures 29 and 30a and b, with the exception that calculations made in the vicinity of ET_o = 5 mm d^{-1} may deviate from the curves in Figures 30a and b, since curves in the vicinity of ET_o = 5 mm d^{-1} were smoothed before plotting. The smoothing caused small, insignificant differences between the figures and the numerical procedure. The parameters listed above are reduced from equations 5 through 10 and using typical values for θ_{FC} and θ_{WP}.

In situations where wetting events are not equally spaced during the initial period, the dual K_c approach of Chapter 7, along with a daily soil water balance, can provide for more accurate results.

EXAMPLE 7-1
Application of Equation 7-3 to Example 25

As in Example 25 in Section B, small vegetables are cultivated in a dry area on a coarse textured soil and receive 20 mm of water twice a week by means of a sprinkler irrigation system. The average ET_o during the initial stage is 5 mm/day. Estimate the crop evapotranspiration during that stage.

For:	t_w = 7/2 =	3.5	day interval
	ET_o =	5	mm/day
	E_{so} = 1.15 ET_o = 1.15 (5) =	5.75	mm/day
For Fig. 29:	TEW_{cor} =	10	mm
	REW_{cor} = min(max(2.5, 6/($5^{0.5}$), 7) =	2.7	mm
	t_1 = REW/E_{so} = 2.7/5.75 =	0.47	days
	since $t_w > t_1$, use Eq. 7-3: $K_{c\ ini(Fig.\ 29)}$ = (10 – (10-2.7) exp[-(3.5-0.47)(5.75)(1+2.7/(10-2.7))/10])/(3.5(5)) =	0.57	-
For Fig. 30.a:	TEW_{cor} = min(15, 7($5^{0.5}$)) =	15	mm
	REW_{cor} = min(6, 15-0.001) =	6	mm
	t_1 = REW/E_{so} = 6/5.75 =	1.04	days
	since $t_w > t_1$, use Eq. 7-3: $K_{c\ ini(Fig.\ 30a)}$ = (15 – (15-6) exp[-(3.5-1.04)(5.75)(1+6/(15-6))/15])/(3.5(5)) =	0.75	-
For:	I =	20	mm
From Eq. 59:	$K_{c\ ini}$ = 0.57 + [(20-10)/(40-10)] (0.75-0.57) = 0.57+0.33(0.12)=	0.63	-
From Eq. 58:	ET_c = 0.63 (5) =	3.2	mm/day

The average crop evapotranspiration during the initial growth stage for the small vegetables is 3.2 mm/day. The values in this example agree relatively closely with those obtained from Example 25.

Annex 8

Calculation example for applying the dual K_c procedure in irrigation scheduling

This annex illustrates in more detail the application of the various equations for calculating K_{cb}, K_e and ET_c using the dual K_c approach of Chapter 7. The example is in the form of a computer spreadsheet and is applied to the dry, edible bean crop that was used in example boxes 15 and 16 of Chapters 6 and 7. The spreadsheet is shown in Figure 8.1, where the irrigation schedule is determined using the daily soil-water balance procedure described in Chapter 8. The timing of irrigations is based on the management allowed depletion (MAD) of the available water that can be stored in the root zone. The irrigation schedule and the corresponding estimated wet soil evaporation are different from the actual values shown in Box 16 of Chapter 7, since Box 16 represents the actual irrigation schedule used at Kimberly during 1974. The actual schedule deviated somewhat from the theoretical schedule of Figure 8.1.

The spreadsheet formulas used for calculations and the references to equations in the text are indicated in Box 8.1. The variable names used for parameters follow the same convention used in Chapters 1 to 9. The variable names are defined in the List of principal symbols and acronymns in the introduction to this paper. A few exceptions are defined in Table 8.1.

The spreadsheet in Figure 8.1 includes columns for variables T_{max}, u_2, and T_{dew}. The T_{max} and T_{dew} columns are used to calculate daily RH_{min}. The u_2 and RH_{min} columns are used to adjust $K_{cb\ mid}$ and $K_{cb\ end}$ using Equation 70 of Chapter 7 and to calculate $K_{c\ max}$ using Equation 72 on a daily basis. The data in the first 7 rows of Figure 8.1 that appear within boxes represent the specific crop and soils information that is entered by the user for a particular crop and soil combination. All other information (outside of boxes) is calculated automatically by the spreadsheet program. The columns having double underlined headings represent the data that are input by the user into the spreadsheet.

The calculations in Figure 8.1 can be used to verify other computer programs or spreadsheet calculations for K_e, K_c and ET_c. Small differences may result, depending on the assumptions of timing of irrigations. The spreadsheet of Figure 8.1 presumes that all irrigation and precipitation events occur early in the morning. The scheduling and magnitudes of irrigations are based on the soil water depletion at the end of the previous day. The spreadsheet also presumes that all drainage from the root zone due to excess precipitation occurs on the day of the precipitation event. It is assumed that runoff from precipitation is zero. If necessary, procedures for predicting precipitation runoff can be entered into the spreadsheet using procedures described in most standard hydrology textbooks. It is assumed that the net depth of irrigation that is retained in the crop root zone is exactly equal to the depletion depth of the previous day. This assumption presumes perfect knowledge of soil water depletion by the irrigator or that all irrigations are adequate or excessive. This assumption may not hold for some irrigation conditions and can be changed by the user as needed.

Spreadsheet formulas used to create the spreadsheet of Figure 8.1 are listed in Box 8.1 for the Microsoft Excel language (versions 5 and higher). Formulae for other types of spreadsheets would be similar. Formulae for the Corel Quattro-Pro language (versions 5 and higher) can be downloaded from the FAO internet site.

BOX 8.1. Spreadsheet formulas and corresponding equations for Excel spreadsheet programs.

Formulas for Rows 1 to 15 of Figure 8.1 (for MicroSoft Excel, versions 5/95 and later)

Equation in text or footnote	***Cell***	***Text, value, or formula***
		Underlined numeric values are input by the user
	A1:	Example Spreadsheet for Calculating $ET_c = (K_{cb} + K_e)ET_o$ and an Irrigation Schedule
	P2:	Computed Dates for Stages:
	A3:	Crop:
	B3:	Dry, Edible Beans
	F3:	Table 11:
	I3:	Table 12:
	J3:	Following Adjustment:
	P3:	J_{Plant}
Table 2.5	Q3:	=TRUNC(275*C5/9-30+C6)+IF(C5>2,-2,0)+ IF(MOD(C14,4)=0,+1,0)
	V3:	f_w (irrig.):
	X3:	0.5
	AE3:	$Root_{min}$
	AF3:	0.2
	AG3:	m
	AH3:	MAD during Initial Stage
	AK3:	70
	AL3:	%
	E4:	L_{ini}
	F4:	25
	H4:	$K_{cb\ ini}$
	I4:	0.15
	J4:	=I4
	L4:	K_{cmin}
	M4:	=J4
	P4:	J_{Dev}
	Q4:	=Q3+F4
	V4:	REW:
	X4:	8
	Y4:	mm
	AE4:	$Root_{max}$
	AF4:	0.8
	AG4:	m
	AH4:	MAD after Initial Stage
	AK4:	45
	AL4:	%
	A5:	Planting:
	B5:	Month
	C5:	5
	E5:	L_{dev}
	F5:	25
	H5:	$K_{cb\ mid}$
	I5:	1.1
Eq. 70	J5:	=I5+(0.04*($K$8-2)-0.004*($K$9-45))*($M$5/3)^0.3
	L5:	Max.Ht.:
	M5:	0.4
	N5:	m
	P5:	J_{Mid}
	Q5:	=Q4+F5
	V5:	TEW:
	X5:	22
	Y5:	mm

BOX 8.1, continued.

	AE5:	Avail.Water
	AF5:	160
	AG5:	mm/m
	B6:	Day
	C6:	22
	E6:	L_{mid}
	F6:	30
	H6:	$K_{cb\ end}$
	I6:	0.25
Eq. 70	J6:	=IF(I6<0.45,I6,I6+(0.04*($K$8-2)-0.004*($K$9-45))*($M$5/3)^0.3)
	P6:	J_{Late}
	Q6:	=Q5+F6
	V6:	initial D_e:
	X6:	18
	Y6:	mm
	E7:	L_{late}
	F7:	20
	P7:	J_{Harv}
	Q7:	=Q6+F7
	V7:	Initial f_w:
	X7:	1
	H8:	Midseas. Av. Wind Speed:
(1)	K8:	=(VLOOKUP(Q6,D14:AP183,38)- VLOOKUP(Q5,D14:AP183,38))/(Q6-Q5)
	L8:	m/s
	M8:	<----Computed automatically from Lookup on column AO
	AH8:	(Irrigation that is needed is presumed applied at beginning of next day)
	H9:	Midseas. Av. RH_{min}:
(1)	K9:	=(VLOOKUP(Q6,D14:AP183,39)- VLOOKUP(Q5,D14:AP183,39))/(Q6-Q5)
	L9:	%
	M9:	<----Computed automatically from Lookup on column AP

First row of formulas (row 14)

Note: some formulas in row 14 (first day) vary from those in rows 15 onward. See row 15 for example calculations for all subsequent days.

	A14:	5
	B14:	15
	C14:	74
Table 2.5	D14:	=TRUNC(275*A14/9-30+B14)+IF(A14>2,-2,0)+IF(MOD(C14,4)=0,+1,0)
	E14:	10
	F14:	5.7655
	G14:	0
	H14:	3.4
Eq. 14	I14:	=0.6108*EXP((17.27*G14)/(G14+237.3))
Eq. 11	J14:	=0.6108*EXP((17.27*E14)/(E14+237.3))
Eq. 63	K14:	=I14/J14*100
	L14:	0
Eq. 66(2)	O14:	=IF(D14<$Q$4,$J$4,IF(D14<$Q$5,$J$4+(D14-$Q$4)/ $F$5*($J$5- $J$4),IF(D14<$Q$6,$J$5,IF(D14<$Q$7, $J$5+(D14-$Q$6)/$F$7*($J$6-$J$5),$J$4))))
(3)	P14:	=MAX(O14/$J$5*$M$5,P13)
Eq. 72	Q14:	=MAX(1.2+(0.04*(F14*0.9-2)-0.004*(K14-45))*(P14/3)^0.3, O14+0.05)
(4)	R14:	0
Eq. 76	S14:	=MAX(((O14-M$4)/(Q14-M$4))^(1+0.5*P14),0.01)
(5)	T14:	=IF(R14>0,X$3,IF(L14>0,1,X7))

BOX 8.1, continued.

Eq. 75	U14:	=MIN(1-S14,T14)
(6)	V14:	=X6
Eq. 74	W14:	=MAX(IF(V14<X$4,1,(X$5-V14)/(X$5-X$4)),0)
Eq. 71	X14:	=MIN(+W14*(Q14-O14),U14*Q14)
	Y14:	=X14*H14
Eq. 79	Z14:	=MAX(L14+R14,0)
Eq. 77(6)	AA14:	=V14-L14-R14+Y14/U14+Z14
(7)	AB14:	=O14+X14
Eq. 69(7)	AC14:	=AB14*H14
Eq. 8.1(8)	AE14:	=MAX((O14-$J$4)/($J$5-$J$4)*($AF$4-$AF$3)+$AF$3,AE13)
Eq. 82	AF14:	=MAX(IF(D14<Q$4,AK$3,AK$4)/100*AE14*$AF$5,AF13)
Eq. 85(9)	AG14:	=$X$6-L14+AC14
(10)	AH14:	=IF(D14>=Q$3,IF(D14<(Q$6+Q$7)/2,IF(AG14>AF14, AG14,0), 0), 0)
Eq. 88	AI14:	=MAX(+L14-AC14-$X$6,0)
Eq. 84(11)	AJ14:	=IF(AG14>AF14,(AE14*AF$5-AG14)/(AE14*AF$5-AF14),1)
Eq. 80	AK14:	=X14+O14*AJ14
Eq. 85(9)	AL14:	=+$X$6-L14+AK14*H14+AI14
(12)	AO14:	=F14
(12)	AP14:	=K14

Second row of formulas

All rows below row 15 are similar.

	A15:	5
	B15:	16
	C15:	74
Table 2.5	D15:	=TRUNC(275*A15/9-30+B15)+IF(A15>2,-2,0)+IF(MOD(C15,4)= 0,+1,0)
	E15:	13.3
	F15:	2.2175
	G15:	-5
	H15:	4.1
Eq. 14	I15:	=0.6108*EXP((17.27*G15)/(G15+237.3))
Eq. 11	J15:	=0.6108*EXP((17.27*E15)/(E15+237.3))
Eq. 63	K15:	=I15/J15*100
	L14:	0
Eq. 66 (2)	O15:	=IF(D15<$Q$4,$J$4,IF(D15<$Q$5,$J$4+(D15-$Q$4)/$F$5*($J$5-$J$4),IF(D15<$Q$6,$J$5,IF(D15<$Q$7,$J$5+(D15-$Q$6)/$F$7*($J$6-$J$5),$J$4))))
(3)	P15:	=MAX(O15/$J$5*$M$5,P14)
Eq. 72	Q15:	=MAX(1.2+(0.04*(F15*0.9-2)-0.004*(K15-45))*(P15/3)^0.3, O15+0.05)
(4)	R15:	=IF(AH14>0,AH14/$X$3,0)
Eq. 76	S15:	=MAX(((O15-M$4)/(Q15-M$4))^(1+0.5*P15),0.01)
(5)	T15:	=IF(R15>0,X$3,IF(L15>0,1,T14))
Eq. 75	U15:	=MIN(1-S15,T15)
(6)	V15:	=MAX(AA14-L15-R15,0)
Eq. 74	W15:	=MAX(IF(V15<X$4,1,(X$5-V15)/(X$5-X$4)),0)
Eq. 71	X15:	=MIN(+W15*(Q15-O15),U15*Q15)
	Y15:	=X15*H15
Eq. 79	Z15:	=MAX(L15+R15-AA14,0)
Eq. 77(6)	AA15:	=AA14-L15-R15+Y15/U15+Z15
(7)	AB15:	=15+X15
Eq. 69(7)	AC15:	=AB15*H15
Eq. 8.1(8)	AE15:	=MAX((O15-$J$4)/($J$5-$J$4)*($AF$4-$AF$3)+$AF$3,AE14)
Eq. 82	AF15:	=MAX(IF(D15<Q$4,AK$3,AK$4)/100*AE15*$AF$5,AF14)
Eq. 85(9)	AG15:	=AK14 -L15-AH14+AC15
(10)	AH15:	=IF(D15>=Q$3,IF(D15<(Q$6+Q$7)/2,IF(AG15>AF15, AG15,0), 0),0)
Eq. 88	AI15:	=MAX(+L15+AH14-AC15-AK14,0)
Eq. 84(11)	AJ14:	=IF(AG15>AF15,(AE15*AF$5-AG15)/(AE15*AF$5-AF15),1)
Eq. 80	AK14:	=X15+O15*AJ15
Eq. 85(9)	AL15:	=+AL14-L15-AH14+AK15*H15+AI15
(12)	AO15:	=AO14+F15
(12)	AP15:	=AP14+K15

BOX 8.1, continued.

Footnotes:

(1) Cells K8 and K9 use the vertical lookup function to automatically calculate the average wind speed and average daily minimum relative humidity during the midseason period. The lookup function uses cumulative totals of wind speed and RH_{min} that are calculated in columns AO and AP.

(2) The formula to calculate K_{cb} for each day uses a series of imbedded IF statements to determine which growing period the day is in. Linear interpolation is applied when the day is within the development and late season growing periods.

(3) The crop height on any day is calculated as proportional to the value of K_{cb} on that day to the $K_{cb\ mid}$ value, multiplied by the maximum crop height that has been entered by the user in cell M5. The value for crop height is not allowed to decrease with time. Hence, the MAX() function is employed, comparing with the value of the previous day.

(4) The value for irrigation depth (divided by f_w to express the depth over the wetted fraction of the soil, only) is presumed to occur early in the day. This value is based on a decision made at the end of the previous day (column AH), based on whether or not the ending soil water depletion on the previous day has exceeded the readily available water (RAW). The irrigation depth on the first day is presumed to be zero.

(5) The value for f_w is determined according to the last occurrence of precipitation or irrigation, as described in Chapter 7.

(6) The depletion of the evaporation layer (top soil layer) at the beginning of the day is presumed to equal the depletion at the end of the previous day less any precipitation or irrigation, which is assumed to occur very early in the day. The value for $D_{e,i}$ is limited to ≥ 0.

The depletion of the evaporation layer at the end of the day is calculated according to Eq. 77, with root extraction of plant transpiration from the evaporation layer assumed to equal zero.

(7) The value for K_c is calculated as $K_c = K_{cb} + K_e$ and the value for ET_c is calculated as $K_c \times ET_o$.

(8) The depth of the effective root zone on any day is calculated as being proportional to the ratio of the value of the K_{cb} on that day (above the value of $K_{c\ min}$) to the $K_{cb\ mid} - K_{c\ min}$, as described in Eq. 1 of this annex. The rooting depth is not allowed to decrease with time. Therefore, the MAX() function is utilised, where the value for the previous day is compared.

(9) The "first" estimate for ending depletion of the root zone ($D_{r,,i}$) is estimated using Eq. 85, with drainage assumed to be zero and with ET_c for nonstressed conditions. The value for $D_{r,\ i}$ is then recalculated in Column AK, after any drainage loss is estimated and after any reduction in ET_c, to account for low soil water content. The value for $D_{r,\ i}$ in column AK represents depletion of the root zone at the end of the day.

(10) The net depth of irrigation needed is based on the value of soil water depletion at the end of the day. It is assumed that irrigation will be applied at the beginning of the following day. The formula in column AH checks to insure that the specific day is within the growing period. The formula assumes that no irrigation will be desired during the last one-half of the late-season period. This assumption may need to be modified for some other crops. The value for management allowed depletion is allowed to have a different (normally higher) value during the initial period as compared to during the rest of the growing season.

(11) The stress coefficient K_s represents the K_s under the current conditions of soil water. The value for K_s is reduced below 1.0 using Eq. 84 if the depletion of the root zone (following any irrigation or precipitation earlier in the day) is greater than the readily available water (RAW). It is presumed that the stress point, p, is the same as the value entered for MAD. This presumption can be modified as needed.

(12) Columns AO and AP contain cumulative sums of daily wind speed and daily minimum relative humidity. These columns are used to calculate mean values for u_2 and RH_{min} during the midseason period (footnote 1).

TABLE 8.1
List of variable names in the spreadsheet that are not included in the List of principal symbols and acronyms in the introduction section of this paper.

Avail. Water	water available to plant (field capacity – wilting point) [mm/m]
J_{Plant}	number of day of the year at time of planting [-]
J_{Dev}	number of day of the year at beginning of development period [-]
J_{Mid}	number of day of the year at beginning of midseason period [-]
J_{Late}	number of day of the year at beginning of late season period [-]
J_{Harv}	number of day of the year at time of harvest or death [-]
Max. Ht.	mean height of vegetation during the midseason period [m]
MAD during initial stage	management allowed depletion fraction during the initial growing period [-]
MAD after initial stage	management allowed depletion fraction following the initial growing period (during all other periods) [-]
$Root_{min}$	average depth of "effective" root zone during the initial period (also described as $Z_{r\ min}$) [m]
$Root_{max}$	maximum depth of "effective" root zone (also described as $Z_{r\ max}$) [m]

FIGURE 8.2
Daily values for K_{cb} from the calculation example of Figure 8.1

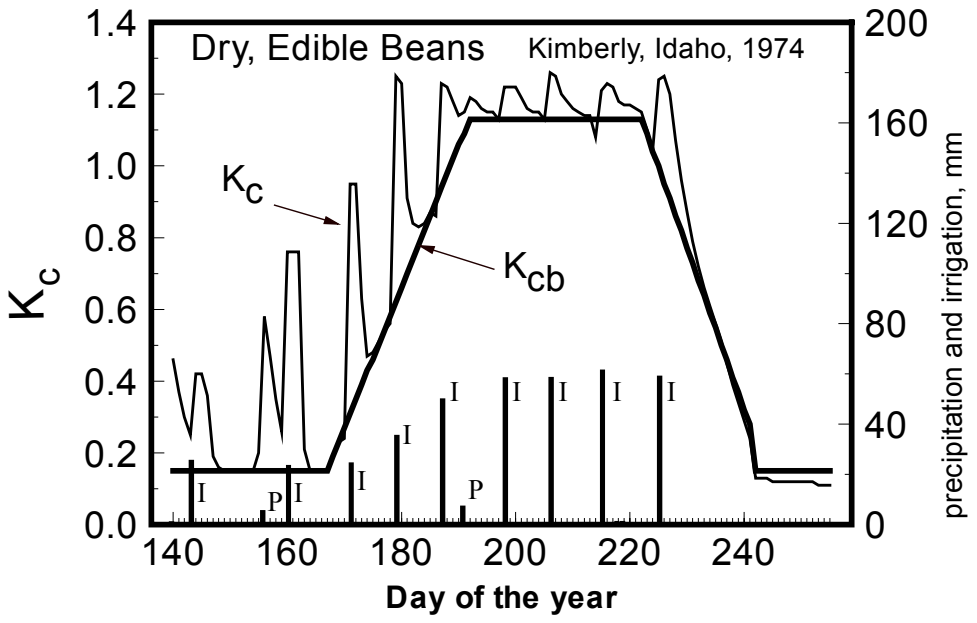

The daily values calculated for K_{cb} and K_c are illustrated in Figure 8.2. The daily soil water depletion at the end of each day calculated in the spreadsheet example is graphed in Figure 8.3. Figure 8.3 illustrates the effect of an increasing root zone on the allowable depletion. The allowable depletion is the same as the readily available water (RAW) when it is assumed that MAD = p, the evapotranspiration depletion factor. The depth of the effective root zone is calculated on each day as:

$$Z_{r\,i} = Z_{r\,min} + \left(Z_{r\,max} - Z_{r\,min}\right) \frac{K_{cb\,i} - K_{cb\,ini}}{K_{cb\,mid} - K_{cb\,ini}} \qquad \text{for } J < J_{mid} \qquad (8\text{-}1)$$

and

$$Z_{r\,i} = Z_{r\,max} \qquad \text{for } J \geq J_{mid} \qquad (8\text{-}2)$$

where

$Z_{r\,i}$	effective depth of the root zone on day i [m]
$Z_{r\,min}$	initial effective depth of the root zone (at the beginning of the initial period (planting))
$Z_{r\,max}$	maximum effective depth of the root zone during the midseason period (from Table 22 of Chapter 8)
J	Day of year [1 to 366]

$Z_{r\,min}$ is the same as variable $Root_{min}$ that is used in Figure 8.1 and $Z_{r\,max}$ is the same as $Root_{max}$. Equations 8-1 and 8-2 presume that the development of the root zone increases in proportion to the increase in K_{cb}. This implies that the maximum effective root depth is reached by the beginning of the midseason. Other approaches to estimate Z_r can be used, including interpolations based on time of season, for example:

$$Z_{r\,i} = Z_{r\,min} + \left(Z_{r\,max} - Z_{r\,min}\right) \frac{J - J_{start}}{J_{max} - J_{start}} \qquad \text{for } J_{start} \leq J \leq J_{max} \qquad (8\text{-}3)$$

and $Z_{r\,i} = Z_{r\,min}$ when $J < J_{start}$, and $Z_{r\,i} = Z_{r\,max}$ when $J > J_{max}$, where:

J_{start}	Day of year at beginning of the increase in $Z_{r\,i}$ beyond $Z_{r\,min}$
J_{max}	Day of year at the attainment of maximum rooting depth

$Z_{r\,min}$ for annual crops should represent the depth of seed placement plus an additional depth of soil that may contribute water to the seed as it extends its initial roots downward following germination. For many annual crops, $Z_{r\,min}$ can be be estimated as 0.15 to 0.20 m.

The value used for MAD is given a separate and larger value during the initial period to account for the ability of roots for some crops to extract water at relatively dry water contents during germination and during the initial period with little impact by stress. In this example, it is assumed that p =MAD.

The irrigation period for the bean crop is presumed to begin at planting and to terminate half-way through the late season period. Therefore, the last irrigation date is on day 225. The bean crop exhibited only a small amount of stress following day 225, since the K_c was declining. The stress coefficient (K_s) is calculated in column AJ of the spreadsheet.

The fact that irrigations are not applied in the spreadsheet until the the soil water depletion at the end of the previous day is greater than or equal to RAW occasionally causes a small amount of stress on the day prior to irrigation (see K_s in column AJ). The impact of K_s on $K_{c\,adj}$ was small before planting and near the end of the growing season because K_{cb} is small relative to the potential value for K_e during these periods.

This particular example is intended only to demonstrate how to apply the soil evaporation equations during scheduling of irrigations. The procedure used to determine the irrigation schedule and the assumptions used may not always be appropriate. The reader should modify the irrigation scheduling procedure to fit the conditions of the local area.

FIGURE 8.3
Soil water depletion at the end of each day calculated in Figure 8.1

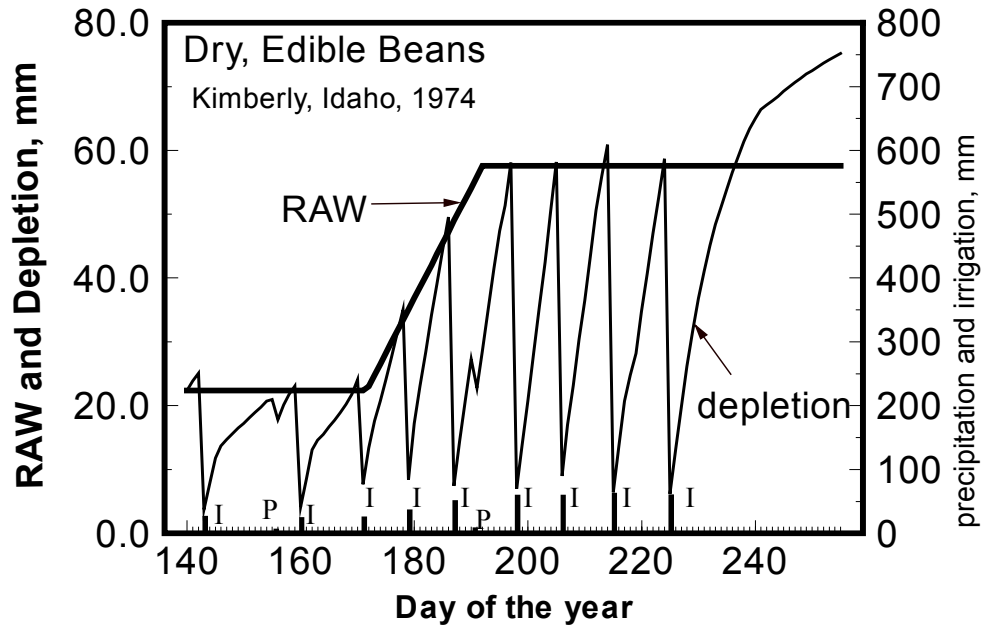

Bibliography

A. BASIC CONCEPTS AND DEFINITIONS

Allen, R.G., Smith, M., Perrier, A., and Pereira, L.S. 1994a. An update for the definition of reference evapotranspiration. *ICID Bulletin*. 43(2). 1-34.

Jensen, M.E., Burman, R.D., and Allen, R.G. (ed). 1990. *Evapotranspiration and Irrigation Water Requirements*. ASCE Manuals and Reports on Engineering Practices No. 70., Am. Soc. Civil Engrs., New York, NY, 360 p.

Monteith, J.L., 1965. Evaporation and Environment. 19th Symposia of the Society for Experimental Biology, University Press, Cambridge, 19:205-234.

Monteith, J.L. 1973. *Principles of Environmental Physics,* Edward Arnold, London.

Monteith, J.L. and Unsworth, M.H. 1990. *Principles of Environmental Physics*, 2nd ed., Edward Arnold, London.

Penman, H. L. 1948. "Natural evaporation from open water, bare soil and grass." *Proc. Roy. Soc. London*, A193, 120-146.

Penman, H.L. 1963. *Vegetation and hydrology*. Tech. Comm. No. 53, Commonwealth Bureau of Soils, Harpenden, England. 125 p.

Pereira, L.S., Perrier, A., Allen, R.G. and Alves, I. 1996. Evapotranspiration: Review of concepts and future trends. *J. Irrig. And Drain. Engrg., ASCE* 25. (in press).

Perrier, A. 1978. Importance des définitions de l'évapotranspiration dans le domaine pratique de la mesure, de l'estimation of de la notion de coefficients culturaux. XV' *Journal of Hydraulics*, Société Hydrotechnique de France, Question IV, Rapport 1:1-7 (in French).

Perrier, A. 1982. Land surface processes: vegetation. pp. 395-448 in P.S. Eagleson (Editor), *Land Surface Processes in Atmospheric General Circulation Models*. Cambridge Univ. Press, Cambridge, Mass.

Perrier, A. 1985. Updated evapotranspiration and crop water requirement definitions. In: Perrier, A. and Riou, C.(eds) *Crop Water Requirements* (ICID Int. Conf., Paris, Sept. 1984). INRA, Paris: 885-887.

Rijtema, P.E., (1965). "Analysis of actual evapotranspiration." Agric. Res. Rep. No. 69, Centre for Agric. Publ. and Doc., Wageningen.

Slatyer, R.O. and McIlroy, I.C. 1961. Evaporation and the principle of its measurement. In: *Practical Meteorology,* CSIRO (Australia) and UNESCO, Paris.

Smith, M., Allen, R.G., Monteith, J.L., Perrier, A., Pereira, L., and Segeren, A. 1992. Report of the expert consultation on procedures for revision of FAO guidelines for prediction of crop water requirements. UN-FAO, Rome, Italy, 54 p.

B. ET EQUATIONS

Allen, R.G. 1986. A Penman for all seasons. *J. Irrig. and Drain. Engrg.* 112(4):348-368.

Allen, R.G. 1992. Evaluation of a temperature difference method for computing grass reference evapotranspiration. Report submitted to UN-FAO Water Resources Development and Management Service, Land and Water Dev. Div., Rome. 50 p.

Allen, R.G., 1995b. Evaluation of procedures for estimating grass reference evapotranspiration using air temperature data only. Report prepared for FAO, Water Resources Development and Management Service, FAO, Rome.

Allen, R.G. and Pruitt, W.O. 1986. Rational use of the FAO Blaney-Criddle formula. *J. Irrig. and Drain. Engrg.*, ASCE 112(IR2):139-155.

Allen, R.G. and Pruitt, W.O. 1991. FAO-24 reference evapotranspiration factors. *J. Irrig. and Drain. Engrg*., ASCE 117(5):758-773.

Allen, R.G., Pruitt, W.O., Businger, J.A., Fritschen, L.J., Jensen, M.E., and Quinn, F.H. 1996. Chapter 4 "Evaporation and Transpiration" in *ASCE Handbook of Hydrology*. New York, NY. p. 125-252.

Batchelor, C.H. 1984. The accuracy of evapotranspiration functions estimated with the FAO modified Penman equation. *Irrig. Science* 5(4): 223-234.

Blaney, H.F. and Criddle, W.D. 1950. Determining water requirements in irrigated areas from climatological and irrigation data. USDA Soil Conserv. Serv. SCS-TP96. 44 pp.

Brutsaert, W.H., 1982. *Evaporation into the Atmosphere*. R. Deidel Publishing Company, Dordrecht, Holland.

Burman, R. and Pochop, L.O. 1994. *Evaporation, Evapotranspiration and Climatic Data.* Elsevier Science B.V., Amsterdam.

Businger, J.A. 1956. Some remarks on Penman's equations for the evapotranspiration. *Netherlands J. Agric. Sci.* 4: 77.

Castrignanò, A., de Caro, A., and Tarantino, E. 1985. Verifica sulla validità di alcuni metodi empirici di stima dell'evapotraspirazione potenziale nel Metapontino. (Verification of validity of several empirical methods of estimating potential evapotranspiration in southern Italy). *L'Irrigazione* XXXII (4):23-28 (in Italian).

Chiew, F.H.S., N.N. Kamadalasa, H.M. Malano and McMahon, T.A. 1995. Penman-Monteith, FAO-24 reference crop evapotranspiration and class-A pan data in Australia. *Agric. Water Management* **28**: 9-21.

Choisnel, E., de Villele, O., and Lacroze, F. 1992. *Une approche uniformisée du calcul de l'évapotranspiration potentielle pour l'ensemble des pays de la Communauté Européenne,* Com. Commun. Européennes, EUR 14223 FR, Luxembourg, 176 p.

Christiansen, J.E. 1968. Pan evaporation and evapotranspiration from climatic data. *J. Irrig. and Drain. Div*., ASCE 94:243-265.

Cuenca, R.H. and Nicholson, M.T. 1982. Application of the Penman equation wind function. *J. Irrig. and Drn. Engrg. Div*., ASCE 108(IR1):13-23.

Doorenbos, J. and Kassam, A.H. 1979. *Yield response to water*. FAO Irrig. and Drain. Paper No. 33, FAO, Rome, Italy. 193 pp.

Doorenbos, J. and Pruitt, W.O. 1975. *Guidelines for predicting crop water requirements*, Irrigation and Drainage Paper 24, Food and Agriculture Organization of the United Nations, Rome, 179 p.

Feddes, R.A. 1987. Crop factors in relation to Makkink reference crop evapotranspiration. Tech. Bull. Inst. for Land and Water Management Research. No. 67, pp. 33-45.

Frére, M. and Popov, G.F. 1979. *Agrometeorological crop monitoring and forecasting*. FAO Plant Production and Protection Paper 17. FAO, Rome, Italy., pp 38-43.

Frevert, D.K., Hill, R.W., and Braaten, B.C. 1983. Estimation of FAO evapotranspiration coefficients. *J. Irrig. and Drain Engrg*., ASCE 109(IR2):265-270.

Gunston, H. and Batchelor, C.H. 1983. A comparison of the Priestley-Taylor and Penman methods for estimating reference crop evapotranspiration in tropical countries. *Agric. Water Man*. 6:65-77.

George, W., Pruitt, W.O., and Dong, A. 1985. Evapotranspiration modeling. In: California Irrigation Management Information System, Final Report, by R. Snyder, D.W. Henderson, Pruitt, W.O., and Dong, A. Calif. Dept. Water Resour. Contract. No. B53812. Land, Air and Water Resources Pap. 10013-A, Univ. Calif., Davis, III-36 to III-59.

Gosse, G., Perrier, A., and Itier, B. 1977. Etude de l'évapotranspiration réelle d'une culture de blé dans le bassin parisien. *Ann. Agron*. 28(5):521-541. (in French).

Hargreaves, G.H. 1983. Discussion of 'Application of Penman wind function' by Cuenca, R.H. and Nicholson, M.J. *J. Irrig. and Drain. Engrg*., ASCE 109(2):277-278.

Hargreaves, G.L., Hargreaves, G.H., and Riley, J.P. 1985. Agricultural benefits for Senegal River Basin. *J. Irrigation and Drainage Engr*., ASCE 111:113-124.

Hashemi, F. and Habibian, M.T. 1979. Limitations of temperature based methods in estimating crop evapotranspiration in arid-zone agricultural development project. *Agric. Meteorol.* 20: 237-247.

Hatfield, J.L. and Fuchs, M. 1990. Evapotranspiration models. Chapter 3, pp 33-59 in *Management of Farm Irrigation Systems* (G.J. Hoffman, T.A. Howell, and K.H. Solomon (ed)), ASAE, St. Joseph, Michigan.

Howell, T.A., Schneider, A.D., and Jensen, M.E. 1991. History of lysimeter design and use for evapotranspiration measurements. In Allen, R.G., Howell, T.A., Pruitt, W.O., Walter, I.A., and Jensen, M.E. (Editors), *Lysimeters for Evapotranspiration and Environmental Measurements*, ASCE, New York, NY p. 1-9.

Itier, B. and Perrier, A. 1976a. Presentation d'une étude analytique de l'advection: I. Advection lie'e aux variations horizontales de concentration et de temperature. *Ann. Agron.* 27(2):111-140.

Itier, B., Brunet, Y., Mcaneney, K.J., and Lagouarde, J.P. 1994. Downwind evolution of scalar fluxes and surface resistance under conditions of local adection. Part I: A reappraisal of boundary conditions. *Agric. and For. Meteorol*. 71: 211-255.

Itier, B. 1996. Measurement and estimation of evapotranspiration. In: Pereira, L.S., Feddes, R.A., Gilley, J.R., Leseffre, B. (eds) *Sustainability of Irrigated Agriculture.* Kluwer Acad. Publ., Dordrecht, pp. 171-191.

Jensen, M.E. and Haise, H.R. 1963. Estimating evapotranspiration from solar radiation. *J.Irrig. and Drain. Div.*, ASCE, 89:15-41.

Jensen, M.E. 1974. (ed.) *Consumptive use of water and irrigation water requirements*. Rep. Tech. Com. on Irrig. Water Requirements, Irrig. and Drain. Div., ASCE, 227 pp.

Jensen, M.E., Burman, R.D., and Allen, R.G. (ed). 1990. *Evapotranspiration and Irrigation Water Requirements*. ASCE Manuals and Reports on Engineering Practices No. 70., Am. Soc. Civil Engrs., New York, NY, 360 p.

Katerji, N. and Perrier, A. 1983. Modélization de l'évapotranspiration réelle ETR d'une parcelle de luzerne: rôle d'un coefficient cultural. *Agronomie* 3(6):513-521 (in French).

Makkink, G.F. 1957. Testing the Penman formula by means of lysimeters. *J. Inst. Water Engng.* 11 (3): 277-288.

McNaughton, K.G. and Jarvis, P.G. 1984. Using the Penman-Monteith equation predictively. *Agricultural Water Management* 8:263-278.

Monteith, J.L. 1973. *Principles of Environmental Physics,* Edward Arnold, London.

Monteith, J.L. 1981. Evaporation and surface temperature. *Quart. J. Roy. Meteorol. Soc.* 107:1-27.

Monteith, J.L. 1985. Evaporation from land surfaces: progress in analysis and prediction since 1948. pp. 4-12 in *Advances in Evapotranspiration*, Proceedings of the ASAE Conference on Evapotranspiration, Chicago, Ill. ASAE, St. Joseph, Michigan.

Pelton, W.L., King, K.M. and Tanner, C.B. 1960. An evaluation of the Thornthwaite and mean temperature methods for determining potential evapotranspiration. *Agron. J.* 52: 387-395.

Penman, H. L. 1948. "Natural evaporation from open water, bare soil and grass." *Proc. Roy. Soc. London*, A193, 120-146.

Penman, H.L. 1963. *Vegetation and hydrology*. Tech. Comm. No. 53, Commonwealth Bureau of Soils, Harpenden, England. 125 pp.

Pereira, L.S. and Smith, M. 1989. Proposed procedures for revision of guidelines for predicting crop water requirements. Land and Water Use Div., FAO Rome, 36 p.

Phene, C.J., Clark, D.A. and Cardon, G.E. 1996. Real time calculation of crop evapotranspiration using an automated pan evaporation system. In: Camp, C.R., Sadler, E.J. and Yoder, R.E. (eds.). *Evaporation and Irrigation Scheduling*, ASCE: 189-194.

Piper, B.S. 1989. Sensitivity of Penman estimates of evaporation to errors in input data. *Ag. Water Man*. 15:279-300.

Priestley, C.H.B. and Taylor, R.J. 1972. On the assessment of surface heat flux and evaporation using large scale parameters. *Mon. Weath. Rev*., 100: 81-92. Pruitt, W.O. (1996). "Empirical method of estimating evapotranspiration using primarily evaporation pans." *Proc. Conf. on Evapotanspiration and its Role in Water Resources Management.* Chicago. Dec. pp. 57-61. Stewart, J.B. 1983. A discussion of the relationships between the principal forms of the combination equation for estimating evapotranspiration. *Ag. Meteorol*. 30:111-127.

Rosenberg, N.J., Blad, B.L. and Verma, S.B. 1983. *Microclimate. The Biological Environment* (2nd edition). J. Wiley, New York.

Seemann, J., Chirkov, Y.I., Lomas, J. and Primault, B., 1979. *Agrometeorology.*Springer Verlag, Berlin, Heidelberg.

Seguin, B., Brunet, Y., and Perrier, A. 1982. Estimation of evaporation: a review of existing methods and recent developments. in European Geologic Society Symposium on Evaporation. Leeds, U.K., August, 1982, 21 p.

Sharma, M.L. 1985. Estimating evapotranspiration. p. 213-281 in *Adv. in Irrigation, Vol III*, D. Hillel (Editor)., Academic Press, New York.

Stewart, J.B. 1983. A discussion of the relationships between the principal forms of the combination equation for estimating evaportranspirations. *Ag. Meteorol.* 30:111-127.

Tanner, C.B. and Pelton, W.L. 1960. Potential evapotranspiration estimates by the approximate energy balance of Penman. *J. Geophysical Res*. 65(10):3391-3413.

Tanner, C.B. and Fuchs, M. 1968. Evaporation from unsaturated surfaces: a generalized combination equation. *J. Geophysical Res*. 73(4):1299-1304.

Thompson, N., Barrie, I.A., and Ayles, M. 1981. The Meteorological Office rainfall and evaporation calculation system: MORECS. Hydrological Memorandum 45, Hydrometeorological Services, London, 66 p.

Thornthwaite, C.W. 1948. An approach toward a rational classification of climate. *Geograph. Rev*., 38, 55.

Turc, L. 1961. Evaluation des besoins en eau d'irrigation, evapotranspiration potentielle, formule climatique simplifice et mise a jour. (in French). *Ann. Agron*. 12:13-49.

Watts, P.J. and Hancock, N.H. 1985. Evaporation and potential evaporation- a practical approach for agricultural engineers. *Mech. Engrg. Trans*. 10(4):231-240 plus discussions during 1986.

Wright, J.L. 1982. New evapotranspiration crop coefficients. *J. irrig. and Drain. Div.,* ASCE, 108 (IR2): 57-74.

Wright, J.L. 1988. Daily and seasonal evapotranspiration and yield of irrigated alfalfa in southern Idaho. *Agron. J*. 80: 662-669.

C. ET AND WEATHER MEASUREMENT

Allen, R.G. 1996. Assessing integrity of weather data for use in reference evapotranspiration estimation. *J. Irrig. and Drain. Engng. Div.,* ASCE 122(2): 97-106.

Allen, R.G., Pruitt, W.O., and Jensen, M.E. 1991. Environmental requirements for lysimeters. pp. 170-181 in Allen, R.G., Howell, T.A., Pruitt, W.O., Walter, I.A., and Jensen, M.E. (Editors). *Lysimeters for Evapotranspiration and Environmental Measurements*. Proc. of the ASCE Int. Symp. on Lysimetry, Honolulu, HA, ASCE, New York, NY.

Bastiaanssen, W.G.M. 1995. Regionalization of surface flux densities and moisture indicators in composite terrain. Doctoral thesis, Wageningen Agricultural University, Wageningen, 273 pp.

Beard, J.R. 1985. An assessment of water use by turfgrass. p. 45-60 in Gibeault, V.A. and Cockerham, S.T. (Editors). *Turfgrass Water Conservation*. Publ. 21405, Univ. Calif., Div. of Agric. and Nat. Resour., Berkley, Calif.

Biran, I., Bravdo, B., Bushkin-Harav, I., and Rawitz, E. 1981. Water consumption and growth rate of 11 turfgrasses as affected by mowing height, irrigation frequency and soil moisture. *Agron. J*. 73:85-90.

Blad, B.L. and Rosenberg, N.J. 1974. Lysimetric calibration of the Bowen-ratio energy balance method for evapotranspiration estimation in the Central Great plains. *J. App. Meteorol*. 13(2):227-236.

Brutsaert, W.H., 1982. *Evaporation into the Atmosphere*. R. Deidel Publishing Company, Dordrecht, Holland.

Businger, J.A. 1988. "A note on the Businger-Dyer profiles." *Boundary-Layer Meteorol.* 42: 145-151.

Businger, J.A. and Yaglom, A.M. 1971. "Introduction to Obukhov's paper on 'Turbulence in an atmosphere with a non-uniform temperature'," *Boundary-Layer Meteorol.* 2: 3-6.

Campbell, G.S. 1977. *An Introduction to Environmental BioPhysics*. Springer Verlag, N.Y. 159 p.

Carrijo, O.A. and Cuenca R.H., 1992. Precision of evapotranspiration estimates using neutron probe. *J. Irrig. and Drain. Engrg., ASCE* 118 (6): 943-953.

Dolman, A.J. and Stewart, J. B. 1987. Modelling forest transpiration from climatological data. In: R.H. Swanson, P.Y. Bernier and P.D. Woodard (eds) *Forest Hydrology and Watershed Management,* IAHS Publ. 167: 319-327.

Fritschen, L.J. and Fritschen, C.L. 1991. Design and evaluation of net radiometers. Paper presented at the 7th Symp. on Meteorol. Observations and Instrumentation, Jan. 13-18, 1991., New Orleans, La., U.S.A. 5 p.

Gash, J.H.C., Shuttleworth, W.J., Lloyd, C.R., André, J.C., Goutorbe, J.P., and Gelpe, J. 1989. Micrometeorological measurements in Les Landes forest during HAPEX-MOBILHY. *Ag. and For. Meteorol*. 46:131-147.

Grant, D.R. 1975. Comparison of evaporation from barley with Penman estimates. *Agric. Meteorol.* 15: 49-60.

Grebet, P. and Cuenca, R.H. 1991. History of lysimeter design and effects of environmental disturbances. in Allen, R.G., Howell, T.A., Pruitt, W.O., Walter, I.A., and Jensen, M.E. (Editors), *Lysimeters for Evapotranspiration and Environmental Measurements*, ASCE, New York, NY p. 10-18.

Itier, B. and Perrier, A. 1976a. Presentation d'une étude analytique de l'advection: I. Advection lie'e aux variations horizontales de concentration et de temperature. *Ann. Agron.* 27(2):111-140.

Itier, B., Brunet, Y., Mcaneney, K.J., and Lagouarde, J.P. 1994. Downwind evolution of scalar fluxes and surface resistance under conditions of local adection. Part I: A reappraisal of boundary conditions. *Agric. and For. Meteorol*. (in press).

Itier, B. 1996. Measurement and estimation of evapotranspiration. In: Pereira, L.S., Feddes, R.A., Gilley, J.R., Leseffre, B. (eds) *Sustainability of Irrigated Agriculture.* Kluwer Acad. Publ., Dordrecht, pp. 171-191.

Kessler, J., Perrier, A. and Pescara, C. de, 1990. *La Météo Agricole.* Météole, (Pau).

Kizer, M.A., Elliott, R.L. and Stone, J.F. 1990. Hourly ET model calibration with eddy flux and energy balance data. *J. Irrig. and Drain. Engrg.*, ASCE 116(2):172-181.

Marsh, A.W., Strohman, R.A., Spaulding, S., Younger, V., and Gibeault, V. 1980. Turf grass irrigation research at the University of California: warm and cool season grasses tested for water needs. *Irrig. J.*, July/August. 20-21, 32-33.

Meyer, W.S. and Mateos, L. 1990. Effects of soil type on soybean crop water use in weighing lysimeters. II. effect of lysimeter canopy height discontinuity on evaporation. *Irrig. Sci*. 11:233-237.

Neale, C.M.U., Kruse, E.G., and Yoder, R.E. 1991. Field experience with hydraulic weighing lysimeters. in Allen, R.G., Howell, T.A., Pruitt, W.O., Walter, I.A., and Jensen, M.E. (Editors), *Lysimeters for Evapotranspiration and Environmental Measurements*, ASCE, New York, NY p. 160-169.

Pearce, A.J., Gash, J.H.C., and Stewart, J.B. 1980. Rainfall interception in a forest stand estimated from grassland meteorological data. *J. Hydrol.*, 46:147-163.

Perrier, A., Itier, B., Bertolini, J.M., and Katerji, N. 1976. A new device for continuous recording of the energy balance of natural surfaces. *Agric. Meteor*. 16(1):71-85.

Perrier, A. and Tuzet, A. 1991. Land surface processes: Description, theoretical approaches, and physical laws underlying their measurements. pp. 145-155 in Schmugge, T.J. and Andre, J.-C. (eds) *Land Surface Evaporation: Measurement and Parameterization.* Springer-Verlag. Berlin.

Perrier, A., Archer, P., and de Pablos, B. 1974. Etude de l'évapotranspiration réelle et maximele de diverses cultures. I: Dispositif et mesure. *Ann. Agron.* 25(3:229-243.

Perrier, A., Katerji, N., Gosse, G., and Itier, B. 1980. Etude "in situ" de l'evapotranspiration reelle d'une culture de ble. (In situ study of evapotranspiration rates for a wheat crop). *Agric. Meterol*. 21:295-311. (in French).

Pruitt, W.O., Morgan, D.L., and Lourence, F.J. 1973. Momentum and mass transfers in the surface boundary layer. *Quart. J. Roy. Meteorol. Soc*. 99:370-386.

Pruitt, W.O. 1991. Development of crop coefficients using lysimeters. pp. 182-190 in Allen, R.G., Howell, T.A., Pruitt, W.O., Walter, I.A., and Jensen, M.E. (Editors). *Lysimeters for*

Evapotranspiration and Environmental Measurements. Proc. of the ASCE Int. Symp. on Lysimetry, Honolulu, HA, ASCE, New York, NY.

Pruitt, W.O. and Lourence, F. J. 1985. Experiences in lysimetry for ET and surface drag measurements. pp. 51-69 in: *Advances in Evapotranspiration*, ASAE, St. Joseph, MI.

Rosenberg, N.J., Blad, B.L. and Verma, S.B. 1983. *Microclimate. The Biological Environment* (2nd edition). J. Wiley, New York.

Schulze, K. 1995. Report of expert meeting for the preparation of an intercomparison of instruments and procedures for measurement and estimation of evaporation and evapotranspiration. World Meteorological Organization, Commission for Instruments and Methods of Observation. Geneva, Switzerland. 30 p.

Seemann, J., Chirkov, Y.I., Lomas, J. and Primault, B., 1979. *Agrometeorology.*Springer Verlag, Berlin, Heidelberg.

Shuttleworth, W.J. 1993. Evaporation. In: D.R. Maidment (ed) *Handbook of Hydrology.* McGraw Hill, New York: 4.1-4.53.

Shuttleworth, W.J. and Wallace, J.S. 1985. Evaporation from sparse crops - an energy combination theory. *Quart. J. Roy Meteorol. Soc.* 111: 839-853.

Stringer, W.C., Wolf, D.D., and Baser, R.E. 1981. Summer regrowth of tall fescue: stubble characteristics and microenvironment. *Agron. J.* 73:96-100.

Slatyer, R.O. and McIlroy, I.C. 1961. Evaporation and the principle of its measurement. In: *Practical Meteorology,* CSIRO (Australia) and UNESCO, Paris.

Stewart, J.B. and Gay, L.W. 1989. Preliminary modelling of transpiration from the FIFE stie in Kansas. *Agric. and For. Meteorol*. 48:305-315.

Tarantino, E. 1991. Grass reference measurements in Italy. in Allen, R.G., Howell, T.A., Pruitt, W.O., Walter, I.A., and Jensen, M.E. (Editors), *Lysimeters for Evapotranspiration and Environmental Measurements*, ASCE, New York, NY p. 200-209.

Thom, A.S., Thony, J.L., and Vauclin, M. 1981. On the proper employment of evaporation pans and atmometers in estimating potential transpiration. *Quart. J. Roy. Meteorol. Soc.*, 107: 711-736.

Walter, I.A., Siemer, E., Dirks, L.R., Quinian, J.P., and Burman, R.D. 1991. Lysimeters vs. buffer areas: evapotranspiration and agronomic comparisons. in Allen, R.G., Howell, T.A., Pruitt, W.O., Walter, I.A., and Jensen, M.E. (Editors), *Lysimeters for Evapotranspiration and Environmental Measurements*, ASCE, New York, NY p. 10-18.

Wehner, D.J. and Watschke, T.L. 1981. Heat tolerance of Kentucky bluegrasses, perennial ryegrasses, and annual bluegrass. *Agron. J.* 73:79-84.

WMO 1983 *Guide to Meteorological Instruments and Observing Practices.* WMO nº 8 (fifth edition), Geneva.

Wright, J.L. 1991. Using lysimeters to develop evapotranspiration crop coefficients. in Allen, R.G., Howell, T.A., Pruitt, W.O., Walter, I.A., and Jensen, M.E. (Editors), *Lysimeters for Evapotranspiration and Environmental Measurements*, ASCE, New York, NY p. 191-199.

D. PARAMETERS IN ET EQUATIONS

Allen, R.G., Jensen, M.E., Wright, J.L., and Burman, R.D. 1989. Operational estimates of reference evapotranspiration. *Agron. J.* 81:650-662.

Allen, R.G., Smith, M., Perrier, A., and Pereira, L.S. 1994a. An update for the definition of reference evapotranspiration. *ICID Bulletin*. 43(2). 1-34.

Allen, R.G., Smith, M., Pereira, L.S., and Perrier, A. 1994b. An update for the calculation of reference evapotranspiration. *ICID Bulletin,* 43 (2): 35-92.

Allen, R.G. 1995a. Evaluation of procedures for estimating mean monthly solar radiation from air temperature. Report prepared for FAO, Water Resources Development and Management Service, FAO, Rome.

Bosen, J.F. 1958. An approximation formula to compute relative humidity from dry bulb and dew point temperatures. *Monthly Weather Rev.* 86(12):486.

Brunt, D. 1939. *Physical and dynamical meteorology*, Univ. Press, Cambridge. 400 pp.

Brunt, D. 1952. *Physical and dynamical meteorology*, 2nd ed., Univ. Press, Cambridge. 428 pp.

Brutsaert, W.H., 1982. *Evaporation into the Atmosphere*. R. Deidel Publishing Company, Dordrecht, Holland.

Burman, R.D., Jensen, M.E., and Allen, R.G. 1987. Thermodynamic factors in evapotranspiration. In: James, L.G. and M.J. English (editors), *Proc. Irrig. and Drain. Spec. Conf.*, ASCE, Portland, Ore., p. 28-30.

Burman, R. and Pochop, L.O. 1994. *Evaporation, Evapotranspiration and Climatic Data.* Elsevier Science B.V., Amsterdam.

Businger, J.A. 1988. "A note on the Businger-Dyer profiles." *Boundary-Layer Meteorol.* 42: 145-151.

Choudhury, B.J., Idso, S.B., and Reginato, R.J. 1987. Analysis of an empirical model for soil heat flux under a growing wheat crop for estimating evaporation by an infrared temperature based energy balance equation. *Agric. for. Meteorol*. 39:283-297.

Clothier, B.E., Clawson, K.L., Pinter, P.J., Moran, M.S., Reginato, R.J., and Jackson, R.D. 1986. Estimates of soil heat flux from net radiation during the growth of alfalfa. *Agric. For. Meteorol* 37:319-329.

Duffie, J.A. and Beckman, W.A. 1991. *Solar engineering of thermal processes.* 2nd Ed., John Wiley and sons, New York. 994 p. Harrison, L.P. 1963. Fundamentals concepts and definitions relating to humidity. In Wexler, A (Editor) *Humidity and moisture* Vol 3, Reinhold Publishing Co., N.Y.

Dyer, A.J. 1974. A reviewof flux-profile relationships. *Boundary Layer Meterol.* 7: 363-372.

Dyer, A.J. and Hicks, B.B., 1970. Flux-gradient relationships in the constant flux layer. *Quart. J. Roy. Meteorol. Soc.* 96: 715-721.

Frevert, D.K., Hill, R.W., and Braaten, B.C. 1983. Estimation of FAO evapotranspiration coefficients. *J. Irrig. and Drain Engrg*., ASCE 109(IR2):265-270.

Garratt, J.R. (1992). *The atmospheric boundery layer.* Cambridge Univ. Press, 316 p.

Garratt, J.R. and Hicks, B.B. 1973. Momentum, heat and water vapour transfer to and from natural and artificial surfaces. *Quart. J. Roy. Meteorol. Soc.* 99: 680-687.

George, W., Pruitt, W.O., and Dong, A. 1985. Evapotranspiration modeling. In: California Irrigation Management Information System, Final Report, by R. Snyder, D.W. Henderson, Pruitt, W.O., and Dong, A. Calif. Dept. Water Resour. Contract. No. B53812. Land, Air and Water Resources Pap. 10013-A, Univ. Calif., Davis, III-36 to III-59.

Gosse, G., Perrier, A., and Itier, B. 1977. Etude de l'évapotranspiration réelle d'une culture de blé dans le bassin parisien. *Ann. Agron*. 28(5):521-541. (in French).

Harrison, L.P. 1963. Fundamentals concepts and definitions relating to humidity. In Wexler, A (Editor) *Humidity and moisture* Vol 3, Reinhold Publishing Co., N.Y.

Hashemi, F. and Habibian, M.T. 1979. Limitations of temperature based methods in estimating crop evapotranspiration in arid-zone agricultural development project. *Agric. Meteorol.* 20: 237-247.

Hatfield, J.L. and Fuchs, M. 1990. Evapotranspiration models. Chapter 3, pp 33-59 in *Management of Farm Irrigation Systems* (G.J. Hoffman, T.A. Howell, and K.H. Solomon (ed)), ASAE, St. Joseph, Michigan.

Hottel, H.C. 1976. A simple model for estimating the transmittance of direct solar radiation through clear atmospheres. *Solar Energy* 18:129.

Idso, S.B. and Jackson, R.B. 1969. Thermal radiation from the atmosphere. *J. Geophys. Res.* 74:5397-5403.

Jensen, J.R. 1988. Effect of asymmetric, daily air temperature and humidity waves on calculation of reference evapotranspiration. Proc. European Economic Community Workshop on Management of Water Resources in Cash Crops and in Alternative Production Systems. Brussels, Belg. 24-25 Nov., 1988. 12 p.

List, R.J. 1984. *Smithsonian Meteorological Tables*, 6th rev. ed., Smithsonian Institution, Washington D.C., U.S.A. 539 p.

Liu, B.Y.H., and Jorden, R.C. 1960. The interrelationship and characteristic distribution of direct diffuse and total solar radiation. *Solar Energy* 4(3):1-19.

Matias P.G.M. 1992. SWATCHP, a model for a continuous simulation of hydrologic processes in a system vegetation - soil - aquifer - river. Ph.D.dissertation, Techn. Univ. Lisbon (in Portuguese).

Monteith, J.L. and Unsworth, M.H. 1990. *Principles of Environmental Physics*, 2nd ed., Edward Arnold, London.

Monteith, J.L., 1965. Evaporation and Environment. 19th Symposia of the Society for Experimental Biology, University Press, Cambridge, 19:205-234.

Murray, F.W. 1967. On the computation of saturation vapor pressure. *J. Appl. Meteor.* 6:203-204.

Penman, H.L. 1963. *Vegetation and hydrology*. Tech. Comm. No. 53, Commonwealth Bureau of Soils, Harpenden, England. 125 pp.

Pereira, L.S. and Smith, M. 1989. Proposed procedures for revision of guidelines for predicting crop water requirements. Land and Water Use Div., FAO Rome, 36 p.

Pruitt, W.O. and Doorenbos, J. 1977. Background and Development of Methods to Predict Reference Crop Evapotranspiration (ETo). Appendix II in FAO-ID-24, pp 108-119.

Seguin, B., Brunet, Y., and Perrier, A. 1982. Estimation of evaporation: a review of existing methods and recent developments. in European Geologic Society Symposium on Evaporation. Leeds, U.K., August, 1982, 21 p.

Sharma, M.L. 1985. Estimating evapotranspiration. p. 213-281 in *Adv. in Irrigation, Vol III*, D. Hillel (Editor)., Academic Press, New York.

Smith, M., Allen, R.G., Monteith, J.L., Pereira, L.S., Perrier, A., Pruitt, W.O. 1992. Report on the Expert Consultation on procedures for Revision of FAO Guidelines for Prediction of Crop Water Requirements. Land and Water Development Division, United Nations Food and Agriculture Service, Rome, Italy.

Tetens, O. 1930. Uber einige meteorologische Begriffe. *z. Geophys.* 6:297-309.

van Wijk, W.R. and de Vries, D.A. 1963. Periodic temperature variations in a homogeneous soil. In: van Wijk, W.R. (Editor). *Physics of the plant environment*. North-Holland Publ. Co., Amsterdam, P. 102-143.

Weiss, A. 1982. An experimental study of net radiation, its components and prediction *Agron. J.* 74:871-874.

WMO 1970. *Guide to Hydrometeorological Practices*. WMO nº 168.TP.82. Geneva

WMO 1981. *Guide to Agricultural Meteorological Practices.* WMO nº 134 (second edition), Geneva.

Wright, J.L. 1982. New evapotranspiration crop coefficients. *J. irrig. and Drain. Div.,* ASCE, 108 (IR2): 57-74.

E. CROP PARAMETERS IN PM EQUATION

Allen, R.G., Jensen, M.E., Wright, J.L., and Burman, R.D. 1989. Operational estimates of reference evapotranspiration. *Agron. J.* 81:650-662.

Allen, R.G., Smith, M., Pereira, L.S., and Perrier, A. 1994b. An update for the calculation of reference evapotranspiration. *ICID Bulletin,* 43 (2): 35-92.

Allen, R.G., Vanderkimpen, P.J., and Wright, J.L. 1995. "Development of resistance parameters for operational application of the Penman-Monteith equation." *Agric. and For. Meteorol.*

Alves, I.L. 1995. Modelling crop evapotranspiration. Canopy and aerodynamic resistances. Ph.D. Dissertation, ISA, Univ. Tec. Lisboa (in portuguese).

Alves, I., Perrier, A. and Pereira, L.S., 1998. Aerodynamic and surface resistances of complete over crops: How good in the "big leaf" approach? *Trans. ASAE* 41(2): 345-351.

Ben-Mehrez, M., Taconet, O., Vidal-Madjar, D., and Valencogne, C. 1992. "Estimation of stomatal resistance and canopy evaporation during the HAPEX-MOBILHY experiment." *Agr. and For. Meteorol.* 58: 285-313.

Bevan, K. 1979. A sensitivity analysis of the Penman-Monteith actual evapotranspiration estimates. *J. Hydrol*. 44:169-190.

Brutsaert, W.H., 1982. *Evaporation into the Atmosphere*. R. Deidel Publishing Company, Dordrecht, Holland.

Businger, J.A. and Yaglom, A.M. 1971. "Introduction to Obukhov's paper on 'Turbulence in an atmosphere with a non-uniform temperature'," *Boundary-Layer Meteorol.* 2: 3-6.

Campbell, G.S. 1977. *An Introduction to Environmental BioPhysics*. Springer Verlag, N.Y. 159 p.

Chamberlain, A.C., 1966. Transport of gases to and from grass and grass-like surfaces. *Proc. Roy. Soc. A*, 290:236-259.

DeCoursey, D.G. 1992. Evaporation and evapotranspiration processes. In: *Root Zone Water Quality Model, version 1.0. Technical Documentation.* GPSR, USDA-ARS, Fort Collins, Co, pp 29-74.

Dolman, A.J. and Stewart, J. B. 1987. Modelling forest transpiration from climatological data. In: R.H. Swanson, P.Y. Bernier and P.D. Woodard (eds) *Forest Hydrology and Watershed Management,* IAHS Publ. 167: 319-327.

Frank, A.B. 1981. Effect of leaf age and position on photosynthesis and stomatal conductance of forage grasses. *Agron. J.* 73:70-74.

Jarvis, P.G. 1976. The interpretation of the variations in leaf water potential and stomatal conductance found in canopies in the field. *Phil. Trans. Roy. Soc*., Lond., B 273:593-610.

Kelliher, F.M., Leuning, R. and Schulze, E.D. 1993. Evaporation and canopy characteristics of coniferous forests and grasslands. *Oecologia* 95:153-163.

Kim, J. and Verma, S.B. 1991. Modeling canopy stomatal conductance in a temperate grassland ecosystem. *Agric. and For. Meteorol*. 55:149-166.

Loommis, R.S. and Williams, W.A. 1969. Productivity and the morphology of crop stand patterns with leaves. In: J.D. Eastin (ed) *Physiological Aspects of Crop Yield.* ASA, CSSA and SSSA, Madison, WI: 27-47.

Martin, D.L. and J.R. Gilley 1993. *Irrigation Water Requirements.* Chapter 2 of the SCS National Engineering Handbook, Soil Conservation Service, Washington D.C., 284 pp.

Matias P.G.M. 1992. SWATCHP, a model for a continuous simulation of hydrologic processes in a system vegetation - soil - aquifer - river. Ph.D.dissertation, Techn. Univ. Lisbon (in Portuguese).

McNaughton, K.G. and Jarvis, P.G. 1984. Using the Penman-Monteith equation predictively. *Agricultural Water Management* 8:263-278.

Monin, A.S. and Obukhov, A.M. 1954. "The basic laws of turbulent mixing in the surface layer of the atmosphere." *Akad. Nauk. SSSR Trud. Geofiz. Inst.,* No. 24. (151): 163-187.

Monteith, J.L. 1973. *Principles of Environmental Physics,* Edward Arnold, London.

Monteith, J.L. 1981. Evaporation and surface temperature. *Quart. J. Roy. Meteorol. Soc.* 107:1-27.

Monteith, J.L. 1985. Evaporation from land surfaces: progress in analysis and prediction since 1948. pp. 4-12 in *Advances in Evapotranspiration*, Proceedings of the ASAE Conference on Evapotranspiration, Chicago, Ill. ASAE, St. Joseph, Michigan.

Monteith, J.L. and Unsworth, M.H. 1990. *Principles of Environmental Physics*, 2nd ed., Edward Arnold, London.

Monteith, J.L., 1965. Evaporation and Environment. 19th Symposia of the Society for Experimental Biology, University Press, Cambridge, 19:205-234.

Paulson, C.A. 1970. The mathematical representation of wind speed and temperature profiles in the unstable atmospheric surface layer. *J. Appl. Meteorol.* 9: 857-861.

Perrier, A. 1982. Land surface processes: vegetation. pp. 395-448 in P.S. Eagleson (Editor), *Land Surface Processes in Atmospheric General Circulation Models*. Cambridge Univ. Press, Cambridge, Mass.

Perrier, A. and Tuzet, A. 1991. Land surface processes: Description, theoretical approaches, and physical laws underlying their measurements. pp. 145-155 in Schmugge, T.J. and Andre, J.-C. (eds) *Land Surface Evaporation: Measurement and Parameterization.* Springer-Verlag. Berlin.

Pruitt, W.O., Morgan, D.L., and Lourence, F.J. 1973. Momentum and mass transfers in the surface boundary layer. *Quart. J. Roy. Meteorol. Soc*. 99:370-386.

Shaw, R,H. and Pereira, A.R. 1982. Aerodynamic roughness of a plant canopy: A numerical experiment. *Agric. Meteorol.* 26: 51-65. Stewart, J.B. 1988. Modelling surface conductance of pine forest. *Agric. and For. Meteorol*. 43:19-35.

Shuttleworth, W.J. 1993. Evaporation. In: D.R. Maidment (ed) *Handbook of Hydrology.* McGraw Hill, New York: 4.1-4.53.

Shuttleworth, W.J. and Wallace, J.S. 1985. Evaporation from sparse crops - an energy combination theory. *Quart. J. Roy Meteorol. Soc.* 111: 839-853.

Smith, M., Allen, R.G., Monteith, J.L., Perrier, A., Pereira, L., and Segeren, A. 1992. Report of the expert consultation on procedures for revision of FAO guidelines for prediction of crop water requirements. UN-FAO, Rome, Italy, 54 p.

Stewart, J.B. 1989. On the use of the Penman-Monteith equation for determining areal evapotranspiration. in Estimation of Areal Evapotranspiration, IAHS Publ. no. 177:3-12.

Stewart, J.B. and Verma, S.B. 1992. Comparison of surface fluxes and conductances at two contrasting sites within the FIFE area. *J. Geophysical Research* 97(D17):18623-18628.

Szeicz, G. and Long, I.F. 1969. Surface resistance of crop canopies. *Water Resour. Res.* 5, 622-633.

Thom, A.S. 1971. Momentum absorption by vegetation. *Quart. J. Roy. Meteorol. Soc.* 97:414-428.

Thom, A.S. 1972. Momentum, mass and heat exchange of vegetation. *Quart. J. Roy. Meteorol. Soc.* 98, 124-134.

Thom, A.S. and Oliver, H.R. 1977. On Penman's equation for estimating regional evaporation. *Quart. J. Roy. Meteorol. Soc.* 103: 345-357.

Thom, A.S., Setwart, J.B., Oliver, H.R. and Gash, J.H.C. 1975. Comparison of aerodynamic and energy budget estimates of fluxes over a pine forest. *Quart. J. Roy. Meteorol. Soc.* 101: 93-105.

van Bavel, C.H., Fritschen, L.J., and Reeves, W.E. 1963. Transpiration of sudangrass as an externally controlled process. *Science* 141:269-270.

Verma, S.B. 1989. Aerodynamic resistances to transfers of heat, mass and momentum. *Estimation of Areal Evapotranspiration,* T.A. Black, D.L. Spittlehouse, M.D. Novak and D.T. Price (ed)., IAHS Pub. No. 177. p. 13-20.

Webb, E.K. 1970. "Profile relationships: the log-linear range, and extension to strong stability." *Q.J. Roy. Met. Soc.* 96: 67-90.

Wallace, J.S., Roberts, J.M., and Sivakuma, M.V.K. 1990. "The estimation of transpiration from sparse dryland millet using stomatal condutance and vegetation area indices." *Agric. and Forest Meteorol.* 51: 35-49.

F. ANALYSIS OF WEATHER AND ET DATA

Allen, R.G. 1996. Assessing integrity of weather data for use in reference evapotranspiration estimation. *J. Irrig. and Drain. Engng. Div.,* ASCE 122(2): 97-106.

Allen, R.G. and Brockway, C.E. 1983. Estimating consumptive use on a statewide basis. pp. 79-89 in Proc. 1983 Irrig. and Drain. Specialty Conf. at Jackson, WY. ASCE, New York, NY.

Allen, R.G., Brockway, C.E., and Wright, J.L. 1983. Weather station siting and consumptive use estimates. *J. Water Resour. Plng. and Mgmt. Div*., ASCE 109(2):134-146.

Allen, R.G. 1997. a Self-Calibrating Method for Estimating Solar Radiation from Air Temperature. *J. Hydrologic Engineering,* ASCE 2(2): 56-67.

Allen, R.G. and Wright, J.L. 1977. Translating Wind Measurements from Weather Stations to Agricultural Crops. *J. Hydrologic Engineering,* ASCE 2(1): 26-35.

Burman, R.D., Wright, J.L. and Jensen, M.E. 1975. Changes in climate and estimated evaporation across a large irrigated area in Idaho. *Trans. ASAE* 18 (6): 1089-1091, 1093.

Pereira, L.S. (ed.). 1998. *Water and Soil Management for Sustainable Agriculture in the Huang-Huai-Hai Rivers Plain (North China*). Final report of EC Research Contract CT93-250, Instituto Superior de Agronomia, Lisbon.

Pruitt, W.O. and Doorenbos, J. 1977. Background and Development of Methods to Predict Reference Crop Evapotranspiration (ETo). Appendix II in FAO-ID-24, pp 108-119.

Pruitt, W.O. and Swann, B.D. 1986. Evapotranspiration studies in N.S.W.: Daily vs. hourly meteorological data. Irrigation '86, Darling downs Institute of Advanced Education, Toowoomba, Queensland, Australia, 29 p.

Rosenberg, N.J., Blad, B.L. and Verma, S.B. 1983. *Microclimate. The Biological Environment* (2nd edition). J. Wiley, New York.

Snyder, R.L. and Pruitt, W.O. 1992. Evapotranspiration data management in California. Proceedings of the Irrigation and Drainage sessions of ASCE Water Forum '92, T. Engman, ed. ASCE, New York, New York. p.128-133.

G. CROP EVAPOTRANSPIRATION

Alves, I.L. 1995. Modelling crop evapotranspiration. Canopy and aerodynamic resistances. Ph.D. Dissertation, ISA, Univ. Tec. Lisboa (in portuguese).

Bevan, K. 1979. A sensitivity analysis of the Penman-Monteith actual evapotranspiration estimates. *J. Hydrol*. 44:169-190.

Howell, T.A., Evett, S.R., Tolk, J.A., Schneider, A.D. and Steiner, J.L. 1996. Evapotranspiration of corn – Southern High Plains. In: Camp, C.R., Sadler, E.J. and Yoder, R.E. (eds.). *Evapotranspiration and Irrigation Scheduling*, ASAE: 158-166.

Jensen, M.E. 1968. Water consumption by agricultural plants. In: Kozlowski, T.T. (ed) *Water Deficits and Plant Growth,* vol II, Academic Press, New York: 1-22.

Jensen, M.E. 1974. (ed.) *Consumptive use of water and irrigation water requirements*. Rep. Tech. Com. on Irrig. Water Requirements, Irrig. and Drain. Div., ASCE, 227 pp.

Katerji, N. and Perrier, A. 1983. Modélization de l'évapotranspiration réelle ETR d'une parcelle de luzerne: rôle d'un coefficient cultural. *Agronomie* 3(6):513-521 (in French).

Lee, R. 1980. *Forest Hydrology*. Columbia Univ. Press, New York.

Perrier, A., Archer, P., and de Pablos, B. 1974. Etude de l'évapotranspiration réelle et maximele de diverses cultures. I: Dispositif et mesure. *Ann. Agron.* 25(3:229-243.

Perrier, A., Katerji, N., Gosse, G., and Itier, B. 1980. Etude "in situ" de l'evapotranspiration reelle d'une culture de ble. (In situ study of evapotranspiration rates for a wheat crop). *Agric. Meterol*. 21:295-311. (in French).

Rijtema, P.E., (1965). "Analysis of actual evapotranspiration." Agric. Res. Rep. No. 69, Centre for Agric. Publ. and Doc., Wageningen.

Shuttleworth, W.J. 1993. Evaporation. In: D.R. Maidment (ed) *Handbook of Hydrology*. McGraw Hill, New York: 4.1-4.53.

H. CROP COEFFICIENTS

Abtew, W. and J. Obeysekera. 1995. Lysimeter study of evapotranspiration of cattails and comparison of three estimation methods. *Trans. ASAE* 38(1):121-129.

Allen, R.G., J. Prueger, and R.W. Hill. 1992. Evapotranspiration from Isolated Stands of Hydrophytes: Cattail and Bulrush. *Trans ASAE* 35(4):1191-1198.

Allen, R.G., R.W. Hill, and S. Vemulapali, S. 1994. Evapotranspiration Parameters for Variably-Sized Wetlands. Paper presented at the 1994 Summer Meeting of ASAE. No. 942132, 24 p. Burman, R.D., Nixon, P.R., Wright, J.L. and Pruitt, W.O. 1980 "Water requirements"p. 189-232 in Jensen, M.E. (ed) *Design and operation of farm irrigation systems,* Amer. Soc. Agric. Engr., St. Joseph, Mich.

Allen, R.G., Smith, M., Pereira, L.S. and Pruitt, W.O. 1997. Proposed revision to the FAO procedure for estimating crop water requirements. In: Chartzoulakes, K.S. (ed.). *Proc. 2nd. Int. Sym. on Irrigation of Horticultural Crops*, ISHS, Acta Hort. Vol. I: 17-33.

Doorenbos, J. and Pruitt, W. O., 1977. Crop water requirements. *Irrigation and Drainage Paper No. 24*, (rev.) FAO, Rome, Italy. 144 p.

Doorenbos, J. and Kassam, A.H. 1979. *Yield response to water*. FAO Irrig. and Drain. Paper No. 33, FAO, Rome, Italy. 193 pp.

Elliott, R. L., S. L. Harp, G. D. Grosz and M. A. Kizer. 1988. Crop Coefficients for Peanut Evapotranspiration. Agricultural Water Management15:155-164.

Feddes, R.A. 1987. Crop factors in relation to Makkink reference crop evapotranspiration. Tech. Bull. Inst. for Land and Water Management Research. No. 67, pp. 33-45.

Fereres, E., (1981). (ed.) "Drip irrigation management." Cooperative Extension, Univ. California, Berkeley, CA, Leaflet No. 21259.

Grattan, S.R., W. Bowers, A. Dong, R.L. Snyder, J.J. Carroll, and W. George. 1998. New crop coefficients estimate water use of vegetables, row crops. *California Agriculture* 52(1):16-21.

Howell, T.A., D.A. Bucks, D.A. Goldhamer, and J.M. Lima. 1986. "Management Principles: 4.1 Irrigation Scheduling.", in *Trickle Irrigation for Crop Production: Design, Operation and Management* (F.S. Nakayama and D.A. Bucks (ed)). Elsevier.

Howell, T.A., Steiner, J.L., Schneider, A.D., and Evett, S.R. 1995. Evapotranspiration of irrigated winter wheat - southern high plains. *Trans. ASAE* 38(3):745-759.

Jensen, M.E. 1974. (ed.) *Consumptive use of water and irrigation water requirements*. Rep. Tech. Com. on Irrig. Water Requirements, Irrig. and Drain. Div., ASCE, 227 pp.

Kolar, J.J. and Kohl, R.A. 1976. Irrigating alfalfa for seed production. Univ. Idaho Agric. Exp. Station Current Information Series 357., Moscow, Idaho. 3 p.

Liu, Y., Teixeira, J.L., Zhang, H.J. and Pereira, L.S. 1998. Model validation and crop coefficients for irrigation scheduling in the North China plai. *Agricultural Water Management* 36: 233-246.

Neale, C.M.U. 1987. Development of Reflectance Based Crop Coefficients for Corn. Unpublished PhD Dissertation, Agricultural Engineering , Colorado State University, Fort Collins, USA.

Neale, C.M.U., W.C. Bausch and D. F. Heerman. 1989. Development of reflectance-based crop coefficients for corn. *Trans. ASAE* 32(6):1891-1899.

Pastor, M. and Orgaz, F. 1994. Riego deficitario del olivar: Los programas de recorte de riego en olivar. *Agricultura* no. 746: 768-776 (in Spanish).

Pereira, L.S., Teixeira, J.L., Pereira, L.A., Ferreira, M.I., and Fernando,R.M., 1987. Simulation models of crop response to irrigation management:research approaches and needs. In: J. Feyen (ed) Simulation Models for Cropping Systems in Relation to Water Management. Commission of the European Communities, EUR 10869, Luxembourg: 19-36.

Pereira, L.S., Perrier, A., Allen, R.G. and Alves, I. 1996. Evapotranspiration: Review of concepts and future trends. In: Camp, C.R., Sadler, E.J., Yoder, R.E. (eds) *Evapotranspiration and Irrigation Scheduling*, ASAE: pp. 109-115.

Pruitt, W.O. 1976. "Evapotranspiration and crop coefficients for a windbreak of Monterey pine trees", personal communication, Davis, CA.

Pruitt, W.O. 1986. "Traditional methods 'Evapotranspiration research priorities for the next decade'." *ASAE* Paper No. 86-2629. 23 p.

Pruitt, W.O., E. Fereres, P.E. Martin, H. Singh, D.W. Henderson, R.M. Hagan, E. Tarantino, and B. Chandio. 1984. "Microclimate, evapotranspiration, and water-use efficiency for drip- and furrow-irrigated tomatoes." *Proceedings 12th Congress*, International Commission on Irrigation and Drainage, Ft. Collins, CO., p. 367-394.

Rogers, J.S., Allen, L.H., and Calvert, D.J. 1983. Evapotranspiration for humid regions: developing citrus grove, grass cover. *Trans. ASAE*, 26(6): 1778-83, 92.

Snyder, R.L., Lanini, B.J., Shaw, D.A., and Pruitt, W.O. 1989a. Using reference evapotranspiration (ETo) and crop coefficients to estimate crop evapotranspiration (ETc) for agronomic crops, grasses, and vegetable crops. Cooperative Extension, Univ. California, Berkeley, CA, Leaflet No. 21427, 12 p.

Snyder, R.L., Lanini, B.J., Shaw, D.A., and Pruitt, W.O. 1989b. Using reference evapotranspiration (ETo) and crop coefficients to estimate crop evapotranspiration (ETc) for trees and vines. Cooperative Extension, Univ. California, Berkeley, CA, Leaflet No. 21428, 8 p.

Wright J.L. 1981. Crop coefficients for estimates of daily crop evapotranspiration. *Irrig. Scheduling for Water and Energy Conservation in the 80s,* ASAE, Dec. 1981.

Wright, J.L. 1982. New Evapotranspiration Crop Coefficients. *J. of Irrig. and Drain. Div.*, ASCE, 108:57-74.

Wright, J.L. and Jensen, M.E. 1972. Peak water requirements of crops in southern Idaho. *J. Irrig. and Drain. Div*., ASCE 96(IR1):193-201.

Wright, J.L. 1990. Evapotranspiration data for dry, edible beans at Kimberly, Idaho., unpublished data, USDA-ARS, Kimberly, Idaho.

I. LENGTHS OF CROP GROWTH STAGES

Allen, R.G. and Gichuki, F.N. 1989. Effects of Projected CO_2-induced Climatic Changes on Irrigation Water Requirements in the Great Plains States (Texas, Oklahoma, Kansas, and Nebraska). *The Potential Effects of Global Climate Change on the United States*: Appendix C - Agriculture. Vol. 1. EPA-230-05-89-053 (J.B. Smith and D.A. Tirpak, Eds.), U.S. Environmental Protection Agency, Office of Policy, Planning and Evaluation, Washington, D.C., (6):1-42.

Dingkuhn, M. 1994. Climatic determinants of irrigated rice performance in the Sahel. III. Characterizing environments by simulating crop phenology. *Agricultural Systems* (48): 435-456.

Doorenbos, J. and Pruitt, W. O., 1977. Crop water requirements. *Irrigation and Drainage Paper No. 24*, (rev.) FAO, Rome, Italy. 144 p.

Everson, D.O., M. Faubion and D.E. Amos 1978. "Freezing temperatures and growing seasons in Idaho." Univ. Idaho Agric. Exp. station bulletin 494. 18 p.

Kruse E.G. and Haise, H.R. 1974. "Water use by native grasses in high altitude Colorado meadows." U.S.D.A Agric. Res. Service, Western Region report ARS-W-6-1974. 60 pages

O'Halloran, T.F. 1997. Reported crop acreages by month for the Imperial Irrigation District, Imperial Irrigation District, Imperial, Calif., USA. personal communication.

Ritchie, J.T. 1991. Wheat phasic development. In: R.J. Hanks and J.T. Ritchie (Editors), *Modeling Plant and Soil Systems*, Agronomy Series No. 31, Am. Soc. Agron., Madison, Wisc., Chapter 3, 31-54.

Ritchie, J.T. and D.S. NeSmith. (1991). "Temperature and crop development." In: R.J. Hanks and J.T. Ritchie (Editors). *Modeling Plant and Soil Systems*, Agronomy Series No. 31, Am. Soc. Agron., Madison, Wisc., Chapter 2, 5-29.

Ritchie, J.T. and Johnson, B.S. (1990). "Soil and plant factors affecting evaporation." Chapter 13 of *Irrigation of Agricultural Crops*, (Stewart, B.A. and Nielsen, D.R (ed.)), Agronomy Series 30. Am. Soc. Agron. p. 363-390.

Snyder, R.L., Lanini, B.J., Shaw, D.A., and Pruitt, W.O. 1989a. Using reference evapotranspiration (ETo) and crop coefficients to estimate crop evapotranspiration (ETc) for agronomic crops, grasses, and vegetable crops. Cooperative Extension, Univ. California, Berkeley, CA, Leaflet No. 21427, 12 p.

Snyder, R.L., Lanini, B.J., Shaw, D.A., and Pruitt, W.O. 1989b. Using reference evapotranspiration (ETo) and crop coefficients to estimate crop evapotranspiration (ETc) for trees and vines. Cooperative Extension, Univ. California, Berkeley, CA, Leaflet No. 21428, 8 p.

Wright, J.L. 1982. New evapotranspiration crop coefficients. *J. Irrig. and Drain. Div.,* ASCE, 108(IR2):57-74.

J. EFFECTS OF SOIL MULCHES

Battikhi, A.M. and Hill, R.W. 1986. Irrigation scheduling and watermelon yield model for the Jordan Valley. *J. Agronomy and Crop Science* 157:145-155.

Battikhi, A.M. and Hill, R.W. 1986. Irrigation scheduling and cantaloupe yield model for the Jordan Valley. *Agricultural Water Management* 15:177-187.

Ghawi, I. and Battikhi, A.M. 1986. Watermelon (*Citrullus lanatus*) production under mulch and trickle irrigation in the Jordan Valley. *J. Agronomy and Crop Science* 156:225-236.

Ghinassi, G. and Neri, L. 1998. Effect of mulching with black polyethylee sheets on sweet pepper evapotranspiration losses. In: Pereira, L.S. and Gowing, J.W. (eds.). *Water and the Environment: Innovative Issues in Irrigation and Drainage.* E. & F.N. Spon, London. Pp. 396-403.

Haddadin, S.H. and Ghawi, I. 1983. Effect of plastic mulches on soil water conservation and soil temperature in field grown tomato in the Jordan Valley. Dirasat 13(8): 25-34

Safadi, A.S. 1991. Squash and cucumber yield and water use models. unpublished Ph.D. dissertation, Dept. Biological and Irrigation Engineering, Utah State Univ., Logan, UT 84322-4105. 190 p.

K. NON-GROWING SEASON EVAPOTRANSPIRATION

Flerchinger, G.N. and Pierson, F.B. 1991. Modeling plant canopy effects on variability of soil temperature and water. *Agr. and For., Meteorol*. 56:227-246.

Running, S.W. and Coughlan, J.C. 1988. A general model of forest ecosystem processes for regional applications: I. Hydrologic balance, canopy gas exchange and primary production processes. *Ecological Modeling* 42:125-154.

Saxton, K.E., Johnson, H.P., and Shaw, R.H. (1974). "Modeling evapotranspiration and soil moisture." *Trans. ASAE* 17(4):673-677.

Sinclair, T.R. (1984). "Leaf area development in field-grown soybeans." Agron. J. 76:141-146.

Liu, Y., Teixeira, J.L., Zhang, H.J. and Pereira, L.S. 1998. Model validation and crop coefficients for irrigation scheduling in the North China plai. *Agricultural Water Management* 36: 233-246.

L. SOIL WATER HOLDING CHARACTERISTICS

Jensen, M.E., Burman, R.D., and Allen, R.G. (1990). *Evapotranspiration and Irrigation Water Requirements*. ASCE Manuals and Reports on Engineering Practice No. 70. 332 p.

Keller, J. and Bliesner, R.D. (1990). *Sprinkle and Trickle Irrigation*. van Nostrand Reinhold., New York, NY. 652 p.

Ratliff, L.F., Ritchie, J.T., and Cassel, D.K. 1983. Field-measured limits of soil water availability as related to laboratory-measured properties. *Soil Sci. Soc. Am. J*., 47:770-775.

M. ROOTING DEPTHS

Doorenbos, J. and Kassam, A.H. 1979. Yield response to water. FAO Irrig. and Drain. Paper No. 33, FAO, Rome, Italy. 193 pp.

Keller, J. and Bliesner, R.D. (1990). *Sprinkle and Trickle Irrigation*. van Nostrand Reinhold., New York, NY. 652 p.

N. SALINITY IMPACTS ON EVAPOTRANSPIRATION

Ayers, R.S. and D.W. Westcot. 1985. *Water quality for agriculture*. Irrigation and Drainage Paper 29, Rev. 1. Food and Agriculture Organization of the United Nations, Rome, 174 pages.

Doorenbos, J. and A.H. Kassam. 1979. *Yield response to water*. Irrigation and Drainage Paper 33. Food and Agriculture Organization of the United Nations, Rome, 193 pages.

Hanks, R.J. 1984. Prediction of crop yield and water consumption under saline conditions. Section 8.2, pages 272-283, in Shainberg, I. and J. Shalhevet (ed), *Soil Salinity under Irrigation: Processes and Management*, Springer-Verlag, Berlin.

Hoffman, G.J., J.A. Jobes, and W.J. Alves. 1983. Response to tall fescue to irrigation water salinity, leaching fraction, and irrigation frequency. *Agric. Water. Management* 7:439-456.

Letey, J. and A. Dinar. 1986. Simulated crop-water production functions for severa crpos when irrigated with saline waters. *Hilgardia* 54(1):1-32.

Letey, J., A. Dinar, and K.C. Knapp. 1985. Crop-water production function model for saline irrigation waters. *Soil Sci. Soc. Am. J*., 49:1005-1009.

Maas, E.V., 1990. Crop salt tolerance. In: K.K. Tanji (Ed.), *Agricultural Salinity Assessment and Management*. ASCE Manuals and Reports on Engineering Practice No. 71. Am Soc. Civil Engineers, New York, pp. 262-304.

Mieri, A. 1984. Plant response to salinity: experimental methodology and application to the field, Section 8.3, pages 284-297, in Shainberg, I. and J. Shalhevet (ed), *Soil Salinity under Irrigation: Processes and Management*, Springer-Verlag, Berlin.

Oster, J.D. 1994. Irrigation with poor quality water – review article. *Agricult. Water management* 25:271-297.

Oster, J.D., I. Shainberg, and I.P. Abrol. 1996. Reclamation of salt-affected soil, Ch. 14. In: M. Agassi (ed.). *Soil Erosion, Conservation, and Rehabilitation*. Marcel Dekker, Inc. New York. pp 315-35.

Rhodes, J.D., A. Kandiah, and A.M. Mashali.. 1992. *The use of saline waters for crop production*. Irrigation and Drainage Paper 48. Food and Agriculture Organization of the United Nations, Rome, 133 pages.

Shalhevet, J. 1984. Management of Irrigation with Brackish Water, Section 8.4, pages 298-318, in Shainberg, I. and J. Shalhevet (ed), *Soil Salinity under Irrigation: Processes and Management*, Springer-Verlag, Berlin.

Shalhevet, J. 1994. Using water of marginal quality for crop production: major issues – review article. *Agricult. Water management* 25:233-269.

Stewart, J.I., R.M. Hagan, and W.O. Pruitt. 1976. Salinity effects on corn yield, evapotranspiration, leaching fraction, and irrigation efficiency. pages 316-331 in H.E. Dregne (ed). *Managing Saline Water for Irrigation*, Proceedings of the Int. Conf. on Managing Saline Water for Irrig.: Planning for the Future, Lubbock, TX.

Tanji, K.K. (Ed.), *Agricultural Salinity Assessment and Management*. 1990. ASCE Manuals and Reports on Engineering Practice No. 71. Am Soc. Civil Engineers, New York, pp. 113-137

O. SOIL EVAPORATION

Hanks, R.J. 1974. Model for predicting plant growth as influenced by evapotranspiration and soil water. *Agron. J.* 66:660-665.

Hanks, R.J. 1985. Crop coefficients for transpiration. *Advances in Evapotranspiration.* Proceedings, National Conf. Advances in Evapotranspiration., ASAE, Chicago, IL., 431-438.

Hanks, R.J. and Hill, R.W. 1980. *Modeling Crop Response to Irrigation in Relation to Soils, Climate and Salinity.* International Irrigation Information Center, No. 6, Pergamon Press, Elmsford, New York. 63 p.

Kanemasu, E.T., Stone, L.R., and Powers, W.L. 1976. Evapotranspiration model tested for soybean and sorghum. *Agron. J.* 68:569-572.

Pruitt, W.O. 1995. Background information on development of Fig. 6 in FAO-ID-24, personal communication, Davis, CA.

Ritchie, J.T. 1972. Model for predicting evaporation from a row crop with incomplete cover. *Water Resources Res.* 8:1204-1213.

Ritchie, J.T. 1974. Evaluating irrigation needs for southeastern U.S.A. 262-273. *Proc. Irrig. and Drain. Spec. Conf.*, ASCE.

Ritchie, J.T., Godwin, D.C., and Singh, U. 1989. Soil and weather inputs for the IBSNAT crop models. *Proceedings of the IBSNAT Symposium: Decision Support System for Agrotechnology Transfer*: Part I., IBSNAT, Dept. Agronomy and Soil Science, College of Tropical Agriculture and Human Resources, University of Hawaii, Honolulu, HA. p. 31-45.

Ritchie, J.T. and Johnson, B.S. 1990. "Soil and plant factors affecting evaporation". Chapter 13 of *Irrigation of Agricultural Crops,* (Stewart, B.a. and Nielsen, D.R. (ed.)), Agronomy Series 30. Am. Soc. Agron. p. 363-390.

Tanner, C.B. and Fuchs, M. 1968. Evaporation from unsaturated surfaces: a generalized combination equation. *J. Geophysical Res*. 73(4):1299-1304.

Tanner, C.B. and Jury, W.A. 1976. Estimating evaporation and transpiration from a crop during incomplete cover. *Agron. J.* 68:239-242.

Wright, J.L. 1989. Evaporation data for a dry soil surface condition, unpublished data, USDA-ARS, Kimberly, Idaho.

P. FACTORS AFFECTING ET_C

Allen, I.H., Jones, P. and Jones, J. W. 1985. Rising atmospheric CO_2 and evapotranspiration. Proc. Natl. Conf. on Advances in Evapotranspiration (Chicago, IL, 16-17 Dec.), ASAE, St. Joseph, MI.

Burman, R.D., Wright, J.L. and Jensen, M.E. 1975. Changes in climate and estimated evaporation across a large irrigated area in Idaho. *Trans. ASAE* 18 (6): 1089-1091, 1093.

Doorenbos, J. and Kassam, A.H. 1979. *Yield response to water*. FAO Irrig. and Drain. Paper No. 33, FAO, Rome, Italy. 193 pp.

Loommis, R.S. and Williams, W.A. 1969. Productivity and the morphology of crop stand patterns with leaves. In: J.D. Eastin (ed) *Physiological Aspects of Crop Yield.* ASA, CSSA and SSSA, Madison, WI: 27-47.

Rhoades, J.D., Kandiah, A. and Mashali A.M. 1992. *The Use of Saline Waters for Crop Production.* Irrig. and Drain. Pap. 48, FAO, Rome.

Shuttleworth, W.J. and Wallace, J.S. 1985. Evaporation from sparse crops - an energy combination theory. *Quart. J. Roy Meteorol. Soc.* 111: 839-853.

Wallace, J.S., Roberts, J.M., and Sivakuma, M.V.K. 1990. "The estimation of transpiration from sparse dryland millet using stomatal condutance and vegetation area indices." *Agric. and Forest Meteorol.* 51: 35-49.

Q. SOIL WATER BALANCE AND IRRIGATION SCHEDULING

Bastiaanssen, W.G.M. 1995. Regionalization of surface flux densities and moisture indicators in composite terrain. Doctoral thesis, Wageningen Agricultural University, Wageningen, 273 pp.

Belmans, C., Wesseling, J.G. and Feddes, R.A. 1983. Simulation model of the water balance of a cropped soil: SWATRE. *I. Hydrology,* 63: 271-286.

Camp, C.R., Sadler, E.J. and Yoder, R.E. 1996. Evapotranspiration and irrigation scheduling. *Proc. Int. Conf. on Evapotranspiration and Irrigation Scheduling.* Am. Soc. Ag. Engineers, St. Joseph, MI. ISBN 0-929355-82-2. 1166 p.

Doorenbos, J. and Kassam, A.H. 1979. *Yield response to water*. FAO Irrig. and Drain. Paper No. 33, FAO, Rome, Italy. 193 pp.

Jordan, W.R. and Ritchie, J.T. 1971. Influence of soil water stress on evaporation, root absortion and internal water status of cotton. *Plant Phisiol.* 48: 783-788.

Kabat, P., van den Broek, B.J. and Feddes, R.A. 1992. SWACROP: a water management and crop production simulation model. *ICID Bull.* 41 (2): 61-84.

Merriam, J.L. 1966. A management control concept for determining the economical depth and frequency of irrigation. *Trans. Am. Soc. Agric. Engrs.* 9: 492-498.

Pereira, L.S., Perrier, A. Ait Kadi, M. and Kabat, P. (eds) 1992. *Crop Water Models.* Special issue of the *ICID Bulletin.* 41 (2), 200 pp.

Pereira, L.S., van den Broek, B.J., Kabat, P. and Allen, R.G. (eds) 1995. *Crop-Water Simulation Models in Practice.* Wageningen Pers, Wageningen, 339 pp.

Raes, D., Lemmens, H., Van Aelst, P., Vanden Bulcke, M. and Smith, M. 1988. IRSIS - Irrigation Scheduling Information System. Reference Manual n° 3. Institute for Land and Water Management, K.U.Leuven, Belgium. Volume 1&2, 119 & 71 p.

Smith, M. 1992. *CROPWAT, a computer program for irrigation planning and management.* FAO Irrigation and Drainage Paper 46, FAO, Rome.

Teixeira, J.L., Farrajota, M.P. and Pereira, L.S. 1995. PROREG simulation software to design demand in irrigation projects. In: Pereira, L.S., van den Broek, B.J., Kabat, P. and Allen, R.G. (eds) *Crop-Water Simulation Models in Practice.* Wageningen Pers, Wageningen: 273-285.

Tuzet, A., Perrier, A. and Masaad, C. 1992. Crop water budget estimation of irrigation requirement. *ICID Bull.* 41(2): 1-17.

Xevi, E. and Feyen, J. 1992. Combined soil water dynamic model (SWATRER) and summary crop simulation model (SUCROS). *ICID Bull.* 41(2): 85-98.

R. GENERAL

Doorenbos, J. and Pruitt, W.O. 1975. *Guidelines for predicting crop water requirements*, Irrigation and Drainage Paper 24, Food and Agriculture Organization of the United Nations, Rome, 179 p.

Doorenbos, J. and Pruitt, W.O. 1977. *Guidelines for predicting crop water requirements*, Irrigation and

Jensen, M.E., Burman, R.D., and Allen, R.G. (ed). 1990. *Evapotranspiration and Irrigation Water Requirements*. ASCE Manuals and Reports on Engineering Practices No. 70., Am. Soc. Civil Engrs., New York, NY, 360 p.

Martin, D.L. and J.R. Gilley 1993. *Irrigation Water Requirements.* Chapter 2 of the SCS National Engineering Handbook, Soil Conservation Service, Washington D.C., 284 pp.

Pereira, L.S. and Allen, R.G. 1998. Crop water requirements. Chapter I.5.1 of *Handbook of Agricultural Engineering*, CIGR and ASAE (in press).